REPORT UAG - 24
PART II

# WORLD DATA CENTER A
# for
# Solar-Terrestrial Physics

# DATA ON SOLAR - GEOPHYSICAL ACTIVITY ASSOCIATED WITH THE MAJOR GROUND LEVEL COSMIC RAY EVENTS OF 24 JANUARY AND 1 SEPTEMBER 1971

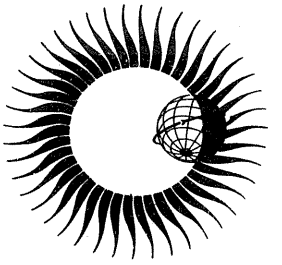

DECEMBER 1972

# WORLD DATA CENTER A

National Academy of Sciences
2101 Constitution Avenue, N. W. Washington, D. C. U.S.A., 20418

World Data Center A consists of the Coordination Office

and eight subcenters:

World Data Center A
Coordination Office
National Academy of Sciences
2101 Constitution Avenue, N.W.
Washington, D. C., U.S.A. 20418
Telephone (202) 961-1478

Solar and Interplanetary Phenomena, Ionospheric Phenomena, Flare-Associated Events, Geomagnetic Variations, Magnetospheric and Interplanetary Magnetic Phenomena, Aurora, Cosmic Rays, Airglow:
World Data Center A
for Solar-Terrestrial Physics
National Oceanic and Atmospheric Administration
Boulder, Colorado, U.S.A. 80302
Telephone (303) 499-1000 Ext. 6467

Geomagnetism, Seismology, Gravity (and Upper Mantle Project Archives):
World Data Center A:
Geomagnetism, Seismology and Gravity
Environmental Data Service, NOAA
Boulder, Colorado, U.S.A. 80302
Telephone (303) 499-1000 Ext. 6311

Glaciology:
World Data Center A:
Glaciology
U. S. Geological Survey
1305 Tacoma Avenue South
Tacoma, Washington, U.S.A. 98402
Telephone (206) 383-2861 Ext. 318

Longitude and Latitude:
World Data Center A:
Longitude and Latitude
U. S. Naval Observatory
Washington, D. C., U.S.A. 20390
Telephone (202) 698-8422

Meteorology (and Nuclear Radiation):
World Data Center A:
Meteorology
National Climatic Center
Federal Building
Asheville, North Carolina, U.S.A. 28801
Telephone (704) 254-0961

Oceanography:
World Data Center A:
Oceanography
National Oceanic and Atmospheric Administration
Rockville, Maryland, U.S.A. 20852
Telephone (202) 426-9052

Rockets and Satellites:
World Data Center A:
Rockets and Satellites
Goddard Space Flight Center
Code 601
Greenbelt, Maryland, U.S.A. 20771
Telephone (301) 982-6695

Tsunami:
World Data Center A:
Tsunami
National Oceanic and Atmospheric Administration
P.O. Box 3887
Honolulu, Hawaii, U.S.A. 96812
Telephone (808) 546-5698

---

Notes:

(1) World Data Centers conduct international exchange of geophysical observations in accordance with the principles set forth by the International Council of Scientific Unions. WDC-A is established in the United States under the auspices of the National Academy of Sciences.
(2) Communications regarding data interchange matters in general and World Data Center A as a whole should be addressed to: World Data Center A, Coordination Office (see address above).
(3) Inquiries and communications concerning data in specific disciplines should be addressed to the appropriate subcenter listed above.

# WORLD DATA CENTER A
# for
# Solar-Terrestrial Physics

## REPORT UAG - 24 PART II

# DATA ON SOLAR - GEOPHYSICAL ACTIVITY ASSOCIATED WITH THE MAJOR GROUND LEVEL COSMIC RAY EVENTS OF 24 JANUARY AND 1 SEPTEMBER 1971


compiled by

Helen E. Coffey and J. Virginia Lincoln
WDC-A for Solar-Terrestrial Physics
Boulder, Colorado


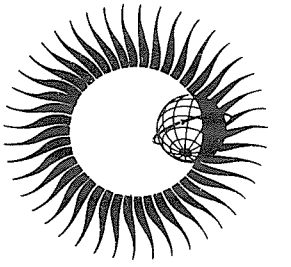


Prepared by World Data Center A for
Solar-Terrestrial Physics, NOAA, Boulder, Colorado
and published by

U.S. DEPARTMENT OF COMMERCE
NATIONAL OCEANIC AND ATMOSPHERIC ADMINISTRATION

ENVIRONMENTAL DATA SERVICE
Asheville, North Carolina, USA 28801

**DECEMBER 1972**

SUBSCRIPTION PRICE: $9.00 a year; $2.50 additional for foreign mailing; single copy price varies.* Checks and money orders should be made payable to the Department of Commerce, NOAA. Remittance and correspondence regarding subscriptions should be sent to the National Climatic Center, Federal Building, Asheville, NC 28801, Attn: Publications.

*PRICE THIS ISSUE $2.00

TABLE OF CONTENTS

Table of Contents (Continued)



* Article covers both the January and September events.

Table of Contents (Continued)



* Article covers both the January and September events.

# 1. INTRODUCTION AND BACKGROUND DATA

by

Helen E. Coffey
World Data Center A for Solar-Terrestrial Physics
NOAA, Boulder, Colorado 80302

## General Activity

The sun on September 1, 1971 was relatively quiet. Since no large flare occurred on the visible solar disk, it is proposed that a large flare occurred in McMath Region 11482, a very active region which passed over the West limb three days earlier. Figure 1 shows this region at central meridian passage (August 23.8). Figure 2 shows the activity on the visible disk on September 1, 1971.

An historical review of McMath Region 11482 is given in Table 1:

Table 1

McMath Region 11482 CMP Date 23.8 Return of Region 11445 Rotation 2

| | | | | Calcium Page Data | | | | | | Sunspot Data | | | | | | | | 9.1 cm | |
|---|---|---|---|---|---|---|---|---|---|---|---|---|---|---|---|---|---|---|---|
| YR | MO | DA | MC NO. | LAT | CMD | L | AREA | INT | MW NO. | LAT | CMD | L | MAG. | H | AREA | CNT | C | INT | FLUX |
| 71 | 8 | 17 | 11482 | S13 | E85 | 268 | 900 | 3.5 | 18538 | S13 | E80 | 272 | (αp) | 4 | 310 | 7 | H | 29 | 9 |
| | | 18 | | S13 | E71 | 269 | 2000 | 4.0 | | S13 | E70 | 269 | (βp) | 4 | 470 | 47 | F | 58 | 18 |
| | | 19 | | S13 | E58 | 268 | 3500 | 3.5 | | S13 | E58 | 268 | (δ ) | 6 | 180 | 40 | F | 69 | 21 |
| | | 20 | | S13 | E43 | 270 | 4000 | 3.5 | | S13 | E42 | 270 | (δ ) | 6 | 240 | 67 | F | 99 | 31 |
| | | 21 | | S12 | E30 | 269 | 4800 | 3.0 | | S12 | E26 | 270 | (δ ) | 6 | | | | | |
| | | 22 | | S12 | E17 | 270 | 4700 | 3.5 | | S12 | E15 | 270 | (βp) | 6 | | | | | |
| | | 23 | | S12 | E04 | 270 | 4800 | 3.5 | | S12 | E01 | 271 | (βγ) | 6 | 610 | 23 | F | 84 | 26 |
| | | 24 | | S12 | W08 | 268 | 4400 | 3.5 | | S12 | W12 | 271 | (δ ) | 6 | 530 | 36 | F | 96 | 29 |
| | | 25 | | S12 | W20 | 268 | 4600 | 3.5 | | S12 | W25 | 270 | (βp) | 6 | 180 | 26 | E | 83 | 25 |
| | | 26 | | S12 | W35 | 269 | 4400 | 3.5 | | S13 | W39 | 270 | (βγ) | 5 | 0 | 29 | F | | |
| | | 27 | | S12 | W50 | 270 | 4600 | 3.5 | | S13 | W52 | 271 | (βγ) | 5 | 900 | 63 | F | 70 | 22 |
| | | 28 | | S12 | W63 | 269 | 4500 | 3.0 | | S13 | W65 | 270 | (βp) | 5 | 730 | 52 | F | | |
| | | 29 | | S12 | W74 | 269 | 3800 | 2.5 | | S12 | W78 | 270 | (βp) | 5 | | | | | |
| | | 30 | | S11 | W88 | 270 | 3000 | 2.5 | | S14 | W88 | 268 | | 0 | | | | | |

The final Relative Sunspot Numbers ($R_z$) and the observed 2800 MHz flux ($S_a$) for the period August 29 - September 5, 1971 are given below; the monthly means for September are: $\overline{R}_z$ = 50.2, $\overline{S}_a$ = 105.1.

| | $R_z$ | $S_a$ | | $R_z$ | $S_a$ |
|---|---|---|---|---|---|
| Aug. 29 | 29 | 112.0 | Sept. 2 | 19 | 90.1 |
| 30 | 21 | 103.3 | 3 | 26 | 92.5 |
| 31 | 21 | 96.3 | 4 | 29 | 92.6 |
| Sept. 1 | 22 | 90.3 | 5 | 42 | 95.2 |

A small confirmed grouped flare, Group 40225, occurred at 2045 UT on September 1 in Region 11496. This, however, was not considered large enough to be responsible for the cosmic ray ground-level increase around 2200 UT.

AUGUST 24, 1971 (P = 18.71, $B_o$ = 7.00, $L_o$ = 266.61)

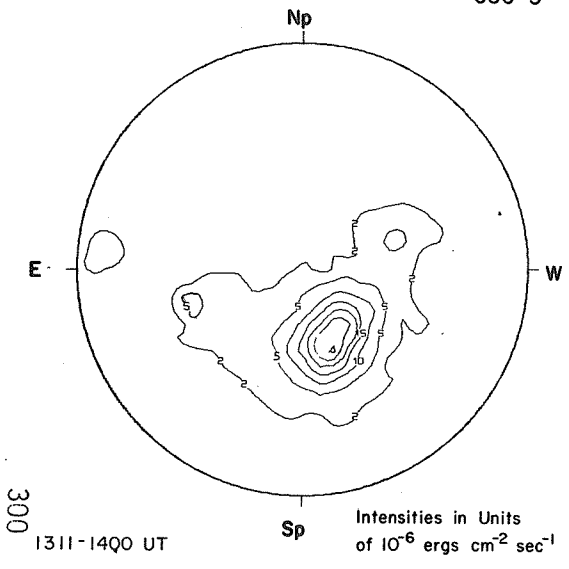


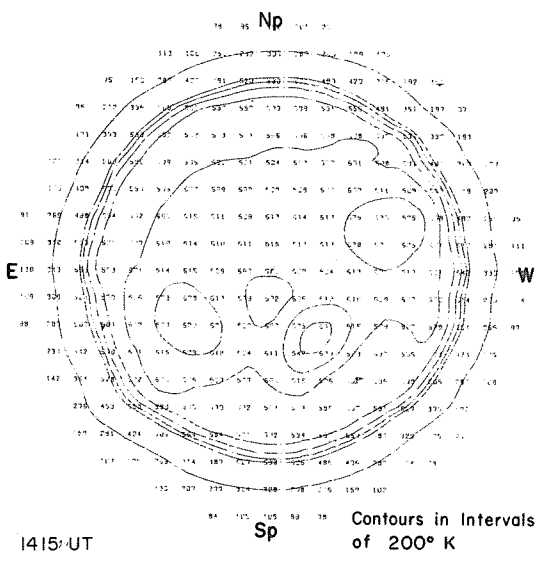


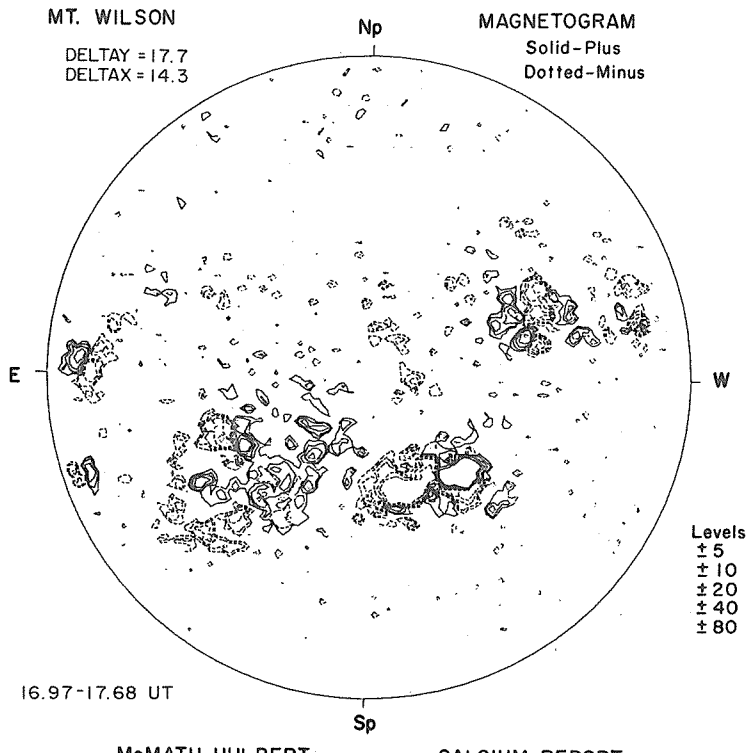


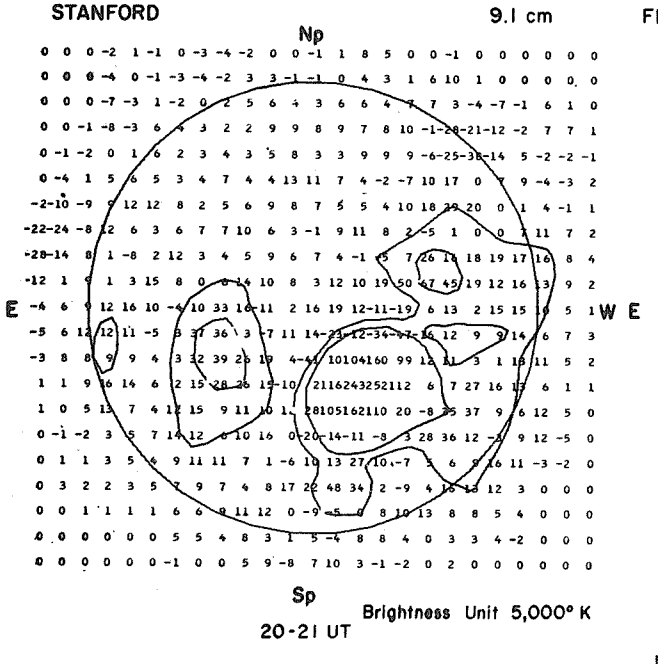


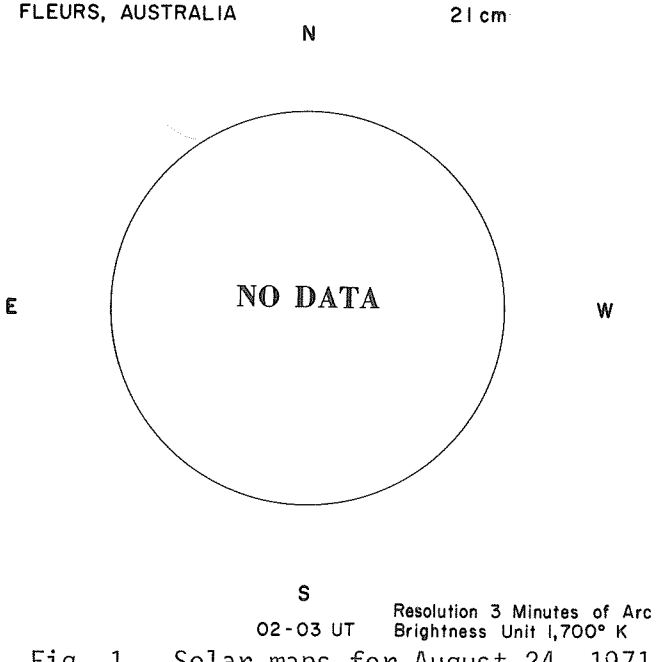


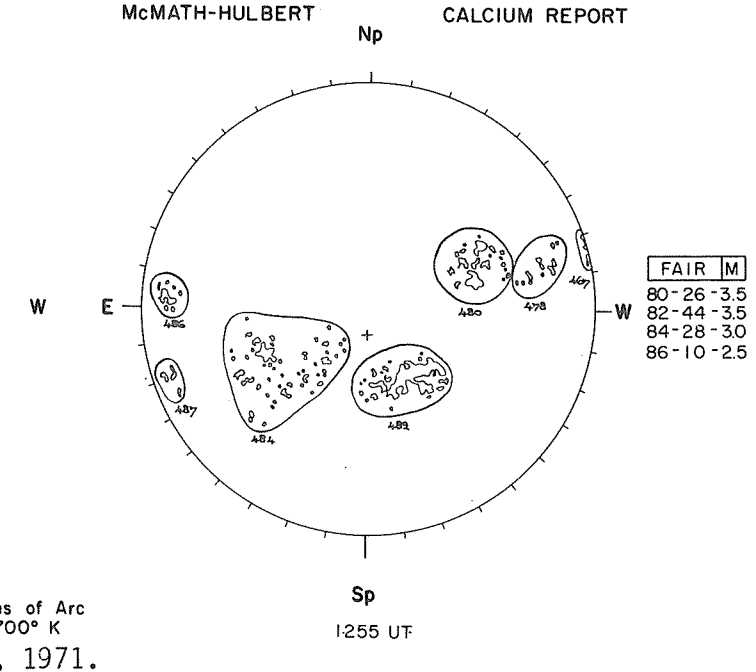


Fig. 1. Solar maps for August 24, 1971.

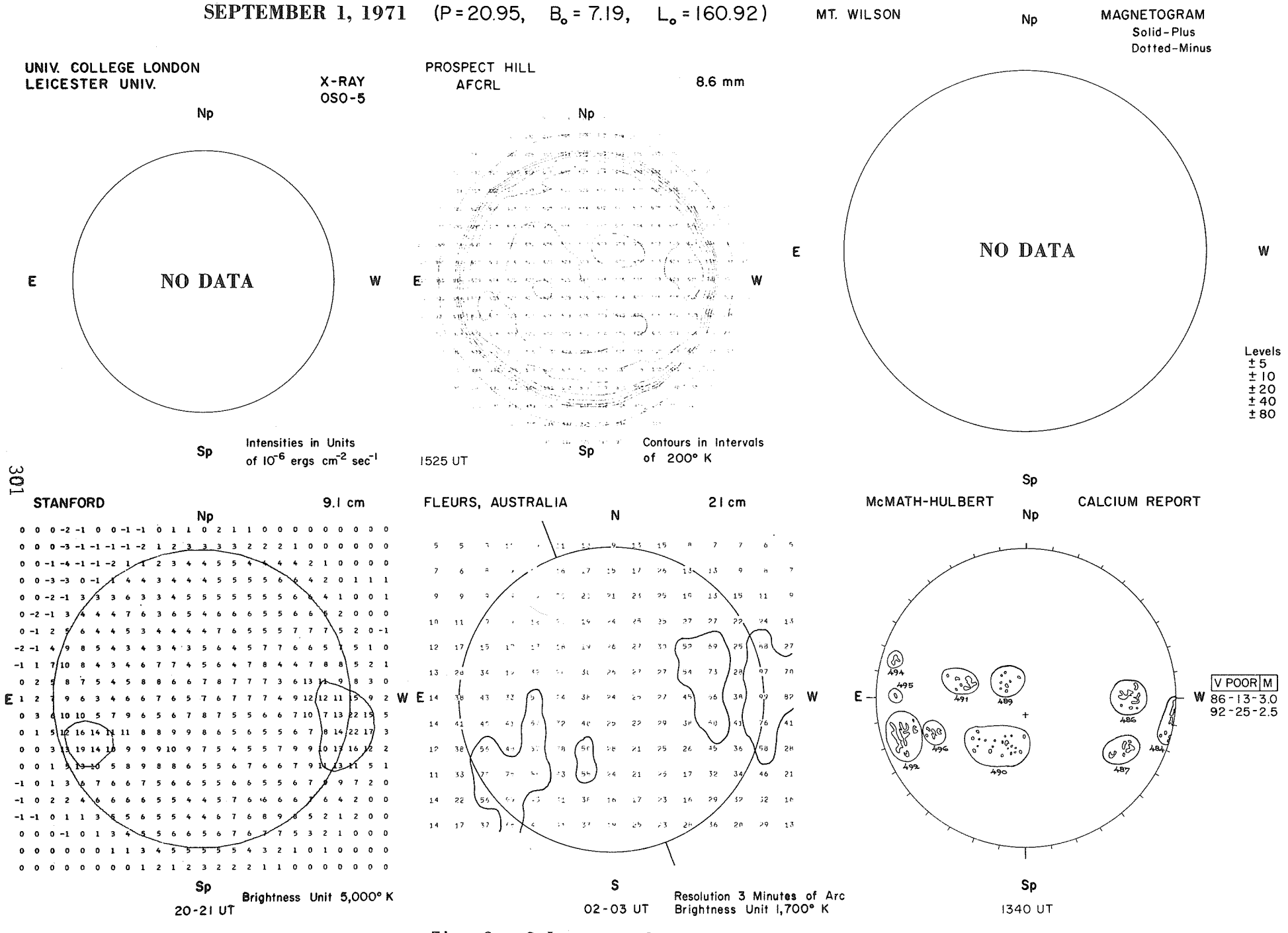


Fig. 2. Solar maps for September 1, 1971.

Spectral observations at the time of the ground-level increase are as follows:

## SOLAR RADIO EMISSION
## SPECTRAL OBSERVATIONS
SEPTEMBER 1971

| SEP. 1971 | TIMES OF OBSERVATION START UT | TIMES OF OBSERVATION END UT | STATION | EVENTS CENTIMETRIC BAND START UT | CENTIMETRIC BAND END UT | CENTIMETRIC BAND INT. | DECIMETRIC BAND START UT | DECIMETRIC BAND END UT | DECIMETRIC BAND INT. | METRIC BAND START UT | METRIC BAND END UT | METRIC BAND INT. | DEKAMETRIC BAND START UT | DEKAMETRIC BAND END UT | DEKAMETRIC BAND INT. | SPECTRAL TYPE |
|---|---|---|---|---|---|---|---|---|---|---|---|---|---|---|---|---|
| 01 | 1300 | 2400 | HARV | | | | 1934 | | 1 | 1933.8 | 1948 | 3 | 1934.8 | 1946 | 3 | II |
| | 1230 | 2400 | BOUL | | | | | | | 1934.2 | 1935.4 | 2 | 1934.2 | 1935.4 | 2 | III |
| | 0953 | 2304 | SGMR | | | | | | | | | | 1934.2 | 1936.3 | 2 | IIIG |
| | | | HARV | | | | 1934.5 | 1950 | 2 | | | | | | | IV |
| | | | SGMR | | | | | | | | | | 1937.0 | 1946.9 | 2 | IV |
| | | | BOUL | | | | | | | 1937.5 | 2009.5 | 2 | 1937.5 | 2009.5 | 2 | IV |
| | | | SGMR | | | | | | | | | | 1950.2 | 2002.3 | 1 | CONT |
| | 2033 | 2400 | CULG | | | | | | | 2034 | 2037 | 1 | | | | I |
| 02 | 0000 | 0129 | CULG | | | | | | | | | | | | | |
| | 0000 | 0130 | BOUL | | | | | | | | | | | | | |
| | 0000 | 0101 | HARV | | | | | | | | | | | | | |
| | 0204 | 0731 | CULG | | | | | | | | | | | | | |
| | 0520 | 1730 | HEIS | | | | | | | | | | | | | |
| | 0938 | 2313 | SGMR | | | | | | | | | | | | | |
| | 1230 | 2400 | BOUL | | | | | | | | | | | | | |
| | 1300 | 2400 | HARV | | | | | | | | | | | | | |
| | 2032 | 2400 | CULG | | | | | | | | | | | | | |

Outstanding solar radio emission occurrences on September 1-2, 1971 are shown in Table 2.

Table 2

## SOLAR RADIO EMISSION
## OUTSTANDING OCCURRENCES
SEPTEMBER 1971

| SEP. 1971 | FREQUENCY | STATION | TYPE | STARTING TIME UT | TIME OF MAXIMUM UT | DURATION MINUTES | FLUX DENSITY $10^{-22}$ Wm$^{-2}$ Hz$^{-1}$ PEAK | FLUX DENSITY MEAN | INT | REMARKS |
|---|---|---|---|---|---|---|---|---|---|---|
| 1 | 2800 | OTTA | 29 | 1950 | | 40 | 13.8 | 3.9 | | |
| | 7000 | SAOP | 29 | 1953 | | 12 | | | | |
| | 18 | BOUL | 48 | 1958 | 2005 | 11 | | | 3 | |
| | 18 | MCMA | 48 | 1958 | 2004 | 15 | | | 3 | |
| | 1415 | SGMR | 29 | 2000.7 | 2000.7 | 32.7 | 15.4 | 7.7 | | |
| | 606 | SGMR | 29 | 2000 | 2000 | 37 | 14.7 | 7.3 | | |
| | 2695 | SGMR | 29 | 2002.2 | 2002.2 | 27.8U | 13.0 | 5.5 | | |
| | 960 | PENN | 29 | 2010 | 2010 | 110 D | 5.8 | 2.9 | | |
| | 2700 | PENN | 29 | 2012.1 | 2012.1 | 135 D | 9.8 | 4.9 | | |
| | 2695 | BOUL | 40 | 2125.5 | 2127 | 3.5 | 30.0 | | | |
| | 2695 | BOUL | 40 | 2156 | 2156.5 | 5.5 | 108.0 | | | |
| | 184 | BOUL | 42 | 2226 | 2248 | 125 | | | 1 | |
| 2 | 930 | BORD | 40 | 0931 | 0932.2 | 2 | 11.0 | 2.0 | | |
| | 930 | BORD | 45 | 0940 | 0940.8 | 1 | 7.0 | 2.0 | | |
| | 930 | BORD | 3 | 1015 | 1016 | 1 | 11.0 | 1.0 | | |
| | 536 | ONDR | 5 | 1205.5E | 1212 | 6.5 | 60.0 | | | |
| | 808 | ONDR | 1 | 1210 | 1212 | 2.5 | | | | |
| | 930 | BORD | 40 | 1400 | 1401.4 | 2 | 7.0 | 2.0 | | |
| | 184 | BOUL | 42 | 1936 | 2107 | 106 | | | 2 | |
| | 2695 | BOUL | 41 | 2243.5 | 2245.5 | 4.5 | 36.0 | | | |

Magnetic activity is indicated in the following chart. An sc followed by a magnetic storm occurred at 1646 UT on September 4, 1971, reported by 22 stations (ssc: 22[A: 3; B: 13; C: 6]; si: A: 2). Storm data follows:

## PRINCIPAL MAGNETIC STORMS
SEPTEMBER 1971

| DATE 1971 MO DA | STORM TIME UT START | STORM TIME UT END MO DA HR | OBS | GEO-MAG LAT. | SUDDEN COMMENCEMENT TYPE | AMPLITUDES D(') | AMPLITUDES H(γ) | AMPLITUDES Z(γ) | C FIGURE DEGREE OF ACTIVITY | MAXIMAL ACTIVITY ON K-SCALE 0 TO 9 MO DA | 3-HOUR PERIOD | K INDEX | RANGES D (') | RANGES H (γ) | RANGES Z (γ) | STORM NUMBERS |
|---|---|---|---|---|---|---|---|---|---|---|---|---|---|---|---|---|
| 09 04 | 1646 | 09 05 22 | COLL | 64.6N | SC * | + 1 | +16 | - 8 | MS | 09 05 | 4.5.6 | 6 | 101 | 890 | 480 | 37 |
| | 1646 | 09 05 16 | MBOR | 21.3N | SC * | - 0.4* | +36 | - 4 | | 09 04 | 8 | 4 | 3 | 45 | 7 | 37 |
| | 1645 | 09 05 22 | HYDE | 7.6N | SC | - 0.1 | +10 | - 1 | M | 09 04 | 8 | 4 | 6 | 72 | 33 | 37 |
| | 1646 | 09 05 14 | AABA | 5.4N | SC | - 0.3 | +11 | - 3.5 | - | -- -- | - | - | --- | --- | --- | 37 |
| | 1646 | 09 05 21 | HRMN | 33.3S | SC | -- | + 5 | -- | M | 09 04 | 8 | 5 | 14 | 67 | 67 | 37 |

# 2. SOLAR REGION OF SEPTEMBER 1971

Sunspots and H-alpha Plage in McMath Region #11482

by

Patrick S. McIntosh
NOAA Environmental Research Laboratories
Boulder, Colorado 80302

The ground-level cosmic ray event of 1 September 1971 occurred two days after the west-limb passage of McMath Region #11482, and since no active centers crossed east limb for five days following this activity, we must associate the GLE event with this region. This report presents the evolution of the active center as viewed in white light and H-alpha from observations obtained at NOAA-Boulder, Gran Canary Island (NASA/NOAA SPAN), Carnarvon, West Australia (NASA/NOAA SPAN), Culgoora, New South Wales (C.S.I.R.O.), Ramey Air Force Base, Puerto Rico (U.S.A.F. Air Weather Service), and the Sacramento Peak Observatory (Air Force Cambridge Research Laboratories) at Sunspot, New Mexico.

This active center, located at S12 and Carrington longitude 270, was formed on the visible disk during the previous solar rotation as McMath Region #11445. The small group was born on 25 July near the low-latitude terminus of a large quiescent filament and exhibited some growth on 30 July. The region returned to east limb on 17 August as a giant spot group still increasing in area. Maximum area was reached on 21 August at about 1700 millionths of the solar hemisphere. The central meridian aspect of this naked-eye group is presented in Figure 1 below.

It is well known that only a few of the very large sunspot groups are associated with particle-producing solar flares. In looking for some distinguishing characteristic for this region, we are attracted to the conspicuous sunspot motions that were visible during the entire disk passage of the region. This author has noted that unusually large motions of sunspots and sunspot rotation are characteristics that may be peculiar to particle-producing active regions [McIntosh, 1969, 1970]. The regions from which this conclusion was made were also notable for having complex magnetic field configurations, usually with the "delta" configuration of two large spots of opposite polarity enclosed in a common penumbra. We cannot identify such a complex configuration for this active center.

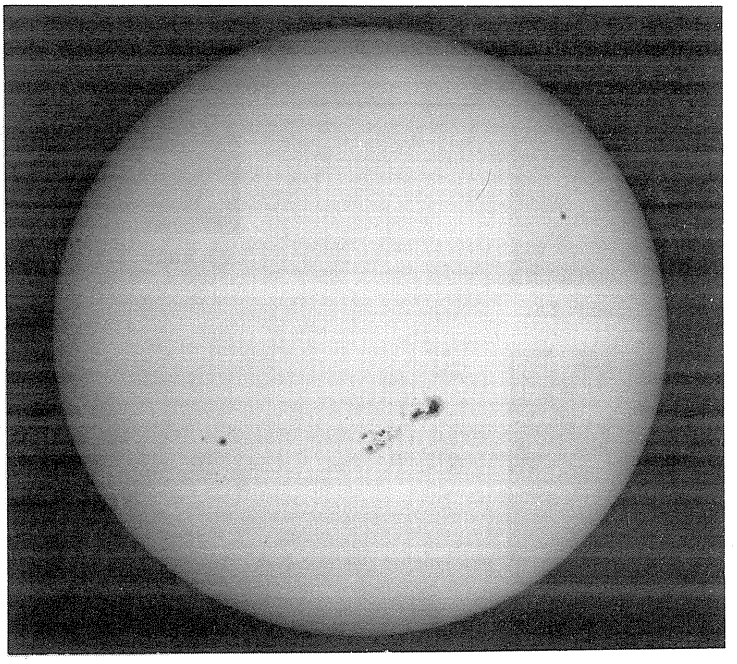

Fig. 1 The white-light patrol photograph from Culgoora, New South Wales (C.S.I.R.O., Australia) for 23 August 1971 at 2246 U.T. with the sunspots of McMath Region #11482 at central meridian. The orientation is geocentric with west to the right.

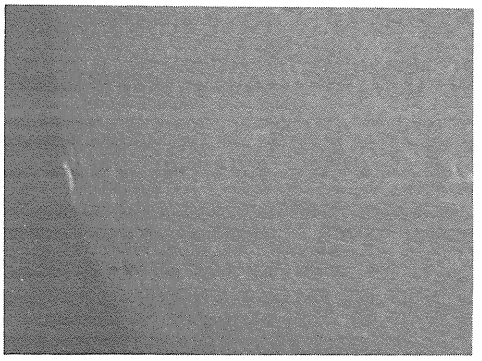

17 Aug. 71 1349 U.T. Ramey AFB

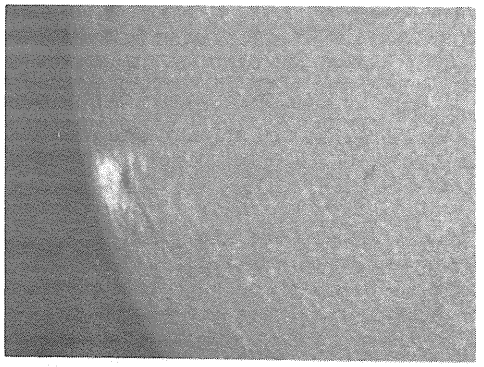

18 Aug. 71 1112 U.T. Ramey AFB

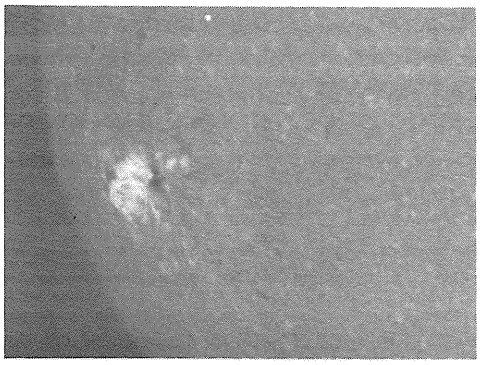

19 Aug. 71 0925 U.T. Canary Is.

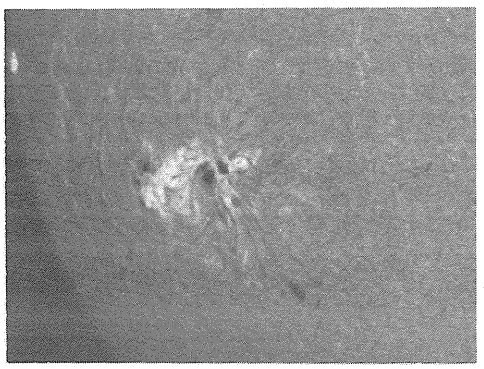

20 Aug. 71 0908 U.T. Canary Is.

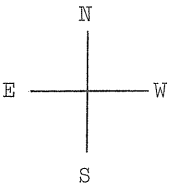


Heliographic

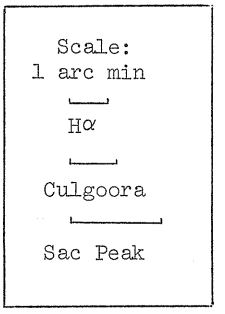


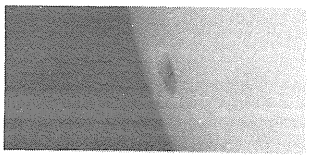

18 Aug. 71 0100 U.T. Culgoora

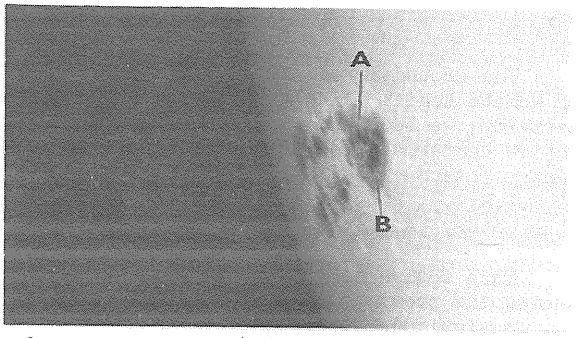


18 Aug. 71 1438 U.T. Sac Peak

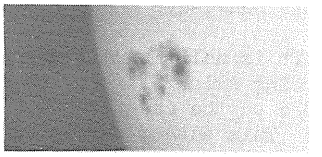

18 Aug. 71 2240 U.T. Culgoora

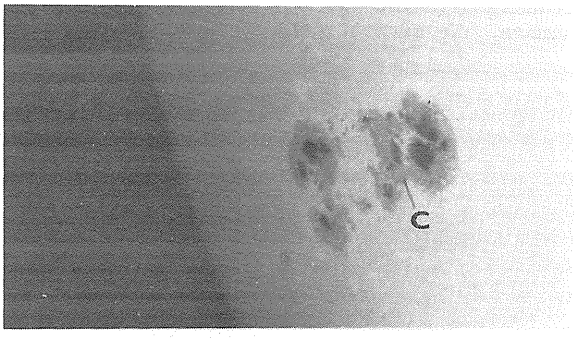


19 Aug. 71 1345 U.T. Sac Peak

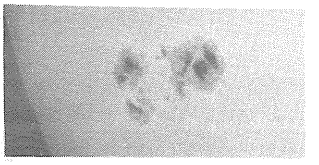

19 Aug. 71 2400 U.T. Culgoora

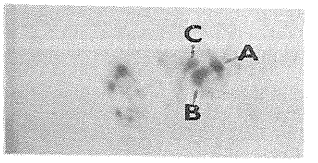


20 Aug. 71 0909 U.T. Canary Is.(Hα+1Å)

Fig. 2 H-alpha (left) and white light (right) patrol photographs for 17-20 August 1971 showing an expanding fibril field and sunspot rotation, respectively.

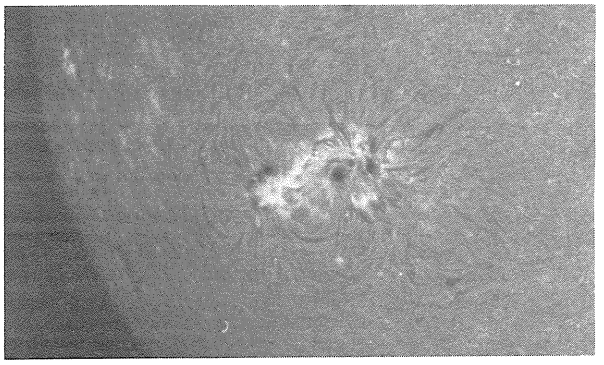

21 Aug. 71 0821 U.T. Canary Is.

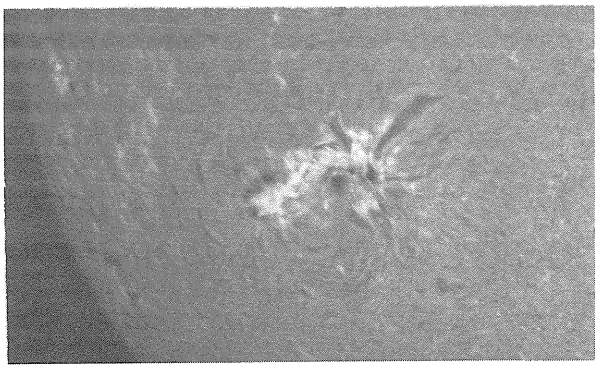

21 Aug. 71 1050 U.T. Ramey AFB

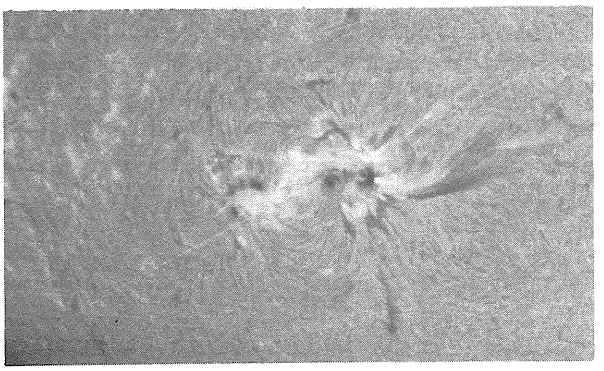

22 Aug. 71 0835 U.T. Canary Is.

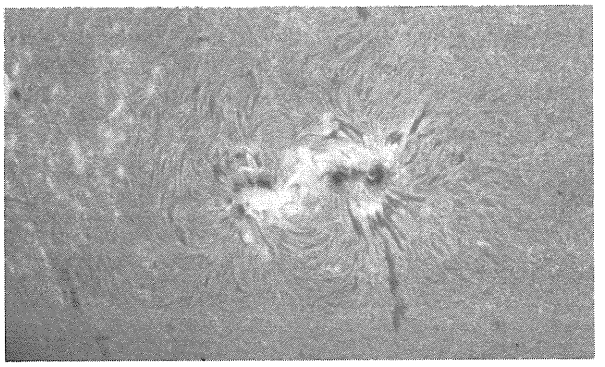

22 Aug. 71 1127 U.T. Ramey AFB

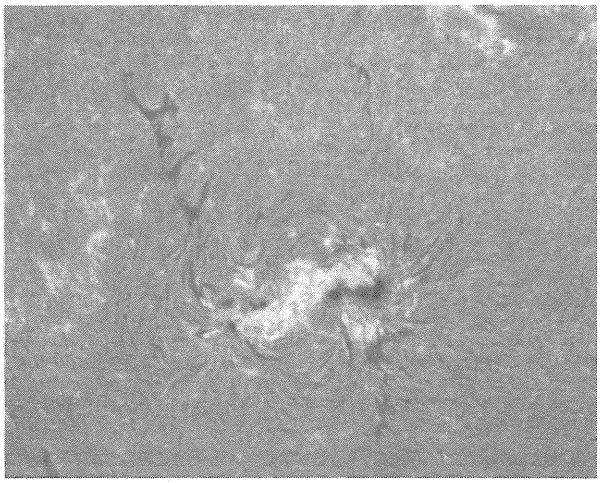

23 Aug. 71 1059 U.T. Ramey AFB

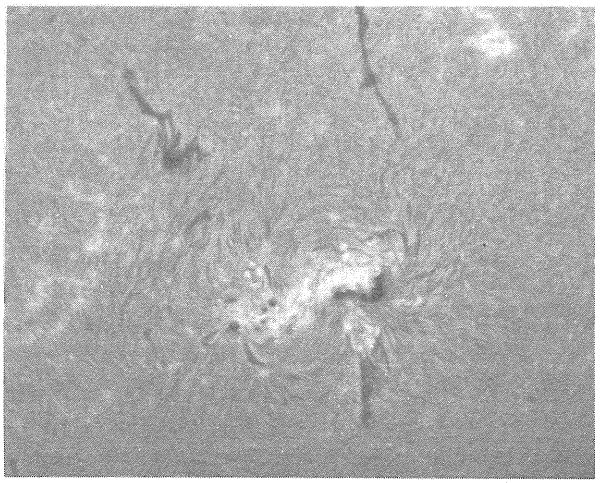

24 Aug. 71 1519 U.T. Ramey AFB

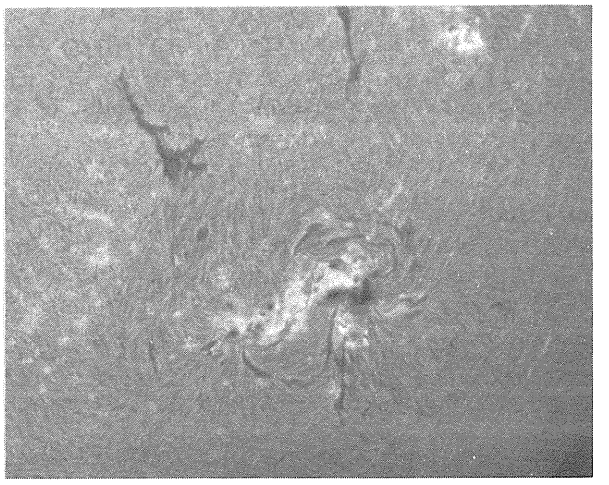

25 Aug. 71 1133 U.T. Ramey AFB

Fig. 3 Dark surge activity (left) and active filaments (right) were associated with the region in H-alpha observations.


20 Aug. 71 1600 U.T. Boulder

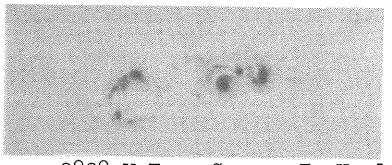

21 Aug. 71 0828 U.T. Canary Is. H$\alpha$+1Å

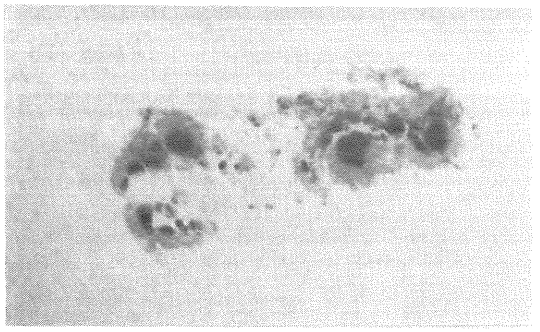

21 Aug. 71 1355 U.T. Sac Peak

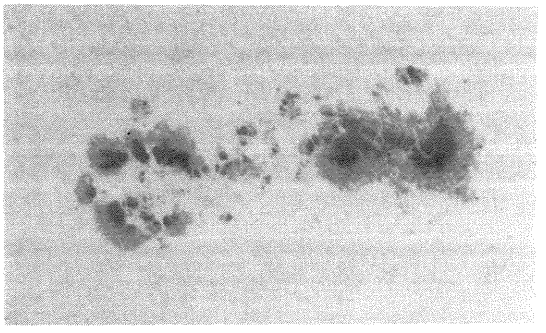

22 Aug. 71 1320 U.T. Sac Peak

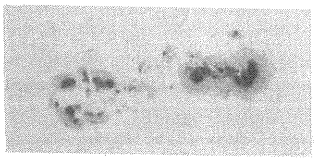

22 Aug. 71 2245 U.T. Culgoora

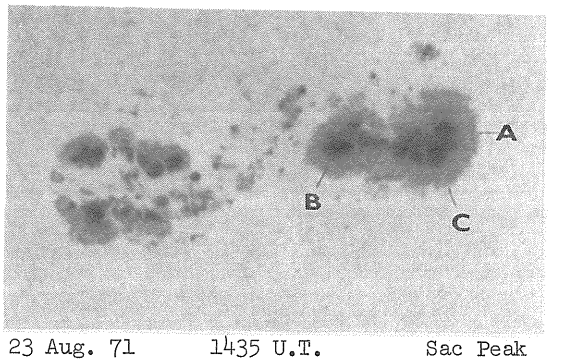


23 Aug. 71 1435 U.T. Sac Peak

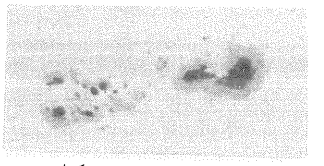

23 Aug. 71 2246 U.T. Culgoora

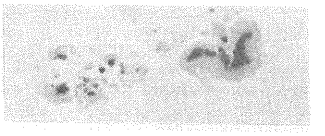

24 Aug. 71 2335 U.T. Culgoora

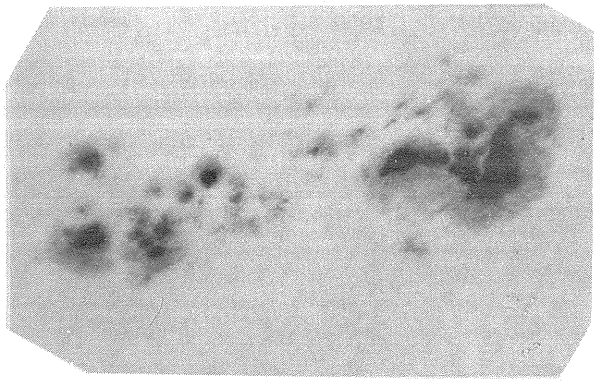

25 Aug. 71 0730 U.T. W. M. Baxter

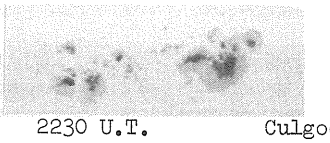

25 Aug. 71 2230 U.T. Culgoora

Fig. 4 Sunspot evolution during 20-25 August 1971 was highlighted by the movement of spot C over the same path covered by spot A during the previous two days. Spot C penetrates spot A on 22 August, becoming surrounded by photospheric and chromospheric bright material (see also Fig. 3). After this collision a portion of spot A is ejected from the leader penumbra, becoming detached by the end of the 25th.

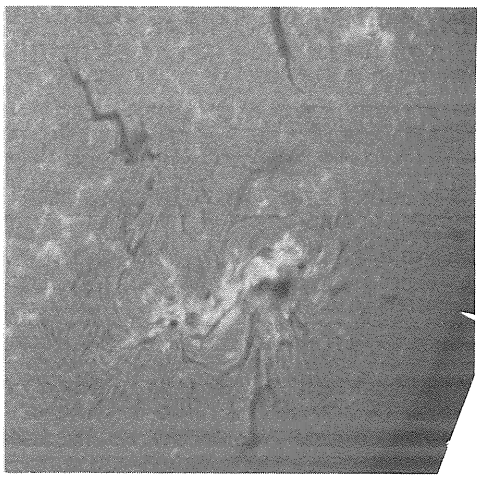

26 Aug. 71 1116 U.T. Ramey AFB

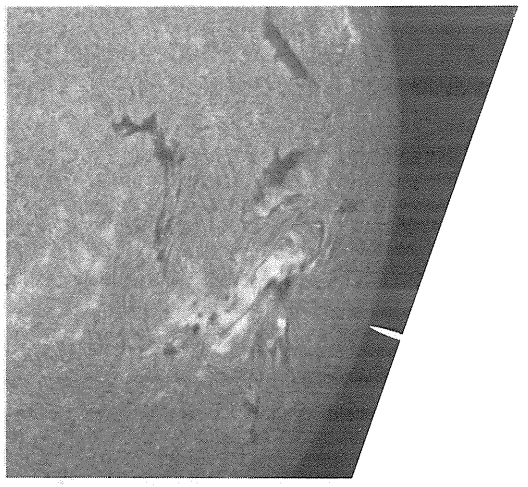

27 Aug. 71 1115 U.T. Ramey AFB

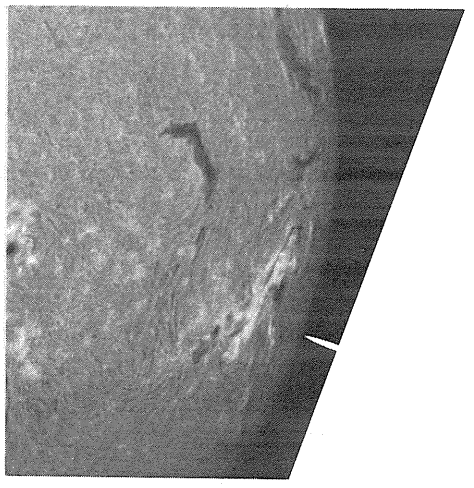

28 Aug. 71 1111 U.T. Ramey AFB

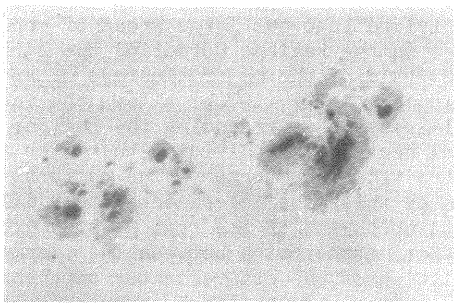

26 Aug. 71 1345 U.T. Sac Peak

27 Aug. 71 1435 U.T. Sac Peak

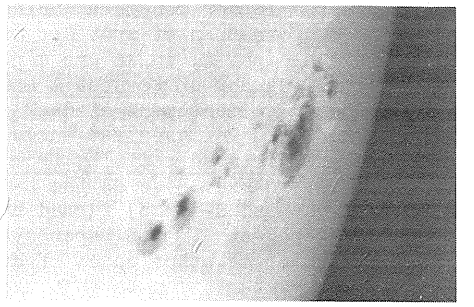

28 Aug. 71 1600 U.T. Sac Peak

Fig. 5 H-alpha (left) and white light (above) observations as the region approached the west limb. The scales are the same as in Fig. 2. The only notable activity during this interval seemed to be increased filament activity north of the main spot, both within the plage and further north near, and north of, the solar equator. The spots were decreasing steadily in area.

The magnetic field distribution in an active region can be studied either as part of the large-scale magnetic field patterns over much of the visible sun, or in a restricted view of just the internal parts of the active region. The latter view was presented for McMath Region #11482 by Livingston [1972, Fig. 4]. This high resolution subtraction magnetogram gives the impression that the region was basically divided into two large areas of opposite magnetic polarity, but with considerable mixing of polarities in the regions bordering the large leader spot and in the vicinity of the longitudinal neutral line dividing the major clusters of spots. The interpretation of H-alpha structures as magnetic fields, [McIntosh, 1972a, 1972b] allows the integration of this close-up view with the large-scale magnetic field patterns surrounding the region. The plage corridor within the bright plage mapped the longitudinal neutral line dividing the major spots, coinciding with the general polarity division seen on the subtraction magnetogram. The patterns of fibrils immediately outside the plage permits the continuation of this line to connect with a filament channel to the east of the region and to connect with filaments northwest of the region, even crossing the solar equator. These connections reveal a large-scale physical association between the flaring region and filament activity viewed in Figs. 3 and 5. The evolution of the active center apparently affected large-scale "quiet" solar features, or both the active center and the large-scale chromospheric patterns were responding to a common evolutionary force. The sunspot motions in this region suggest that the common evolutionary force was mass motions in the photosphere.

The sequence of sunspot photographs in Fig. 2 shows considerable sunspot movements even early in the disk passage of the region. A line connecting spots A and B rotated clockwise through nearly 90 degrees during the 48 hours from 18 August to 20 August. Careful measurement of the absolute heliographic coordinates of these spots revealed that both A and B were in motion, spot A moving west and spot B moving east, during the early part of this interval. Spot B came to rest early on the 20th, but spot A continued its westward motion and moved slightly south in latitude. This motion continued during the 21st and 22nd, as seen in Fig. 4, placing spots A and B at equal latitude at opposite ends of a large penumbra for the remainder of the disk passage. The motion of spot A can be considered as an arc with the center of radius approximately located in spot B, as if spot B were the center of a vortex of Coriolis-type mass motion in the photospheric gases. The direction of motion, clockwise as viewed in "sky" directions, agrees with southern hemisphere atmospheric motions in a planetary atmosphere. The observation of vortical motions of opposite senses in opposite hemispheres has been reported for solar structures by Hale [1927], Richardson [1941], Sakurai [1967], and McIntosh [1969, 1970, 1972c].

The sunspot photographs of Fig. 2 also show the movement of a sunspot from the follower cluster of spots toward the leader penumbra during 18-19 August. This spot became attached to the leader penumbra at the time of formation of spot C. Spot C then moved during 19-22 August over almost the identical path followed by spot A, in an arc centered on spot B. On 22 August, a very significant event took place as spot C caught up to spot A and penetrated through spot A! As spot C approached spot A there was a pronounced commencement of dark surge activity surrounding the western perimeter of the leader penumbra (Fig. 3). The greatest surge activity occurred during the 22nd, as spot C moved into spot A. The surges were directed radially from the point of contact between the merging spots (see photograph at 22/0835 U.T. in Fig. 3). As the two spots came into contact, a bright ring of material (visible in both white light and H-alpha) formed around spot C. This ring is easily seen in Figs. 3 and 4 and in the sunspot photograph in the paper by Bumba and Sykora elsewhere in this compilation. This observer has noted a number of other cases of bright rings surrounding spots that were in the process of coalescing. It is important to note that these cases of coalescence, including our region of interest here, involved spots of the same magnetic polarity.

The proper motion velocities of spots A and C, measured with respect to Carrington coordinates, were 0.20 km/sec and 0.35 km/sec, respectively, during the period 19-21 August. The southern hemisphere proton-flare region of October 30, 1968 also contained a spot moving in an arc about a larger spot, both of leader polarity (like our case here). The measured proper motion velocity in that case was 0.12-0.20 km/sec [McIntosh, 1970].

On the 23rd of August, spot C had fully penetrated spot A, apparently splitting A into two parts. Late on the 24th, the northern portion of spot A formed a satellite umbra which separated and detached from the leader penumbra by the end of the 25th (Fig. 4). This satellite spot appears related to the development of complex absorption features north of the leader during the days just prior to west-limb passage.

The spots in the following portion of the region formed a configuration of a ring. The motions among these spots had a pattern of movement south (to higher latitude) then westward along the lower border of the ring. The movements of spots in leader and follower together depicted a continuous line of movement in the shape of the letter "S" from latitudes above the follower to latitudes between the leader and the solar equator. The line of motion paralleled the longitudinal neutral line. The spot motions then suggest the transport of momentum from higher latitudes to lower latitudes, in agreement with the mass motions required by recent dynamo theories of the solar cycle.

The most rapid sunspot motions occurred close to the time of greatest sunspot growth (early in the disk passage) and also during the time of most frequent flare activity detected from the earth. The reasons for the occurrence of a great event two days past west-limb passage are not obvious. Close

study of the H-alpha photographs provided some clues. The motions of the spots were paralleled with a gradual alteration of the shape of the line of polarity reversal inferred from the H-alpha structures. The curvature of the S-shaped line became more pronounced as the region approached west limb, as if the mass motions deduced from the spot motions resulted in the transport of follower-polarity magnetic fields to a position between the leader and the solar equator. An accumulation of follower magnetic field strength might be inferred by the increase in plage brightness and the appearance of filaments north of the leader spot just prior to west-limb passage (Fig. 5). If this trend is extrapolated there may have formed sufficient field strength by the time of the proton flare to create a configuration like the "delta" configuration. Our extrapolation would give an increasing gradient in the longitudinal magnetic field across a neutral line that was oriented east-west. Such a configuration is especially common in proton-flare regions.

Another subtle evolution in H-alpha structures may be part of the explanation for the proton flare. The inferred longitudinal neutral line in the center of the region was positioned midway between leader and follower spots for most of the disk passage. Beginning about four days before west-limb passage, the position of this line began to shift westward toward the leader spots, implying an increase in magnetic field gradient. Foreshortening of our view of the region interfered with careful measurements during the last two days before west-limb passage, so an extrapolation to the time of the flare is not reliable. Perhaps the magnetic field gradient increased throughout the longitudinal neutral line positioned over a 90-degree arc north and east of the leader spot, and thereby increased the potential for a proton flare.

The return of the region on 13 September as McMath Region #11516 showed a bright plage with a relatively small, but complex, sunspot group. The configuration of the inferred longitudinal neutral line was almost identical to the configuration inferred just prior to west-limb passage two weeks earlier, with a six-degree westward shift in Carrington longitude. The neutral line was still S-shaped, with an east-west oriented section directly north of the old leader spot. The plage on the north side of the returning leader sunspot was brighter than when the region was last seen two weeks earlier, and a narrow plage corridor extended east-west through this plage. This tends to confirm the speculation above that magnetic field strengths may have increased in the vicinity of the leader just beyond the west limb, with a resulting increase in magnetic field gradient across a longitudinal neutral line.

In summary, we are missing the most important observations pertinent to explaining the occurrence of the proton flare of 1 September 1971 because the region was out of view for two days before the event. The evolution of the sunspots and H-alpha structures suggest that large-scale photospheric mass motions in this region may have led to the formation of a magnetic field configuration favorable for the generation of the proton flare. The extrapolation of these observations to the time of the flare, and therefore our conclusions, must remain speculative.

Acknowledgements

We are grateful for the loan of observational material from several observatories, making it possible to monitor active center evolution in greater detail than in most previous studies. Special thanks are given to the late W. M. Baxter, Director of the Solar Section of the British Astronomical Association until his untimely death. Mr. Baxter volunteered his sunspot photograph published here, one of the last to be taken before his death. The white light patrol films from the Sacramento Peak Observatory (Air Force Cambridge Research Labs) were provided by L. Gilliam and copied into large-scale internegatives [McIntosh, 1972d]. Other observations are the courtesy of Capt. J. Smith (USAF) at the solar observatory at Ramey Air Force Base, Puerto Rico, J. Hirman at the NASA/NOAA S.P.A.N. observatory on Gran Canary Island (Spain), R. Giovanelli of the C.S.I.R.O. Culgoora Solar Observatory, and the several observers at the NOAA observatory in Boulder, Colorado.

The study was performed under NASA Contract G.O. #H-42710A for the purpose of flare forecasting technique development.

## REFERENCES


HALE, G. E. 1927 The Fields of Force in the Atmosphere of the Sun, Nature, 119, 708.

LIVINGSTON, W. C. 1972 Measuring Solar Photospheric Magnetic Fields, Sky and Telesc., 43, 344-349.

McINTOSH, P. S. 1969 Sunspots Associated with the Proton Flare of 23 May 1967, World Data Center A, Upper Atmosphere Geophysics Report UAG-5, 14-19, February 1969.

McINTOSH, P. S. 1970a Sunspots Associated with the Proton Flares of Late October 1968, World Data Center A, Upper Atmosphere Geophysics Report UAG-8, 22-29, March 1970.

McINTOSH, P. S. 1972a Solar Magnetic Fields Derived from Hydrogen-alpha Filtergrams, Topical Review in Reviews of Geophysics and Space Physics, 11,

McINTOSH, P. S. 1972b Inference of Solar Magnetic Polarities from H-alpha Observations, in Solar Activity Observations and Predictions, edited by P. S. McIntosh and M. Dryer, Volume 30 of Progress in Astronautics and Aeronautics series, Martin Summerfield, series editor, MIT Press, pp. 65-92.

McINTOSH, P. S. 1972c Sunspots and H-alpha Plage Associated with the GLE Event of 24 January 1971, this compilation.

RICHARDSON, R. S. 1941 The Nature of Solar Hydrogen Vortices, Astrophys. J., 93, 24.

SAKURAI, K. 1967 Solar Cosmic Ray Flares and Related Sunspot Magnetic Fields, Report of Ionos. and Space Res. in Japan 21, 113-124.

# Large-Scale Magnetic Field and Activity Distribution Connected with the Proton-Flare of September 1, 1971 Region

by

V. Bumba
Astronomical Institute
of
The Czechoslovak Academy of Sciences, Ondrejov

and

J. Sýkora
Astronomical Institute
of
The Slovak Academy of Sciences, Skalnaté Pleso

## 1. Introduction

The relation of particle-emitting flares to a characteristic large-scale configuration of solar magnetic fields has been described in the previous paper concerning the proton-flare of January 24, 1971 [Bumba, Sýkora, present compilations] as well as in some other papers [Bumba, 1971 a, b; Bumba et al., 1972]. We demonstrate in this short note that the studied proton-flare from September 1, 1971 developed in a similar large-scale magnetic and activity situation. The same kinds of observational data as in the previous paper are used. These include the Mt. Wilson daily magnetic maps, Fraunhofer Institute, Freiburg, daily activity "Maps of the Sun", "Daily Geomagnetic Character Figures" from the Institut für Geophysik, Göttingen and the "Magnetic Field of Sunspots" published by the Pulkovo Observatory of the U. S. S. R. Academy of Sciences.

## 2. Development of the Large-scale Situation in which the Studied Proton-flare Took Place

It is noted that the proton-flare from September 1, 1971 occurred in the same magnetic stream as the proton-flare of January 24, 1971 (in the Carrington network tilted by the 27 day rotation, therefore, with a difference of about 40° to the West in heliographic longitude). The only difference is that this time it developed in the southern hemisphere while the first one took place in the northern solar hemisphere. The large-scale situation in more detail is shown in Figure 1 which represents the series of consecutively mounted synoptic charts (with two consecutive maps overlapped for integration). These describe separately the negative and positive polarity magnetic fields, geomagnetic activity (with four days shift) and calcium plages, filaments and sunspot group activity. Although it is more difficult to find in these magnetic synoptic charts the characteristic large-scale patterns of the supergiant drop-shaped body with which the proton-flare regions are correlated, the skilled observer may agree that at least some indications of this characteristic feature may be found in the negative polarity distribution having its head again about 90° to the West. Again the faster redistribution of the negative polarity fields in comparison with the relatively more stable (or still more pronounced) positive polarity fields following the proton-flare occurrence are seen.

The development of photospheric and chromospheric activity which precedes and follows the appearance of the proton-flare region is also shown.

The enhanced periods of the geomagnetic activity correlate this time in the upper left corner (western half of the Figure 1d) and in the middle lower part with the negative polarity fields. The recurrent geomagnetic events in the western half of the Figure 1d form the prolongation of the recurrent geomagnetically enhanced intervals connected with the older negative polarity magnetic fields which are westward of the proton-flare of January 24, 1971. In the lower right hand corner (eastern part of the Figure 1d) the recurrent enhanced geomagnetic activity correlates with the magnetic stream of positive polarity as in preceding years of activity.

## 3. Development of the Proton-flare Region

From Figure 1c we see that one rotation before the proton-flare region developed, a small β type group is observed in its central meridian passage. From the form of calcium plage one rotation after the proton-flare, we judge that the plage represents the remains of at least two active regions (or spot groups), the new one being east of the original group.

Studying the development of the huge sunspot group in which the flare took place we notice its fast growth just after it appears from behind the eastern limb. This growth proceeds from the central part of the group (from the close-vicinity of the dividing line between the field polarities), but this process reaches its maximum sometime around August 23, 1971 (see Figure 2 representing the photographs of this group on August 22, 1971) and then the area as well as the activity of the group diminishes very fast as the group approaches to the western solar limb.

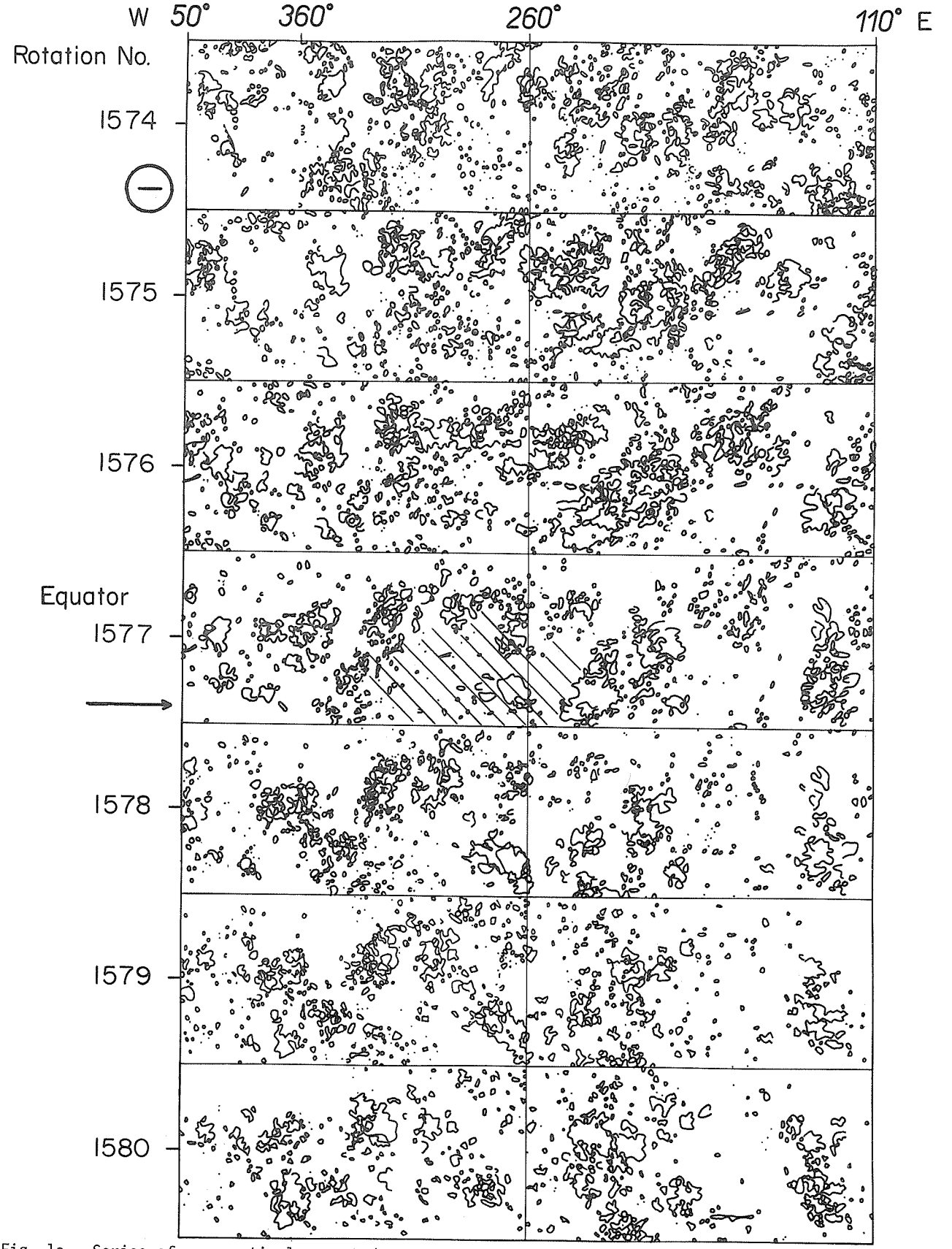


Fig. 1a. Series of consecutively mounted magnetic synoptic charts (within the heliographic latitudes ± 40°) of negative polarity for rotations Nos. 1574-1581. For integration two consecutive maps, one of which is repeated are overlapped. The rotation with the proton-flare which occurred close to the indicated heliographic longitude 260° (south from the equator) is shown by an arrow.

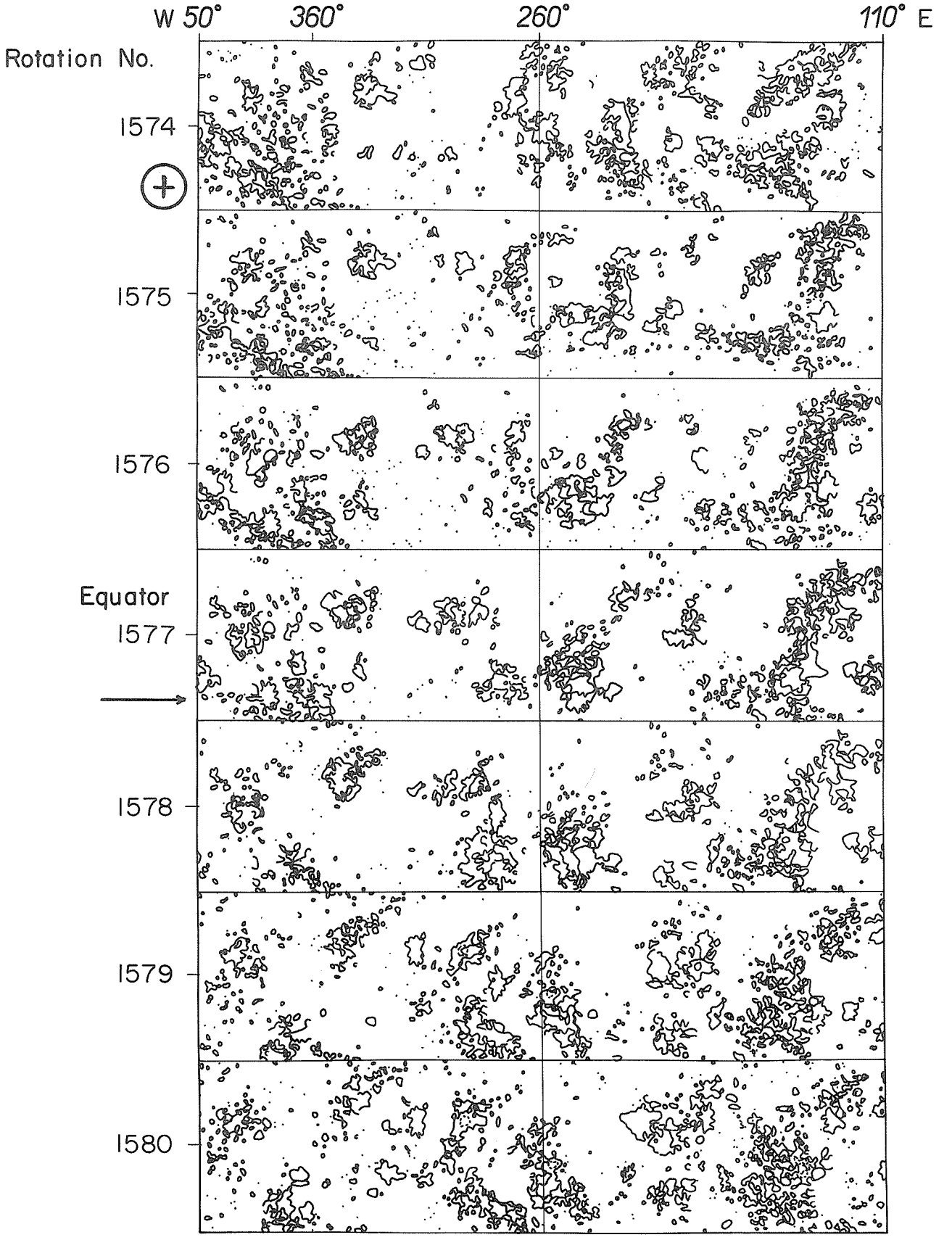


Fig. 1b. The same series of consecutively mounted magnetic synoptic charts for positive polarity fields as in Figure 1a.

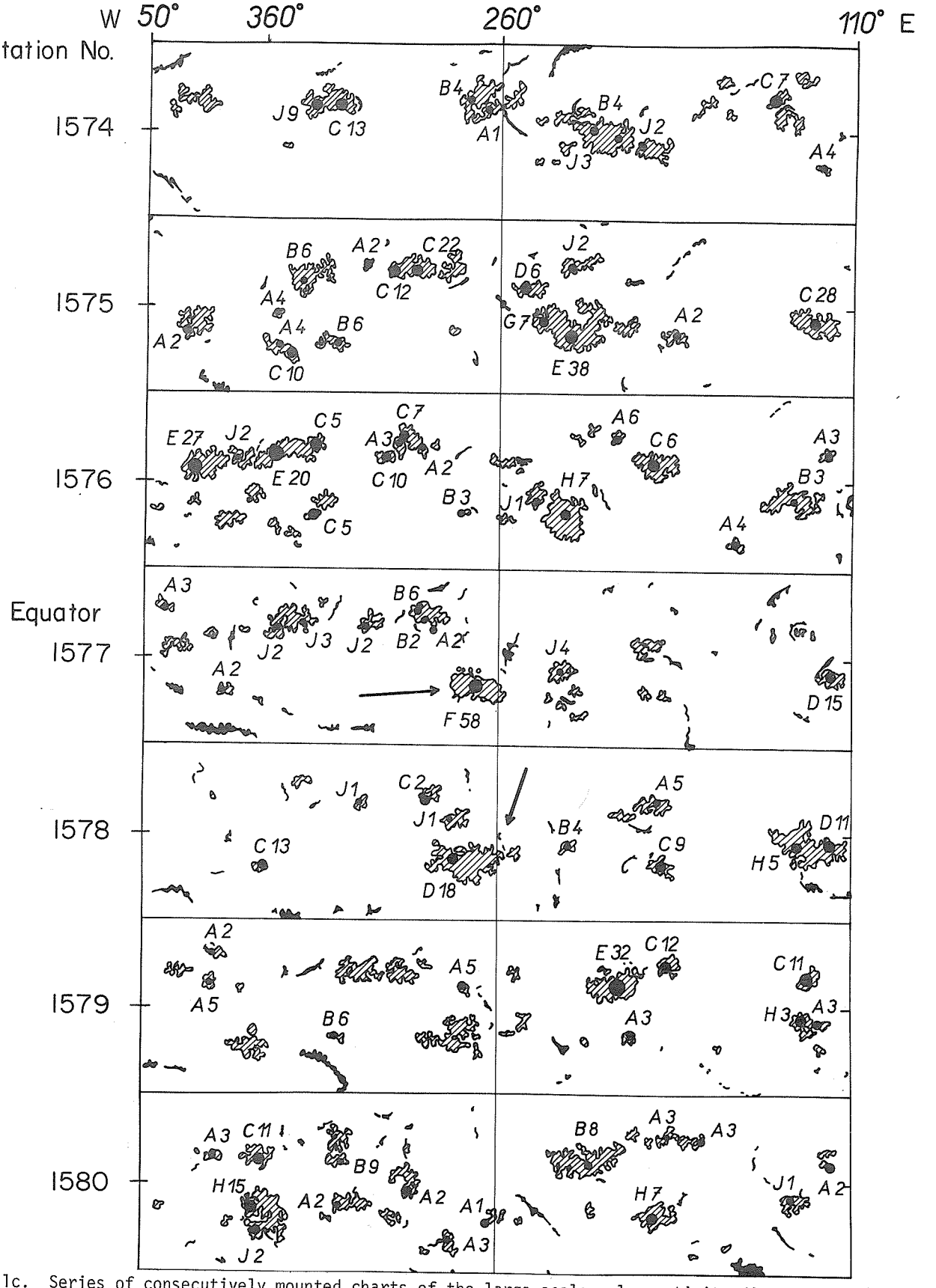


Fig. 1c. Series of consecutively mounted charts of the large-scale solar activity distribution (Fraunhofer Institute, Freiburg) without the overlapping of maps for rotations Nos. 1575-1581. The studied active region F 58 as well as the calcium plage remains of the probable newly developed group in the following rotation are indicated by an arrow.

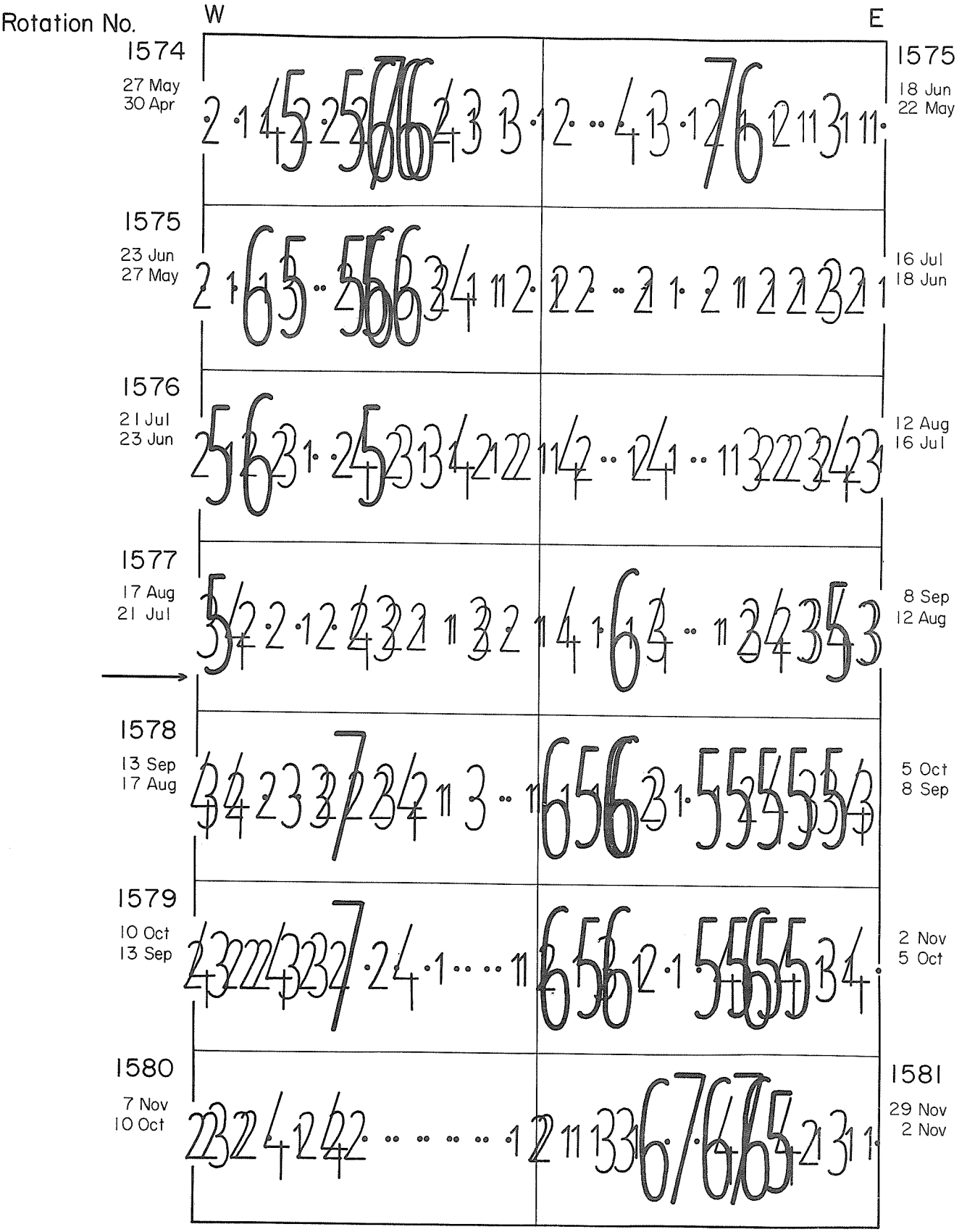


Fig. 1d. Series of consecutively mounted charts of geomagnetic activity distribution (Institut fUr Geophysik, Göttingen) for the same time interval with the same overlapping of charts. The four days, needed by the particles to arrive at the Earth, are taken into account.

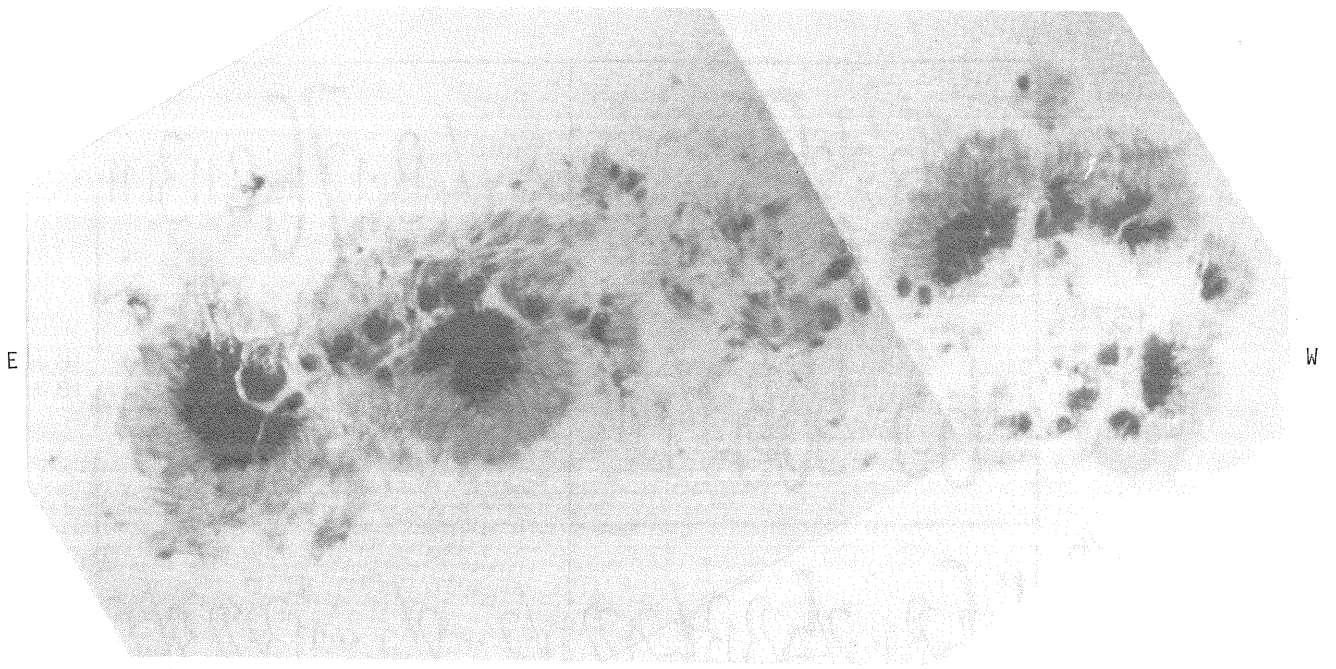


Fig. 2. Photograph of the studied sunspot group from August 22, 1971 obtained at the Astronomical Institute of the Slovak Academy of Sciences, Skalnaté Pleso with the objective lens having the diameter of 16 cm and focal length 304 cm. West is to the right, North to the top of the Figure. The exposure time of the right hand part: $5^h36^m57^s$ UT; of the left hand part: $6^h37^m50^s$ UT.

From all that has been said it is very difficult to make some conclusions about what happened during the two days the region was behind the limb. Probably new activity developed (see the form of the plage the next rotation) in the closest neighborhood of the described group, although no sign of such renewal of activity is seen in the photosphere or in the chromosphere before the group disappears behind the limb.

## 4. Coronal Situation Above the Proton-flare Region

Again not enough observational material exists for construction of synoptic charts demonstrating the green corona large-scale distribution. In Figure 3 the coronal situation development as was observed above the proton-flare region is shown. We see in the corona the enhanced level of green ($\lambda$5303 Å) emission during the western limb passage of the studied longitudinal interval in the preceding rotation, where the photospheric activity was very low, which signals the future development of larger activity. On the eastern and still more on the western limb during the main rotation with the large developed sunspot group the level of green coronal emission is very high. It seems even higher at the beginning of the rotation following the proton-flare occurrence, although the whole figure is not drawn because of the lack of observational data. But later a fast decrease of emission is observed.

## REFERENCES


BUMBA, V. and J. SÝKORA, 1972: Development of the Large-Scale Situation in which the Proton-Flare of January 24, 1971 Took Place, present compilation, p. 43.

BUMBA, V., 1971 a: Large-Scale Negative Polarity Magnetic Fields on the Sun and Particle-Emitting Flares, Submitted to the Proceedings of the Solar Wind Conference, Asilomar, Pacific Grove, California, March 21-26, 1971.

BUMBA, V., 1971 b: Large-Scale Regularities in Solar Magnetic Field Distribution and Occurrence of Large Flares, Submitted to the Proceedings of the 6th Regional Consultation on Solar Physics, Gyula, Hungary, September 6-11, 1971.

BUMBA, V., L. KRIVSKÝ and J. SÝKORA, 1972: Development and Spatial Structure of Proton-Flares near the Limb and Coronal Phenomena. IV Proton-flare from Nov. 2, 1969 and its Active Region, Bull. Astr. Inst. Czech., 23, 85.

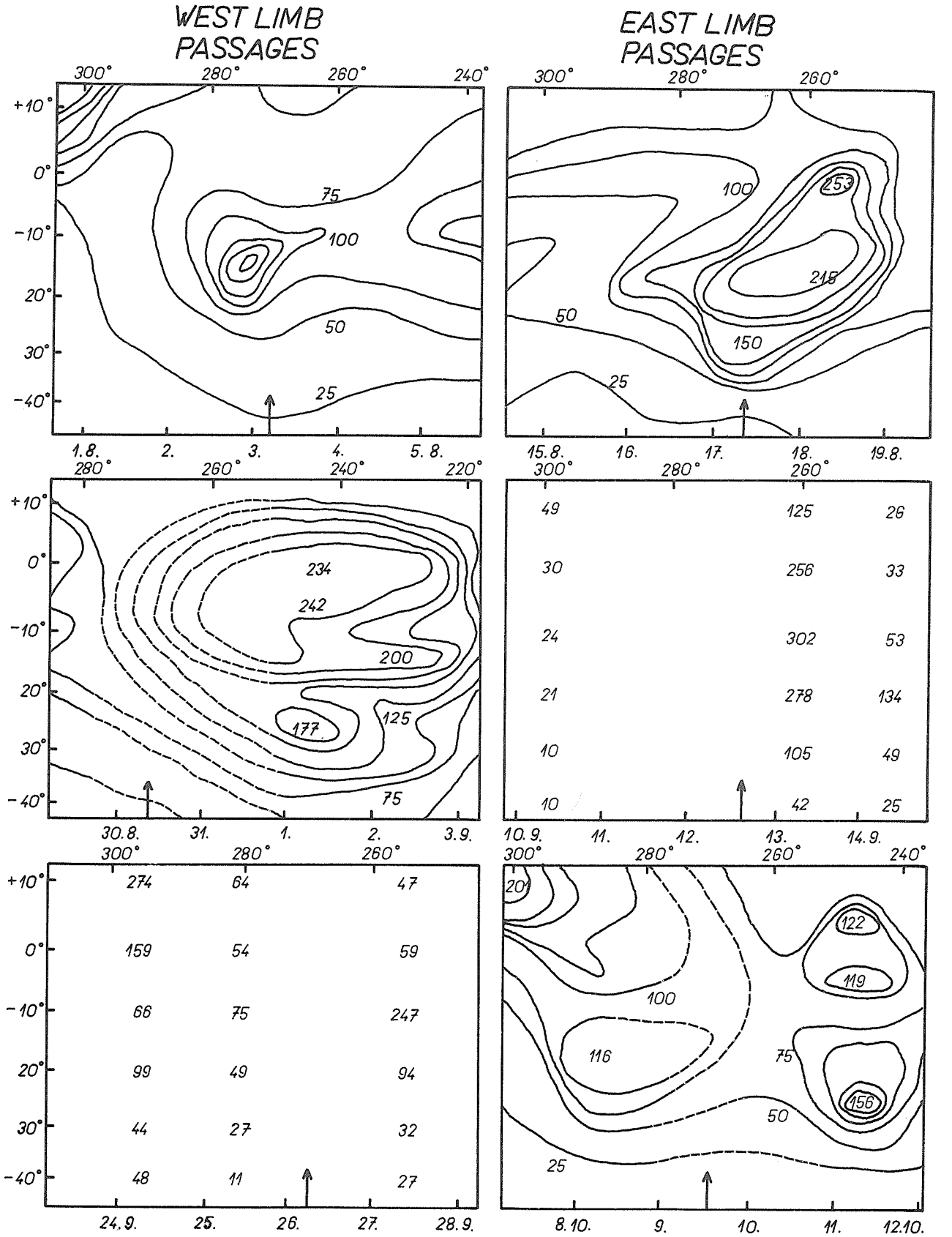


Fig. 3. Coronal situation above the proton-flare region for the preceding, main and the following rotations. Lines of equal mean intensity or the values of the intensity of the green (λ5303 Å) coronal emission in absolute coronal units are shown. Heliographic coordinates are indicated. Also the passages of the region on the eastern and western limb are shown by the data and the arrows.

# 3. SOLAR RADIO EVENTS

## Early Development of Radio Emission from MMH 11482

by

D. S. Lund
NOAA Environmental Research Laboratories
Boulder, Colorado 80302

### Introduction

In a previous volume in this series, we reported on our efforts to apply synchrotron emission theory to flare-associated radio spectra [Lund, 1970]. Our interest was in rapid diagnosis of physical conditions within the flare region which would be premonitory of energetic particle arrival in the near-earth environment. Since that time, we have been studying the radio spectra of active centers, as observed well before major flare activity, and we will now apply some of our results to the observations of McMath-Hulbert Region Number 11482. Although a thorough explanation of active-center emission requires discussion of the radiative transfer equation, with a source function that includes gyroemission and gyroabsorption, we will defer such discussion and will here comment on a number of aspects which do not require such rigorous derivation.

Microwave observations of active center emission may be of several types: the spectrum may be inferred from whole-sun measurements, or the spectrum may be derived from observations which seek to isolate the individual center of activity. In this note, we shall confine our attention to the latter class. Further the spectrum may be described in terms of its polarization. Observations at Pulkovo [Gel'freikh and Peterova, 1970] indicate that bipolar regions often display a circular polarization excess which maximizes near the limbs, and is nearly zero close to the central meridian (CM), with sense inverting near CM passage. Unipolar regions show a simple maximum near CM passage. Unfortunately, this type of data was not available to us during the research we are reporting. Thus we must discuss the spectrum of one linearly polarized component, and see what (if anything) can be deduced about development of either the coronal extension of the active region, or the chromosphere-to-corona interface, during the period before the flare of September 1, 1971.

### Discussion of Observations

In Figure 1, we show a schematic spectrum of the radio emission from an active center, representing the spectral flux density in one polarized component, integrated (spatially) over the entire active center, and viewed close to the central meridian. At the longer wavelengths (10 to 50 centimeters) the spectral flux density varies as $\lambda^{-2}$, and corresponds to a brightness temperature of one or two million degrees. In this portion of the spectrum (marked A in the Figure), the corona is optically thick, and the emission at the several observed wavelengths is born in a thin shell; thin enough that thermal

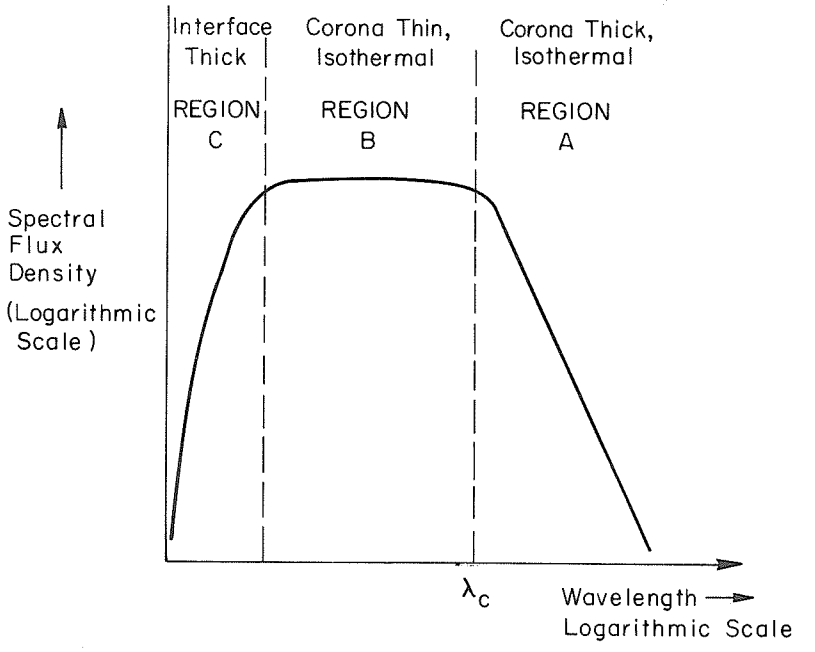


Fig. 1 Idealized Spectrum of an Active Center

gradients in the corona are unimportant. By this we mean that the kinetic temperature is nearly the same for small and large optical depths. In Region B, the corona is optically thin, comparatively speaking, but still isothermal in the sense defined above. Despite the coronal transparency, the coronal temperature is sufficiently high as to provide most of the flux. If the electron density and temperature were constant, then the flux would be independent of wavelength, and Figure 1 would be flat. We have sketched it in this way on the basis of Drago's [1970] observations, although the evidence we will show doesn't support such interpretation. At the shortest wavelengths, in Region C, the interface between corona and chromosphere is opaque, while the corona itself is quite transparent. The shorter the wavelength, the deeper within the active region is the origin of the radiation. Deeper portions are cooler, hence the source function decreases at the shorter wavelengths in this oversimplified view.

Two further observational facts are needed later: the first that the spectral flux density, as observed at a fixed frequency in active centers that are not changing rapidly, seems to follow a cosinusoidal dependency on apparent longitude [Christiansen et al., 1957; Gutmann and Steinberg, 1957; Khangil'din, 1964, present the evidence at various wavelengths]. This result appears valid over the wavelength range 0.8 to 20 centimeters, and offers a crude way of distinguishing spatial and temporal variations. The absence of wavelength dependence in this experimental result leads us to expect that the entire spectrum should increase and decrease in magnitude, but not be deformed (i.e. change slope), as the region is carried across the visible disk by solar rotation. The second empirical result we shall need relates to the 'size' of active centers. Neglecting for the moment the question of structure within the active center [the 'core and halo' of Kundu, 1959; the aureole structure of Khangil'din, op. cit.], it appears from eclipse observations [Straka, 1970; Drago, op.cit.] that the angular extent of the emission region is less than the beamwidth of the antennas in use at the Fleurs, Stanford and Prospect Hill observatories. For this reason we shall treat the emission region as if it were an unresolved source.

In the context of the previous paragraphs, we can now examine the observational evidence contained in the spectroheliograms published in "Solar-Geophysical Data." Pertinent maps at wavelengths 0.8, 9.1 and 21 centimeters have been drawn from this source during the visibility of MMH 11482 on the disk. We have supplemented these data with our own observations at 3.2 centimeters. During the period 17-31 August, 1971, observations were obtained with a prototype polarimeter installed at prime focus of a sixty-foot-diameter antenna. During that time, only linearly-polarized components were observed, thus making our results comparable with those from the other observatories. In Table I, we list the solid angle to half beamwidth ($\Omega_A$) of the several observatories, together with the factors $\frac{2k\Omega_A}{\lambda^2}$, which when applied to the reported temperatures represent the conversion factors to flux. We note in passing that a relatively poor antenna pattern in our own measurements has been compensated for by integrating the antenna pattern and deriving a Gaussian function of equivalent area.

Table 1.

| | $\Omega_A$ | $\frac{2k\Omega_A}{\lambda^2}$ |
|---|---|---|
| Fleurs | $(1.27 \times 10^{-6})^{*}$ | $7.96 \times 10^{-28}$ |
| Stanford | $(8.95 \times 10^{-7})^{*}$ | $2.97 \times 10^{-27}$ |
| Boulder | $(1.77 \times 10^{-5})^{**}$ | $4.89 \times 10^{-25}$ |
| Prospect Hill | $1.49 \times 10^{-6}$ | $5.02 \times 10^{-25}$ |
| | Steradians | Watts Meter$^{-2}$ Hertz$^{-1}$ Degree$^{-1}$ |

*Adjusted for beamwidth in $\delta$ coordinate

**Equivalent Gaussian FWHM

In Figures 2, 3 and 4 the daily spectra are shown for the entire passage of the active center across the visible disk. Comparing these Figures with earlier published results [Christiansen et al., 1960; Kakinuma and Swarup, 1962; Swarup et al., 1963; Tsuchiya and Takahashi, 1968; Straka, op. cit.; Drago, op. cit.] we find general agreement with the earlier results. However, our results are the first showing the effects of rotation and region development.

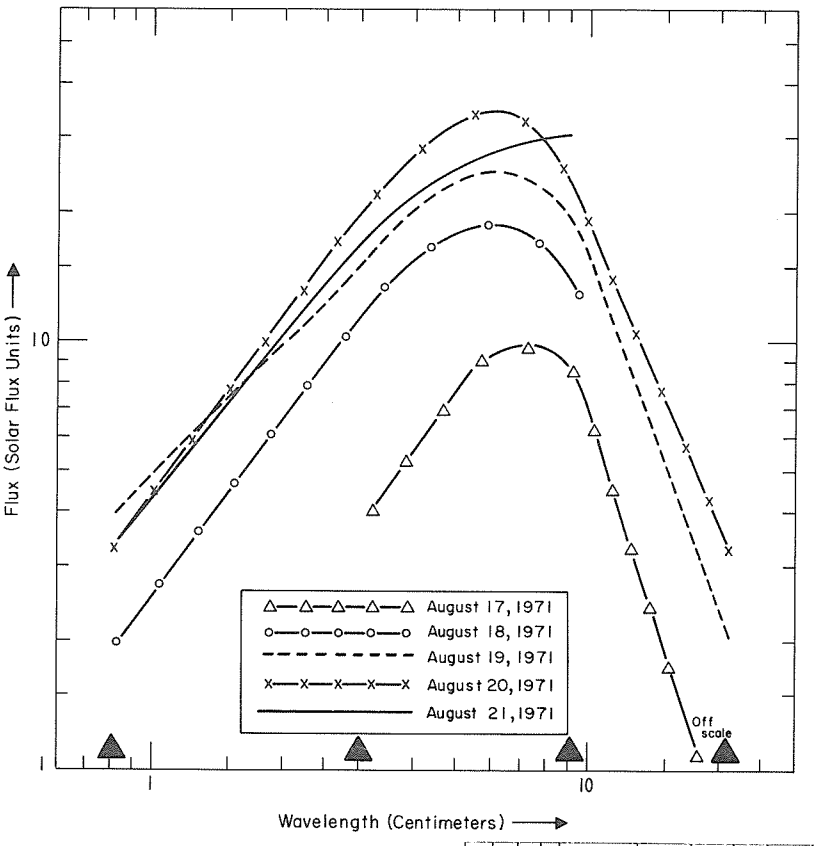


Fig. 2

Observed Spectra from MMH 11482 (east limb toward CM)

▲ denotes observed wavelengths. Smooth curve drawn through observations.

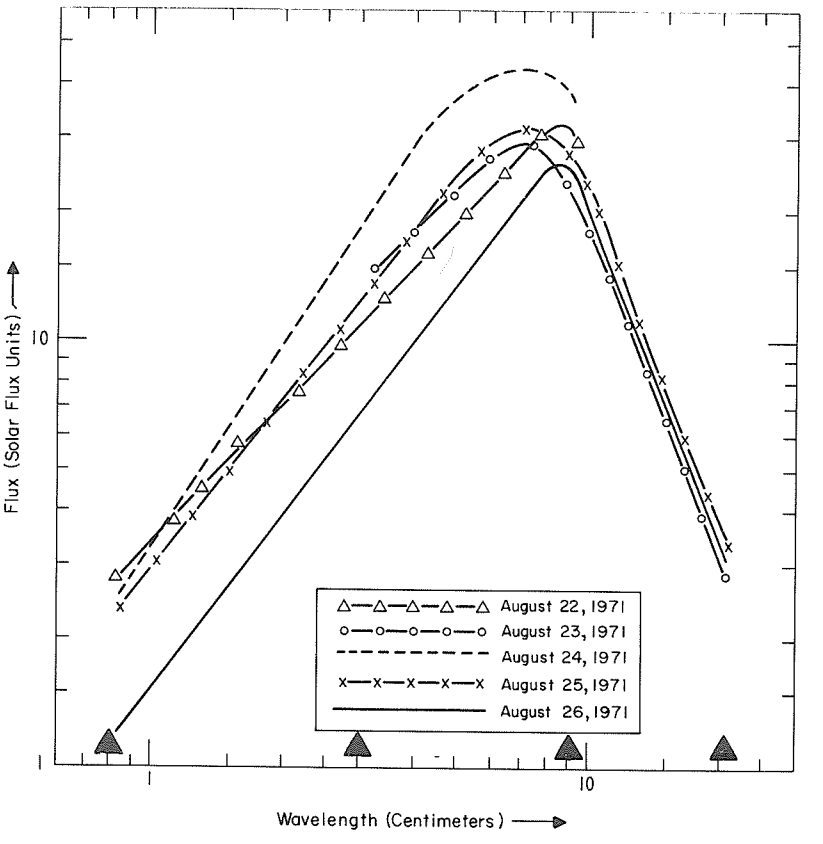


Fig. 3

Observed Spectra from MMH 11482 (before and after CMP).

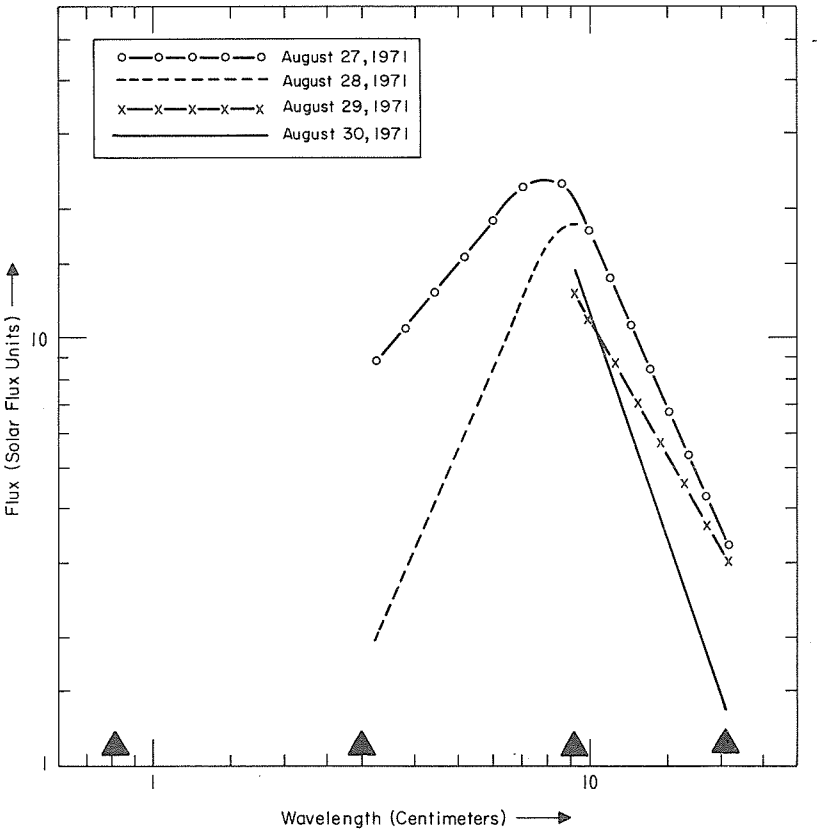


Fig. 4 Observed Spectra from MMH 11482 (CMP to West limb)

Analysis and Conclusions

A careful examination of Figures 2-4 will show three points of interest, which deal with a) coronal development, b) developments in the interface region, and c) a curious change in the spectrum as the active center progresses toward West Limb (and the flare which is the subject of this volume). We will expand on each of these items separately.

Consider the longer-wavelength portions of the spectra shown in Figures 2-4. These correspond to Region A of Figure 1. Of the nine days for which data are available at both 9.1 and 21 cm., eight show a spectral index of about 2. Recalling that spectral index ($\alpha$) is defined as $S \propto \lambda^{-\alpha}$, where S denotes spectral flux density, a spectral index of 2 is characteristic of thermal emission from a quasi-isothermal region. Formally, if $S_\infty$ is a constant

$$S = S_\infty \lambda^{-\alpha} \text{ (long wavelengths)}$$

seems a valid description of the long-wavelength spectrum with $\alpha \sim 2$. The transition between Regions A and B occurs at a critical wavelength $\lambda_c$, where

$$S = \left(1 - \frac{1}{e}\right) S_\infty \lambda_c^{-\alpha}$$

which may be taken as a definition of the wavelength at which the coronal extension of the active region is close to unit optical depth. Unit optical depth means

$$\tau = \int_{\text{outside}}^{S^*} \frac{0.16\, N_e^2\, \lambda_c^2}{c^2 T_e^{3/2}}\, ds = 1$$

Where the c in the denominator is the velocity of light, and $N_e$ and $T_e$ are electron density and temperature. In Figure 5 we plot $\lambda_c$ as a function of time.

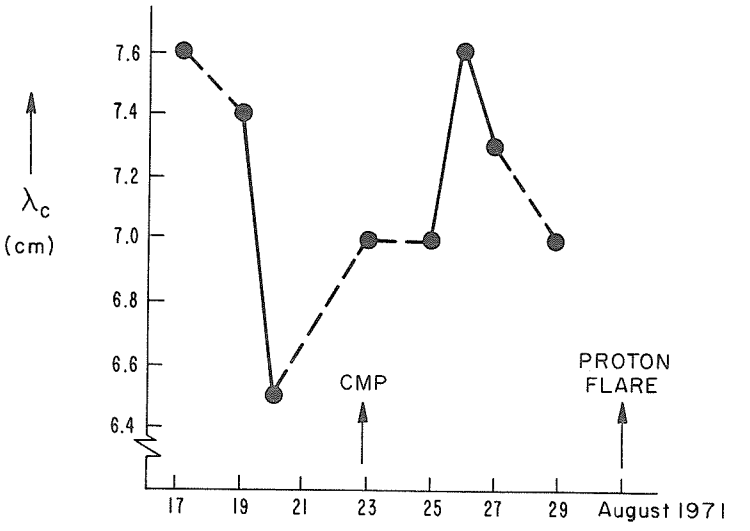


Fig. 5 Critical wavelength of spectra (as a function of time).

Considering the crudeness of our spectra, the relative constancy of $\lambda_c$ is surprising, for if $\lambda_c$ is indeed constant then

$$\int N_e^2 \, T_e^{-3/2} \, ds \neq f(\theta, t)$$

where $\theta$ is the angle between the line of sight and the outward normal from the active center. Thus, to the limits of accuracy of our data, we find no evidence for pumping of material (enhanced $N_e$) into the corona in advance of the proton flare, such as would increase $\lambda_c$.

Turning now to the short wavelengths, there is a wealth of information about the interface between chromosphere and corona, that may be gained by studying Region C of Figure 1. However, such studies are very difficult. One of the difficulties is coronal contamination of the observations: we have argued that the coronal portion of the active center has unit optical depth at around 7 cm., and if the optical depth varies as $\lambda^2$, one might expect an optical depth of $10^{-2}$ from just the active corona at 8 mm. Since this results in a brightness temperature an order of magnitude greater than enhancements observed at 8 mm., we conclude that coronal contamination may be severe at the shorter wavelengths. Another difficulty is that the source function in the interface region must include a non-negligible contribution from gyroemission, and this is not well understood. Because of these, and other, difficulties let us discuss the short-wavelength information in qualitative fashion. Although there is no theoretical reason for believing that a power-law spectrum represents the correct dependence of flux on wavelength (Region C), we have calculated such a spectral index from the ratio of 0.8/3.2 cm. flux. In Figure 6 spectral indices derived from short-, and long-wavelength slopes are shown, as functions of time, together with the Daily Flare Indices. It may be easily seen from Figure 6 that there were anomalies in the short-wavelength spectral index on the 19th, 24th, 28th and 29th. The last two will be discussed in the next paragraph. The softening on the 19th corresponds to an increase in the 0.8 cm. flux, which did not presage major activity, either in the optical or the X-ray portions of the spectrum. The hardening of the short-wavelength portion of the spectrum on the 24th, which can be seen in the enhanced fluxes at 3.2 and 9.1 cm., is thought to be associated with a slow rise and fall of the X-ray emission from the region beginning at about 12 hours (GMT) and ending at about 23 hours. This X-ray 'gradual rise and fall' can be clearly seen in the Solrad 9 data. In summary, then, if $\partial S/\partial \lambda$ at the short wavelengths is truly indicative of physical conditions in the interface region, then there is little evidence of change within that region.

Initial examination of Figures 3 and 4 might make one speculate that the active center began decaying on the 26th. However, no decay is evident at the longer wavelengths, and optical observations of the lower-lying portions of the active center offer further evidence that the region was not decaying. Another explanation is that the region was displaying the limb darkening we have described previously. However, comparison of Figures 2 and 4 show that this explanation is incorrect. One explanation that is consistent with the evidence is that the spectral changes are due to obscuration. Examine the $H_\alpha$ pictures of the region as reproduced in the optical section of this volume. Note the

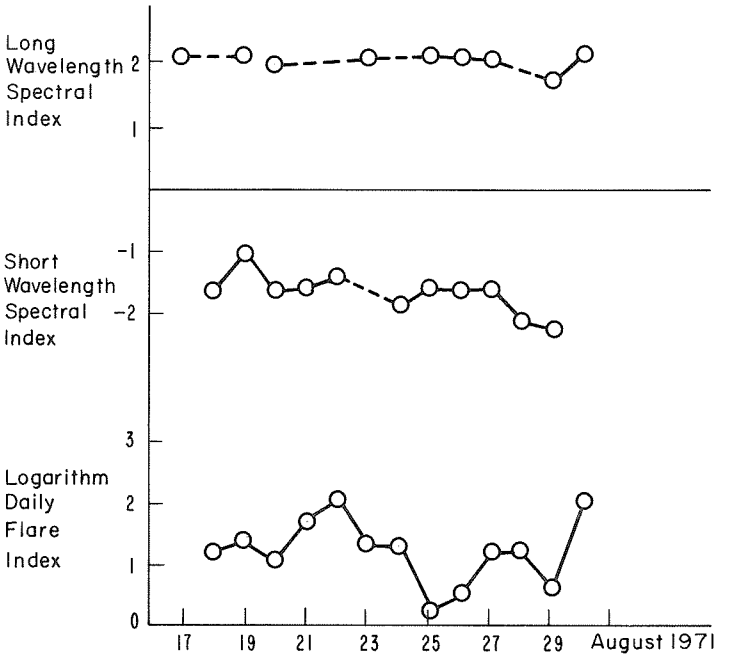


Fig. 6 Comparison of Spectral Indices with Flare Activity

extensive filamentary system trailing the region, and especially observe that the filament crosses the equator of the sun. Such systems are, on occasion, associated with 'coronal holes'. Further evidence for this speculation may be found by examining the radio maps, and noting that as the region approached west limb, the center of gravity of the radio emission was increasingly displaced from the optical plage. Further, the effect was greater at 21 cm. than at 9 cm. We offer this as evidence that the region was progressively occulted at the shorter wavelengths, and that refraction at the longer wavelengths was responsible for the displacement between optical and radio positions.

Let us quickly summarize our conclusions:

a) The radio evidence indicates that temporal changes in the corona either were nonexistent, or proceeded with a time scale of hours.

b) The observations suggest a coronal structure of possible high density and low temperature trailing behind the active region.

c) There is no evidence for substantial changes in the interface region, although the obscuration noted makes this conclusion weak.

## REFERENCES


CHRISTIANSEN, W. N., J. A. WARBURTON and R. D. DAVIES — 1957 — The Distribution of Radio Brightness Over the Solar Disk at a Wavelength of 21 Centimeters, IV. The Slowly Varying Component, Aust. J. Phys., 10, 491-514.

CHRISTIANSEN, W. N., D. S. MATHEWSON, J. L. TAWSEY, S. F. SMERD, A. BOISCHOT, J. F. DENISSE, P. SIMON, T. KAKINUMA, HELEN DODSON-PRINCE and JOHN FIROR — 1960 — A Study of a Solar Active Region Using Combined Optical and Radio Techniques, Ann. d'Ap., 23, No. 1, 75-101.

DRAGO, F. C. — 1970 — Radio Spectrum of Two Active Regions, Solar Physics, 13, 357-371.

GEL'FREIKH, G. B., and N. G. PETEROVA — 1970 — Polarization of Local Sources of Solar Radio Emission at 4.4 cm., Astronomicheskii Zh., 47, No. 4, 689-701.

GUTMANN, M., and J. L. STEINBERG — 1957 — Resultats Preliminaires Obtenus avec L'Interferometre a 8 Antennes sur 3 Cm de Longeur d'Onde, in Paris Symposium on Radio Astronomy, R. N. Bracewell (ed), pp. 123-124, Stanford University Press, Stanford, California.

KAKINUMA, T., and G. SWARUP — 1962 — A Model for the Sources of the Slowly Varying Component of Microwave Solar Radiation, Ap. J., 136, 975-994.

KHANGIL'DIN, U. V. — 1964 — Characteristics of Solar Active Regions Obtained from Observations on Millimeter Wavelengths, Astronomicheskii Zh., 41, No. 2, 302-312.

KUNDU, M. R. — 1959 — Structures et Proprietes des Sources d'Activite Solaire sur Ondes Centimetriques, Ann. d'Ap., 22, No. 1, 1-100.

LUND, D. S. — 1970 — Radio Burst Spectra Associated with Proton Flux Increases, Upper Atmosphere Geophysics Report UAG-8, 103-111.

STRAKA, R. M. — 1970 — Microwave Spectral Observations of Coronal Condensations, AFCRL-70-0241, 1-24.

SWARUP, G., T. KAKINUMA, A. E. COVINGTON, GLADYS A. HARVEY, R. F. MULLALY and J. ROME — 1963 — High-Resolution Studies of Ten Solar Active Regions at Wavelengths of 3-21 cm., Ap. J., 137, 1251-1267.

TSUCHIYA, A., and TAKAHASHI, K. — 1968 — Spectrum of Slowly Varying Component of Solar Radio Emission on Millimeter Wavelengths, Solar Physics, 3, 346-348.

# The Microwave Sun at the Time of the Cosmic Ray Increase of September 1, 1971

by

J. H. Deuter and R. N. Bracewell
Radio Astronomy Institute
Stanford University
Stanford, California

Between 2000 and 2100 UT on the day of September 1, 1971 the microwave solar emission at a wavelength of 9.1 cm was distributed as shown in Figure 1. Equal brightness temperatures are represented by contours; the outermost contour is for 10,000°K and the contour interval is 10,000°K. The photospheric disk is shown by a circle. The north pole of the sun is at the top and east is at the left. The contours presented here refer to a smoothed map in which each observation is replaced by the mean of the nine values centered on it. Details regarding the instrument can be obtained from Bracewell and Swarup [1961], and further details about the presentation are given in the annually published Descriptive Text that accompanies "Solar-Geophysical Data".

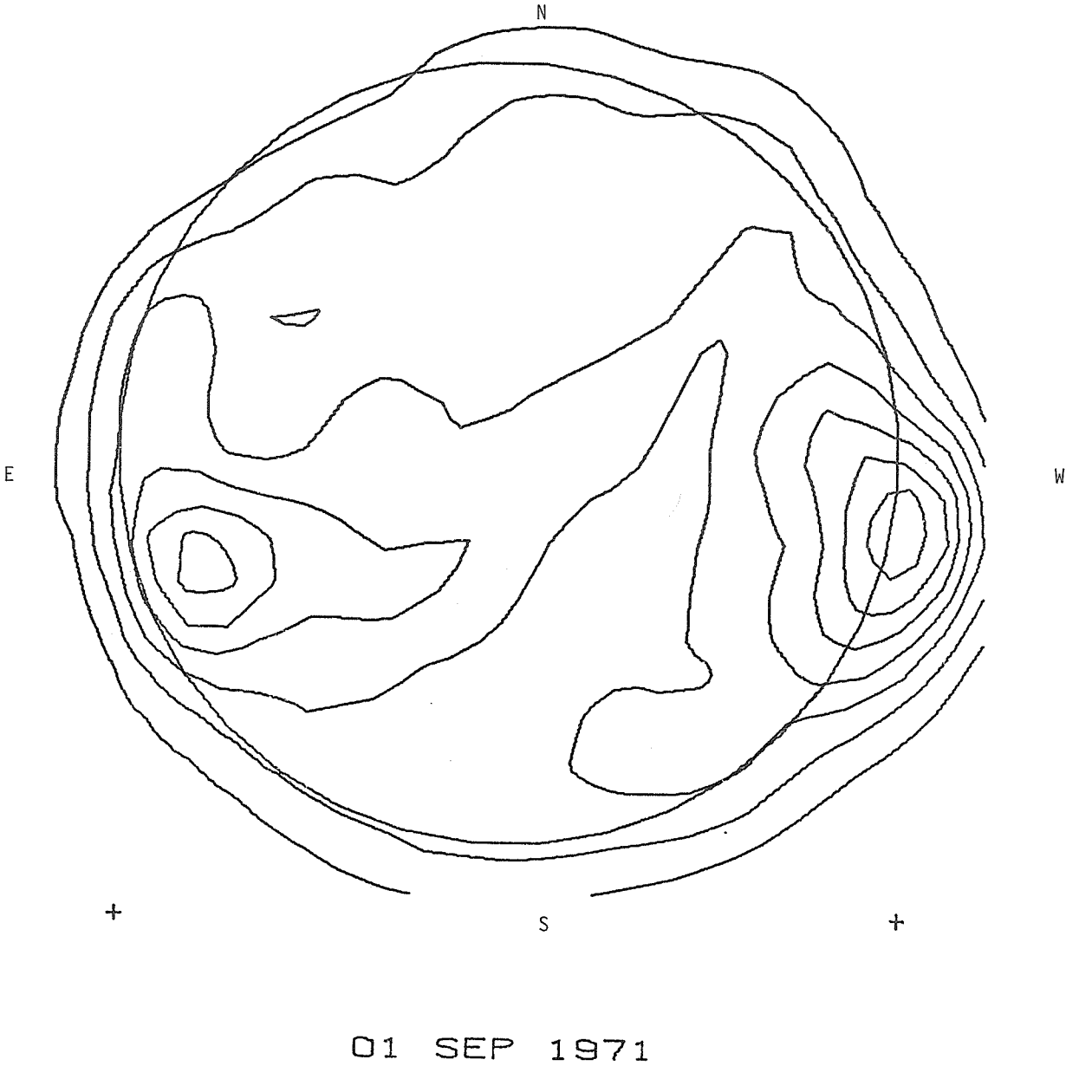


Fig. 1. Stanford 9.1 cm solar emission between 2000 and 2100 UT, September 1, 1971.

A microwave burst was recorded just before the map was taken, as shown in Figure 2. Records of this type are made as the sun moves through the fan beams of the east-west arm of the instrument. The beam width is 2.3 minutes of arc and the spacing of successive fringes is 41 minutes of arc when the source is near the meridian, as in this case.

The burst occurred on the west limb. It was not in existence at 1928 UT but had acquired considerable strength by 1931 UT. After a further increase a maximum was reached between 1936 and 1939 and by 2000 UT, when observations were started for Figure 1, recovery was not quite complete.

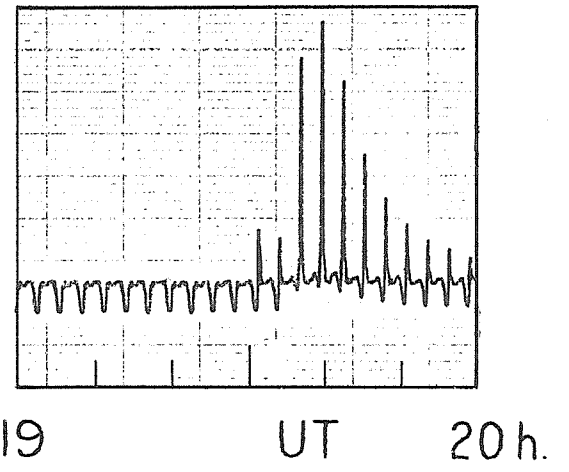


Fig. 2. Microwave burst between 1900 and 2000 UT, September 1, 1971.

Acknowledgement

This research was supported by the Air Force Office of Scientific Research under Contract AF44620-70-C-0076.

REFERENCE

BRACEWELL, R. N. and G. SWARUP 1961 The Stanford Microwave Spectroheliograph Antenna, a Microsteradian Pencil Beam Interferometer, Trans. I.R.E., Vol. AP-9, 22-30.

"Centimeter Wavelength Observations of
the Behind-the-Limb Flare of 1 September 1971"

by

Fred L. Wefer
Department of Astronomy
The Pennsylvania State University
University Park, Pennsylvania

## Introduction

The data pertaining to the behind the limb event of 1 September 1971 presented below are from observations made at The Pennsylvania State University Radio Astronomy Observatory (PSURAO) with fixed frequency radiometers operating at 10.7 GHz, 2.70 GHz and 960 MHz. The radiometers and their calibration have been discussed in detail by Hagen and Wefer [1971]. A brief discussion of the radiometer systems is given in Solar-Geophysical Data [1972]. The radiometers are operated primarily as a burst patrol. The behavior of the background solar flux density with radio frequency during a two month period centered on 1 September 1971 is first discussed. Then detailed data on the microwave flare of 1 September 1971 are presented.

## Background Solar Flux Density

It has been fairly well established that the proton event of 1 September 1971 was a behind-the-limb-event [Solar-Geophysical Data, 1971b]. Additional evidence for this can be gained from a study of the behavior of the undisturbed or background solar flux density. The unpublished measurements made at PSURAO, combined with the published values at other frequencies from AFCRL [Solar-Geophysical Data, 1971a and 1971c], provide values of the background solar flux density at nine frequencies in the range 245 MHz through 15.4 GHz during the period 1 August through 30 September 1971.

In Figure 1 is shown the fractional change in the background solar flux density as a function of radio frequency and time, in the form of a contour map. The contour interval is 0.1, the zero contour being indicated by tic marks on the downward (negative) side. The single ambiguity on the map is that the region just to the left of the asterisk is a depression rather than a hump. The fractional change is defined by

$$\zeta_\nu(t) = \frac{S_\nu(t) - \overline{S}_\nu}{\overline{S}_\nu}$$

where $\zeta_\nu(t)$ = fractional change in background solar flux density at frequency $\nu$ and time t,

$S_\nu(t)$ = background solar flux density at frequency $\nu$ and time t, and

$\overline{S}_\nu$ = average value of $S_\nu(t)$ over the time interval of interest.

The quantity $\zeta_\nu(t)$ is used instead of $S_\nu(t)$ directly for three reasons. It is the change in $S_\nu(t)$ with time which is of interest here, not the actual values of $S_\nu(t)$. The time average of $\zeta_\nu(t)$ is zero at each frequency, yielding a contour map much easier to interpret than a contour map of $S_\nu(t)$. Finally the values of $\zeta_\nu(t)$ are independent of errors in the values of the antenna effective areas used to compute $S_\nu(t)$, thus eliminating one of the largest sources of error in the data.

Focusing attention on frequencies above 600 MHz, it is seen that during the period 1 through 17 August 1971 the background solar flux density remained within about 10% of the two month average. The value of $\zeta_\nu(t)$ increased on 18 August at 5 GHz, the increase spreading to both higher and lower frequencies on 19 and 20 August. These increases correspond to the appearance on the east limb on 17 August

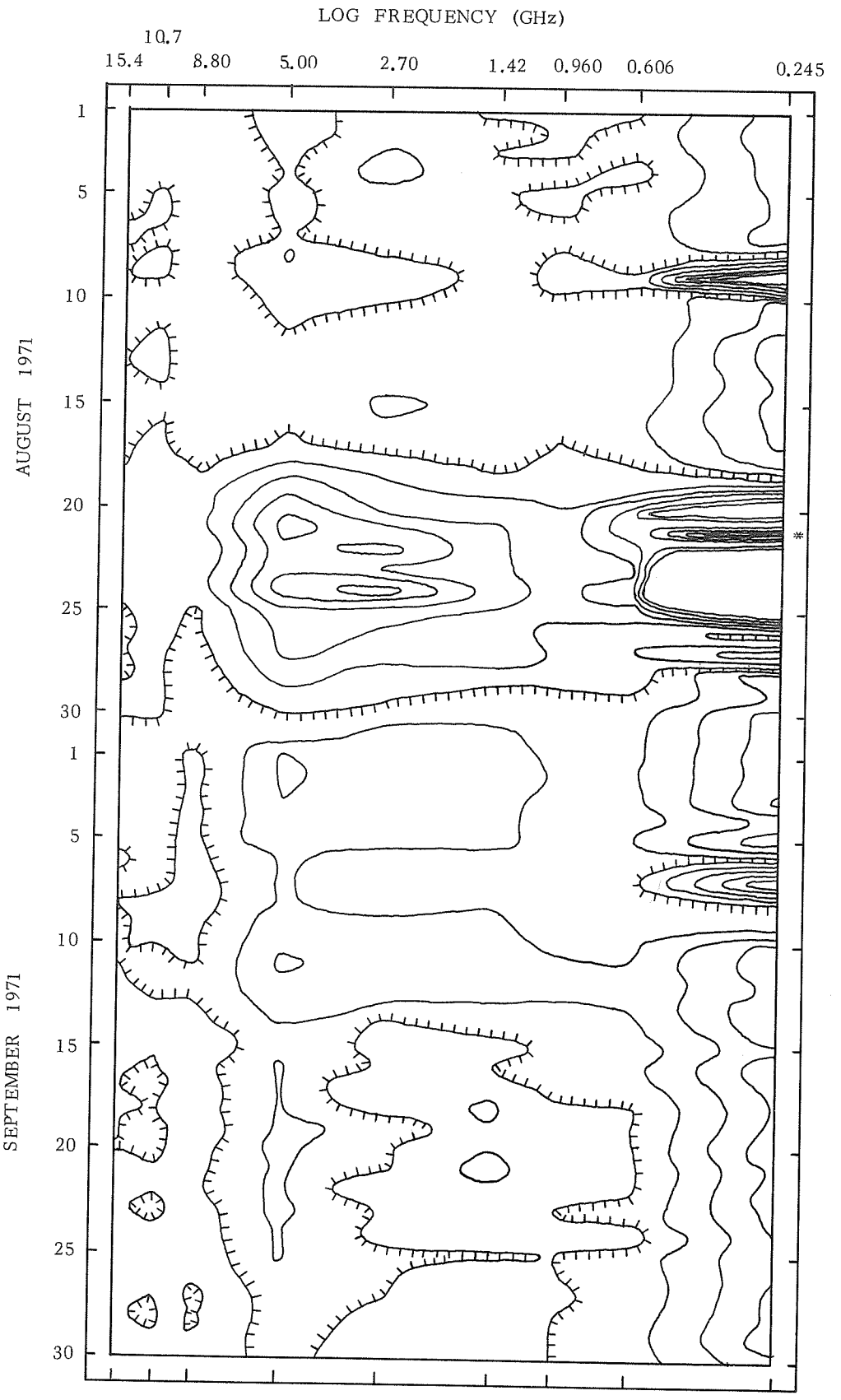


Figure 1. Contour map in the time-frequency plane of the fractional change in the background solar flux density during the period 1 August through 30 September 1971. The contour interval is 0.1, the zero contour being indicated by tic marks on the downward (negative) side.

of Mt. Wilson sunspot region 11445 (McMath Region 11482) [Solar-Geophysical Data, 1971d]. While there were a number of other regions on the visible surface of the sun, the increase in $\zeta$ did not begin until McMath region 482 appeared on the east limb. The center of region 482 crossed the central meridian on 23 August, near the center of the broad peak in $\zeta$. The fractional change in the background solar flux density reached a peak value of 0.54 at 2.70 GHz on 24 August. Following this, $\zeta$ steadily declined, reaching a level of 0.1 at 5 GHz on 29 August, when region 482 began west limb passage. While there were a number of regions remaining on the visible surface of the sun, $\zeta$ decreased as region 482 approached the west limb. The 9.1 cm Stanford and 21 cm Fleurs spectroheliograms [Solar-Geophysical Data, 1971d] substantiate that the increase in $\zeta$ was caused almost entirely by region 482. McMath region 482 was, therefore, the most "active" by far of the various regions on the sun during this period.

The values of $\zeta$ were low and relatively constant during the month of September. When region 482 (McMath region 11516) reappeared on the east limb on 13 September, only a slight increase in the values of $\zeta$ was observed. The Stanford and Fleurs spectroheliograms also showed much reduced brightness temperatures associated with the region at this time.

McMath region 482 is thus seen to be the most likely candidate for the seat of the proton event of 1 September 1971.

## The Microwave Flare

The microwave outbursts associated with the proton event of 1 September 1971 began at 19:26.3 UT, 19:28.6 UT and 19:31.8 UT at 2.70 GHz, 960 MHz and 10.7 GHz, respectively. The radiometer chart records of these events were digitized in preparation for the construction of the dynamic spectrum of the microwave flare. These digitized records are plotted in Figure 2. The flux density scale is the same for the three records. The 2.70 GHz and 960 MHz traces have been offset by 40 fu and 80 fu, respectively, in an attempt to improve clarity. The time is marked at ten minute intervals along the lower abscissa; tic marks appear every minute along the upper abscissa.

Three things should be noted in the figure. In spite of the above mentioned offsets, the 2.70 GHz and 960 MHz traces cross twice. The peak of the 2.70 GHz burst went slightly off-scale on the high gain channel causing the apparent 1.2 minute long flat maximum. Finally, the two minute long gaps in the traces beginning at 20:01 UT are caused by the automatic hourly calibration of the radiometers.

The recordings at the three frequencies are presented again in Figure 3, with the peaks of the traces normalized to unity. The two lower frequencies have again been offset to improve clarity. This figure shows the striking similarity of the shapes of the burst at the three frequencies.

While it is normally risky to attempt to construct dynamic spectra of microwave flares from only three single frequency records, the AFCRL observations [Solar-Geophysical Data, 1971e] indicated that the flare was quite regular and smooth in the frequency range 960 MHz through 10.7 GHz. The dynamic spectrum constructed from the PSURAO data alone is shown in Figure 4. The contours are logarithmic in their spacing, successive contour levels differing by a factor of two. The shape of the 128 fu contour line indicates that the peak flux density of the microwave flare occurred somewhere between 2.70 GHz and 1.42 GHz.

Hagen and Wefer [1972] have analyzed this microwave flare in some detail and were able to show that the spectrum of the peak flux densities is consistent with synchrotron radiation due to 3 Mev electrons interacting with a magnetic field of approximately 50 Gauss at a level of about 150,000 km above the photosphere.

## REFERENCES


Hagen, J. P. and Wefer, F. L. 1971 A Catalog of Distinct Solar Radio Events for Fixed Frequency Observations Made at The Pennsylvania State University Radio Astronomy Observatory During the Period 1 July 1964 through 30 June 1970, The Penna. State University, Dept. of Astronomy Scientific Report No. 023.

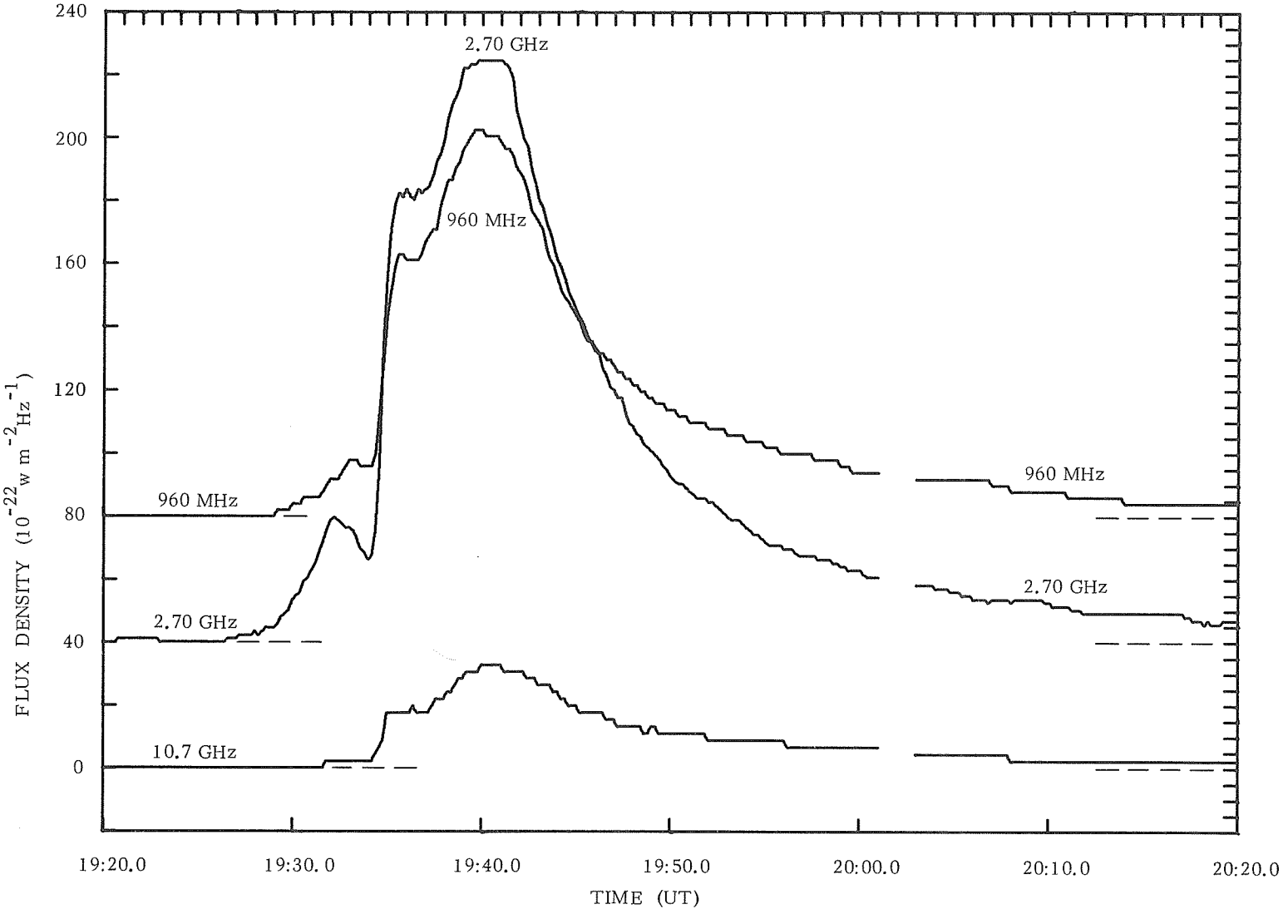


Figure 2. Plots of the digitized radiometer records of the behind-the-limb flare of 1 September 1971.

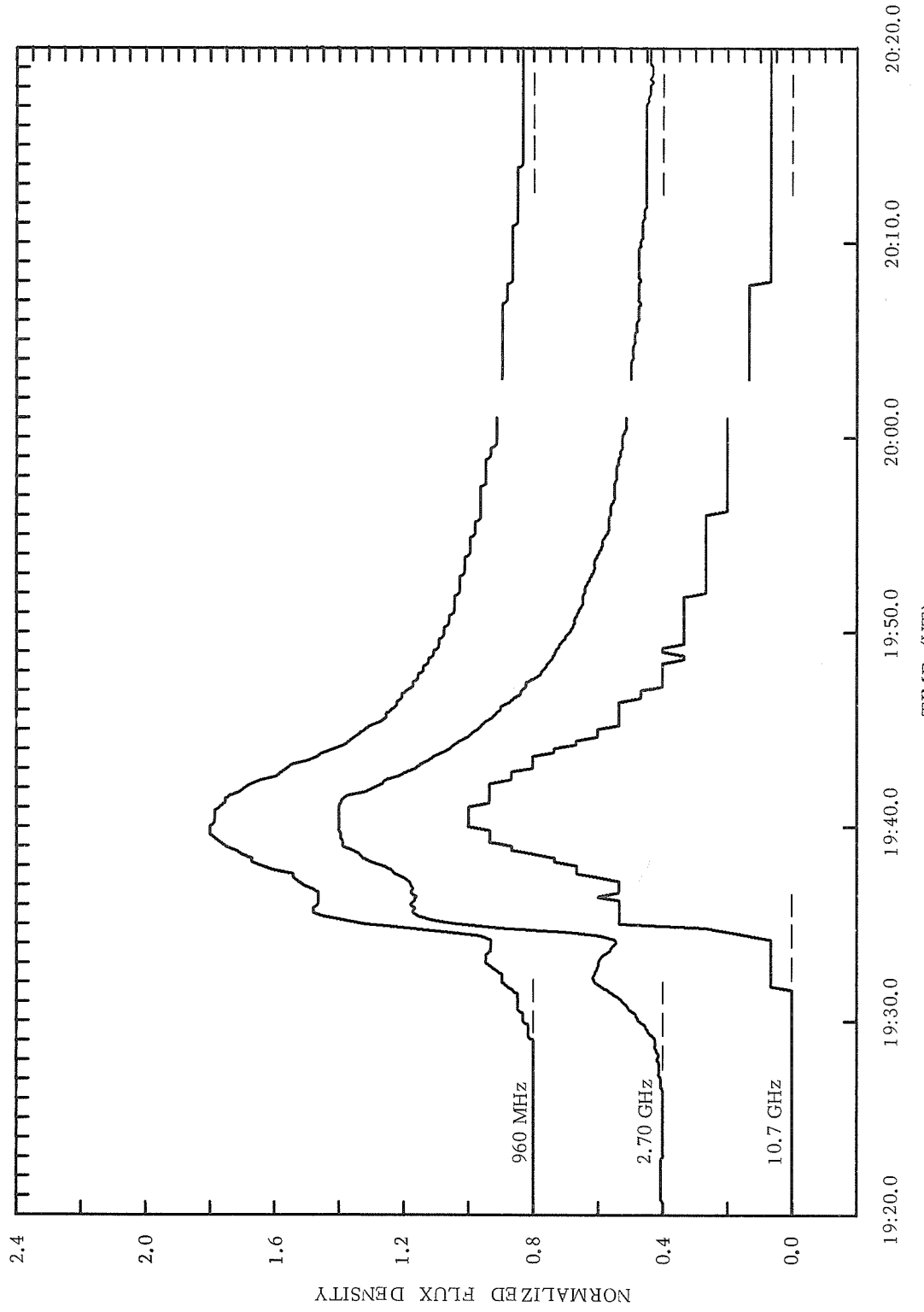


Figure 3. Plots of the digitized radiometer records with the peak flux densities normalized to unity, for the 1 September 1971 behind-the-limb flare.

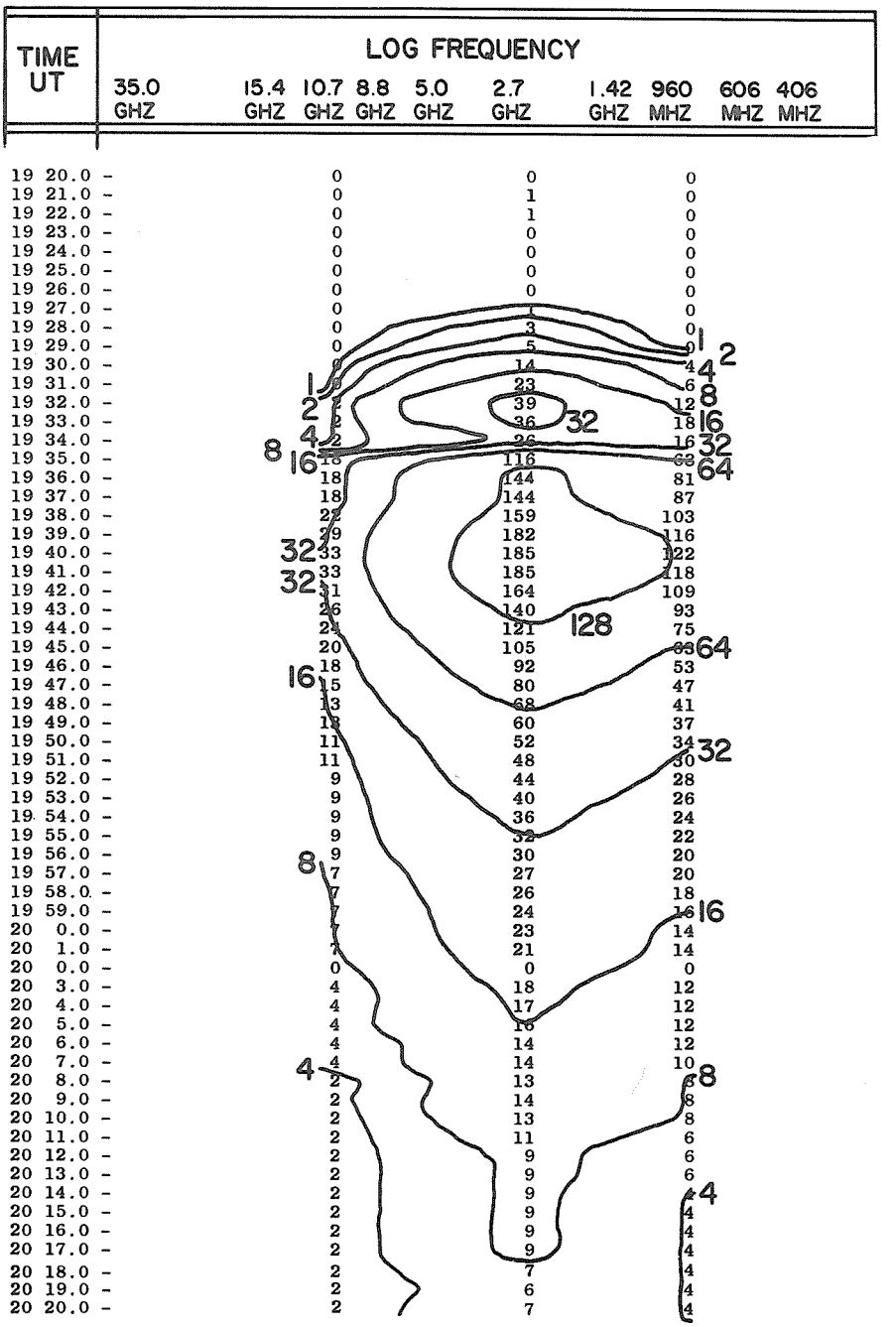


Figure 4. Dynamic spectrum of the 1 September 1971 behind-the-limb microwave flare, constructed from three fixed frequency records.

| | | |
|---|---|---|
| Solar-Geophysical Data | 1972 | No. 330 (Supplement), pp. 47-49, February 1972, U.S. Department of Commerce, (Boulder, Colorado). |
| Solar-Geophysical Data | 1971a | No. 325-Part I, p. 7, September 1971. |
| Solar-Geophysical Data | 1971b | No. 326-Part I, pp. 27-28, October 1971. |
| | 1971c | _____ p. 7. |
| | 1971d | _____ pp. 30-71 and p. 78. |
| | 1971e | _____ p. 19. |
| Solar-Geophysical Data | 1971f | No. 327-Part I, pp. 28-67, November 1971. |
| Hagen, J. P. and Wefer, F. L. | 1972 | Radio Observations of the Behind the Limb Flare of 1 September 1971 and Theory of Origin, paper given at American Astronomical Society meeting, April 1972. |

# On the S-Component and Noise Storms in September, 1971

by

A. Böhme and A. Krüger
German Academy of Sciences
Central Institute for Solar-Terrestrial Physics
(Heinrich-Hertz-Institute)
Berlin-Adlershof, GDR

[Editor's Note: See contribution by these authors on pages 61 to 63 for the January 1971 event.]

This report is restricted to a representation of radio flux and polarization data referring to the development of the active regions before the occurrence of the proton event on September 1, 1971. The observed data are shown in Table 1, and are condensed in form of synthetic spectral diagrams of the S-component and the noise storm emission (Figure 1).

It is widely believed that the S-component and noise storm spectra carry some significance about conditions facilitating the outflow of high and medium energetic solar particles, respectively [cf. also Sakurai, 1971]. However, it is indicated by the present examples that the observing conditions by directivity and angular dependence of the emission properties are not always favorable for an exact prediction of energetic events.

## The August-September 1971 Period

As demonstrated by Figure 1, during the last decade of August 1971 well-expressed centers of the S-component and the noise storm component were observed, which were closely linked together. The S-component spectrum was evident up to the 3 cm-region as early as August 19, (Figure 2) indicating a proton-dangerous situation, but the event came more than 10 days later when the related active center on the southern hemisphere had passed over the west limb.

The complex of the noise storm was visible between August 20-25. A modulation of the radiation as shown in Figure 1 perhaps could be interpreted by motions of the magnetic structure of the noise storm emitting region or by the passing of different tubes of force through the line of sight. On several days the polarization was varying. The noise storm flux spectrum was broader than that of the former period of January 1971 (cf. Figure 2). After 25 August the noise storm radiation disappeared. The disappearance of the source of the S-component occurred on August 30.

Table 1

Daily Flux and Polarization data
Heinrich-Hertz-Institute

| 1971 August | 9500 | 3000 | 1490 | 510 | 287 | 234 | 113 | 68 | 40 MHz |
|---|---|---|---|---|---|---|---|---|---|
| 16 | 271 l | 83 | 86 0 | 28 | 7 | 7 | 2 0 | < | < 0 |
| 17 | 273 l | 84 | 88 0 | 28 | 7 | 7 | 2 0 | < | < 0 |
| 18 | 286 0 | 91 | 93 0 | 28 | 8 | 11 | 3 0 | < | < 0 |
| 19 | 300 r | - | 101 l | 33 | 11 | 11 | 20 r-l | < | < 0 |
| 20 | 293 - | 115 | 110 l | 48 | 28 | 57 | 73 L | 120 | 197 l |
| 21 | - - | 126 | 112 0 | 53 | 41 | 89 | 14 l | < | < l |
| 22 | - - | - | 111 0 | 35 | 52 | 124 | 170 L | 166 | 306 l |
| 23 | - r | 130 | 112 0 | 35 | 37 | 120 | 98 l | < | < - |
| 24 | 274:r | 130 | 108 0 | 39 | 83 | 183 | 586 R-l | 741 | 316 r |
| 25 | 276:0 | 125 | 109 r: | 28 | 16 | 36 | 137 l-r | 164 | 331 0 |
| 26 | 270:l | 118 | 105 r: | 28 | 10 | 9 | 11 l | < | < 0 |
| 27 | 269:0 | 115 | 102 r: | 28 | 11 | 16 | 4 l | < | < 0 |
| 28 | 270:r | 128 | 97 r: | 32 | 5 | 9 | 2 0 | < | < 0 |
| 29 | 262:0 | 96 | 87 - | 28 | 5 | 8 | 2 0 | < | < 0 |
| 30 | 256:0 | 88 | 85 r: | 35 | 7 | 8 | 2 0 | < | < 0 |
| 31 | 253 0 | 79 | 80 r: | 35 | 9 | 7 | 2 0 | < | < 0 |

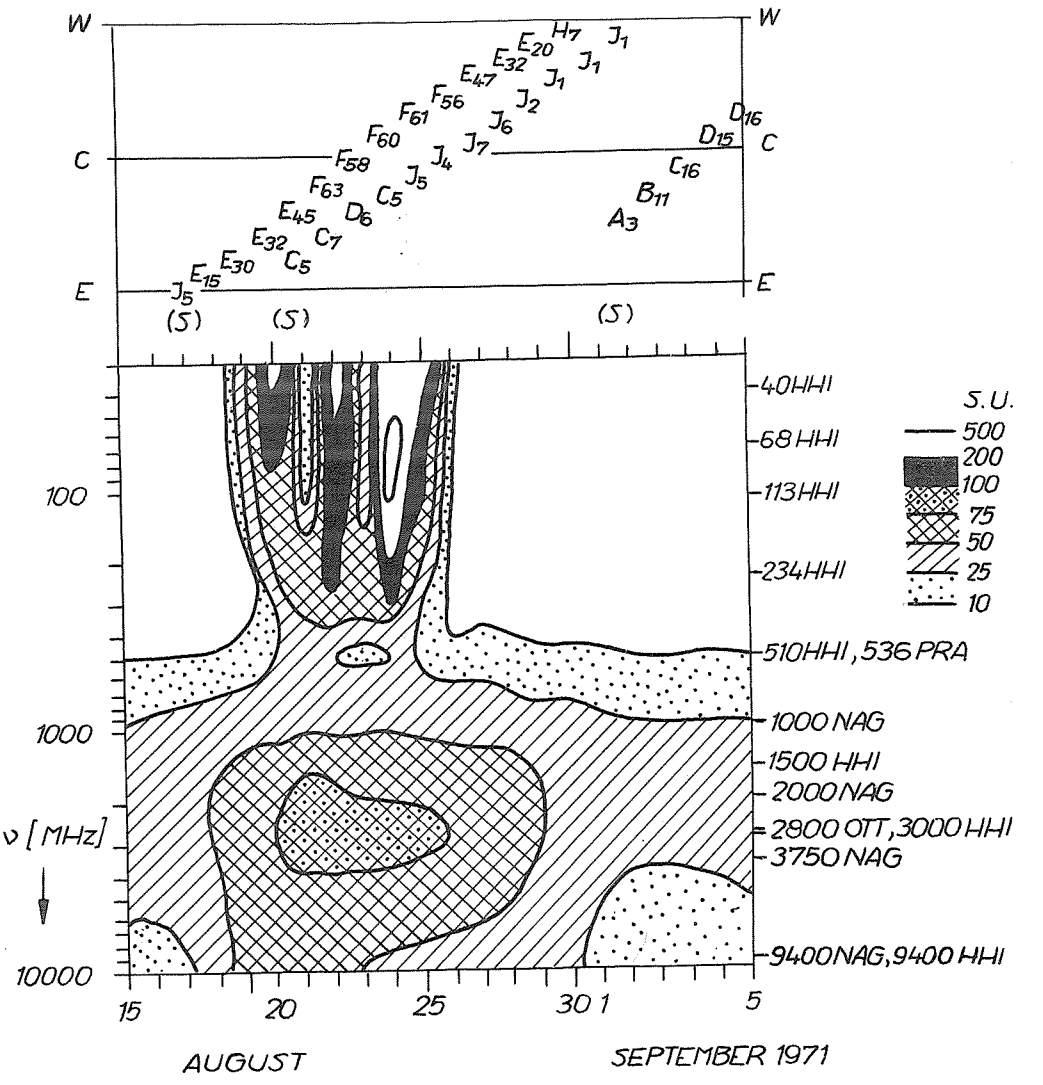


Fig. 1 Spectral diagrams of S- and noisestorm components and major spot groups (top).

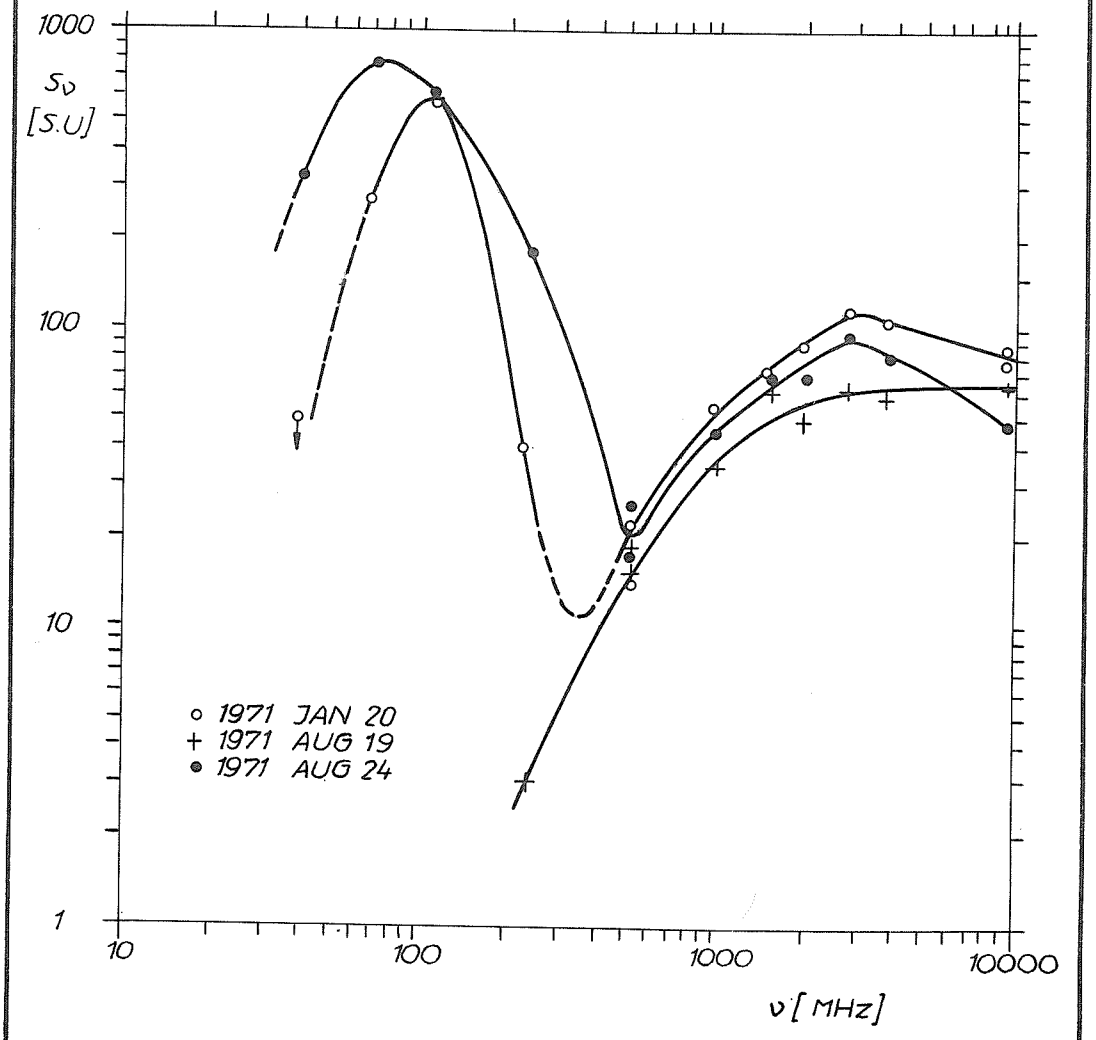


Fig. 2 Spectra of daily mean fluxes of noisestorms and the S-component for selected cases

## REFERENCES


BOHME, A. and A. KRUGER 1971 Characteristics of Noise Storms and the S-Component of Solar Radio Emission in March, 1970. World Data Center A - Upper Atmosphere Geophysics Report UAG-12, 71.

SAKURAI, K. 1971 Type I Noise Active Regions and Energetic Electrons from 1 to 10 March 1970. World Data Center A - Upper Atmosphere Geophysics Report UAG-12, 52.

# Millimeter Wave Spectroheliograms Associated with the September 1, 1971 Solar Terrestrial Event

by

Larry E. Telford
Air Force Cambridge Research Laboratories
L. G. Hanscom Field, Bedford, Massachusetts 01730

8.6 mm spectroheliograms have been taken on a daily basis (weather and equipment permitting) since the Summer, 1968. In March, 1971, 20 mm spectroheliograms were added to the daily routine. The 8.6 mm and 20 mm spectroheliograms are taken concurrently using a dual frequency feed system on the AFCRL 29-Foot Millimeter Wave Antenna. This submission represents a collection of 8.6 mm spectroheliograms and 20 mm spectroheliograms covering two weeks prior to the September 1 event. Equipment problems prevented the generation of an 8.6 mm spectroheliogram on August 18 and the generation of 20 mm spectroheliograms on August 20, 21, and 24 and September 1.

The following comments apply to the spectroheliograms presented in Figures 1 through 5:

1. All spectroheliogram radio brightness temperatures are to be multiplied by ten, i.e., 520° = 5200°K.
2. All spectroheliogram radio brightness temperatures are antenna temperatures corrected for atmospheric attenuation but not corrected for antenna pattern effects.
3. The 8.6 mm antenna pattern and radiometer parameters are given in the latest "Solar-Geophysical Data Descriptive Text".
4. The antenna half power beamwidth at 20 mm is 8 minutes of arc with first side lobe levels at approximately -18 dB. The 20 mm radiometer is a standard Dicke type with a sensitivity of 2°K for a one second time constant.
5. The difference between the average antenna temperatures in the January (p. 64) and the September sets of 8.6 mm spectroheliograms is due to a change in the calibrate noise tube in the intervening period.
6. The contour levels for the plotted spectroheliograms are:
   Figures 1, 2, and 3 - 3000°K, 5200°K and up in 200°K increments.
   Figures 4 and 5 - 3000°K, 5000°K and up in 100°K increments.
7. The times associated with each spectroheliogram is the time the center grid point was observed. The spectroheliogram observation sequence starts at the upper left corner of the plotted grid and ten seconds are spent at each grid point. The sequence moves from left to right for each line. Using this sequence, the exact observation time for each grid point can be calculated.

In addition to the plotted spectroheliograms, Tables 1 and 2 represent the output of a data reduction computer program which interpolates the original radio brightness temperature grid and searches for maxima with a fixed set of searching constraints. The tables represent the heliographic location and enhancement, or temperature above the average surface background temperature, for each maxima found for each spectroheliogram. In reproducing the table, all maxima with enhancements less than 100°K were ignored. Since the input grid data are not corrected for antenna effects, the maxima locations are not accurate when the region is greater than ±45° from Central Meridian at 8.6 mm or ±25° from Central Meridian at 20 mm. Within these limits, the locations are accurate to ±2° in heliographic coordinates.

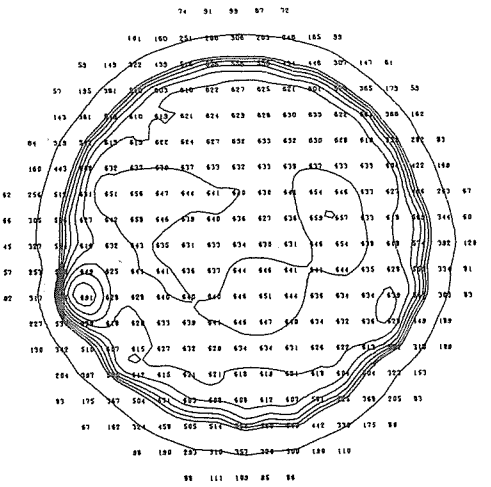
8.6 MM SPECTROHELIOGRAM
PROSPECT HILL RADIO OBSERVATORY
1647 UT DAY 231 1971
CONTOURS IN INTERVALS OF 200 DEGREES KELVIN
DEGREES KELVIN/10

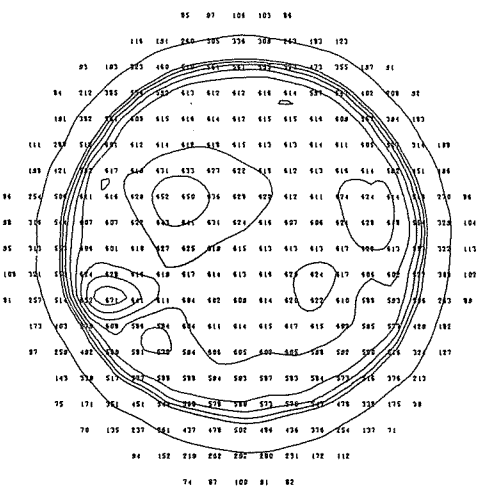
8.6 MM SPECTROHELIOGRAM
PROSPECT HILL RADIO OBSERVATORY
1813 UT DAY 232 1971
CONTOURS IN INTERVALS OF 200 DEGREES KELVIN
DEGREES KELVIN/10

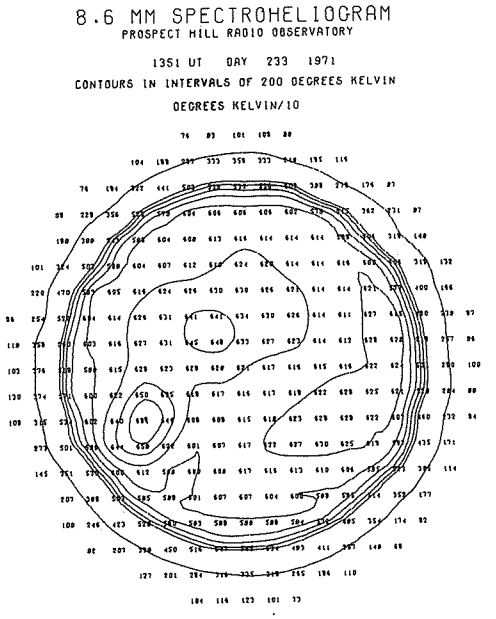
8.6 MM SPECTROHELIOGRAM
PROSPECT HILL RADIO OBSERVATORY
1351 UT DAY 233 1971
CONTOURS IN INTERVALS OF 200 DEGREES KELVIN
DEGREES KELVIN/10

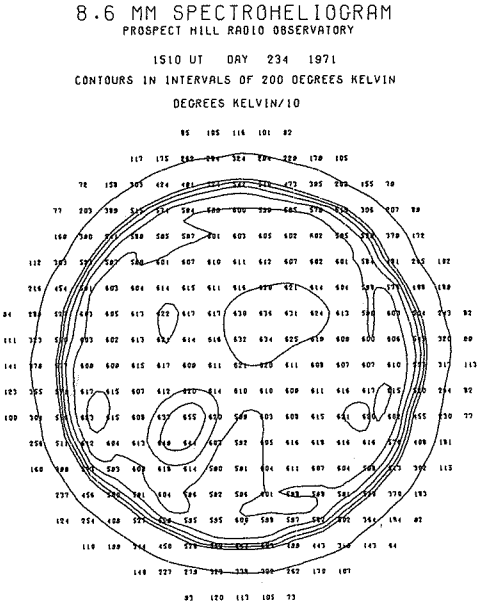
8.6 MM SPECTROHELIOGRAM
PROSPECT HILL RADIO OBSERVATORY
1510 UT DAY 234 1971
CONTOURS IN INTERVALS OF 200 DEGREES KELVIN
DEGREES KELVIN/10

Fig. 1.

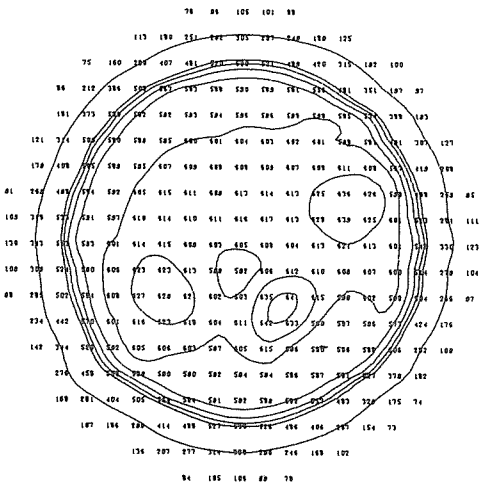
8.6 MM SPECTROHELIOGRAM
PROSPECT HILL RADIO OBSERVATORY
1415 UT DAY 236 1971
CONTOURS IN INTERVALS OF 200 DEGREES KELVIN
DEGREES KELVIN/10

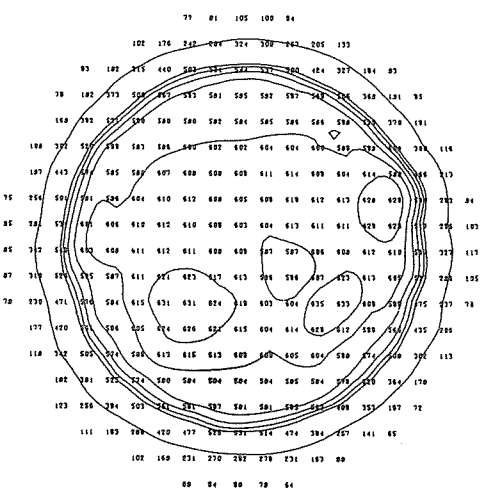
8.6 MM SPECTROHELIOGRAM
PROSPECT HILL RADIO OBSERVATORY
1454 UT DAY 237 1971
CONTOURS IN INTERVALS OF 200 DEGREES KELVIN
DEGREES KELVIN/10

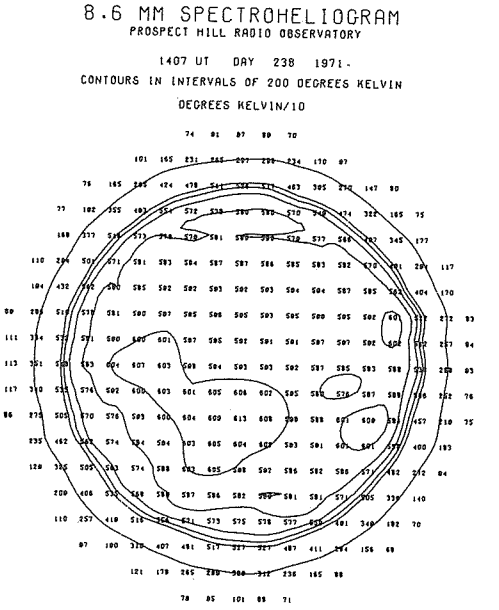
8.6 MM SPECTROHELIOGRAM
PROSPECT HILL RADIO OBSERVATORY
1407 UT DAY 238 1971
CONTOURS IN INTERVALS OF 200 DEGREES KELVIN
DEGREES KELVIN/10

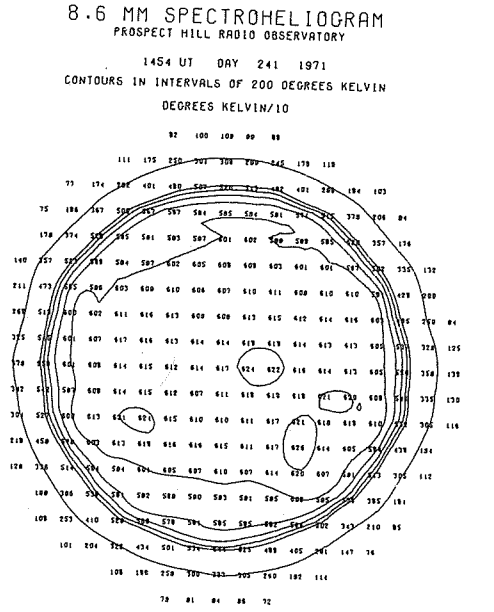
8.6 MM SPECTROHELIOGRAM
PROSPECT HILL RADIO OBSERVATORY
1454 UT DAY 241 1971
CONTOURS IN INTERVALS OF 200 DEGREES KELVIN
DEGREES KELVIN/10

Fig. 2.

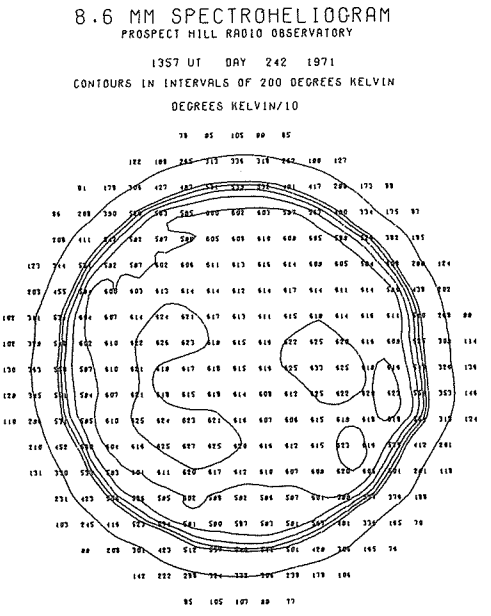
8.6 MM SPECTROHELIOGRAM
PROSPECT HILL RADIO OBSERVATORY
1357 UT DAY 242 1971
CONTOURS IN INTERVALS OF 200 DEGREES KELVIN
DEGREES KELVIN/10

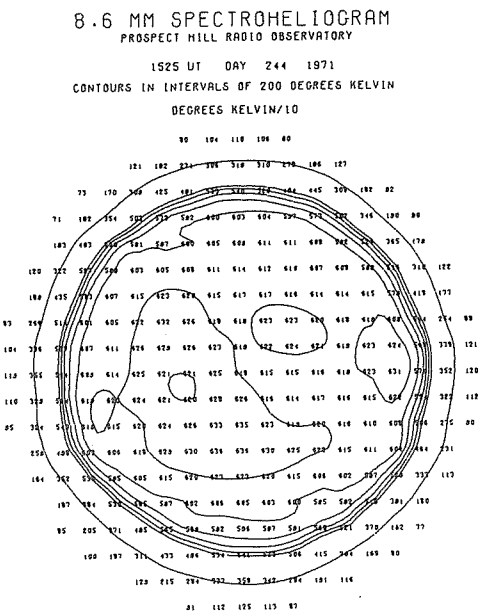
8.6 MM SPECTROHELIOGRAM
PROSPECT HILL RADIO OBSERVATORY
1525 UT DAY 244 1971
CONTOURS IN INTERVALS OF 200 DEGREES KELVIN
DEGREES KELVIN/10

Fig. 3.

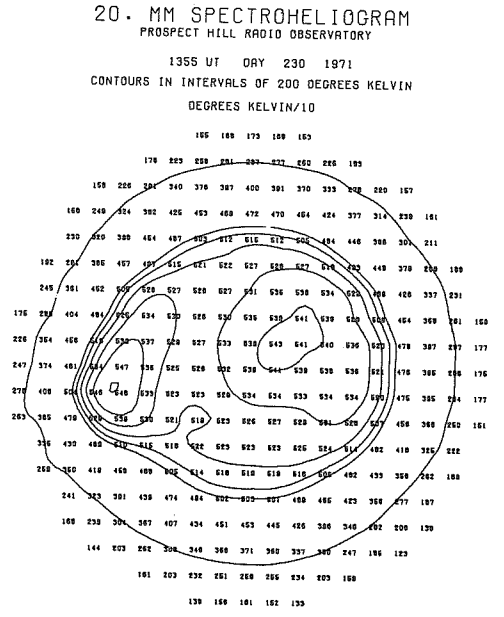
20. MM SPECTROHELIOGRAM
PROSPECT HILL RADIO OBSERVATORY
1355 UT DAY 230 1971
CONTOURS IN INTERVALS OF 200 DEGREES KELVIN
DEGREES KELVIN/10

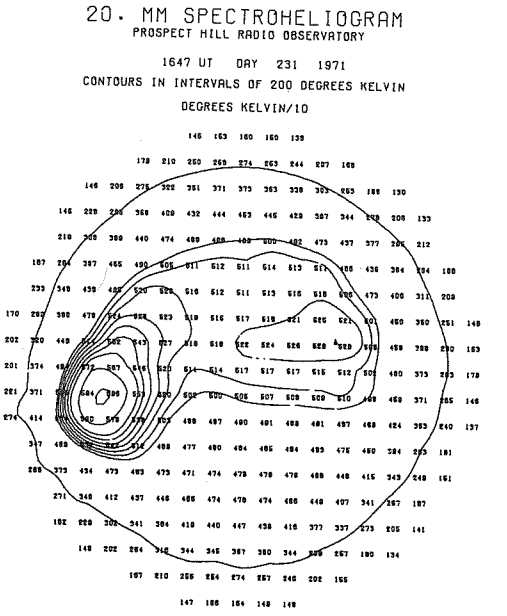
20. MM SPECTROHELIOGRAM
PROSPECT HILL RADIO OBSERVATORY
1647 UT DAY 231 1971
CONTOURS IN INTERVALS OF 200 DEGREES KELVIN
DEGREES KELVIN/10

Fig. 4.

20. MM SPECTROHELIOGRAM
PROSPECT HILL RADIO OBSERVATORY

1510 UT DAY 234 1971
CONTOURS IN INTERVALS OF 200 DEGREES KELVIN
DEGREES KELVIN/10

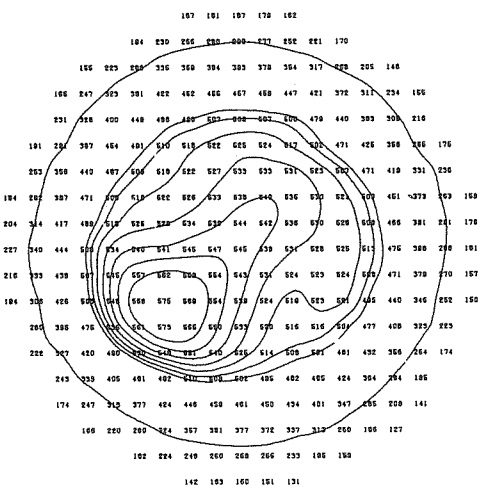

20. MM SPECTROHELIOGRAM
PROSPECT HILL RADIO OBSERVATORY

1454 UT DAY 237 1971
CONTOURS IN INTERVALS OF 200 DEGREES KELVIN
DEGREES KELVIN/10

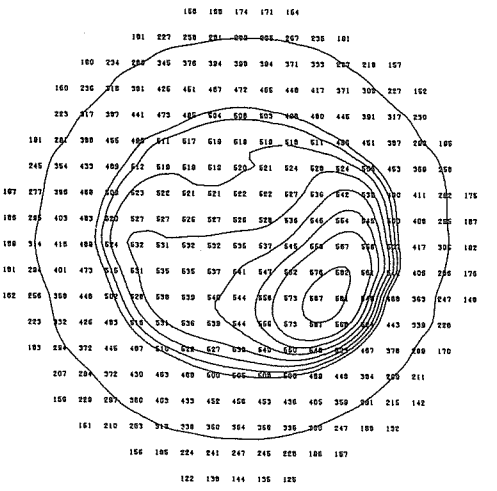

20. MM SPECTROHELIOGRAM
PROSPECT HILL RADIO OBSERVATORY

1407 UT DAY 238 1971
CONTOURS IN INTERVALS OF 200 DEGREES KELVIN
DEGREES KELVIN/10

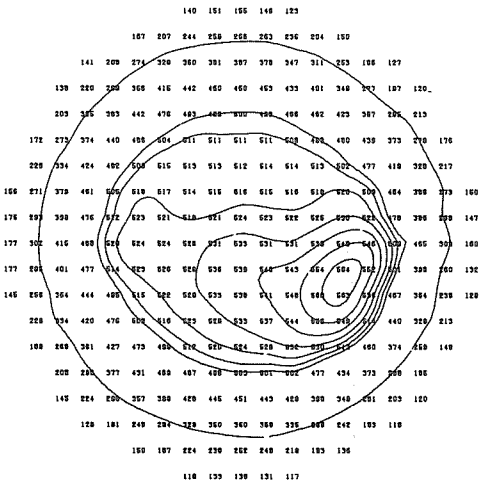

20. MM SPECTROHELIOGRAM
PROSPECT HILL RADIO OBSERVATORY

1454 UT DAY 241 1971
CONTOURS IN INTERVALS OF 200 DEGREES KELVIN
DEGREES KELVIN/10

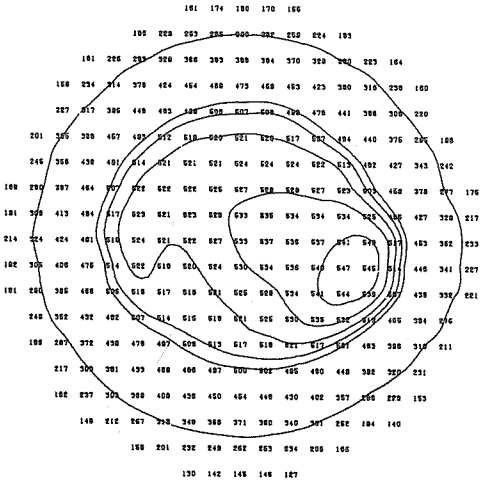

20. MM SPECTROHELIOGRAM
PROSPECT HILL RADIO OBSERVATORY

1357 UT DAY 242 1971
CONTOURS IN INTERVALS OF 200 DEGREES KELVIN
DEGREES KELVIN/10

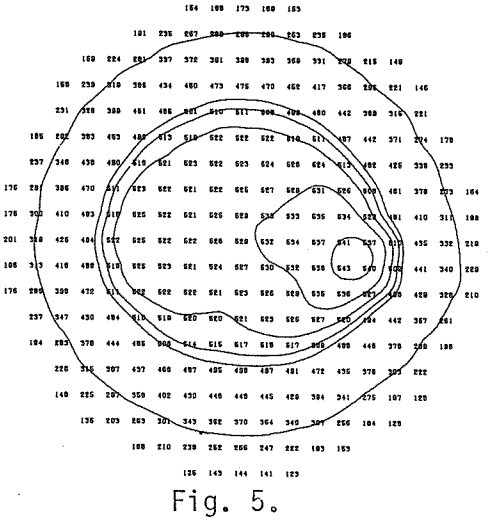

Fig. 5.

TABLE 1

Day 231
AUGUST 19, 1971 1647 UT
$L_o = 326^o$, $B_o = +7^o$

| L | LAT | CMD | 8 mm |
|---|---|---|---|
| 282 | 09N | 44E | 220 K |
| 294 | 07N | 32E | 295 K |
| 350 | 04N | 24W | 320 K |
| 300 | 07S | 26E | 140 K |
| 332 | 10S | 06W | 210 K |
| 271 | 14S | 55E | 835 K |

Day 232
AUGUST 20, 1971 1813 UT
$L_o = 311^o$, $B_o = +7^o$

| L | LAT | CMD | 8 mm |
|---|---|---|---|
| 266 | 12N | 45E | 160 K |
| 292 | 09N | 19E | 455 K |
| 349 | 05N | 38W | 185 K |
| 353 | 03N | 42W | 180 K |
| 334 | 08S | 23W | 150 K |
| 269 | 13S | 42W | 655 K |

Day 233
AUGUST 21, 1971 1351 UT
$L_o = 299^o$, $B_o = +7^o$

| L | LAT | CMD | 8 mm |
|---|---|---|---|
| 288 | 05N | 11E | 340 K |
| 344 | 03N | 45W | 200 K |
| 341 | 07S | 42W | 110 K |
| 328 | 09S | 29W | 150 K |
| 268 | 13S | 31E | 665 K |
| 321 | 16S | 22W | 155 K |

Day 234
AUGUST 22, 1971 1510 UT
$L_o = 286^o$, $B_o = +7^o$

| L | LAT | CMD | 8 mm |
|---|---|---|---|
| 262 | 09N | 24E | 130 K |
| 291 | 08N | 05W | 290 K |
| 234 | 12S | 52E | 180 K |
| 269 | 14S | 17E | 495 K |

TABLE 1 Continued

Day 236
AUGUST 24, 1971 1415 UT
$L_o = 260^o$, $B_o = +7^o$

| L | LAT | CMD | 8 mm |
|---|---|---|---|
| 237 | 09N | 23E | 150 K |
| 290 | 07N | 30W | 405 K |
| 263 | 05N | 03W | 165 K |
| 234 | 12S | 26E | 295 K |
| 270 | 14S | 10W | 485 K |

Day 237
AUGUST 25, 1971 1454 UT
$L_o = 247^o$, $B_o = +7^o$

| L | LAT | CMD | 8 mm |
|---|---|---|---|
| 262 | 11N | 15W | 160 K |
| 289 | 06N | 42W | 330 K |
| 227 | 13S | 20E | 320 K |
| 271 | 13S | 24W | 390 K |

Day 238
AUGUST 26, 1971 1407 UT
$L_o = 233^o$, $B_o = +7^o$

| L | LAT | CMD | 8 mm |
|---|---|---|---|
| 257 | 08N | 22W | 130 K |
| 283 | 06N | 50W | 190 K |
| 200 | 02S | 33E | 210 K |
| 232 | 11S | 01E | 260 K |
| 270 | 14S | 37W | 250 K |

Day 241
AUGUST 29, 1971 1454 UT
$L_o = 194^o$, $B_o = +7^o$

| L | LAT | CMD | 8 mm |
|---|---|---|---|
| 235 | 09N | 41W | 120 K |
| 166 | 05N | 28E | 135 K |
| 203 | 00 | 09W | 200 K |
| 226 | 08S | 32W | 175 K |
| 168 | 13S | 26E | 175 K |
| 187 | 17S | 07E | 115 K |
| 215 | 17S | 21W | 215 K |

Day 242
AUGUST 30, 1971 1357 UT
$L_o = 181^o$, $B_o = +7^o$

| L | LAT | CMD | 8 mm |
|---|---|---|---|
| 158 | 06N | 23E | 180 K |
| 202 | 01S | 21W | 240 K |
| 226 | 09S | 45W | 150 K |
| 153 | 12S | 28E | 180 K |
| 163 | 17S | 18E | 185 K |
| 212 | 19S | 31W | 155 K |

Day 244
SEPTEMBER 1, 1971 1525 UT
$L_o = 154^o$, $B_o = +7^o$

| L | LAT | CMD | 8 mm |
|---|---|---|---|
| 131 | 09N | 23E | 200 K |
| 166 | 08N | 12W | 125 K |
| 202 | 03S | 48W | 195 K |
| 103 | 09S | 51E | 120 K |
| 109 | 13S | 45E | 115 K |
| 150 | 15S | 04E | 250 K |
| 136 | 17S | 18E | 180 K |

TABLE 2

Day 230
AUGUST 18, 1971 1355 UT
$L_o = 339^\circ$, $B_o = +7^\circ$

| | L | LAT | CMD | 20 mm |
|---|---|---|---|---|
| | 346 | 04N | 07W | 175 K |
| * | 296 | 07S | 44E | 250 K |

Day 231
AUGUST 19, 1971 1647 UT
$L_o = 326^\circ$, $B_o = +7^\circ$

| | L | LAT | CMD | 20 mm |
|---|---|---|---|---|
| | 352 | 04N | 26W | 160 K |
| * | 281 | 09S | 45E | 870 K |

Day 234
AUGUST 22, 1971 1510 UT
$L_o = 286^\circ$, $B_o = +7^\circ$

| L | LAT | CMD | 20 mm |
|---|---|---|---|
| 263 | 14S | 23E | 540 K |

Day 237
AUGUST 25, 1971 1454 UT
$L_o = 247^\circ$, $B_o = +7^\circ$

| L | LAT | CMD | 20 mm |
|---|---|---|---|
| 269 | 13S | 22W | 610 K |

Day 238
AUGUST 26, 1971 1407 UT
$L_o = 233^\circ$, $B_o = +7^\circ$

| | L | LAT | CMD | 20 mm |
|---|---|---|---|---|
| | 199 | 03S | 34W | 045 K |
| * | 262 | 09S | 29W | 460 K |

Day 241
AUGUST 29, 1971 1454 UT
$L_o = 194^\circ$, $B_o = +7^\circ$

| | L | LAT | CMD | 20 mm |
|---|---|---|---|---|
| | 163 | 09N | 31E | 060 K |
| | 161 | 01S | 33E | 070 K |
| * | 226 | 08S | 32W | 310 K |

Day 242
AUGUST 30, 1971 1357 UT
$L_o = 181^\circ$, $B_o = +7^\circ$

| | L | LAT | CMD | 20 mm |
|---|---|---|---|---|
| | 146 | 01S | 35E | 080 K |
| * | 213 | 08S | 32W | 260 K |

* Heliographic longitude given for reference only and is in error due to large beamwidth at 20 mm. Region corresponds to L269,S13.

REFERENCE

1972 Solar-Geophysical Data, Descriptive Text, Number 330 (Supplement), February, 1972, U.S. Department of Commerce, (Boulder, Colorado U.S.A. 80302), 21.

# Dynamic Radio Spectra of the Solar Flare of 1971 September 1 1930 UT

by

A. Maxwell
Harvard Radio Astronomy Station, Fort Davis, Texas 79734

During 1971, the solar dynamic radio-spectrum analyzer at the Harvard Radio Astronomy Station, Fort Davis, Texas, operated over the complete band 10-2000 MHz. Descriptions of the equipment will be found elsewhere [Thompson, 1961; Maxwell, 1971]. The receivers in the band 500-2000 MHz were put into operation in 1970 and are connected to a steerable 85-ft antenna, whose large collecting area permits solar bursts in this band to be recorded at high sensitivity.

The radio burst recorded on 1971 September 1 at Fort Davis was of much shorter duration than that of January 24 (see p. 69 ). Figure 1 shows a type II burst commenced in the meter band at 19hr 33min 40sec and continued until about 1948 UT. Type IV radiation was recorded in the decimeter band from 19hr 34min 30sec until approximately 1950 UT. In the optical band, the Lockheed, Boulder, and Palehua Observatories, although making observations at the time, did not report sighting any flare. However, Dr. Helen Dodson-Prince (private communication) reports that at the McMath-Hulburt Observatory, although observing conditions were poor, prominence activity was observed off the West limb of the sun at latitude S10 when the clouds cleared at 1953 UT. Further prominence activity was observed at the same location during the following hour. Dr. Dodson-Prince also reports that one of the biggest active areas of the present solar cycle had just passed over the solar limb, and suggests that the whole solar event fits the pattern of proton storm events that have originated from flares that have occurred just beyond the West limb.

REFERENCES

MAXWELL, A. 1971 Solar Phys., 16, 224.

THOMPSON, A. R. 1961 Astrophys. J., 133, 643.

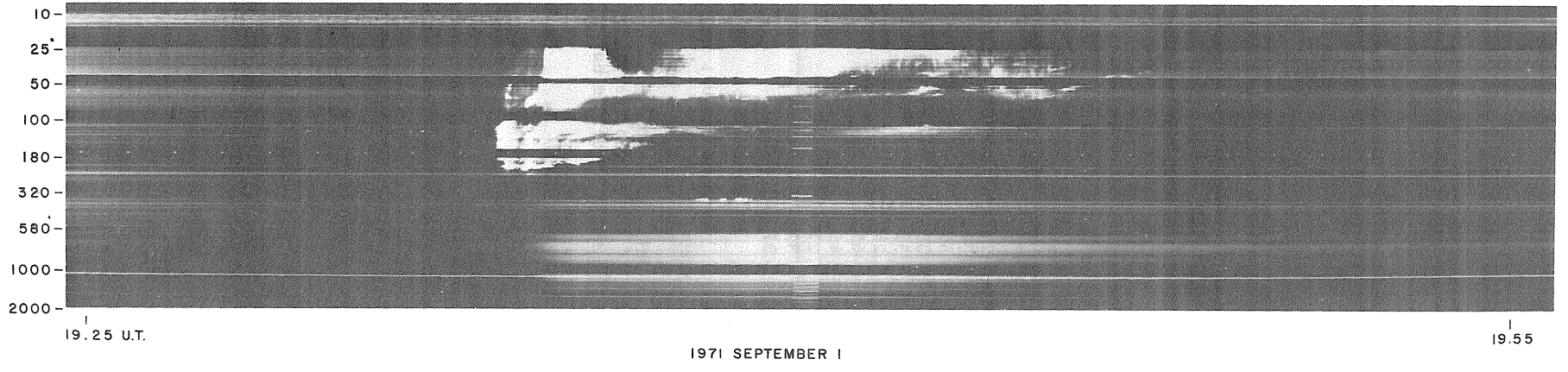


Fig. 1. Dynamic spectra of the solar radio burst recorded at the Harvard Radio Astronomy Station, Fort Davis, Texas.

# September 1, 1971, Solar Radio Burst Observation

by

W. R. Barron
Air Force Cambridge Research Laboratories
Bedford, Massachusetts

A proton and ground-level event started this date which was associated with a solar radio burst beginning about 1926 UT. The PCA at 30 MHz, which started September 1 at about 2030 UT, ultimately reached 5.6 dB absorption at 1800 UT on September 2 at Thule Air Base, Greenland. The ground level event reached a maximum of 12% above normal near 2250 UT on September 1. Satellite sensors of greater than 25 Mev particles reached a maximum September 2 near 0400 UT with an enhancement of greater than 50 times normal. Only small X-ray increases were observed.

The solar radio burst was the best indicator of the parent event which apparently took place in McMath Region 11482 at S11, L = 269° which was then estimated to be 30° beyond the west limb. No flare was observed. The only optical evidence was an active prominence seen starting on September 1 at 1944 UT on the west limb near S11.

The Sagamore Hill solar radio data are as follows:

| Frequency (MHz) | Time (UT) | | Duration | Flux Density $10^{-22}$ W m$^{-2}$(Hz)$^{-1}$ | | Type of Event |
|---|---|---|---|---|---|---|
| | Start | Max | Min | Peak | Mean | (SGD Classification) |
| 15400 | 1934.3 | 1941.2 | 21.7 | 21.6 | 10.1 | 20 |
| 8800 | 1930.7 | 1940.9 | 34.0 | 36.1 | 18.0 | 22 |
| 4995 | 1929.1 | 1940.5 | 50.1 | 68.0 | 26.2 | 22 |
| 2695 | 1926.9 | 1940.5 | 35.3 | 120.0 | 40.0 | 04 |
| 1415 | 1926.9 | 1939.6 | 33.8 | 160.0 | 45.0 | 04 |
| 606 | 1931.1 | 1940.4 | 28.9 | 150.0 | 45.0 | 04 |
| 410 | 1932.1 | 1940.3 | 65.0 | 88.0 | 40.0 | 06 |
| 245 | 1931.3 | 1934.4 | 65.7 | 810.0 | 320.0 | 47 |
| 2695 | 2002.2 | 2002.2 | 27.8U | 13.0 | 5.5 | 29 |
| 1415 | 2000.7 | 2000.7 | 32.7 | 15.4 | 7.7 | 29 |
| 606 | 2000.0 | 2000.0 | 37.0 | 14.7 | 7.3 | 29 |

24-48 MHz Group of type III's: 1934.2-1936.3 UT; intensity 2; type IV: 1937.0-1946.9 UT; intensity 2; 30 MHz burst increase.

One of the important uses of these data is in studies of the solar radio burst heights and probable electron densities from knowledge of the probable angular burst position beyond the solar limb, the observed burst spectrum, and probable spectrum of the burst if it had occurred on the visible disk.

# Analysis of the Polarization of the Solar Radio Emission at 237 MHz, during the Period 17-31 August 1971, Coming from the McMath Region 11482, Responsible for the Event of September 1, 1971

by

Paolo Santin
Astronomical Observatory
Trieste, Italy

The event that determined the ground level cosmic ray increase of September 1, 1971 originated in the McMath Region 11482, which on that day was not visible on the solar disk since it crossed the West limb on August 31, 1971.

In this paper the solar radio emission at 237 MHz coming from that active zone will be analyzed with particular emphasis on the circular polarization of the background radiation. The period considered is August 17-31, 1971, viz. the whole passage on the visible disk of McMath Region 11482. It was possible to make this analysis, even with an instrument with low resolution power, since during that period McMath Region 11482 was the only active solar region from a radio point of view.

Our receiver, fed by a ten meter parabolic antenna, is a radiopolarimeter functioning at 237 MHz with a bandwidth of 0.5 MHz [Sedmak, 1970]. Its output gives the sum and the difference of the two circularly polarized components, L + R and L - R, with a low time resolution (20 cm/h) and also the details of the two separate components L and R with high time resolution ( $\geq$ 2 mm/sec). We thus have the total flux and the degree of circular polarization m = (L-R)/(L+R), whose accuracy can generally be considered better than 10%.

Figure 1 shows the behavior of the daily mean emission during the whole passage of the active region on the visible disk. A noise storm developed with its characteristic directivity in a rather large frequency range, at least from 30 to 540 MHz (see Spectral Data from Weissenau Bulletin). The maximum emission occurred on August 24 at 1330.36 UT, with a flux density of 546 solar flux units ($10^{-22}$ $Wm^{-2}Hz^{-1}$).

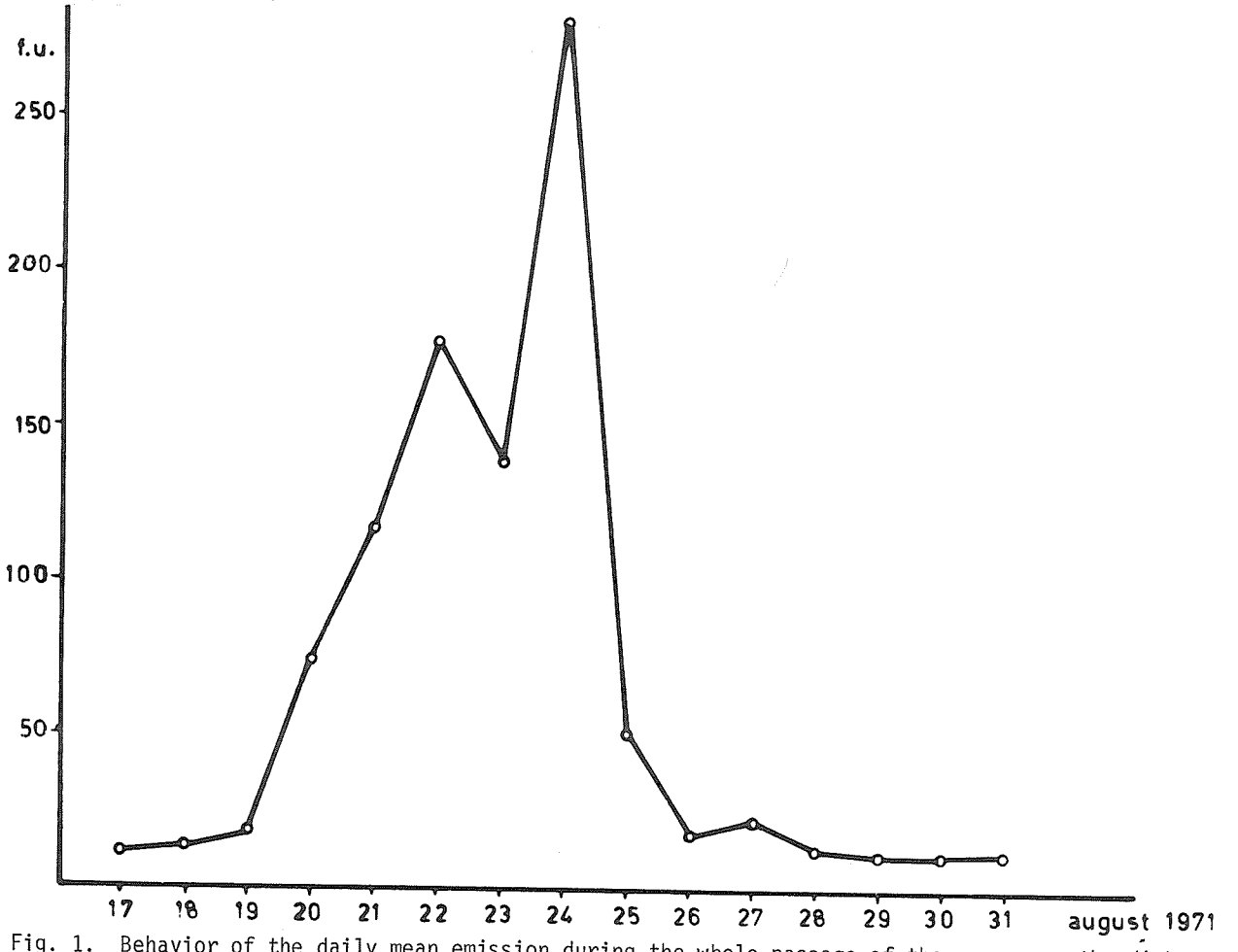


Fig. 1. Behavior of the daily mean emission during the whole passage of the source on the disk.

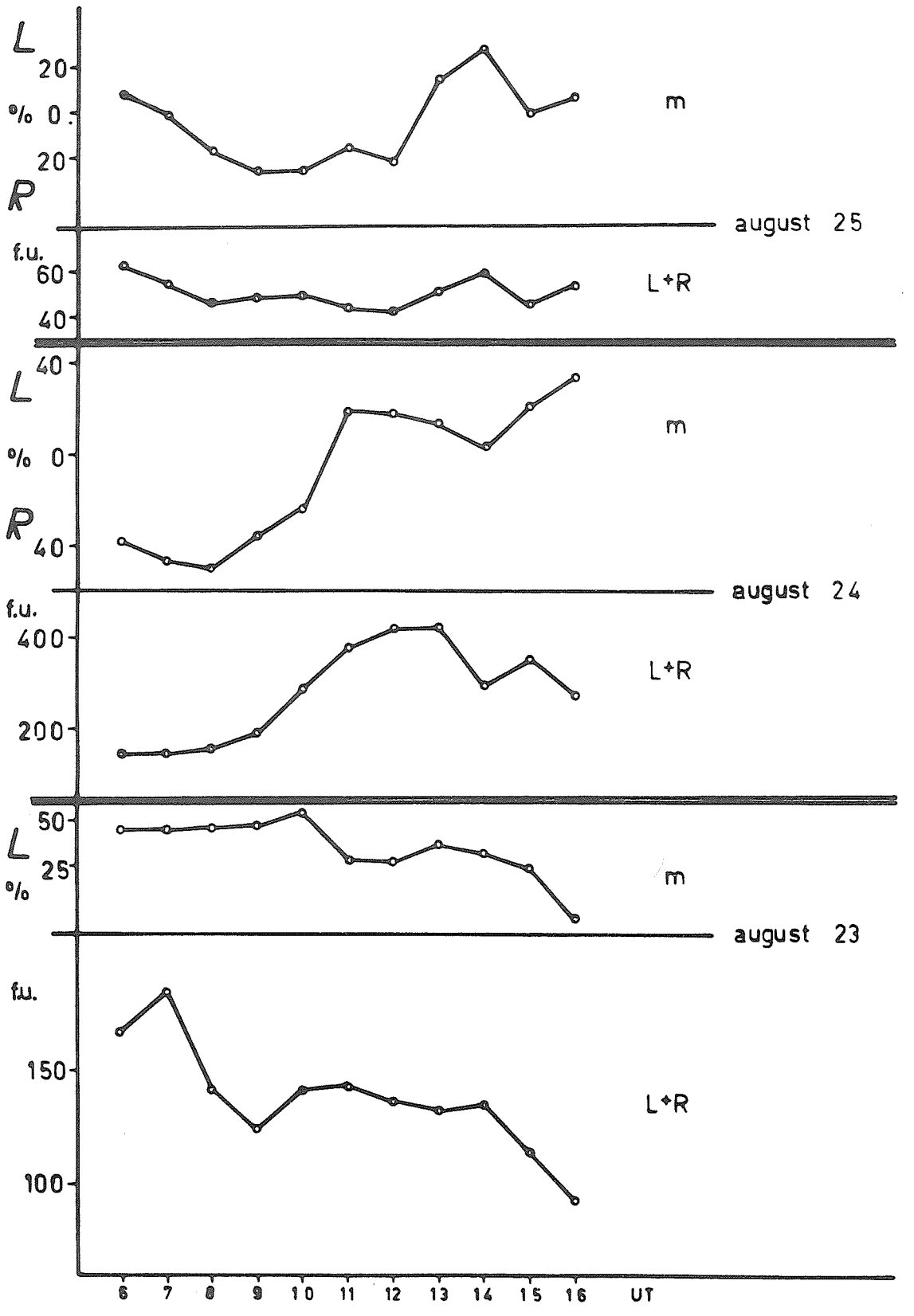


Fig. 2. Total flux and degree of circular polarization during the days of August 23, 24 and 25. The means are referred to the hour following that marked.

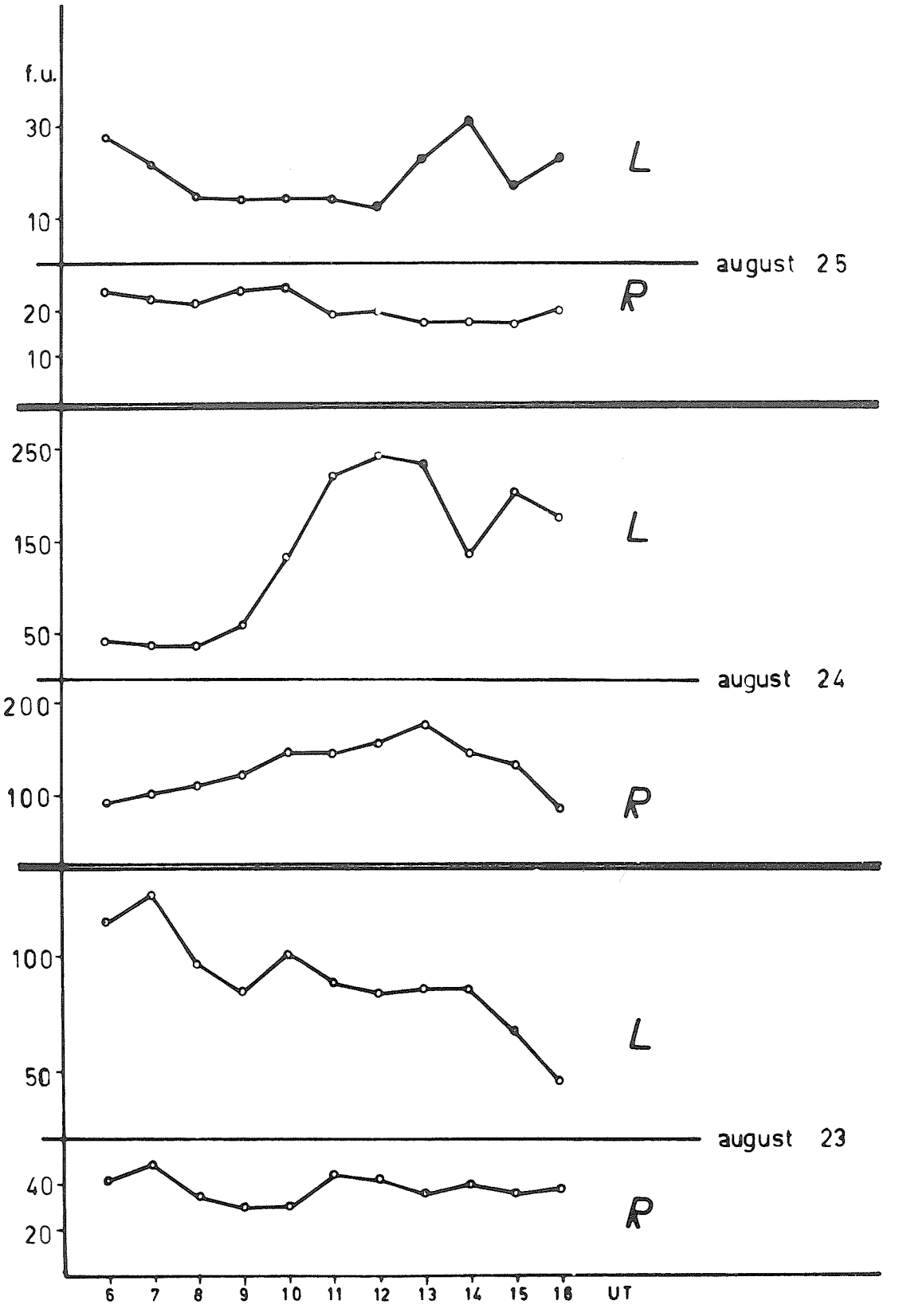


Fig. 3. Behavior of the two separate components, oppositely polarized, during the days of August 23, 24 and 25. The means are referred to the hour following that marked.

Figures 2 and 3 show the behavior of the total flux and of the degree of polarization on the days of August 23, 24 and 25, the most peculiar days of the whole passage. During the other days the polarization percentage was rather stable, at about 50% left polarization.

From a general analysis of the diagrams, and also of the recordings on the other days, one can draw two conclusions: (1) generally the left-handed polarized radiation prevails. This causes the variability of the degree of circular polarization. (2) Since the general trend of the two components is often similar, it is probable that unpolarized radiation is present which in our case splits up equally in the two channels, thus determining the parallel behavior of the two components.

As far as August 24 is concerned, enhancement of the background is present in both channels, but with a delay between them. This delay seems to exclude the presence of unpolarized radiation, and, therefore, we probably have a quasi-contemporary enhancement of the two different sources caused by a unique agent. Moreover, the behavior of type I activity on the same day is rather interesting, although they are not directly considered in this paper: type I bursts are present with a prevalent left-handed polarization until 1000 UT. They disappear almost completely from 1000 until 1400 UT, reappear again, practically unpolarized, from 1400 until 1500 UT, and finally disappear from 1500 UT until the end of the recording. It is interesting to note that the periods during which type I disappear correspond to the two enhancements of the background and to the two periods during which the radiation is left-handed polarized. This behavior of type I activity is perhaps understood by supposing that the two enhancements are due to a type IV event not perfectly recognized. In fact, spectral data published in "Solar-Geophysical Data", 326 Part I, show a type IV event from 1000 UT only in the dekametric band, while in the metric band there is a type IV only from 1400 UT. This is also supported by the fact that the continuum is very similar to the continuum of a type IV burst when observed at a single frequency.

On September 1, 1971, after the sources crossed the West limb, the emisssion decreased to a minimum level (12 flux units) and stayed absolutely quiet all day.

REFERENCES

SEDMAK, G. 1970 Osservazioni Solari, 18 suppl., Trieste.

# Radio Bursts Associated with Solar Proton Flare on September 1, 1971

by

Kunitomo Sakurai
Radio Astronomy Branch
Laboratory for Extraterrestrial Physics
NASA/Goddard Space Flight Center
Greenbelt, Maryland 20771

## 1. Introduction

Solar flares which produce high-energy particles, so-called solar cosmic rays, generally accompany radio bursts of spectral type IV. It is known that the microwave component of these bursts is a good indicator of the generation of high-energy particles in solar flares [e.g., Kundu and Haddock, 1960; Sakurai and Maeda, 1961].

In this paper, we will consider some characteristics of solar radio bursts as obtained by satellite and ground-based observations on September 1, 1971. Since the IMP-I satellite has been recording solar radio emissions after launch on March 13, 1971, we are able to show the observed results on hectometric radio emissions as observed by this satellite in the case of the September 1, 1971 event along with the Clark Lake Observatory data. In this case, we can analyze frequency-onset time relationship for the initial stage of the development of radio bursts of wide frequency band.

## 2. Radio Bursts on September 1, 1972

Decametric and hectometric radio bursts were associated with the solar flare which seemed to have occurred at about 1925 UT on September 1, 1971. This flare was not directly observed since it occurred about 40 degrees beyond the west limb of the solar disk, but it accompanied the generation of solar cosmic rays and extensive solar radio bursts, both of which were observed on the earth. The record on decametric radio bursts as observed at the Clark Lake Observatory is shown in Figure 1. This shows that weak continuum emission, which seems to be classified as decametric type IV burst, was only observed in addition to intense type II and IV radio bursts. Radio emissions at hectometric frequencies were detected by the IMP-I satellite.

As has been mentioned above, we do not know the exact position of the flare because the sunspot group which produced this flare had already disappeared behind the west limb on August 29, 1971. For this reason, we have no optical data on this flare. By making use of radio data from microwave to hectometric frequencies, we have estimated the starting time of the explosive phase for this flare. Relation between frequency and the onset time of radio emissions is shown in Figure 2.

The result indicates that the start of microwave emissions was delayed more than 7 minutes in comparison with decametric emission around 2000 MHz. However, we do not know as yet whether this delay was produced in connection with the development of the flare, though it seems that this delay was related to some screening effect by the solar disk itself on microwave emissions. If this effect can really explain such a delay, we may estimate a possible relation of the starting times of microwave emissions to frequency by extrapolating the observed relation between onset time and frequency in metric and decimetric frequencies. In doing this, we need to consider the result as obtained in the case of the solar flare on July 7, 1966 [Sakurai, 1971]. Thus we have obtained a possible trend for starting times on microwave frequency range as indicated by the dot-dash line in Figure 2. This trend suggests that the explosive phase started around 1925 UT.

About 15 minutes later after the onset of the explosive phase, the peak flux for each frequency of type IV burst was reached at about 1940 UT as indicated in Figure 2. The spectrum of peak fluxes for microwave and decimetric frequencies is not similar to that which has been deduced by Castelli et al. [1967, 1968] in regard to solar proton flares. The result is shown in Figure 3.

In this event, several trends of drifting radio bursts were detected in low frequency range. Evidence of such radio bursts suggests that several radio sources were consecutively ejected from the flare region.

The relation of observed frequency to angular-distance from the sun-earth line has been obtained for the path of the radio source of type III bursts at hectometric frequencies. Though the result thus obtained is very tentative, two trends for the path of such source have been detected as shown in Figure 4.

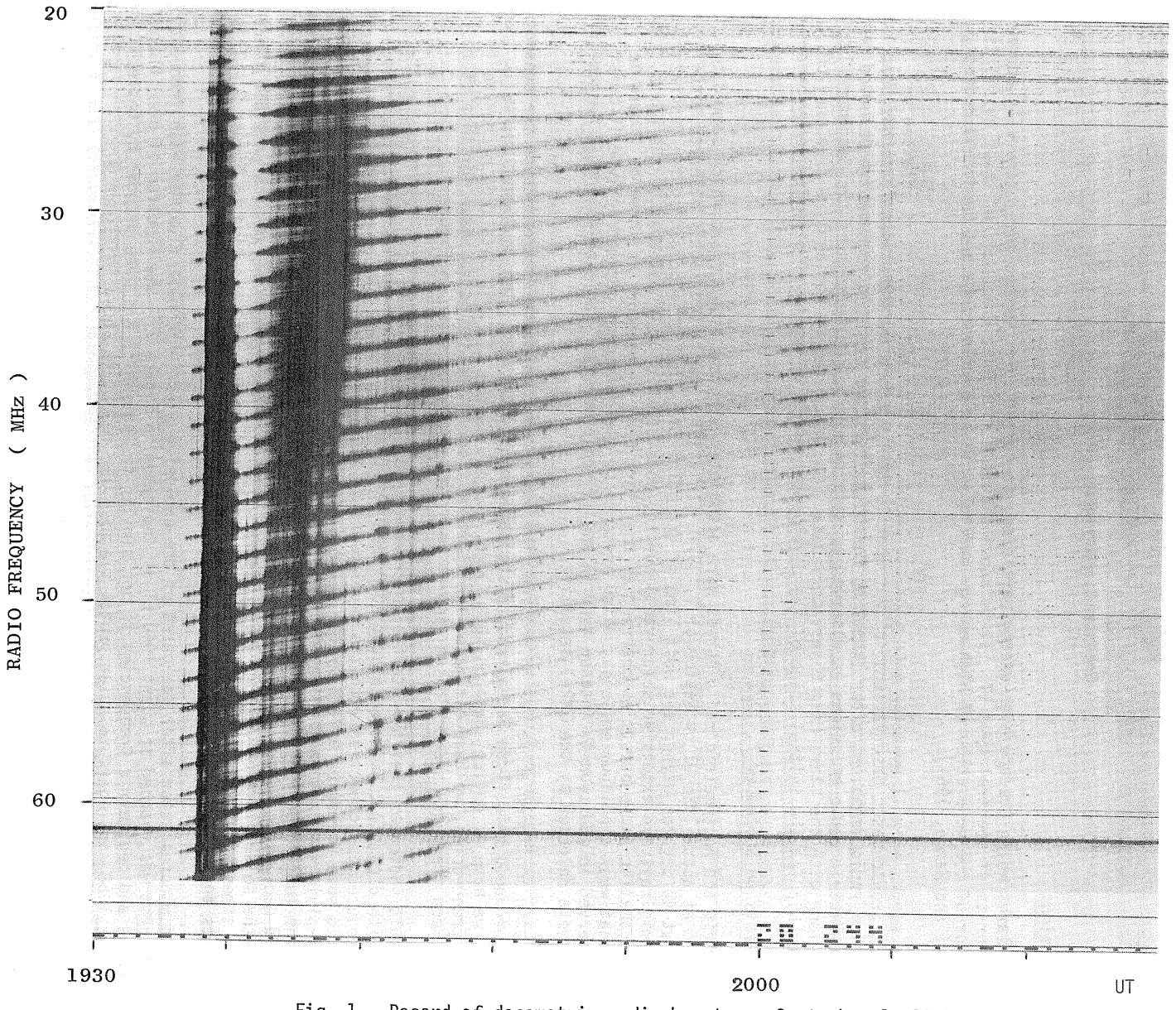


Fig. 1. Record of decametric radio bursts on September 1, 1971.

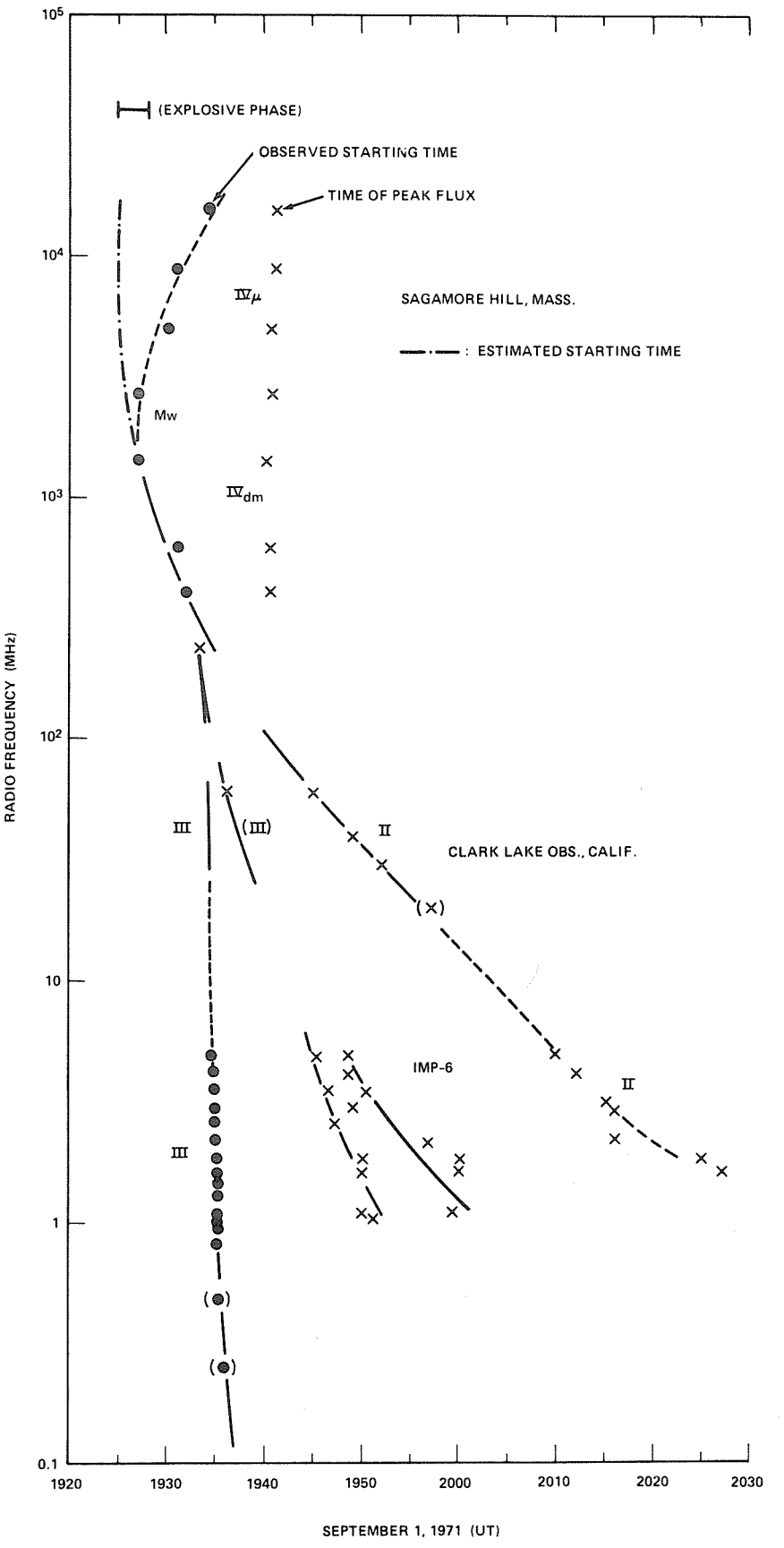


Fig. 2. The time sequence of the occurrence of radio burst of spectral type MW, IV, II and III. Hectometric type II and III radio bursts are seen.

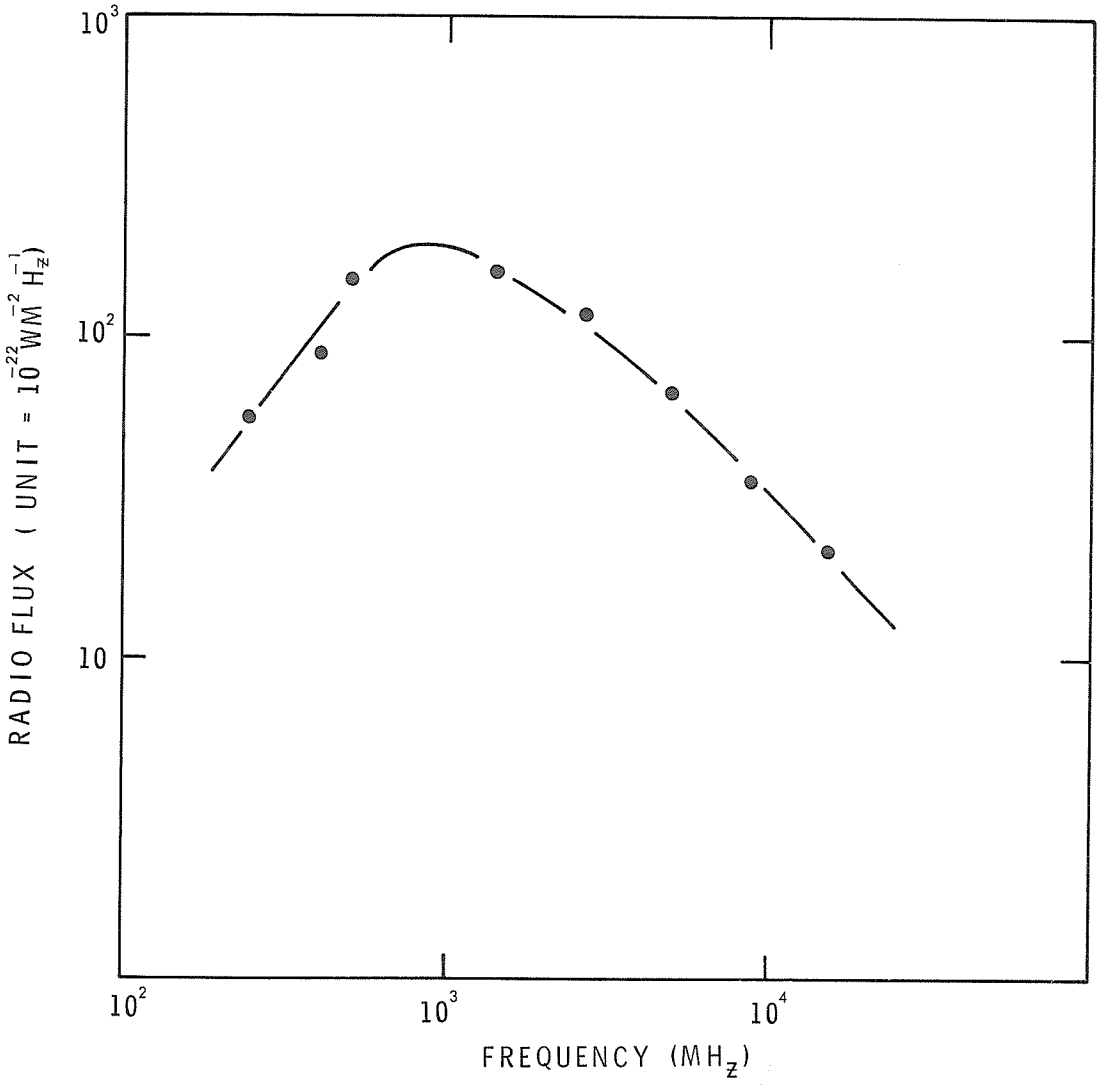


Fig. 3. The peak flux spectrum of type IV radio burst on September 1, 1971.

## 3. Discussion

In the case of the solar flare on September 1, 1971, the sources for type II and III radio bursts were ejected from the flare site during the explosive phase. During this phase, both microwave impulsive and type IV radio bursts at microwave frequencies must have been emitted, although we have not observed them at all, as is evident from Figure 2. We do not know as yet what mechanism produced such depression of the intensity of these bursts, but we may consider two alternative interpretations for such results. The first takes into account that the source for these bursts was too low to be seen from the earth, because the flare site was beyond the west limb of the solar disk. This is a reason why the onset of both bursts was so much delayed in comparison with that of decimetric radio emissions, a component of microwave impulsive bursts on the lower frequency side. The second one assumes that the position of the source for microwave emissions was high enough in order to be seen from the earth, but the emission directivity at microwave frequencies was so narrow that the emission did not directly reach the earth's observers.

## Acknowledgement

I would like to thank Dr. R. G. Stone and Dr. J. Fainberg for their supply of the valuable data on solar radio emission for this event. Comments by Dr. J. Fainberg are appreciated.

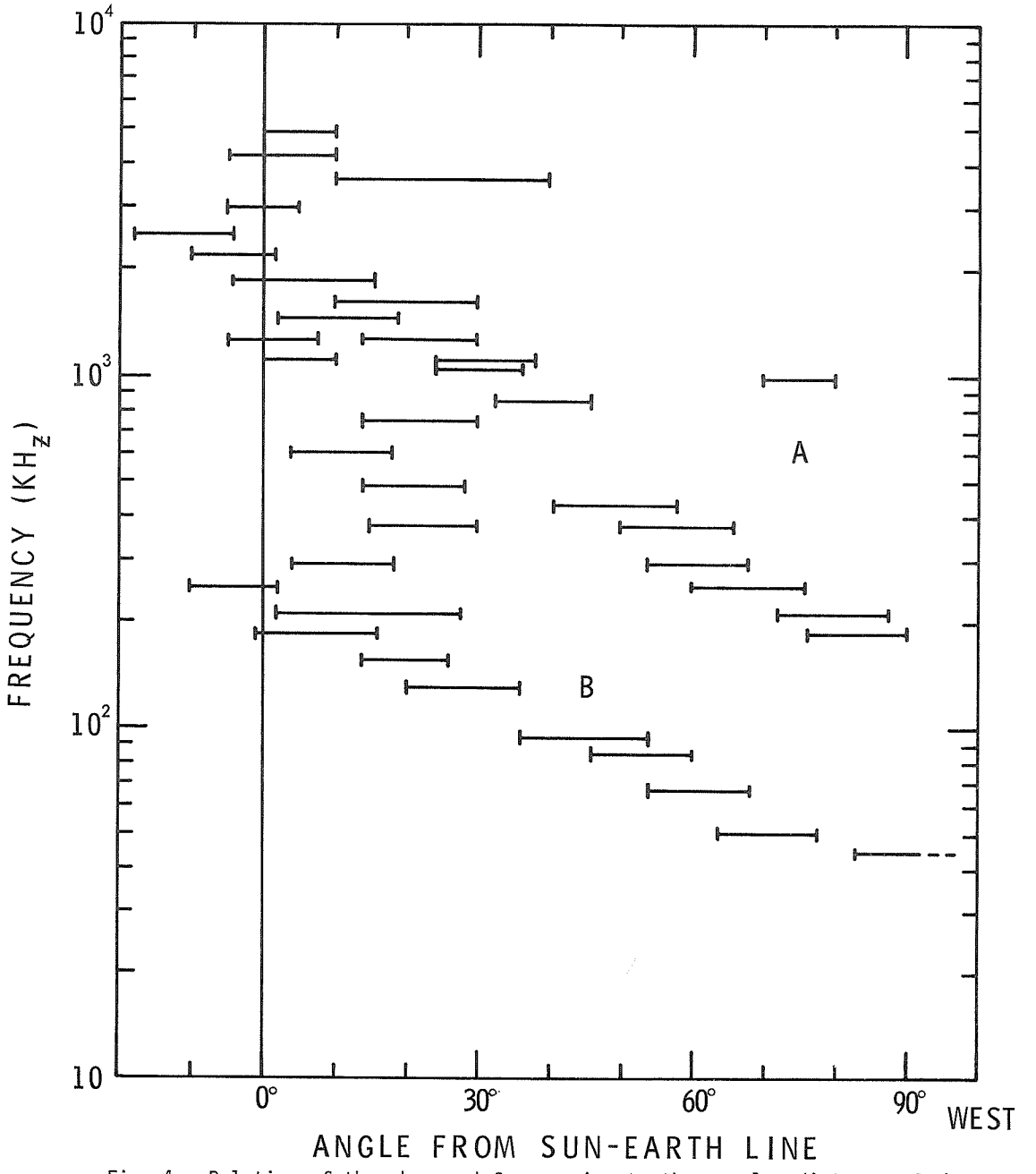


Fig. 4. Relation of the observed frequencies to the angular distance of the radio source with respect to the sun-earth line.

REFERENCES


| | | |
|---|---|---|
| CASTELLI, J. P., J. AARON, and G. A. MICHAEL | 1967 | J. Geophys. Res., 72, 5491. |
| CASTELLI, J. P., J. AARON, and G. A. MICHAEL | 1967 | Ap. J., 153, 26. |
| KUNDU, M. R. and F. T. HADDOCK | 1960 | Nature, 186, 610. |
| SAKURAI, K. | 1971 | Solar Physics, 20, 147. |
| SAKURAI, K. and H. MAEDA | 1961 | J. Geophys. Res., 66, 1966. |

# VLF and Solar Observations during the Event of September 1, 1971

by

S. Ananthakrishnan, D. Basu, L. R. Piazza and M. E. Z. Mellone
Centro de Rádio Astronomia e Astrofísica
Universidade Mackenzie
São Paulo, Brazil

## VLF Observations

The phase of VLF signals from transmitters NAA (17.8 kHz), Cutler, Maine, U.S.A. and NLK (18.6 kHz), Seattle, Washington, U.S.A., was recorded at São Paulo, Brazil during September 1971. No noticeable effect was present on the phase of either trajectory during the daytime, in the period August 29 to September 5. However the nighttime phase on NAA showed a deviation of $\simeq$ 7 μsec from normal on the 3rd and 5th of September (see Figure 1). In this Figure the quiet days are August 29 and September 8. Values of $\sigma$ (the standard deviation) are $\pm$ 2 μsec at night on the NAA-São Paulo path. Hence both on September 3 and September 5 there were significant deviations from normal. Possible reasons for this have been discussed in a recent paper [Ananthakrishnan, S. and B. Hackradt, 1972].

The trajectory NLK-São Paulo exhibited marked deviations from normal on the 3rd and 5th of September (between 0400 and 0700 UT), shown in Figure 2. Maximum deviations were of the order of 7 μsec ($\sigma = \pm$ 4 μsec).

## Solar Radio Observations

The sun was observed by the 7 GHz polarization-radio telescope [Kaufmann, P., 1971] at the Itapetinga Radio Observatory (22° 11' S, 46° 33' W), São Paulo, Brazil between the hours 1040-2015 UT (with interruption 1520-1537 UT). The daily mean flux value of the day was $201 \times 10^{-22}$ $Wm^{-2}Hz^{-1}$ with no appreciable polarization. The bursts observed during the patrol period are summarized in Table 1 and the unpolarized burst (Simple 2F with PBI), the largest event of the day, is reproduced in Figure 3.

Table 1

| Type* | Class | Start UT | Max UT | Duration Min. | Peak Flux $\times 10^{-22} Wm^{-2}Hz^{-1}$ | Peak Polarization Percent |
|---|---|---|---|---|---|---|
| 23 | Simple 3AF | 1717.6 | 1723.1 | 50.9 | 8.2 | 70.7 L |
| 8 | Spike | 1722.6 | 1723.1 | 0.6 | 6.5 | 88.4 L |
| 1 | Simple 1 | 1931.0 | 1933.0 | 3.0 | 4.6 | 0.0 |
| 4 | Simple 2F | 1934.0 | 1941.0 | 19.0 | 53.3 | 0.0 |
| 29 | PBI | 1953.0 | - | 12.0 | - | - |

* As given in "Solar-Geophysical Data".

## REFERENCES

ANANTHAKRISHNAN, S. and B. HACKRADT 1972 Forbush Decrease in the Flux of Galactic Cosmic Rays and Associated VLF Nighttime Propagation Phenomenon, Planetary and Space Science, 20, 81-87.

KAUFMANN, P. 1971 Report from Solar Institute, Pierre Kaufmann/The New Intapetinga Radio Observatory, from Mackenzie University, São Paulo, Brazil, Solar Physics, 18, 336.

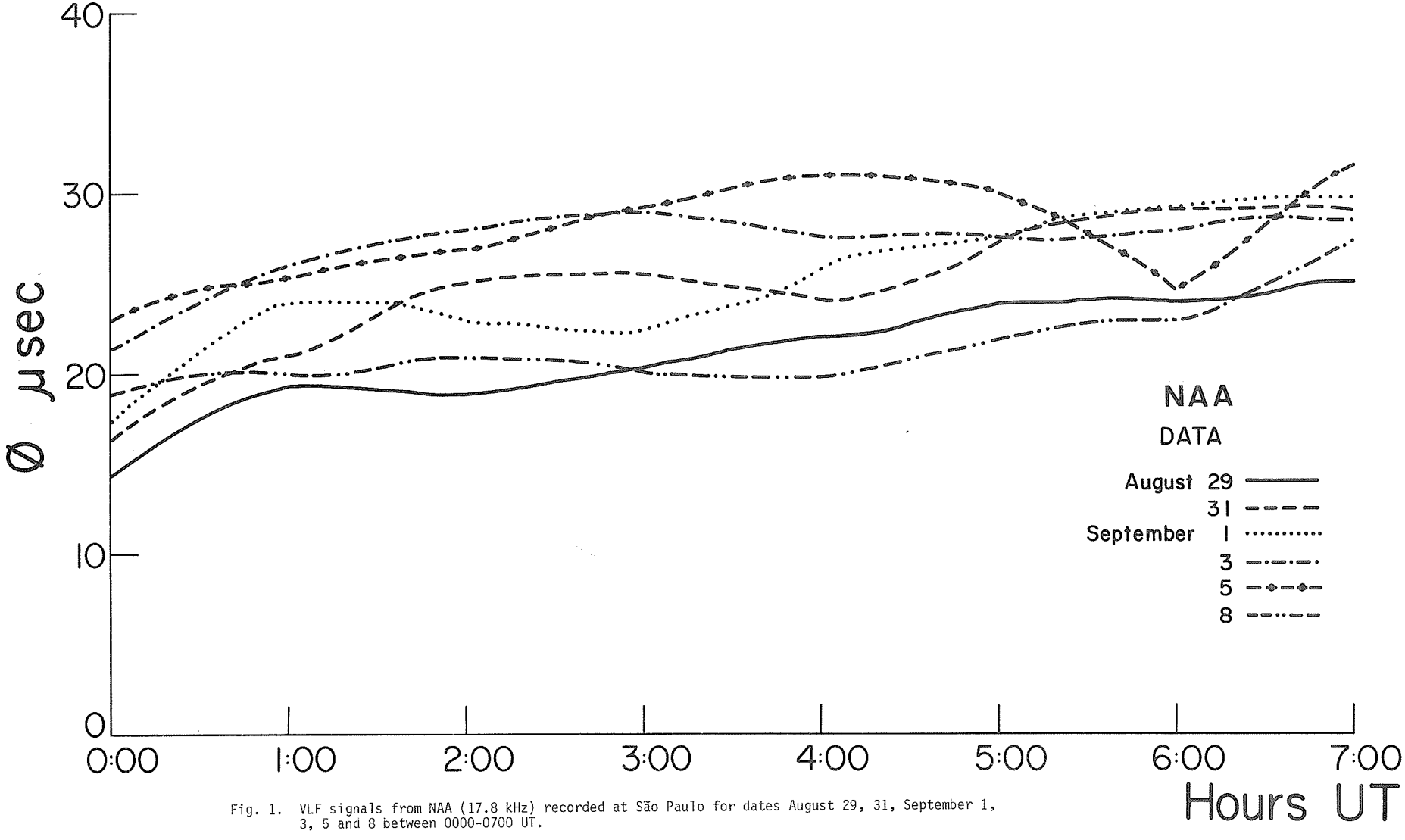


Fig. 1. VLF signals from NAA (17.8 kHz) recorded at São Paulo for dates August 29, 31, September 1, 3, 5 and 8 between 0000-0700 UT.

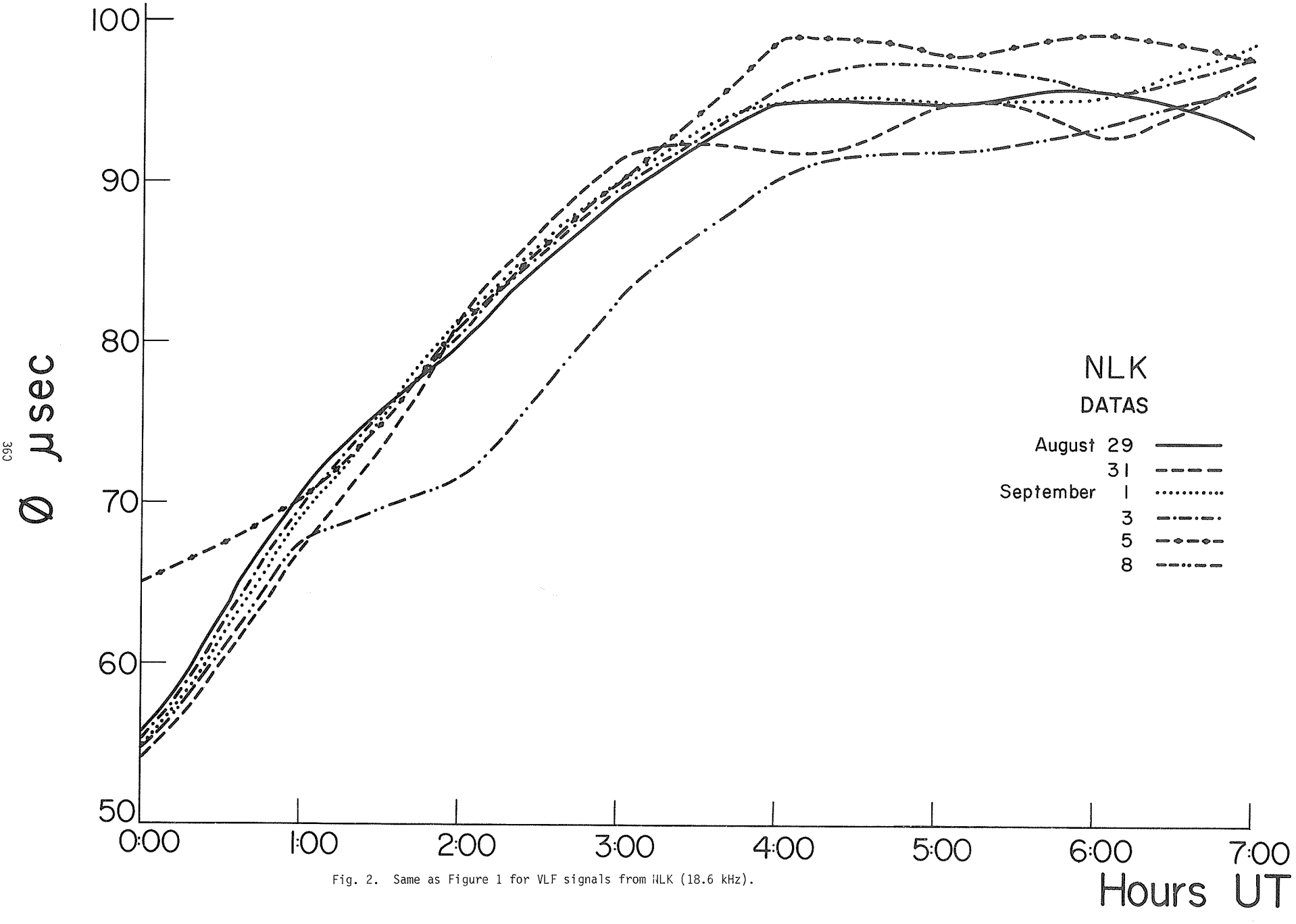


Fig. 2. Same as Figure 1 for VLF signals from NLK (18.6 kHz).

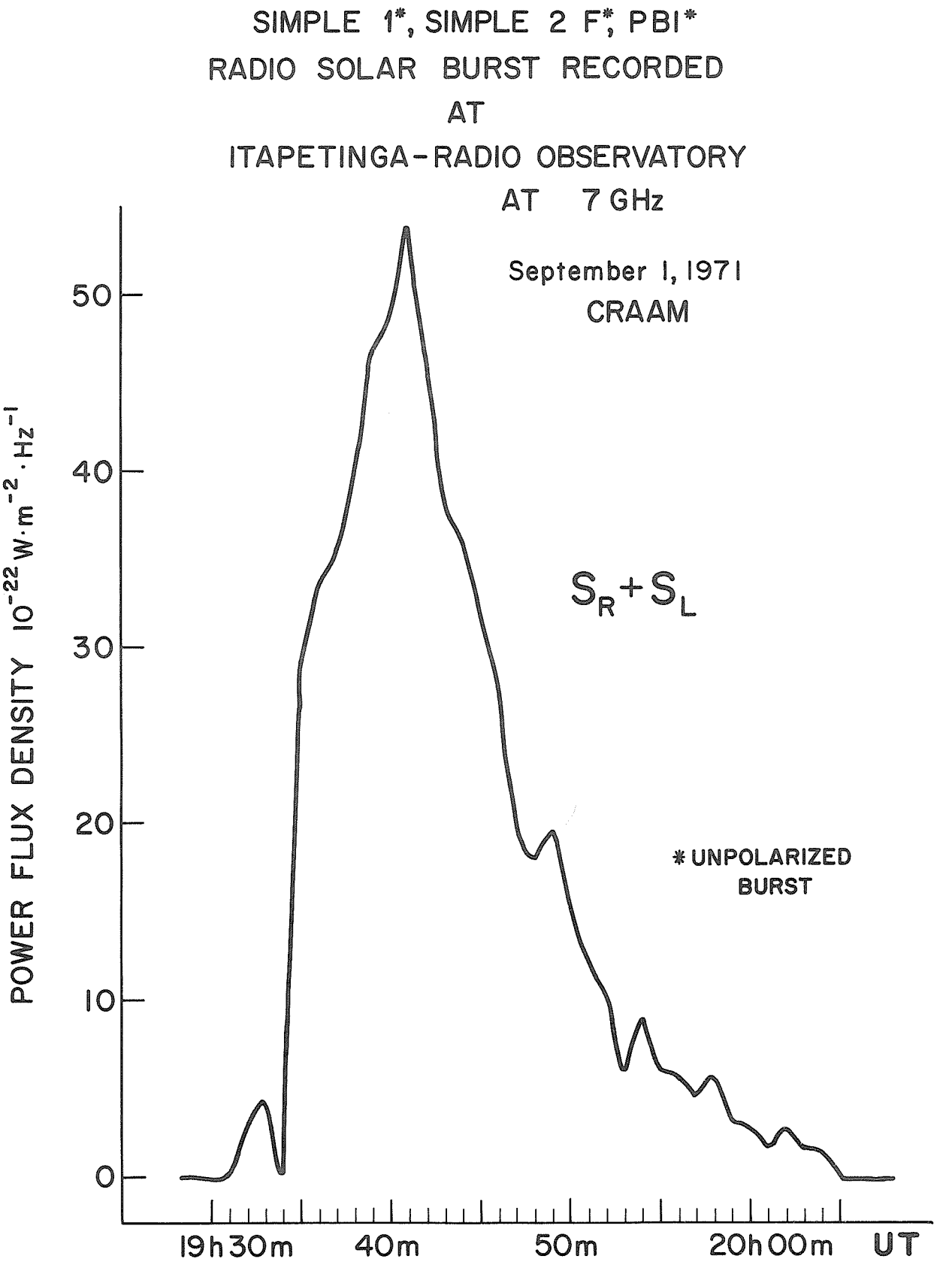
SIMPLE 1*, SIMPLE 2 F*, PBI*
RADIO SOLAR BURST RECORDED
AT
ITAPETINGA-RADIO OBSERVATORY
AT 7 GHz
September 1, 1971
CRAAM
$S_R + S_L$
* UNPOLARIZED BURST
POWER FLUX DENSITY $10^{-22}$ W·m$^{-2}$·Hz$^{-1}$
50
40
30
20
10
0
19h30m
40m
50m
20h00m
UT

Fig. 3.

## 4. SPACE OBSERVATIONS

## Solar X-Ray and Ultraviolet Emission on September 1, 1971

by

D. M. Horan, R. W. Kreplin, and R. G. Taylor
E. O. Hulburt Center for Space Research
Naval Research Laboratory
Washington, D. C. 20390

The records of solar X-ray emission obtained by the Naval Research Laboratory's SOLRAD 9 satellite (Explorer 37, 1968-17A) on September 1, 1971 are shown as Figure 1. The top curve on each plot represents the solar X-ray energy flux in the 8 to 20 Å band. In both cases, a gray-body solar emission spectrum [Kreplin, 1961] with a 2 x $10^6$°K color temperature was assumed in converting from ionization chamber current levels to energy flux units. The third curve from the top represents solar energy flux in the 0.5 to 3 Å band based on a gray-body emission spectrum with a 10 x $10^6$°K color temperature for the emitting solar region. The curve is quite intermittent because the 0.5 to 3 Å solar energy flux is usually below the threshold level of the detector.

The X-ray emission is plotted in units of ergs/cm$^2$ sec on a logarithmic scale. The abscissa is linear with the integers denoting hours in Universal Time (UT). Charged particle interference with the X-ray sensors, which can cause the plotted flux values to be higher or lower than the actual flux, is indicated by the lowest data curve. The ionization chamber current caused by the charged particle background is digitized and recorded as a "count". The number of "counts" plotted is linearly related to the current generated in the 0.5 to 3 Å ionization chamber by penetrating charged particles when the detector is facing away from the sun. Counts of 10 to 15 indicate negligible particle interference. Counts of 20 to the maximum value of 127 indicate significant particle interference. The data processing computer program inhibits the plotting of data obviously contaminated by particle interference, and this feature causes randomly spaced data gaps of 30 minutes duration or less.

The record of solar X-ray emission obtained by SOLRAD 9 on September 1, 1971 is shown as Figure 1. The solar X-ray emission in the 1 to 8 and 8 to 20 Å bands was at a very low level at the beginning of the day, and decreased steadily until the satellite passed behind the Earth at 1920 UT. For several hours after 1500 UT, the 1 to 8 Å band emission was so low that the solar signals were at the experiment amplifier's noise level. When the satellite emerged from the Earth's shadow at 1959 UT, a small X-ray flare was in progress. Data from NRL's SOLRAD 10 satellite (1971-058A) were used to verify that the X-ray enhancement began prior to 1928 UT and that peak emission of 1.9 x $10^{-3}$ ergs/cm$^2$ sec in the 1 to 8 Å band occurred at 2004 UT. By 2400 UT, the emission in the 1 to 8 Å band had decayed to approximately 3 x $10^{-4}$ ergs/cm$^2$ sec with no additional flare activity. X-ray emission in the 1 to 8 Å and 8 to 20 Å bands decreased steadily throughout the day on September 2 with no flare activity. Therefore, the X-ray activity on September 1 was insignificant as viewed from Earth. This does not eliminate the possibility that the X-ray emission seen at Earth was a small portion of the X-ray emission from a large event extending high into the corona and centered over an active region 20° or 30° around the west limb.

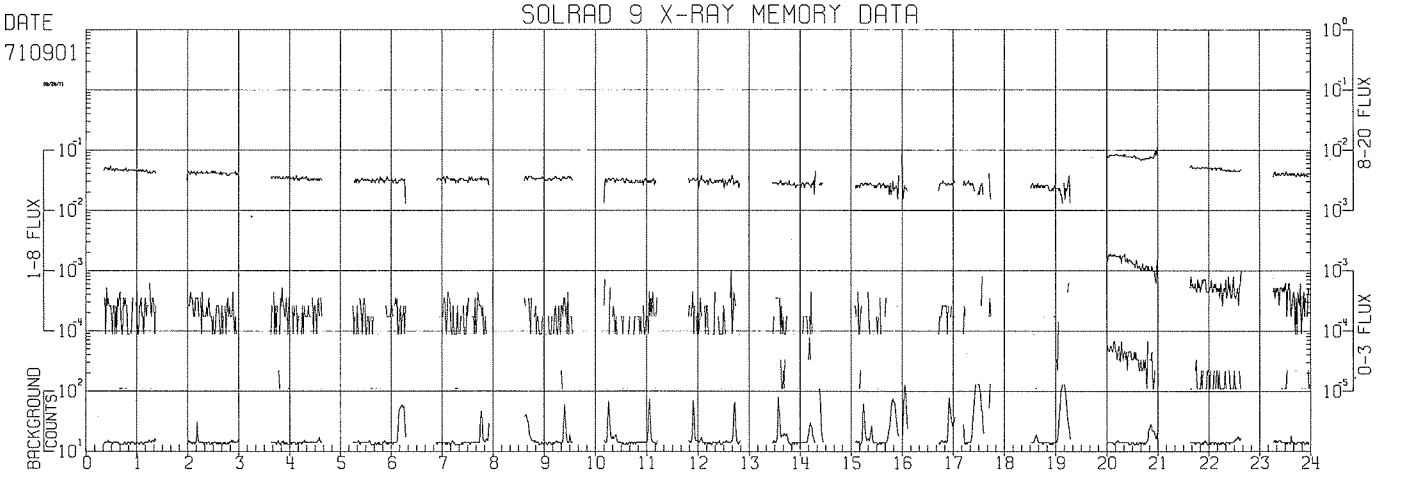


Fig. 1. Solar X-ray flux on September 1, 1971.

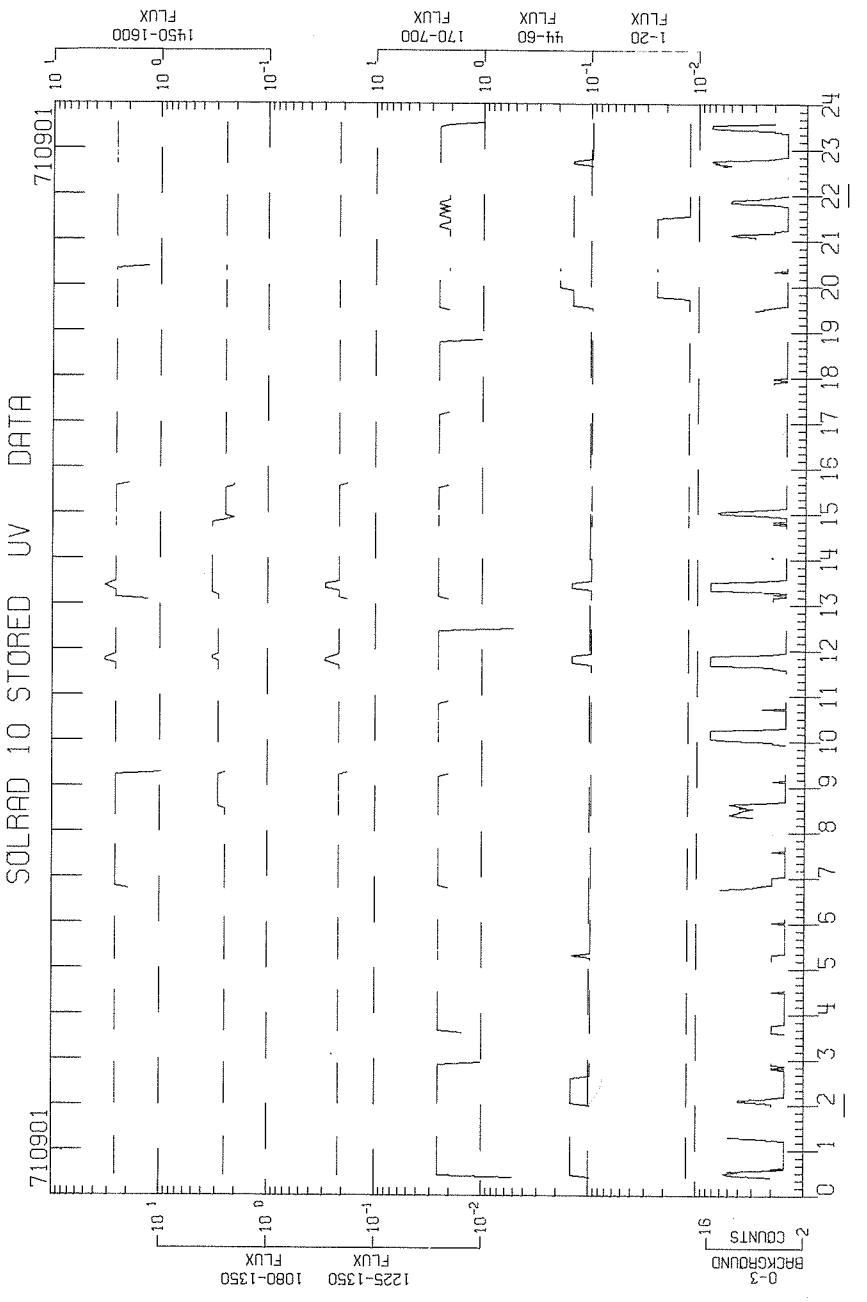


Fig. 2. Solar ultraviolet flux on September 1, 1971.

The record of solar ultraviolet emission on September 1, 1971 is shown as Figure 2. The data were obtained from sensors aboard NRL's SOLRAD 10 satellite (Explorer 44, 1971-058A). The general structure of the plot is identical to the SOLRAD 9 X-ray plots in that the abscissa is linearly scaled in hours of Universal Time, and the ordinate is logarithmically scaled in units of energy flux, ergs/cm$^2$ sec. Charged particle interference, which can cause the plotted flux values to be higher than the actual flux, is indicated by the lowest data curve. The number of "counts" plotted is linearly related to the current generated by penetrating charged particles in an ionization chamber collimated to prevent it from viewing the sun. On the plot shown in Figure 2, a count of 3 indicates negligible particle interference, and counts of 4 to the maximum value of 15 indicate increasing particle interference. A complete description of the SOLRAD 10 experiments and the assumptions used in converting the data from telemetered numbers to flux units is given in NRL Report No. 7408 [Horan and Kreplin, 1972].

The data curve shown at the top of Figure 2 displays the ultraviolet flux in the 1450 to 1600 Å band. Within the limits of very coarse digitization of the experiment, solar emission was constant throughout the day at a value of 2.56 ± 0.32 ergs/cm$^2$ sec. The sharp changes which appear several times at the beginning or end of a darkness period are caused by attenuation of the solar emission as it passes through the Earth's atmosphere. The increases at approximately 1150 and 1325 UT are due to interference by trapped charged particles.

The second data curve from the top displays solar emission in the 1080 to 1350 Å band which is dominated by the Lyman-alpha line at 1216 Å. Until 0830 UT the flux was constant within the limits of digitization of the experiment at 2.46 ± 0.41 ergs/cm$^2$ sec. The absolute flux values presented for the 1080 to 1350 Å band should not be accepted with great confidence because the sensor continuously degraded in sensitivity since launch, and finally became inoperative in February 1972. The absolute values presented are low, probably by a factor of 2 or 3. However, relative changes should still be valid. Between 0830 and 1315 UT the flux level was constant at 2.87 ± 0.41 ergs/cm$^2$ sec, and then it decreased over six minutes to 2.05 ± 0.41 ergs/cm$^2$ sec at 1454 UT. The flux value at 1457 UT was 2.46 ± 0.41 ergs/cm$^2$ sec and it remained at that level for the remainder of the day. The real-time data, which are not subjected to the coarse digitization of the stored data, show a value of 2.00 ± 0.10 ergs/cm$^2$ sec at 1831 and 2010 UT.

The third data curve from the top displays coarsely digitized stored data for the solar emission in the 1225 to 1350 Å band. Except for deviations caused by atmospheric attenuation or trapped particle interference, the flux level was constant throughout the day at 0.216 ± 0.036 ergs/cm$^2$ sec.

The fourth data curve from the top displays the solar emission in the 170 to 700 Å band. Again, the stored data are coarsely digitized. The emission in this band was constant throughout the day at 2.55 ± 0.51 ergs/cm$^2$ sec except for several drops to a level of 2.04 ± 0.51 ergs/cm$^2$ sec between 2100 and 2220 UT. However, if this represents any actual change in solar emission, it could have been as small as a few hundredths of an erg/cm$^2$ sec. The real-time data are not subjected to coarse digitization and show a value of 2.15 ± 0.15 ergs/cm$^2$ sec at 1831 and 2010 UT.

Clearly, within the stored data digitization limits of the ultraviolet experiments, there are no flux changes which occur in conjunction with the X-ray flare at 2004 UT. However, if the X-ray flare observed is centered over a photospheric region well around the west limb, it would be impossible for any lower attitude ultraviolet emission associated with the flare to be visible from Earth. There is evidence of at least a 17 percent change in the 1080 to 1350 Å emission between 0830 and 1457 UT. We believe that the change is real, but we also believe that additional data should be studied in order to rule out possible cumulative particle effects in the sensor response function.

The fifth and sixth data curves from the top show the measured solar emission in the 44 to 60 Å and 1 to 20 Å X-ray bands, respectively. These curves agree with those of Figure 1 in displaying a low X-ray emission level throughout the day with a small X-ray flare around 2000 UT.

REFERENCES


HORAN, D. M. and R. W. KREPLIN — 1972 — The SOLRAD 10 Satellite, Explorer 44, 1971-058A, NRL Report # 7408.

KREPLIN, R. W. — 1961 — Solar X-Rays, Annales de Geophysique, 17, 151-161.

# Proton and Alpha Particle Fluxes Measured Aboard OV5-6

by
G. K. Yates and J. G. Kelley
Air Force Cambridge Research Laboratories
L. G. Hanscom Field, Bedford, Massachusetts

and

B. Sellers and F. A. Hanser
Panametrics, Inc., Waltham, Massachusetts

Satellite OV5-6 (International designation 1969-046B) measures solar fluxes of protons and alpha particles. The perigee is 16,341 km and the apogee is 112,196 km. Thus, for most of the time the instuments are outside the earth's magnetosphere. The data presented here do not include fluxes within this region. The orbit was described in greater detail in an earlier report in this series [Yates et al., 1971].

The proton-alpha particle detector on OV5-6 consists of two totally depleted silicon surface barrier detectors in a telescope configuration. The detectors each have a 2 $cm^2$ area and are separated by 2.54 cm. The outer one is 200 microns thick and the inner one 750 microns. The outer detector is shielded from light by 0.6 mil of aluminum foil. In the coincidence mode of operation, the telescope has a geometric factor of 0.52 $cm^2$-sr, with a detection cone of 30° half angle. The average angle of detection is 17°. A coincidence is set by an energy loss window on the first detector and a threshold on the second detector. The resulting coincidences detect protons and alpha particles (principally) in the following ranges: protons 5.3 to 8 Mev, 8 to 17 Mev, 17 to 40 Mev, and 40 to 100 Mev; alpha-particles 20 to 32 Mev, 32 to 68 Mev, and 68 to 100 Mev. The telescope cycles sequentially through these seven ranges, each range is counted and then read out. The complete cycle is completed in approximately two minutes. The telescope looks in the equatorial plane of the satellite.

The satellite spin axis is stable and is directed toward $0^h$ and $40^m$ RA and 32° declination in celestial coordinates. In September 1971 the sun appeared fifty degrees below (-50°) the satellite's equator. Since the spin period at this time was approximately 4.7 seconds, the telescope accumulated counts in a given particle energy range for approximately two satellite rotations.

The Figure shows 30 minute averages of the data from the four coincidence proton channels and the lowest energy alpha particle channel. Fluxes are given in particles/$cm^2$-sec-sr-Mev; most gaps correspond to periods of no telemetry; points when the satellite was within the trapped radiation belt are omitted.

Armstrong and Krimigis [1971] have shown that there is an inverse correlation between the proton/alpha-particle flux ratio and the hardness of the proton energy spectrum. These data agree with their results. A comparison of the two lower proton energy intervals in the Figure with those of the January event (see p. 120) shows that the January event was the harder of the two. At 0730 hours UT, September 2, the proton/alpha particle flux ratio in the 5 to 8 Mev/nucleon interval was 23.

REFERENCES

ARMSTRONG, T. P. and S. M. KRIMIGIS — 1971 — Statistical study of solar protons, alpha particles, and $Z \geq 3$ nuclei in 1967-1968, J. Geophys. Res., 76, 4230-4244.

YATES, G. K., J. G. KELLEY, B. SELLERS, F. A. HANSER, and P. R. MOREL — 1971 — Proton, alpha and bremsstrahlung fluxes measured aboard OV5-6, World Data Center A, Upper Atmosphere Geophysics Report UAG-12, Part I, 139-146.

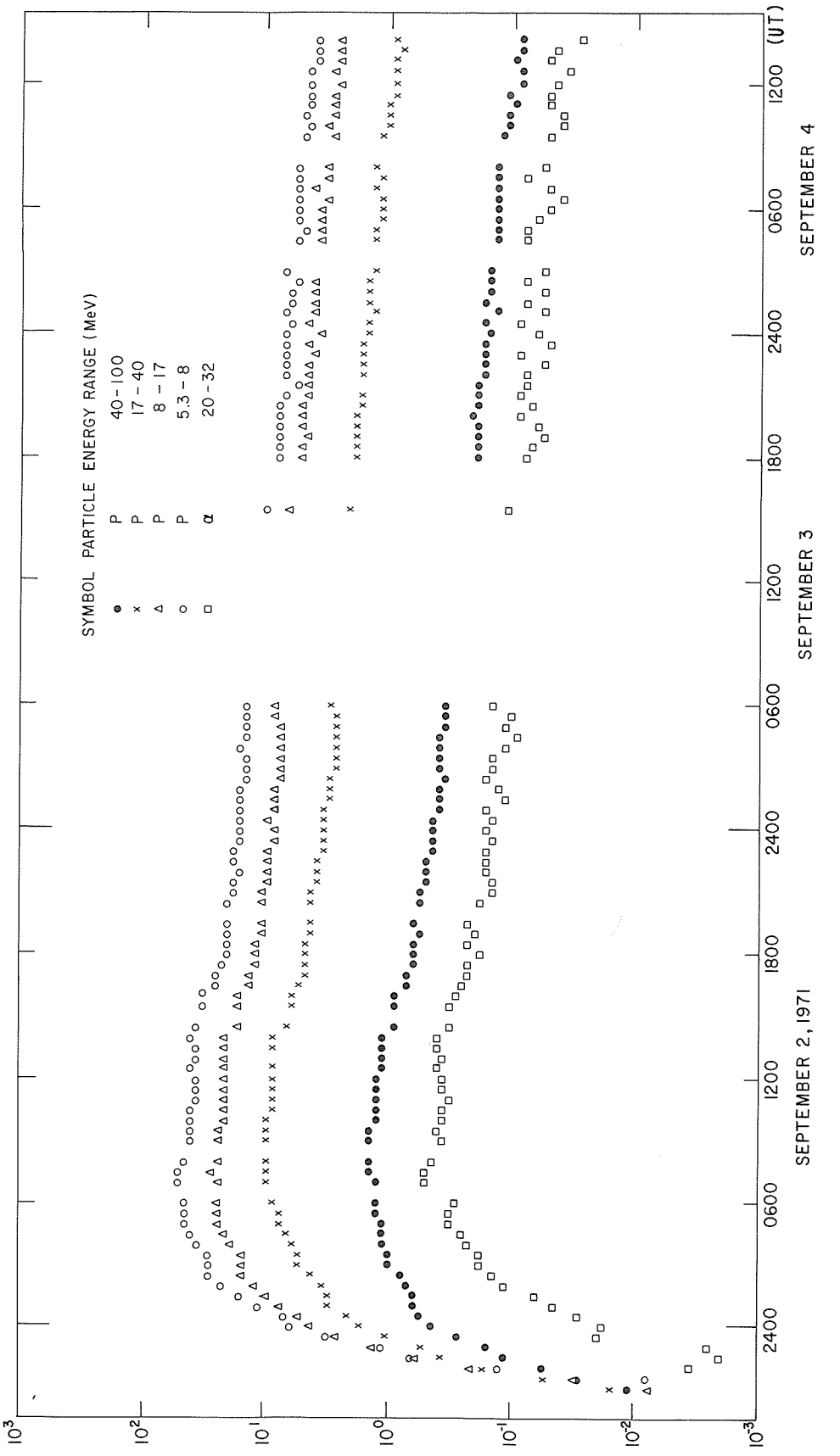


FIGURE 1. TIME VARIATION OF PARTICLE FLUXES (30 minute AVERAGES)

# "Solar Wind Plasma Observations Subsequent to the Solar Proton Event of September 1, 1971"

by

H.C. Howe, J.H. Binsack and H.S. Bridge
Center for Space Research
MIT, Cambridge, Massachusetts

At the time of the solar proton event on September 1, 1971, Explorer 33 was in the geomagnetic tail downstream of the earth; therefore, no data for the time of the event are available from the MIT plasma experiment onboard this satellite. Solar wind plasma data were collected starting at 0225 UT, September 3, 1971, when the plasma data indicate Explorer 33 crossed the bow shock into the solar wind. The solar wind was extremely steady from then until 1645 UT, September 4, 1971, when a small but sudden increase in the density and velocity, in the presence of a constant thermal speed, were observed (see Figure 1). A small sudden commencement was observed simultaneously on the earth. It is our opinion that the event observed on Explorer 33 is a tangential discontinuity convected by the solar wind and not a travelling shock, as might have been expected from the flare which caused the proton event of September 1 [Hirshberg et al., 1970]. Therefore, the magnetic unrest observed on the ground on September 4 and 5 is probably unrelated to the solar proton event. Burlaga [1971] gives a general review of shocks and discontinuities.

## REFERENCES

Burlaga, L.F. 1971 Hydromagnetic waves and discontinuities in the solar wind, G.S.F.C. Preprint X-692-71-95, to appear in Space Science Reviews.

Hirshberg, J., A. Alksne, D.S. Colburn, S.J. Bame, and A.J. Hundhausen 1970 Observations of a solar flare induced interplanetary shock and helium-enriched driver gas, J. Geophys. Rev., 75, 1.

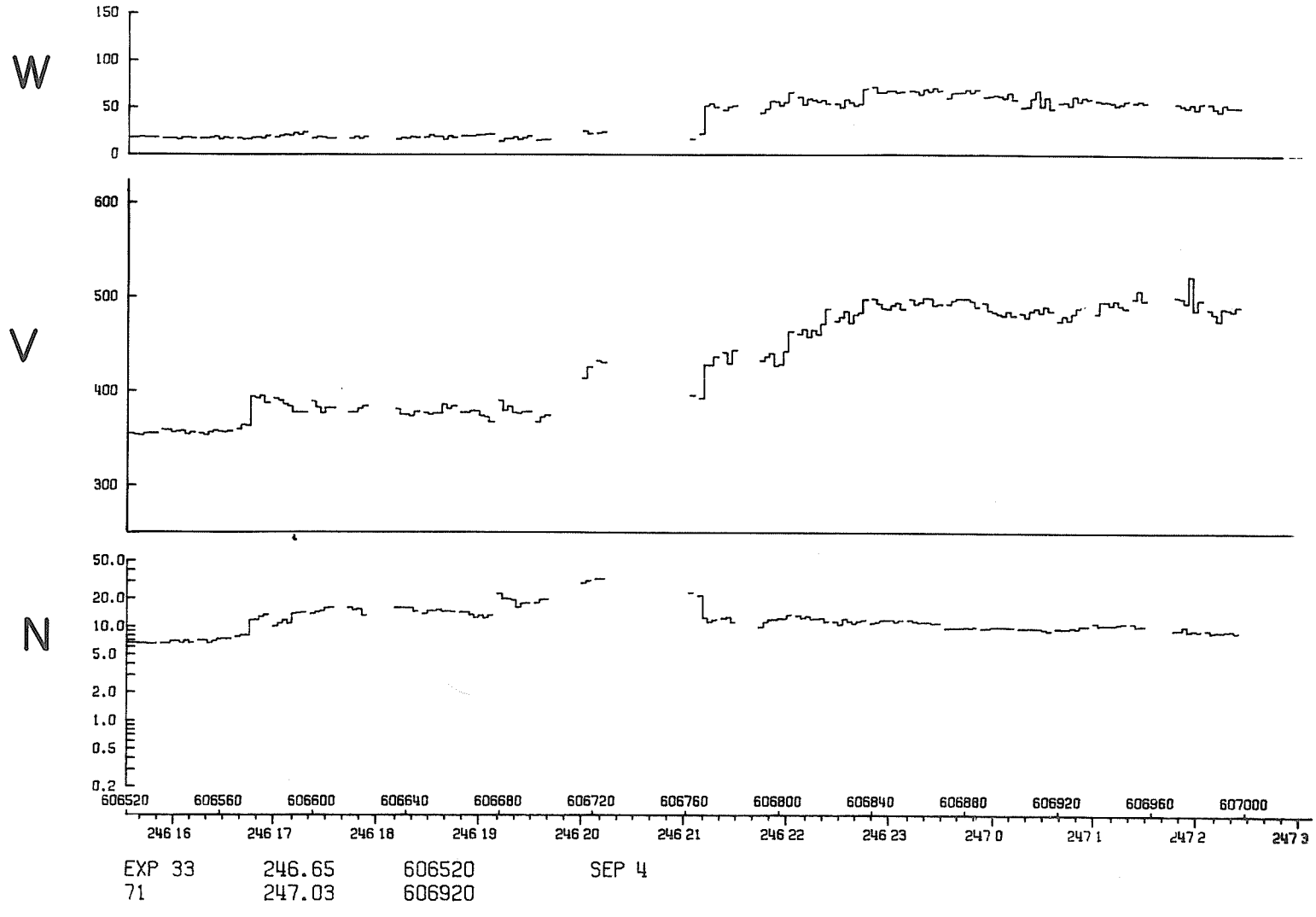


Fig. 1. Solar wind thermal speed (W, km/sec), bulk velocity (V, km/sec) and number density (N, $cm^{-3}$) between 1545 UT, September 4 and 0230 UT, September 5, 1971. The decimal day and hour UT are given for each hour below the horizontal axis. The thermal speed and temperature (T) are related by the expression $\frac{1}{2} m_p W^2 = kT$, where $m_p$ and k are the proton mass and Boltzmann constant.

## 5. COSMIC RAYS

## Tables of Neutron Monitor Data and Selected Graphs for the September 1, 1971 Event

by

Helen E. Coffey
World Data Center A for
Solar-Terrestrial Physics
NOAA, Boulder, Colorado 80302

Cosmic ray neutron monitor data for the September 1, 1971 event are presented both in tabulated form and graphical displays. In many cases the data for this period were forwarded to us upon special request. We thank all reporting observatories for their cooperation.

Table 1 lists the stations, their equipment, geographical coordinates, cutoff rigidities, scaling factors, pressure coefficients, mean station pressure in mm Hg and multiplication factors, if any. Following is Table 2 which presents hourly values for September 1-2, 1971 from the 28 stations, listed in cutoff rigidity order. Again, the incompleteness of data is due to the lag in compiling cosmic ray data. The data does however cluster around the period we are most interested in, i.e., 2200-0200 UT.

Graphical displays of selected stations show both the variation of data with cutoff rigidity and a quick graphical look at the event. These include: a.) Alert, Deep River, General Belgrano and Inuvik five-minute data given in percentage deviations for 1900 UT September 1 - 1800 UT September 2 (Figure 1); b.) Syowa Base, Mt. Norikura and Tokyo Itabashi five-, fifteen- and ten-minute data, respectively, given in percentage deviations for 1900 UT September 1 - 0900 UT September 2 (Figure 2).

Finally, 24 individual stations data in 5-, 10- and 15-minute hourly rates are presented in Table 3. Information pertinent to each station is given in the headings. All data is pressure corrected except for Tixie Bay and Leeds. Pressure values for Tixie Bay are listed. No pressure data for Leeds was available.

The 24 stations listed in cutoff rigidity order are:

| Station | Cutoff rigidity | Hourly rate |
|---|---|---|
| Alert | 0.00 | Five-minute |
| Dumont d'Urville | 0.01 | Fifteen-minute |
| Inuvik | 0.18 | Five-minute |
| Fort Churchill | 0.21 | " " |
| Syowa Base | 0.42 | " " |
| Goose Bay | 0.52 | " " |
| Tixie Bay | 0.53 | " " |
| Kiruna | 0.54 | " " |
| General Belgrano | 0.75 | " " |
| Oulu | 0.81 | " " |
| Deep River | 1.02 | " " |
| Sanae | 1.02 | Ten-minute |
| Port aux Francais | 1.19 | Five-minute |
| Mt. Washington | 1.24 | " " |
| Durham | 1.41 | " " |
| Leeds | 2.20 | " " |
| Lomnicky Stit | 4.00 | Ten-minute |
| Dallas | 4.35 | Five-minute |
| Jungfraujoch | 4.48 | Six-minute |
| Ushuaia | 5.68 | Fifteen-minute |
| Mexico City | 9.53 | Five-minute |
| Buenos Aires | 10.63 | " " |
| Mt. Norikura | 11.39 | Fifteen-minute |
| Tokyo/Itabashi | 11.61 | Ten-minute |

Table 1

| Abb-rev. | Station | Equip | Geographic Coordinates Lat | East | Cutoff Rigidity | Scaling Factors | Pressure Coefficient | Mean Station Pressure mm HG | Real Counts |
|---|---|---|---|---|---|---|---|---|---|
| ALE | Alert | SNM | 82.5 N | 297.6 | 0.0 | -- | 0.987%/mm Hg | 725 | 100x tabulated |
| DUM | Dumont d'Urville | SNM | 66.4 S | 140.0 | 0.01 | -- | .99 %/mm Hg | --- | 200x " |
| INU | Inuvik | SNM | 68.35N | 226.2 | 0.18 | -- | .987%/mm Hg | 758 | 100x " |
| CHU | Fort Churchill | NM | 58.75N | 265.9 | 0.21 | -- | -- | 1010mb | 40x " |
| | Syowa Base | SNM | 69.03S | 39.6 | 0.42 | -- | -.74 %/mb | 965mb | 100x " |
| GOO | Goose Bay | SNM | 53.33N | 299.5 | 0.52 | -- | .987%/mm Hg | 758 | 100x " |
| | Tixie Bay | SNM | 71.55N | 128.9 | 0.53 | -- | -.96 %/mm Hg | 758 | 100x " |
| | Kiruna | SNM | 67.83N | 20.4 | 0.54 | -- | -.99 %/mm Hg | 720 | 100x " |
| OUL | Oulu | SNM | 65.0 N | 25.4 | 0.81 | -- | .735%/mb | 1000mb | 100x " |
| DEE | Deep River | SNM | 46.1 N | 282.5 | 1.02 | -- | .987%/mm Hg | 747 | 300x " |
| OTT | Ottawa | NM | 45.4 N | 284.4 | 1.08 | 6.4 | -- | --- | --- |
| BEG | Bergen | NM | 60.4 N | 5.3 | 1.13 | 16 | .74 %/mb | 990mb | --- |
| SUL | Sulphur Mountain | SNM | 51.2 N | 244.39 | 1.14 | -- | .7665%/mb | --- | 100x " |
| POR | Port aux Francais | SNM | 49.35S | 70.2 | 1.19 | -- | 1.01 %/mm Hg | --- | 400x " |
| MTW | Mt. Washington | NM | 44.3 N | 288.7 | 1.24 | -- | Pressure Corrected | | |
| DUR | Durham | SNM | 43.1 N | 289.1 | 1.41 | -- | Pressure Corrected | | |
| LEE | Leeds | NM | 53.82N | 358.4 | 2.20 | -- | -- | --- | 100x " |
| KIE | Kiel | SNM | 54.33N | 10.1 | 2.29 | -- | .961%/mm Hg | 755 | 100x " |
| | Utrecht | SNM | 52.08N | 5.13 | 2.76 | -- | .99 %/mm Hg | 760 | 100x " |
| LOM | Lomnicky Stit | NM | 49.2 N | 20.22 | 4.00 | -- | -1.024%/mm Hg | 550 | 8x " |
| PRE | Predigstuhl | SNM | 47.7 N | 12.88 | 4.30 | -- | -.9 %/mm Hg | 625 | 100x " |
| DAL | Dallas | NM | 32.78N | 263.2 | 4.35 | -- | -- | 995mb | 120x " |
| JUN | Jungfraujoch | NM | 46.55N | 7.9 | 4.48 | 100 | -- | --- | --- |
| USH | Ushuaia | NM | 54.8 S | 291.7 | 5.68 | 8 | -- | 750 | -3000x " |
| | Mexico City | SNM | 19.33N | 260.8 | 9.53 | -- | -.72 %/mb | 778.6mb | 100x " |
| BUE | Buenos Aires | SNM | 34.58S | 301.5 | 10.63 | -- | -- | --- | 32x " |
| MTN | Mt. Norikura | SNM | 36.12N | 137.5 | 11.39 | 128 | -.7 %/mb | 720mb | --- |
| | Tokyo/Itabashi | SNM | 35.67N | 139.75 | 11.61 | 128 | .666%/mb | 1013.3mb | --- |

Table 2

September 1, 1971

| HOUR | 13 | 14 | 15 | 16 | 17 | 18 | 19 | 20 | 21 | 22 | 23 | 24 |
|---|---|---|---|---|---|---|---|---|---|---|---|---|
| ALERT | | | | | | | | 7180 | 7653 | 8151 | 8127 | 8007 |
| TERRE ADELIE | | | | | 2053 | 2059 | 2064 | 2066 | 2224 | 2354 | 2373 | 2323 |
| INUVIK | | | | | | | | 82227 | 86792 | 91644 | 91437 | 90813 |
| CHURCHILL | | | | 18944 | 18966 | 19105 | 19154 | 19075 | 19927 | 21186 | 21259 | 20934 |
| SYOWA BASE | | | | | | | | 6517 | 6766 | 7114 | 7159 | 7114 |
| GOOSE BAY | | | | | | | | 7038 | 7208 | 7602 | 7660 | 7606 |
| TIXIE BAY | | | | | | | 6681 | 7114 | 7486 | 7511 | 7464 | 7373 |
| KIRUNA | | | | | | | | | 7064 | 7428 | 7916 | 8035 |
| OULU | 3790 | 3804 | 3808 | 3800 | 3792 | 3797 | 3804 | 3788 | 3937 | 4187 | 4260 | 4170 |
| DEEP RIVER | | | | | | | | 6970 | 7208 | 7570 | 7677 | 7622 |
| OTTAWA | 2980 | 3003 | 2981 | 3012 | 2973 | 2977 | 3014 | 3085 | 3125 | 3319 | 3322 | 3311 |
| BERGEN | 531 | 535 | 531 | 528 | 532 | 520 | 525 | 520 | 560 | 575 | 592 | 575 |
| SULPHUR MT | 8603 | 8633 | 8687 | 8660 | 8684 | 8724 | 8757 | 8763 | 9260 | 9998 | 10233 | 10129 |
| KERGUELEN | | | | | | 19574 | 19434 | 19502 | 20907 | 21912 | 21903 | 21519 |
| MT WASHINGTON | | | | | | | 2309 | 2309 | 2444 | 2637 | 2649 | 2584 |
| DURHAM | | | | | | | 2277 | 2282 | 2369 | 2455 | 2458 | 2416 |
| LEEDS | 7122 | 7050 | 7039 | 7003 | 6954 | 6883 | 6890 | 6803 | 6915 | 6986 | 6865 | 6788 |
| KIEL | 6324 | 6296 | 6307 | 6312 | 6304 | 6301 | 6299 | 6256 | 6401 | 6445 | 6412 | 6350 |
| UTRECHT | 6325 | 6348 | 6335 | 6313 | 6336 | 6327 | 6342 | 6293 | 6394 | 6380 | 6335 | 6334 |
| LOMNICKY STIT | | | | | | | | 10754 | 10788 | 10799 | 10803 | 10853 |
| PREDIGTSTUHL | 3778 | 3788 | 3780 | 3800 | 3755 | 3759 | 3758 | 3750 | 3761 | 3743 | 3763 | 3750 |
| DALLAS | 6236 | 6254 | 6255 | 6270 | 6272 | 6277 | 6318 | 6325 | 6319 | 6323 | 6328 | 6325 |
| JUNGFRAUJOCH | | | | | | 6085 | 6064 | 6065 | 6086 | 6054 | 6062 | 6049 |
| USHUAIA | 410 | 455 | 486 | 439 | 423 | 398 | 447 | 427 | 371 | 426 | 334 | 353 |
| MEXICO CITY | | | | | | | 654 | 655 | 655 | 656 | 656 | 654 |
| BUENOS AIRES | | | | | | 13265 | 13258 | 13197 | 13212 | 13246 | 13304 | 13239 |
| MT NORIKURA | | | | 5249 | 5248 | 5255 | 5258 | 5272 | 5274 | 5270 | 5293 | 5288 |
| TOKYO/ITABASHI | | | | 3552 | 3554 | 3546 | 3550 | 3547 | 3562 | 3576 | 3571 | 3583 |

Table 2 (continued)

September 2, 1971

| 01 | 02 | 03 | 04 | 05 | 06 | 07 | 08 | 09 | 10 | 11 | 12 | AVERAGE |
|---|---|---|---|---|---|---|---|---|---|---|---|---|
| 7845 | 7726 | 7637 | 7549 | 7514 | 7450 | 7409 | 7352 | 7347 | 7333 | 7307 | 7292 | 7581.1 |
| 2269 | 2254 | 2216 | 2193 | 2173 | 2162 | 2146 | 2129 | 2122 | 2125 | 2105 | 2101 | 2175.5 |
| 89848 | 88748 | 87526 | 86463 | 86003 | 85233 | 84495 | 84371 | 84062 | 83310 | 83115 | 83153 | 86425.9 |
| 20713 | 20519 | 20173 | 20034 | 19884 | 19683 | 19484 | 19480 | 19454 | 19332 | 19311 | | 19830.9 |
| 6996 | 6896 | 6829 | 6743 | 6725 | 6707 | 6713 | 6689 | 6713 | 6739 | 6798 | 6765 | 6822.5 |
| 7522 | 7467 | 7324 | 7286 | 7197 | 7137 | 7129 | 7094 | 7088 | 7070 | 7040 | 7031 | 7264.6 |
| 7250 | 7238 | 7197 | 7139 | 7068 | 7072 | 7003 | 7020 | 6977 | 6950 | 6961 | 6945 | 7136.1 |
| 7888 | 7734 | 7614 | 7499 | 7432 | 7387 | 7319 | 7302 | 7275 | 7304 | 7277 | 7256 | 7490.0 |
| 4111 | 4035 | 4004 | 3961 | 3929 | 3904 | 3895 | 3898 | 3901 | 3925 | 3899 | 3885 | 3928.5 |
| 7511 | 7423 | 7282 | 7207 | 7148 | 7103 | 7066 | 7054 | 7022 | 7004 | 6996 | | 7241.4 |
| 3295 | 3236 | 3152 | 3067 | 3041 | 3117 | 3056 | 3117 | 3035 | 3038 | 3068 | 3009 | 3097.2 |
| 570 | 547 | 545 | 538 | 546 | 539 | 535 | 535 | 535 | 543 | 536 | 539 | 543.8 |
| 9981 | 9777 | 9596 | 9456 | 9286 | 9138 | 9099 | 9057 | 8996 | 8966 | 8896 | 8866 | 9176.8 |
| 21191 | 20929 | 20726 | 20477 | 20448 | 20322 | 20283 | 20271 | 20232 | 20092 | 20080 | 20161 | 20524.3 |
| 2554 | 2482 | 2429 | 2381 | 2384 | 2379 | 2350 | | | | | | 2607.0 |
| 2383 | 2363 | 2329 | 2309 | 2308 | 2292 | | | | | | | 2353.4 |
| 6775 | 6683 | 6660 | 6653 | 6607 | 6578 | 6613 | 6632 | 6613 | 6623 | 6619 | 6633 | 6791.1 |
| 6335 | 6316 | 6281 | 6289 | 6281 | 6264 | 6279 | 6315 | 6328 | 6346 | 6356 | 6357 | 6323.1 |
| 6306 | 6314 | 6295 | 6298 | 6293 | 6301 | 6304 | 6330 | 6346 | 6371 | 6339 | 6361 | 6329.9 |
| 10840 | 10711 | 10705 | 10698 | 10795 | 10787 | 10763 | 10751 | 10816 | 10805 | 10815 | | 10780.1 |
| 3760 | 3747 | 3737 | 3736 | 3741 | 3749 | 3757 | 3769 | 3773 | 3775 | 3771 | 3771 | 3761.3 |
| 6312 | 6272 | 6267 | 6245 | 6253 | 6236 | 6255 | 6259 | 6255 | 6263 | 6253 | 6261 | 6276.4 |
| | | | | | | | | | | | | 6066.5 |
| 486 | 401 | 383 | 425 | 394 | 435 | 380 | 426 | 422 | 434 | 424 | 434 | 417.2 |
| 653 | 655 | 653 | 652 | 651 | 652 | 653 | 652 | 655 | 652 | | | 653.8 |
| 13172 | 13162 | 13179 | 13143 | 13171 | 13227 | 13252 | 13223 | 13216 | 13230 | 13316 | 13259 | 13224.7 |
| 5262 | 5278 | 5246 | 5245 | 5250 | 5251 | 5250 | 5244 | | | | | 5260.8 |
| 3593 | 3573 | 3594 | 3571 | 3580 | 3569 | 3566 | 3562 | 3545 | | | | 3566.3 |

Table 3

ALERT 82.5N 62.20W CANADA

NEUTRON MONITOR 18-NM-64

REAL COUNTS 100 TIMES TABULATED COUNTS

FIVE-MINUTE BAROMETER CORRECTED HOURLY RATES

SEPTEMBER 1-2, 1971

| TIME U.T. | MINUTES AT END OF INTERVAL 05 | 10 | 15 | 20 | 25 | 30 | 35 | 40 | 45 | 50 | 55 | 60 | AVERAGE |
|---|---|---|---|---|---|---|---|---|---|---|---|---|---|
| 1900-2000 | 7206 | 7185 | 7195 | 7153 | 7195 | 7217 | 7121 | 7142 | 7206 | 7163 | 7174 | 7206 | 7180 |
| 2000-2100 | 7259 | 7280 | 7326 | 7454 | 7485 | 7613 | 7730 | 7836 | 7857 | 7977 | 8019 | 7998 | 7653 |
| 2100-2200 | 8008 | 8104 | 8136 | 8083 | 8168 | 8231 | 8231 | 8221 | 8178 | 8093 | 8199 | 8157 | 8151 |
| 2200-2300 | 8093 | 8125 | 8242 | 8199 | 8189 | 8136 | 8051 | 8146 | 8168 | 7998 | 8072 | 8104 | 8127 |
| 2300-2400 | 8149 | 8011 | 8001 | 8043 | 8054 | 7990 | 8064 | 8054 | 7937 | 7905 | 7916 | 7961 | 8007 |
| 2400-0100 | 7940 | 7823 | 7866 | 7876 | 7813 | 7813 | 7844 | 7855 | 7866 | 7802 | 7834 | 7802 | 7845 |
| 0100-0200 | 7749 | 7749 | 7763 | 7752 | 7784 | 7742 | 7742 | 7699 | 7731 | 7692 | 7649 | 7660 | 7726 |
| 0200-0300 | 7649 | 7755 | 7660 | 7639 | 7607 | 7607 | 7639 | 7649 | 7652 | 7578 | 7578 | 7631 | 7637 |
| 0300-0400 | 7529 | 7571 | 7571 | 7603 | 7603 | 7595 | 7448 | 7521 | 7574 | 7595 | 7521 | 7458 | 7549 |
| 0400-0500 | 7521 | 7564 | 7606 | 7458 | 7469 | 7535 | 7535 | 7482 | 7451 | 7493 | 7524 | 7524 | 7514 |
| 0500-0600 | 7472 | 7514 | 7493 | 7430 | 7496 | 7517 | 7370 | 7443 | 7391 | 7380 | 7454 | 7443 | 7450 |
| 0600-0700 | 7380 | 7436 | 7457 | 7373 | 7415 | 7405 | 7418 | 7418 | 7450 | 7366 | 7408 | 7376 | 7409 |
| 0700-0800 | 7334 | 7338 | 7296 | 7401 | 7372 | 7372 | 7362 | 7372 | 7341 | 7299 | 7362 | 7372 | 7352 |
| 0800-0900 | 7375 | 7313 | 7281 | 7355 | 7396 | 7365 | 7355 | 7292 | 7355 | 7365 | 7334 | 7375 | 7347 |
| 0900-1000 | 7292 | 7334 | 7334 | 7344 | 7368 | 7316 | 7400 | 7368 | 7316 | 7222 | 7337 | 7361 | 7333 |
| 1000-1100 | 7350 | 7288 | 7256 | 7267 | 7260 | 7249 | 7395 | 7333 | 7291 | 7281 | 7406 | 7305 | 7307 |
| 1100-1200 | 7305 | 7294 | 7284 | 7305 | 7287 | 7308 | 7256 | 7277 | 7297 | 7287 | 7308 | 7301 | 7292 |
| 1200-1300 | 7301 | 7290 | 7301 | 7335 | 7293 | 7262 | 7283 | 7297 | 7369 | 7362 | 7269 | 7269 | 7303 |
| 1300-1400 | 7165 | 7331 | 7289 | 7248 | 7297 | 7276 | 7248 | 7372 | 7258 | 7248 | 7230 | 7303 | 7272 |
| 1400-1500 | 7303 | 7282 | 7262 | 7285 | 7327 | 7285 | 7306 | 7265 | 7316 | 7247 | 7237 | 7247 | 7280 |
| 1500-1600 | 7144 | 7278 | 7309 | 7340 | 7268 | 7302 | 7219 | 7343 | 7292 | 7264 | 7233 | 7264 | 7271 |
| 1600-1700 | 7154 | 7257 | 7298 | 7205 | 7246 | 7185 | 7288 | 7280 | 7250 | 7280 | 7222 | 7222 | 7241 |
| 1700-1800 | 7284 | 7273 | 7253 | 7263 | 7242 | 7253 | 7246 | 7338 | 7246 | 7228 | 7269 | 7276 | 7264 |

DUMONT DURVILLE 66.4S 140.02E ANTARCTICA

NEUTRON MONITOR 9-NM-64

CORRECTED FOR BAROMETRIC PRESSURE

COEFFICIENT 9.9 PER CENT PER CM HG

MULTIPLY INDICATED NUMBERS BY 200

FIFTEEN-MINUTE HOURLY RATES

SEPTEMBER 1-2, 1971

| TIME U.T. | MINUTES AT END OF INTERVAL 15 | 30 | 45 | 60 |
|---|---|---|---|---|
| 1600-1700 | 513 | 510 | 516 | 514 |
| 1700-1800 | 512 | 515 | 516 | 516 |
| 1800-1900 | 518 | 514 | 515 | 517 |
| 1900-2000 | 515 | 517 | 514 | 520 |
| 2000-2100 | 531 | 568 | 574 | 551 |
| 2100-2200 | 578 | 594 | 591 | 591 |
| 2200-2300 | 596 | 595 | 598 | 584 |
| 2300-2400 | 585 | 579 | 581 | 578 |
| 2400-0100 | 573 | 569 | 566 | 561 |
| 0100-0200 | 568 | 566 | 557 | 563 |
| 0200-0300 | 558 | 556 | 551 | 551 |
| 0300-0400 | 548 | 551 | 548 | 546 |
| 0400-0500 | 544 | 545 | 543 | 541 |
| 0500-0600 | 542 | 543 | 541 | 536 |
| 0600-0700 | 538 | 536 | 537 | 535 |
| 0700-0800 | 536 | 529 | 535 | 529 |
| 0800-0900 | 528 | 530 | 532 | 532 |
| 0900-1000 | 534 | 533 | 531 | 527 |
| 1000-1100 | 527 | 526 | 527 | 525 |
| 1100-1200 | 527 | 523 | 524 | 527 |

Table 3 (continued)

INUVIK 68.21N 133.43W CANADA

NEUTRON MONITOR 18-NM-64

REAL COUNTS 100 TIMES TABULATED COUNTS

FIVE-MINUTE BAROMETER CORRECTED HOURLY RATES

SEPTEMBER 1-2, 1971

| TIME | MINUTES AT END OF INTERVAL | | | | | | | | | | | | |
|---|---|---|---|---|---|---|---|---|---|---|---|---|---|
| U.T. | 05 | 10 | 15 | 20 | 25 | 30 | 35 | 40 | 45 | 50 | 55 | 60 | AVERAGE |
| 1900-2000 | 6802 | 6849 | 6837 | 6868 | 6915 | 6880 | 6832 | 6856 | 6832 | 6844 | 6880 | 6832 | 6852 |
| 2000-2100 | 6939 | 6934 | 7041 | 7124 | 7160 | 7339 | 7339 | 7260 | 7367 | 7410 | 7469 | 7410 | 7233 |
| 2100-2200 | 7457 | 7457 | 7612 | 7605 | 7616 | 7712 | 7747 | 7640 | 7628 | 7735 | 7747 | 7688 | 7637 |
| 2200-2300 | 7557 | 7688 | 7652 | 7593 | 7680 | 7728 | 7633 | 7605 | 7550 | 7640 | 7656 | 7455 | 7620 |
| 2300-2400 | 7478 | 7514 | 7526 | 7692 | 7633 | 7502 | 7538 | 7597 | 7609 | 7514 | 7585 | 7625 | 7568 |
| 2400-0100 | 7578 | 7566 | 7483 | 7518 | 7447 | 7447 | 7495 | 7495 | 7381 | 7511 | 7475 | 7452 | 7487 |
| 0100-0200 | 7499 | 7416 | 7440 | 7428 | 7475 | 7393 | 7345 | 7373 | 7373 | 7397 | 7326 | 7283 | 7396 |
| 0200-0300 | 7331 | 7331 | 7272 | 7295 | 7319 | 7319 | 7331 | 7307 | 7272 | 7248 | 7260 | 7241 | 7294 |
| 0300-0400 | 7205 | 7229 | 7276 | 7182 | 7170 | 7193 | 7182 | 7229 | 7229 | 7158 | 7276 | 7134 | 7205 |
| 0400-0500 | 7193 | 7205 | 7163 | 7198 | 7234 | 7116 | 7245 | 7127 | 7139 | 7175 | 7057 | 7151 | 7167 |
| 0500-0600 | 7151 | 7080 | 7097 | 7050 | 7132 | 7132 | 7137 | 7090 | 7078 | 7054 | 7090 | 7142 | 7103 |
| 0600-0700 | 7083 | 7048 | 7052 | 7041 | 7012 | 6977 | 7024 | 7118 | 7088 | 7029 | 6994 | 7029 | 7041 |
| 0700-0800 | 7005 | 7076 | 7045 | 6963 | 7069 | 7003 | 7062 | 7008 | 7031 | 6978 | 7071 | 7060 | 7031 |
| 0800-0900 | 6989 | 7060 | 7071 | 7071 | 7041 | 6989 | 6978 | 6982 | 6994 | 6924 | 6964 | 6999 | 7005 |
| 0900-1000 | 6976 | 7022 | 6999 | 6859 | 6987 | 6999 | 6957 | 6957 | 6915 | 6857 | 6850 | 6932 | 6943 |
| 1000-1100 | 6955 | 6908 | 6955 | 6920 | 6932 | 6827 | 7025 | 6955 | 6978 | 6838 | 6920 | 6902 | 6926 |
| 1100-1200 | 6948 | 6913 | 6872 | 6918 | 6988 | 6976 | 6941 | 6941 | 6941 | 6923 | 6876 | 6916 | 6929 |
| 1200-1300 | 6928 | 6898 | 6898 | 6898 | 6960 | 6914 | 6838 | 6919 | 6896 | 6884 | 6981 | 6900 | 6910 |
| 1300-1400 | 6970 | 6912 | 6947 | 6889 | 6889 | 6842 | 6870 | 6829 | 6887 | 6910 | 6972 | 6880 | 6900 |
| 1400-1500 | 6919 | 6827 | 6878 | 6901 | 6848 | 6791 | 6860 | 6825 | 6830 | 6853 | 6922 | 6841 | 6858 |
| 1500-1600 | 6818 | 6880 | 6938 | 6857 | 6857 | 6862 | 6874 | 6855 | 6833 | 6936 | 6883 | 6883 | 6873 |
| 1600-1700 | 6894 | 6860 | 6945 | 6910 | 6949 | 6954 | 6908 | 6890 | 6940 | 6895 | 6854 | 6940 | 6912 |
| 1700-1800 | 6826 | 6910 | 6865 | 6881 | 6881 | 6806 | 6954 | 6851 | 6874 | 6931 | 6935 | 6895 | 6884 |

FORT CHURCHILL 58.75N 265.90E CANADA

IGY NEUTRON MONITOR

BAROMETER REFERENCE 1010 MILLIBARS

ATTENUATION LENGTH 137.2 MILLIBARS

REAL COUNTS 40 TIMES TABULATED COUNTS

FIVE-MINUTE BAROMETER CORRECTED HOURLY RATES

SEPTEMBER 1-2, 1971

| TIME | MINUTES AT END OF INTERVAL | | | | | | | | | | | |
|---|---|---|---|---|---|---|---|---|---|---|---|---|
| U.T. | 05 | 10 | 15 | 20 | 25 | 30 | 35 | 40 | 45 | 50 | 55 | 60 |
| 1500 | 1567 | 1578 | 1584 | 1581 | 1574 | 1579 | 1575 | 1586 | 1580 | 1579 | 1588 | 1572 |
| 1600 | 1578 | 1565 | 1597 | 1580 | 1577 | 1577 | 1594 | 1581 | 1572 | 1581 | 1566 | 1598 |
| 1700 | 1614 | 1576 | 1593 | 1588 | 1596 | 1586 | 1582 | 1606 | 1576 | 1602 | 1593 | 1591 |
| 1800 | 1589 | 1596 | 1601 | 1600 | 1595 | 1604 | 1594 | 1591 | 1604 | 1592 | 1603 | 1584 |
| 1900 | 1586 | 1590 | 1590 | 1592 | 1602 | 1587 | 1591 | 1593 | 1593 | 1589 | 1583 | 1580 |
| 2000 | 1600 | 1622 | 1621 | 1647 | 1631 | 1655 | 1662 | 1661 | 1684 | 1701 | 1719 | 1725 |
| 2100 | 1733 | 1732 | 1755 | 1750 | 1736 | 1765 | 1768 | 1782 | 1782 | 1787 | 1804 | 1792 |
| 2200 | 1809 | 1807 | 1790 | 1769 | 1760 | 1774 | 1773 | 1756 | 1746 | 1752 | 1747 | 1776 |
| 2300 | 1752 | 1749 | 1770 | 1764 | 1733 | 1761 | 1732 | 1745 | 1729 | 1733 | 1734 | 1732 |
| 2400 | 1710 | 1725 | 1732 | 1740 | 1734 | 1724 | 1717 | 1715 | 1714 | 1728 | 1737 | 1734 |
| 0100 | 1709 | 1715 | 1718 | 1717 | 1720 | 1709 | 1730 | 1702 | 1696 | 1693 | 1708 | 1702 |
| 0200 | 1695 | 1674 | 1689 | 1686 | 1696 | 1694 | 1681 | 1690 | 1665 | 1668 | 1666 | 0 |
| 0300 | 0 | 1677 | 1669 | 1681 | 1674 | 1678 | 1674 | 1669 | 1659 | 1655 | 1666 | 1659 |
| 0400 | 1672 | 1650 | 1661 | 1666 | 1644 | 1641 | 1661 | 1667 | 1668 | 1658 | 1648 | 1648 |
| 0500 | 1622 | 1644 | 0 | 1646 | 1631 | 1636 | 1636 | 1662 | 1644 | 1657 | 1620 | 1638 |
| 0600 | 1617 | 1642 | 1609 | 1630 | 1642 | 1627 | 1625 | 1604 | 1621 | 1622 | 1622 | 1622 |
| 0700 | 1627 | 1636 | 1618 | 1629 | 1624 | 1615 | 1644 | 1626 | 1614 | 1599 | 1612 | 1634 |
| 0800 | 1612 | 1624 | 1630 | 1623 | 1632 | 1611 | 1617 | 1619 | 1617 | 1624 | 1630 | 1617 |
| 0900 | 1610 | 1607 | 1616 | 1613 | 1615 | 1602 | 1600 | 1619 | 1622 | 1607 | 1602 | 1616 |
| 1000 | 1602 | 1628 | 1618 | 1597 | 1601 | 1603 | 1603 | 1622 | 1606 | 1609 | 1616 | 1605 |
| 1100 | 1617 | 1614 | 1600 | 1602 | 1615 | 1618 | 1625 | 1605 | 1607 | | | |

Table 3 (continued)

SYOWA BASE 69.0S 39.58E ANTARCTICA

NEUTRON MONITOR 12-NM-64

PRESSURE CORRECTED TO 965 MILLIBARS

COEFFICIENT -0.74 PER CENT PER MILLIBAR

SCALING FACTOR 100

FIVE-MINUTE COUNTING RATES

SEPTEMBER 1-2, 1971

| TIME U.T. | MINUTES AT END OF INTERVAL 05 | 10 | 15 | 20 | 25 | 30 | 35 | 40 | 45 | 50 | 55 | 60 |
|---|---|---|---|---|---|---|---|---|---|---|---|---|
| 1900-2000 | 547 | 544 | 543 | 540 | 539 | 536 | 544 | 546 | 547 | 542 | 550 | 539 |
| 2000-2100 | 554 | 545 | 547 | 555 | 566 | 566 | 567 | 572 | 572 | 571 | 574 | 577 |
| 2100-2200 | 586 | 584 | 593 | 592 | 592 | 596 | 592 | 593 | 598 | 598 | 595 | 595 |
| 2200-2300 | 589 | 589 | 589 | 596 | 601 | 601 | 594 | 598 | 597 | 601 | 605 | 599 |
| 2300-2400 | 602 | 602 | 597 | 601 | 592 | 591 | 588 | 592 | 583 | 595 | 591 | 580 |
| 2400-0100 | 586 | 583 | 580 | 585 | 586 | 580 | 585 | 578 | 581 | 578 | 583 | 591 |
| 0100-0200 | 576 | 580 | 578 | 581 | 576 | 578 | 571 | 569 | 571 | 575 | 570 | 571 |
| 0200-0300 | 574 | 578 | 568 | 567 | 574 | 567 | 570 | 568 | 568 | 564 | 566 | 565 |
| 0300-0400 | 563 | 556 | 564 | 568 | 559 | 560 | 566 | 561 | 566 | 561 | 562 | 557 |
| 0400-0500 | 559 | 561 | 565 | 557 | 566 | 556 | 561 | 558 | 556 | 560 | 560 | 556 |
| 0500-0600 | 554 | 558 | 555 | 555 | 564 | 555 | 562 | 561 | 557 | 561 | 558 | 567 |
| 0600-0700 | 562 | 557 | 556 | 567 | 556 | 554 | 558 | 559 | 558 | 563 | 561 | 562 |
| 0700-0800 | 558 | 553 | 557 | 557 | 557 | 558 | 566 | 558 | 558 | 559 | 550 | 558 |
| 0800-0900 | 557 | 554 | 561 | 558 | 558 | 559 | 562 | 558 | 570 | 555 | 558 | 563 |
| 0900-1000 | 566 | 562 | 562 | 552 | 562 | 566 | 564 | 558 | 563 | 564 | 559 | 561 |
| 1000-1100 | 568 | 566 | 573 | 563 | 561 | 571 | 569 | 566 | 562 | 564 | 567 | 568 |
| 1100-1200 | 566 | 566 | 574 | 560 | 560 | 562 | 566 | 561 | 561 | 561 | 563 | 565 |

GOOSE BAY 53.16N 60.24W CANADA

NEUTRON MONITOR 18-NM-64

REAL COUNTS 100 TIMES TABULATED COUNTS

FIVE-MINUTE BAROMETER CORRECTED HOURLY RATES

SEPTEMBER 1-2, 1971

| TIME U.T. | MINUTES AT END OF INTERVAL 05 | 10 | 15 | 20 | 25 | 30 | 35 | 40 | 45 | 50 | 55 | 60 | AVERAGE |
|---|---|---|---|---|---|---|---|---|---|---|---|---|---|
| 1900-2000 | 7093 | 6996 | 7063 | 7000 | 7030 | 7007 | 7075 | 7045 | 7030 | 7045 | 6989 | 7079 | 7038 |
| 2000-2100 | 7144 | 6982 | 7166 | 7065 | 7069 | 7166 | 7245 | 7207 | 7346 | 7391 | 7323 | 7391 | 7208 |
| 2100-2200 | 7507 | 7428 | 7507 | 7484 | 7686 | 7623 | 7578 | 7634 | 7671 | 7772 | 7660 | 7668 | 7602 |
| 2200-2300 | 7757 | 7600 | 7698 | 7653 | 7619 | 7683 | 7615 | 7728 | 7615 | 7702 | 7552 | 7698 | 7660 |
| 2300-2400 | 7701 | 7619 | 7511 | 7600 | 7638 | 7567 | 7623 | 7612 | 7645 | 7649 | 7574 | 7529 | 7606 |
| 2400-0100 | 7544 | 7541 | 7529 | 7589 | 7444 | 7533 | 7511 | 7533 | 7477 | 7544 | 7567 | 7448 | 7522 |
| 0100-0200 | 7492 | 7526 | 7492 | 7459 | 7518 | 7474 | 7489 | 7481 | 7422 | 7444 | 7455 | 7348 | 7467 |
| 0200-0300 | 7392 | 7381 | 7348 | 7385 | 7337 | 7274 | 7333 | 7318 | 7289 | 7278 | 7229 | 7322 | 7324 |
| 0300-0400 | 7366 | 7326 | 7259 | 7404 | 7304 | 7304 | 7274 | 7285 | 7263 | 7274 | 7274 | 7097 | 7286 |
| 0400-0500 | 7186 | 7186 | 7212 | 7152 | 7230 | 7241 | 7208 | 7175 | 7245 | 7186 | 7186 | 7159 | 7197 |
| 0500-0600 | 7071 | 7111 | 7104 | 7159 | 7126 | 7171 | 7189 | 7171 | 7111 | 7137 | 7144 | 7148 | 7137 |
| 0600-0700 | 7119 | 7230 | 7138 | 7057 | 7167 | 7141 | 7108 | 7130 | 7163 | 7086 | 7130 | 7075 | 7129 |
| 0700-0800 | 7053 | 7019 | 7064 | 7152 | 7130 | 7008 | 7141 | 7104 | 7111 | 7122 | 7111 | 7118 | 7094 |
| 0800-0900 | 7118 | 7096 | 7107 | 7140 | 7151 | 7107 | 7029 | 7047 | 7092 | 7121 | 7058 | 6991 | 7088 |
| 0900-1000 | 7032 | 7047 | 7080 | 7058 | 7014 | 7114 | 7136 | 7151 | 6989 | 7085 | 7036 | 7092 | 7070 |
| 1000-1100 | 7092 | 6976 | 7087 | 6976 | 7087 | 6987 | 7076 | 7094 | 7039 | 6994 | 7016 | 7061 | 7040 |
| 1100-1200 | 7009 | 7043 | 7016 | 7128 | 7032 | 7050 | 6994 | 6998 | 7021 | 7009 | 7039 | 7032 | 7031 |
| 1200-1300 | 7039 | 7087 | 7087 | 7043 | 7009 | 7025 | 7062 | 7085 | 7062 | 7073 | 7033 | 7044 | 7054 |
| 1300-1400 | 7044 | 7122 | 6955 | 6993 | 6960 | 7068 | 7079 | 7112 | 7119 | 7134 | 7079 | 7083 | 7062 |
| 1400-1500 | 7017 | 7120 | 7113 | 7073 | 7088 | 7019 | 7092 | 7089 | 7078 | 7045 | 7159 | 7086 | 7082 |
| 1500-1600 | 7064 | 7090 | 7068 | 7017 | 7021 | 7131 | 7146 | 7135 | 7012 | 7005 | 7157 | 7157 | 7084 |
| 1600-1700 | 7085 | 7049 | 7016 | 7082 | 7027 | 7082 | 7125 | 7154 | 7096 | 7169 | 7104 | 7097 | 7091 |
| 1700-1800 | 7040 | 7072 | 7022 | 7062 | 7101 | 7073 | 7023 | 7058 | 7073 | 7073 | 7030 | 7055 | 7057 |

Table 3 (continued)

TIXIE BAY 71.58N 128.9E USSR

NEUTRON MONITOR 18-NM-64

UNCORRECTED FOR PRESSURE

RECALCULATING COEFFICIENT 100

FIVE-MINUTE HOURLY RATES

SEPTEMBER 1-2, 1971

| TIME | MINUTES AT END OF INTERVAL | | | | | | | | | | | |
|---|---|---|---|---|---|---|---|---|---|---|---|---|
| U.T. | 05 | 10 | 15 | 20 | 25 | 30 | 35 | 40 | 45 | 50 | 55 | 60 |
| 1900 | 555 | 555 | 553 | 562 | 556 | 556 | 547 | 559 | 550 | 564 | 563 | 561 |
| 2000 | 561 | 573 | 578 | 582 | 589 | 595 | 591 | 601 | 613 | 615 | 602 | 614 |
| 2100 | 613 | 617 | 618 | 626 | 627 | 626 | 631 | 624 | 629 | 626 | 627 | 622 |
| 2200 | 624 | 624 | 627 | 636 | 624 | 628 | 619 | 627 | 629 | 626 | 617 | 630 |
| 2300 | 626 | 621 | 625 | 623 | 628 | 628 | 615 | 622 | 616 | 622 | 618 | |
| 2400 | 622 | 622 | 615 | 616 | 612 | 616 | 618 | 616 | 610 | 608 | 612 | 606 |
| 0100 | 611 | 609 | 611 | 610 | 588 | 600 | 595 | 604 | 609 | 603 | 606 | 604 |
| 0200 | 604 | 609 | 605 | 606 | 600 | 606 | 602 | 600 | 605 | 597 | 600 | 604 |
| 0300 | 606 | 600 | 598 | 595 | 599 | 601 | 606 | 598 | 600 | 603 | 597 | 594 |
| 0400 | 610 | 597 | 597 | 596 | 598 | 591 | 593 | 590 | 595 | 597 | 587 | 588 |
| 0500 | 588 | 591 | 586 | 590 | 588 | 582 | 598 | 587 | 592 | 588 | 588 | 590 |
| 0600 | 597 | 587 | 593 | 590 | 592 | 596 | 591 | 583 | 581 | 587 | 583 | 592 |
| 0700 | 587 | 588 | 580 | 589 | 580 | 584 | 586 | 586 | 584 | 580 | 584 | 575 |
| 0800 | 589 | 582 | 590 | 590 | 586 | 587 | 586 | 591 | 577 | 580 | 580 | 582 |
| 0900 | 577 | 580 | 579 | 574 | 584 | 594 | 579 | 583 | 578 | 584 | 583 | 582 |
| 1000 | 579 | 577 | 573 | 581 | 576 | 577 | 580 | 585 | 579 | 581 | 580 | 582 |
| 1100 | 587 | 582 | 578 | 579 | 577 | 573 | 582 | 579 | 578 | 582 | 584 | 580 |
| 1200 | 582 | 574 | 579 | 578 | 584 | 575 | 579 | 575 | 578 | 582 | 577 | 582 |
| 1300 | 574 | 573 | 583 | 577 | 577 | 572 | 572 | 576 | 578 | 571 | 570 | 570 |
| 1400 | 574 | 574 | 573 | 574 | 580 | 572 | 568 | 585 | 576 | 574 | 570 | 572 |
| 1500 | 574 | 580 | 576 | 575 | 571 | 578 | 578 | 575 | 577 | 578 | 577 | 571 |
| 1600 | 572 | 573 | 579 | 576 | 576 | 564 | 572 | 575 | 573 | 571 | 571 | 570 |
| 1700 | 579 | 575 | 574 | 573 | 569 | 575 | 569 | 577 | 573 | 574 | 573 | 570 |
| 1800 | 571 | 571 | 574 | 580 | 577 | 576 | 568 | 578 | 575 | 570 | 575 | 571 |

PRESSURE IN MM HG X 1/10

| | | | | | | | | | | | | |
|---|---|---|---|---|---|---|---|---|---|---|---|---|
| 1900 | 7579 | 7579 | 7579 | 7573 | 7573 | 7578 | 7578 | 7578 | 7578 | 7573 | 7573 | 7578 |
| 2000 | 7578 | 7578 | 7578 | 7578 | 7578 | 7577 | 7577 | 7577 | 7577 | 7577 | 7577 | 7577 |
| 2100 | 7577 | 7577 | 7577 | 7577 | 7577 | 7573 | 7576 | 7576 | 7576 | 7576 | 7576 | 7576 |
| 2200 | 7576 | 7576 | 7576 | 7576 | 7576 | 7576 | 7576 | 7573 | 7576 | 5576 | 7576 | 7575 |
| 2300 | 7575 | 7575 | 7575 | 7575 | 7575 | 7574 | 7573 | 7574 | 7574 | 7574 | 7574 | 7574 |
| 2400 | 7574 | 7574 | 7573 | 7573 | 7573 | 7572 | 7572 | 7572 | 7573 | 7573 | 7573 | 7573 |
| 0100 | 7573 | 7573 | 7573 | 7573 | 7573 | 7573 | 7572 | 7572 | 7572 | 7572 | 7572 | 7572 |
| 0200 | 7572 | 7572 | 7572 | 7572 | 7572 | 7572 | 7571 | 7571 | 7571 | 7571 | 7571 | 7571 |
| 0300 | 7571 | 7571 | 7571 | 7573 | 7570 | 7570 | 7570 | 7570 | 7570 | 7570 | 7569 | 7569 |
| 0400 | 7569 | 7569 | 7569 | 7569 | 7569 | 7569 | 7569 | 7568 | 7568 | 7568 | 7568 | 7568 |
| 0500 | 7568 | 7568 | 7568 | 7568 | 7568 | 7568 | 7568 | 7567 | 7567 | 7567 | 7567 | 7567 |
| 0600 | 7563 | 7566 | 7566 | 7566 | 7566 | 7566 | 7566 | 7566 | 7566 | 7566 | 7566 | 7566 |
| 0700 | 7563 | 7566 | 7566 | 7566 | 7566 | 7566 | 7566 | 7566 | 7566 | 7566 | 7563 | 7566 |
| 0800 | 7563 | 7565 | 7565 | 7565 | 7565 | 7565 | 7563 | 7565 | 7563 | 7564 | 7564 | 7564 |
| 0900 | 7564 | 7564 | 7564 | 7564 | 7564 | 7564 | 7564 | 7564 | 7564 | 7564 | 7564 | 7564 |
| 1000 | 7564 | 7564 | 7564 | 7564 | 7564 | 7564 | 7564 | 7564 | 7564 | 7564 | 7564 | 7564 |
| 1100 | 7563 | 7562 | 7563 | 7563 | 7563 | 7562 | 7562 | 7562 | 7562 | 7561 | 7561 | 7561 |
| 1200 | 7560 | 7560 | 7560 | 7560 | 7560 | 7560 | 7533 | 7559 | 7559 | 7559 | 7559 | 7559 |
| 1300 | 7558 | 7558 | 7559 | 7559 | 7559 | 7533 | 7559 | 7559 | 7560 | 7560 | 7560 | 7560 |
| 1400 | 7560 | 7563 | 7560 | 7560 | 7560 | 7560 | 7530 | 7559 | 7559 | 7559 | 7559 | 7559 |
| 1500 | 7553 | 7558 | 7558 | 7558 | 7558 | 7558 | 7553 | 7559 | 7559 | 7559 | 7559 | 7559 |
| 1600 | 7559 | 7559 | 7559 | 7558 | 7558 | 7558 | 7558 | 7558 | 7558 | 7558 | 7558 | 7558 |
| 1700 | 7558 | 7558 | 7558 | 7558 | 7558 | 7558 | 7558 | 7558 | 7558 | 7558 | 7558 | 7558 |
| 1800 | 7558 | 7558 | 7558 | 7558 | 7558 | 7558 | 7557 | 7557 | 7557 | 7557 | 7557 | 7557 |

Table 3 (continued)

KIRUNA 67.83N 20.43E SWEDEN

NEUTRON MONITOR 12-NM-64

CORRECTED TO 720 MM HG

COEFFICIENT -0.99 PER CENT PER MM HG

REAL COUNTS 10 TIMES TABULATED COUNTS

FIVE-MINUTE HOURLY RATES

SEPTEMBER 1-2, 1971

| TIME U.T. | MINUTES AT END OF INTERVAL | | | | | | | | | | | |
|---|---|---|---|---|---|---|---|---|---|---|---|---|
| | 05 | 10 | 15 | 20 | 25 | 30 | 35 | 40 | 45 | 50 | 55 | 60 |
| 2000 | 5887 | 5915 | 5929 | 5841 | 5897 | 5903 | 5901 | 5888 | 5843 | 5861 | 5876 | 5902 |
| 2100 | 6001 | 5948 | 6085 | 6110 | 6195 | 6121 | 6172 | 6298 | 6263 | 6342 | 6361 | 6388 |
| 2200 | 6390 | 6424 | 6489 | 6567 | 6518 | 6568 | 6636 | 6648 | 6792 | 6702 | 6722 | 6707 |
| 2300 | 6736 | 6645 | 6638 | 6679 | 6730 | 6728 | 6715 | 6812 | 6663 | 6681 | 6684 | 6644 |
| 2400 | 6636 | 6613 | 6634 | 6601 | 6551 | 6499 | 6585 | 6632 | 6554 | 6538 | 6514 | 6523 |
| 0100 | 6494 | 6546 | 6554 | 6512 | 6478 | 6401 | 6392 | 6451 | 6414 | 6414 | 6365 | 6317 |
| 0200 | 6375 | 6354 | 6358 | 6340 | 6415 | 6299 | 6353 | 6335 | 6352 | 6325 | 6360 | 6277 |
| 0300 | 6288 | 6313 | 6271 | 6264 | 6282 | 6236 | 6190 | 6211 | 6227 | 6213 | 6249 | 6247 |
| 0400 | 6215 | 6241 | 6204 | 6150 | 6196 | 6218 | 6269 | 6144 | 6153 | 6175 | 6127 | 6222 |
| 0500 | 6199 | 6191 | 6105 | 6169 | 6167 | 6140 | 6178 | 6114 | 6163 | 6150 | 6162 | 6129 |
| 0600 | 6086 | 6112 | 6114 | 6075 | 6062 | 6076 | 6042 | 6122 | 6101 | 6134 | 6141 | 6122 |
| 0700 | 6051 | 6104 | 6084 | 6130 | 6020 | 6017 | 6046 | 6111 | 6059 | 6164 | 6125 | 6110 |
| 0800 | 6056 | 6033 | 6083 | 5964 | 6101 | 6084 | 6088 | 6084 | 6058 | 6051 | 6088 | 6065 |
| 0900 | 6117 | 6041 | 6111 | 6128 | 6093 | 6038 | 6109 | 6151 | 6073 | 6031 | 6072 | 6078 |
| 1000 | 6036 | 6044 | 6097 | 6072 | 6056 | 6100 | 6082 | 5992 | 6085 | 6079 | 6078 | 6054 |
| 1100 | 6004 | 6126 | 6080 | 6039 | 6045 | 6002 | 6048 | 6074 | 6057 | 6002 | 6063 | 6022 |
| 1200 | 6051 | 6086 | 6034 | 6005 | 6055 | 6058 | 6066 | 6042 | 6052 | 6055 | 6038 | 5992 |
| 1300 | 6001 | 6073 | 6059 | 6038 | 6015 | 6013 | 6003 | 6013 | 6060 | 6035 | 6031 | 6002 |
| 1400 | 6030 | 5989 | 6016 | 5975 | 6039 | 6009 | 5885 | 6049 | 6047 | 6009 | 6020 | 5955 |
| 1500 | 5905 | 6011 | 5962 | 5935 | 6036 | 6014 | 6008 | 5984 | 5907 | 5923 | 5993 | 5929 |
| 1600 | 5939 | 5966 | 6017 | 5999 | 6018 | 5981 | 6016 | 5978 | 6054 | 5981 | 5922 | 5969 |
| 1700 | 6000 | 5976 | 5880 | 5953 | 5896 | 5972 | 5997 | 5956 | 5953 | 5932 | 5989 | 5946 |
| 1800 | 5930 | 5976 | 5978 | 5937 | 5972 | 5918 | 5952 | 5901 | 5971 | 5933 | 5968 | 5877 |
| 1900 | 5944 | 5957 | 5975 | 5959 | 5885 | 5889 | 5885 | 5929 | 5907 | 5964 | 5881 | 5925 |

BELGRANO 77.96S 38.8W ANTARCTIC

NEUTRON MONITOR 6-NM-64

REAL COUNTS 16 TIMES TABULATED COUNTS

FIVE-MINUTE BAROMETER CORRECTED HOURLY RATES

SEPTEMBER 1-2, 1971

| TIME U.T. | MINUTES AT END OF INTERVAL | | | | | | | | | | | |
|---|---|---|---|---|---|---|---|---|---|---|---|---|
| | 05 | 10 | 15 | 20 | 25 | 30 | 35 | 40 | 45 | 50 | 55 | 60 |
| 1700-1800 | 1345 | 1375 | 1352 | 1343 | 1364 | 1369 | 1373 | 1353 | 1372 | 1370 | 1373 | 1356 |
| 1800-1900 | 1376 | 1376 | 1365 | 1368 | 1385 | 1388 | 1363 | 1384 | 1367 | 1379 | 1358 | 1351 |
| 1900-2000 | 1390 | 1364 | 1371 | 1375 | 1388 | 1387 | 1371 | 1399 | 1388 | 1363 | 1352 | 1367 |
| 2000-2100 | 1383 | 1364 | 1385 | 1402 | 1410 | 1406 | 1380 | 1424 | 1429 | 1431 | 1460 | 1464 |
| 2100-2200 | 1454 | 1482 | 1506 | 1489 | 1507 | 1506 | 1515 | 1517 | 1525 | 1522 | 1524 | 1504 |
| 2200-2300 | 1512 | 1474 | 1506 | 1488 | 1510 | 1494 | 1464 | 1462 | 1500 | 1496 | 1509 | 1485 |
| 2300-2400 | 1517 | 1493 | 1495 | 1502 | 1522 | 1495 | 1523 | 1501 | 1494 | 1485 | 1490 | 1484 |
| 2400-0100 | 1511 | 1470 | 1462 | 1505 | 1506 | 1473 | 1486 | 1502 | 1501 | 1461 | 1464 | 1476 |
| 0100-0200 | 1469 | 1483 | 1488 | 1474 | 1484 | 1485 | 1462 | 1445 | 1472 | 1479 | 1468 | 1453 |
| 0200-0300 | 1455 | 1459 | 1413 | 1453 | 1456 | 1451 | 1442 | 1447 | 1430 | 1421 | 1430 | 1426 |
| 0300-0400 | 1423 | 1470 | 1440 | 1423 | 1398 | 1448 | 1452 | 1441 | 1475 | 1448 | 1424 | 1431 |
| 0400-0500 | 1426 | 1431 | 1410 | 1408 | 1415 | 1417 | 1445 | 1422 | 1453 | 1444 | 1424 | 1416 |
| 0500-0600 | 1393 | 1418 | 1405 | 1394 | 1410 | 1397 | 1404 | 1388 | 1398 | 1424 | 1394 | 1407 |

OULU 65.1N 25.3E FINLAND

NEUTRON MONITOR 9-NM-64

CORRECTED FOR PRESSURE

SCALING FACTOR 64

FIVE-MINUTE HOURLY RATES

SEPTEMBER 1-2, 1971

| TIME U.T. | MINUTES AT END OF INTERVAL 05 | 10 | 15 | 20 | 25 | 30 | 35 | 40 | 45 | 50 | 55 | 60 | AVERAGE |
|---|---|---|---|---|---|---|---|---|---|---|---|---|---|
| 1800 | 496 | 498 | 496 | 486 | 497 | 493 | 490 | 503 | 494 | 500 | 488 | 500 | 495.0 |
| 1900 | 489 | 495 | 487 | 488 | 487 | 495 | 494 | 493 | 497 | 497 | 496 | 497 | 493.1 |
| 2000 | 506 | 504 | 508 | 510 | 513 | 519 | 522 | 524 | 519 | 526 | 523 | 537 | 517.6 |
| 2100 | 543 | 549 | 552 | 545 | 547 | 548 | 547 | 553 | 544 | 550 | 556 | 553 | 548.9 |
| 2200 | 566 | 563 | 559 | 556 | 545 | 556 | 551 | 548 | 550 | 552 | 550 | 544 | 553.4 |
| 2300 | 548 | 545 | 544 | 544 | 541 | 543 | 540 | 531 | 546 | 538 | 535 | 535 | 540.5 |
| 2400 | 535 | 541 | 537 | 524 | 539 | 539 | 531 | 530 | 537 | 536 | 526 | 528 | 533.5 |
| 0100 | 525 | 521 | 533 | 529 | 523 | 526 | 526 | 521 | 522 | 524 | 526 | 525 | 525.4 |
| 0200 | 526 | 523 | 526 | 523 | 519 | 518 | 518 | 520 | 517 | 516 | 519 | 517 | 520.4 |
| 0300 | 507 | 521 | 518 | 519 | 513 | 517 | 514 | 520 | 511 | 516 | 511 | 511 | 514.6 |
| 0400 | 505 | 522 | 514 | 512 | 517 | 515 | 503 | 511 | 507 | 513 | 514 | 509 | 511.5 |
| 0500 | 515 | 507 | 513 | 506 | 507 | 505 | 506 | 511 | 505 | 502 | 506 | 509 | 507.9 |
| 0600 | 508 | 507 | 500 | 510 | 505 | 503 | 511 | 513 | 509 | 505 | 511 | 513 | 507.8 |
| 0700 | 503 | 501 | 509 | 511 | 505 | 506 | 514 | 509 | 504 | 503 | 510 | 506 | 506.8 |
| 0800 | 514 | 511 | 506 | 503 | 511 | 500 | 508 | 510 | 508 | 507 | 507 | 499 | 507.1 |

DEEP RIVER 46.1N 77.3W CANADA

NEUTRON MONITOR 48-NM-64

REAL COUNTS 300 TIMES TABULATED COUNTS

FIVE-MINUTE BAROMETER CORRECTED HOURLY RATES

SEPTEMBER 1-2, 1971

| TIME U.T. | MINUTES AT END OF INTERVAL 05 | 10 | 15 | 20 | 25 | 30 | 35 | 40 | 45 | 50 | 55 | 60 | AVERAGE |
|---|---|---|---|---|---|---|---|---|---|---|---|---|---|
| 1900-2000 | 6947 | 6986 | 6973 | 6960 | 6927 | 6998 | 6959 | 6991 | 6965 | 6991 | 6971 | 6971 | 6970 |
| 2000-2100 | 6964 | 7010 | 7029 | 7067 | 7099 | 7222 | 7261 | 7299 | 7331 | 7395 | 7408 | 7414 | 7208 |
| 2100-2200 | 7427 | 7504 | 7504 | 7581 | 7535 | 7612 | 7638 | 7599 | 7586 | 7612 | 7612 | 7625 | 7570 |
| 2200-2300 | 7669 | 7669 | 7695 | 7656 | 7643 | 7695 | 7725 | 7636 | 7700 | 7713 | 7679 | 7648 | 7677 |
| 2300-2400 | 7648 | 7648 | 7641 | 7692 | 7667 | 7628 | 7602 | 7602 | 7590 | 7590 | 7602 | 7551 | 7622 |
| 2400-0100 | 7533 | 7559 | 7559 | 7507 | 7489 | 7491 | 7568 | 7473 | 7473 | 7506 | 7467 | 7506 | 7511 |
| 0100-0200 | 7467 | 7487 | 7462 | 7454 | 7416 | 7454 | 7467 | 7397 | 7403 | 7364 | 7377 | 7332 | 7423 |
| 0200-0300 | 7345 | 7332 | 7320 | 7255 | 7268 | 7307 | 7332 | 7216 | 7242 | 7242 | 7255 | 7268 | 7282 |
| 0300-0400 | 7242 | 7229 | 7203 | 7235 | 7196 | 7216 | 7165 | 7210 | 7198 | 7203 | 7203 | 7183 | 7207 |
| 0400-0500 | 7196 | 7183 | 7145 | 7139 | 7113 | 7203 | 7152 | 7165 | 7087 | 7087 | 7178 | 7126 | 7148 |
| 0500-0600 | 7126 | 7126 | 7087 | 7120 | 7094 | 7107 | 7146 | 7094 | 7120 | 7068 | 7113 | 7029 | 7103 |
| 0600-0700 | 7093 | 7106 | 7042 | 7054 | 7061 | 7074 | 7042 | 7093 | 7080 | 7003 | 7100 | 7048 | 7066 |
| 0700-0800 | 7042 | 7094 | 7074 | 7036 | 7029 | 7099 | 7060 | 7060 | 7086 | 7073 | 6996 | 6996 | 7054 |
| 0800-0900 | 7022 | 7060 | 7022 | 7015 | 7028 | 7021 | 6988 | 7027 | 7039 | 7039 | 7007 | 6994 | 7022 |
| 0900-1000 | 6994 | 7020 | 7020 | 7000 | 6987 | 7000 | 6949 | 7020 | 7058 | 7033 | 6961 | 7000 | 7004 |
| 1000-1100 | 7026 | 7064 | 6993 | 6967 | 6993 | 6987 | 7026 | 6974 | 6974 | 6981 | 6968 | 6994 | 6996 |

Table 3 (continued)

SANAE 70.46S 357.51E ANTARCTICA

3-NM-64 NEUTRON MONITOR

REAL COUNTS 10 TIMES TABULATED VALUES

CORRECTED TO 980 MB

COEFFICIENT 0.73 PER CENT PER MILLIBAR

TEN-MINUTE HOURLY COUNTING RATES

SEPTEMBER 1-2, 1971

| TIME U.T. | MINUTES AT END OF INTERVAL 10 | 20 | 30 | 40 | 50 | 60 |
|---|---|---|---|---|---|---|
| 1700-1800 | 2582 | 2536 | 2524 | 2556 | 2532 | 2564 |
| 1800-1900 | 2537 | 2560 | 2526 | 2526 | 2534 | 2534 |
| 1900-2000 | 2605 | 2542 | 2534 | 2554 | 2552 | 2548 |
| 2000-2100 | 2566 | 2596 | 2602 | 2690 | 2730 | 2728 |
| 2100-2200 | 2748 | 2800 | 2778 | 2812 | 2812 | 2798 |
| 2200-2300 | 2898 | 2897 | 2853 | 2875 | 2859 | 2875 |
| 2300-2400 | 2839 | 2847 | 2827 | 2851 | 2837 | 2821 |
| 2400-0100 | 2828 | 2772 | 2766 | 2744 | 2778 | 2736 |
| 0100-0200 | 2765 | 2744 | 2734 | 2730 | 2692 | 2740 |
| 0200-0300 | 2716 | 2700 | 2692 | 2704 | 2684 | 2677 |
| 0300-0400 | 2683 | 2706 | 2665 | 2623 | 2649 | 2683 |
| 0400-0500 | 2659 | 2616 | 2649 | 2683 | 2657 | 2632 |
| 0500-0600 | 2666 | 2563 | 2626 | 2618 | 2624 | 2667 |
| 0600-0700 | 2593 | 2561 | 2616 | 2628 | 2624 | 2640 |
| 0700-0800 | 2601 | 2620 | 2622 | 2552 | 2595 | 2616 |
| 0800-0900 | 2634 | 2612 | 2583 | 2614 | 2597 | 2589 |
| 0900-1000 | 2646 | 2620 | 2606 | 2583 | 2620 | 2604 |
| 1000-1100 | 2605 | 2600 | 2591 | 2571 | 2597 | 2628 |
| 1100-1200 | 2658 | 2573 | 2585 | 2626 | 2520 | 2602 |

PORT AUX FRANCAIS 49.35S 70.25E KERGUELEN ISLAND

NEUTRON MONITOR 18-NM-64

CORRECTED FOR BAROMETRIC PRESSURE

COEFFICIENT 10.1 PER CENT PER CM HG

MULTIPLY INDICATED NUMBERS BY 400

FIVE-MINUTE HOURLY RATES

| TIME U.T. | MINUTES AT END OF INTERVAL 05 | 10 | 15 | 20 | 25 | 30 | 35 | 40 | 45 | 50 | 55 | 60 |
|---|---|---|---|---|---|---|---|---|---|---|---|---|
| 1800 | 1624 | 1624 | 1623 | 1627 | 1626 | 1624 | 1644 | 1632 | 1631 | 1634 | 1649 | 1636 |
| 1900 | 1608 | 1619 | 1617 | 1640 | 1615 | 1595 | 1607 | 1630 | 1618 | 1630 | 1624 | 1631 |
| 2000 | 1625 | 1628 | 1642 | 1621 | 1619 | 1620 | 1632 | 1627 | 1617 | 1626 | 1620 | 1625 |
| 2100 | 1638 | 1661 | 1684 | 1702 | 1718 | 1760 | 1766 | 1767 | 1775 | 1806 | 1795 | 1835 |
| 2200 | 1811 | 1806 | 1845 | 1817 | 1820 | 1839 | 1849 | 1822 | 1824 | 1832 | 1833 | 1814 |
| 2300 | 1831 | 1845 | 1842 | 1842 | 1829 | 1821 | 1814 | 1815 | 1839 | 1816 | 1799 | 1810 |
| 2400 | 1781 | 1806 | 1807 | 1808 | 1803 | 1792 | 1795 | 1782 | 1782 | 1795 | 1784 | 1784 |
| 0100 | 1769 | 1773 | 1772 | 1775 | 1761 | 1759 | 1769 | 1778 | 1767 | 1759 | 1747 | 1762 |
| 0200 | 1765 | 1758 | 1756 | 1752 | 1746 | 1747 | 1733 | 1737 | 1744 | 1750 | 1705 | 1736 |
| 0300 | 1726 | 1742 | 1727 | 1719 | 1730 | 1737 | 1720 | 1726 | 1733 | 1737 | 1723 | 1706 |
| 0400 | 1710 | 1703 | 1707 | 1717 | 1707 | 1711 | 1699 | 1714 | 1694 | 1707 | 1702 | 1706 |
| 0500 | 1696 | 1705 | 1695 | 1710 | 1682 | 1723 | 1705 | 1702 | 1706 | 1715 | 1702 | 1707 |
| 0600 | 1699 | 1693 | 1686 | 1693 | 1692 | 1696 | 1695 | 1689 | 1692 | 1688 | 1702 | 1697 |
| 0700 | 1694 | 1693 | 1703 | 1697 | 1677 | 1679 | 1688 | 1690 | 1688 | 1698 | 1694 | 1682 |
| 0800 | 1705 | 1689 | 1704 | 1679 | 1688 | 1700 | 1685 | 1688 | 1688 | 1682 | 1674 | 1689 |
| 0900 | 1690 | 1687 | 1697 | 1682 | 1687 | 1676 | 1688 | 1691 | 1675 | 1682 | 1697 | 1680 |
| 1000 | 1690 | 1667 | 1673 | 1679 | 1675 | 1692 | 1664 | 1688 | 1671 | 1664 | 1648 | 1681 |
| 1100 | 1672 | 1674 | 1686 | 1681 | 1673 | 1679 | 1667 | 1664 | 1676 | 1678 | 1671 | 1659 |
| 1200 | 1695 | 1685 | 1683 | 1685 | 1673 | 1691 | 1669 | 1671 | 1681 | 1695 | 1668 | 1665 |

MT WASHINGTON 44.3N 288.7E NEW HAMPSHIRE

IGY NEUTRON MONITOR

CORRECTED FOR BAROMETRIC PRESSURE

FIVE-MINUTE HOURLY RATES

SEPTEMBER 1-2, 1971

| TIME U.T. | MINUTES AT END OF INTERVAL 05 | 10 | 15 | 20 | 25 | 30 | 35 | 40 | 45 | 50 | 55 | 60 |
|---|---|---|---|---|---|---|---|---|---|---|---|---|
| 1800-1900 | 190 | 194 | 196 | 192 | 188 | 191 | 197 | 189 | 194 | 187 | 196 | 194 |
| 1900-2000 | 193 | 189 | 194 | 193 | 190 | 190 | 196 | 194 | 193 | 191 | 198 | 189 |
| 2000-2100 | 192 | 197 | 197 | 201 | 197 | 199 | 204 | 211 | 206 | 214 | 214 | 211 |
| 2100-2200 | 219 | 221 | 215 | 224 | 219 | 220 | 220 | 218 | 222 | 219 | 222 | 220 |
| 2200-2300 | 219 | 225 | 222 | 230 | 222 | 218 | 222 | 217 | 216 | 220 | 222 | 216 |
| 2300-2400 | 216 | 219 | 212 | 215 | 216 | 216 | 212 | 213 | 220 | 212 | 215 | 216 |
| 2400-0100 | 211 | 218 | 212 | 215 | 211 | 214 | 214 | 212 | 212 | 213 | 214 | 207 |
| 0100-0200 | 208 | 207 | 209 | 210 | 206 | 208 | 206 | 205 | 207 | 207 | 202 | 205 |
| 0200-0300 | 0 | 200 | 202 | 203 | 200 | 204 | 199 | 202 | 207 | 203 | 203 | 207 |
| 0300-0400 | 201 | 198 | 204 | 198 | 199 | 198 | 198 | 197 | 193 | 198 | 196 | 201 |
| 0400-0500 | 199 | 198 | 198 | 200 | 197 | 197 | 200 | 198 | 197 | 205 | 195 | 199 |
| 0500-0600 | 200 | 195 | 200 | 195 | 204 | 197 | 194 | 199 | 199 | 203 | 196 | 197 |
| 0600-0700 | 197 | 196 | 195 | 196 | 190 | 198 | 200 | 198 | 196 | 192 | 195 | 197 |

DURHAM 43.1N 289.1E NEW HAMPSHIRE

NEUTRON MONITOR 12-NM-64

CORRECTED FOR BAROMETRIC PRESSURE

FIVE-MINUTE HOURLY RATES

SEPTEMBER 1-2, 1971

| TIME U.T. | MINUTES AT END OF INTERVAL 05 | 10 | 15 | 20 | 25 | 30 | 35 | 40 | 45 | 50 | 55 | 60 |
|---|---|---|---|---|---|---|---|---|---|---|---|---|
| 1800-1900 | 191 | 190 | 190 | 189 | 187 | 189 | 189 | 190 | 191 | 189 | 190 | 192 |
| 1900-2000 | 190 | 191 | 192 | 190 | 190 | 188 | 189 | 192 | 188 | 188 | 192 | 191 |
| 2000-2100 | 193 | 193 | 192 | 194 | 197 | 198 | 197 | 199 | 203 | 200 | 201 | 202 |
| 2100-2200 | 201 | 204 | 205 | 205 | 204 | 207 | 202 | 207 | 204 | 205 | 205 | 205 |
| 2200-2300 | 207 | 204 | 204 | 209 | 206 | 206 | 205 | 204 | 205 | 205 | 203 | 199 |
| 2300-2400 | 202 | 202 | 203 | 202 | 203 | 202 | 198 | 202 | 202 | 202 | 198 | 200 |
| 2400-0100 | 202 | 199 | 202 | 197 | 199 | 198 | 196 | 197 | 200 | 197 | 198 | 198 |
| 0100-0200 | 198 | 199 | 194 | 198 | 198 | 196 | 198 | 198 | 196 | 199 | 194 | 195 |
| 0200-0300 | 195 | 197 | 193 | 194 | 192 | 195 | 193 | 192 | 197 | 195 | 193 | 194 |
| 0300-0400 | 191 | 190 | 192 | 193 | 193 | 194 | 194 | 193 | 193 | 193 | 194 | 191 |
| 0400-0500 | 197 | 191 | 192 | 192 | 192 | 196 | 192 | 193 | 191 | 190 | 190 | 193 |
| 0500-0600 | 193 | 194 | 191 | 192 | 189 | 192 | 190 | 188 | 190 | 192 | 190 | 191 |

Table 3 (continued)

LEEDS 53.8N 01.5W ENGLAND

IGY NEUTRON MONITOR

REAL COUNTS 100 TIMES TABULATED COUNTS

FIVE-MINUTE UNCORRECTED RATES

SEPTEMBER 1-2, 1971

| TIME U.T. | MINUTES AT END OF INTERVAL 05 | 10 | 15 | 20 | 25 | 30 | 35 | 40 | 45 | 50 | 55 | 60 |
|---|---|---|---|---|---|---|---|---|---|---|---|---|
| 2400-0100 | 583 | 584 | 581 | 587 | 584 | 590 | 592 | 585 | 589 | 589 | 589 | 592 |
| 0100-0200 | 592 | 590 | 596 | 590 | 591 | 590 | 592 | 587 | 588 | 588 | 589 | 588 |
| 0200-0300 | 591 | 579 | 587 | 593 | 591 | 583 | 591 | 597 | 586 | 594 | 591 | 601 |
| 0300-0400 | 594 | 592 | 593 | 598 | 598 | 600 | 589 | 592 | 595 | 597 | 597 | 588 |
| 0400-0500 | 590 | 595 | 601 | 599 | 596 | 592 | 592 | 597 | 599 | 594 | 603 | 597 |
| 0500-0600 | 595 | 598 | 591 | 598 | 595 | 595 | 596 | 600 | 589 | 597 | 595 | 589 |
| 0600-0700 | 593 | 590 | 597 | 598 | 587 | 596 | 586 | 605 | 599 | 599 | 599 | 597 |
| 0700-0800 | 597 | 596 | 598 | 593 | 592 | 593 | 593 | 604 | 596 | 596 | 587 | 591 |
| 0800-0900 | 591 | 595 | 595 | 597 | 598 | 595 | 593 | 590 | 599 | 595 | 593 | 596 |
| 0900-1000 | 602 | 592 | 596 | 601 | 583 | 602 | 589 | 596 | 598 | 590 | 595 | 589 |
| 1000-1100 | 597 | 596 | 597 | 595 | 600 | 591 | 597 | 594 | 589 | 596 | 593 | 590 |
| 1100-1200 | 596 | 594 | 595 | 598 | 592 | 601 | 597 | 599 | 600 | 597 | 593 | 588 |
| 1200-1300 | 599 | 593 | 593 | 596 | 590 | 595 | 595 | 597 | 595 | 591 | 590 | 588 |
| 1300-1400 | 583 | 589 | 591 | 587 | 595 | 590 | 590 | 584 | 588 | 589 | 587 | 577 |
| 1400-1500 | 585 | 585 | 586 | 582 | 580 | 585 | 587 | 587 | 591 | 595 | 589 | 587 |
| 1500-1600 | 583 | 579 | 584 | 586 | 585 | 586 | 577 | 588 | 583 | 583 | 585 | 584 |
| 1600-1700 | 577 | 586 | 586 | 578 | 573 | 577 | 583 | 584 | 577 | 579 | 578 | 576 |
| 1700-1800 | 573 | 574 | 573 | 579 | 577 | 567 | 579 | 575 | 574 | 566 | 580 | 566 |
| 1800-1900 | 573 | 574 | 577 | 583 | 572 | 569 | 577 | 575 | 574 | 572 | 569 | 575 |
| 1900-2000 | 571 | 567 | 567 | 570 | 569 | 563 | 568 | 568 | 564 | 563 | 568 | 565 |
| 2000-2100 | 572 | 568 | 573 | 571 | 576 | 576 | 572 | 579 | 573 | 579 | 588 | 588 |
| 2100-2200 | 594 | 583 | 581 | 583 | 588 | 577 | 582 | 579 | 583 | 581 | 577 | 578 |
| 2200-2300 | 574 | 579 | 579 | 578 | 572 | 572 | 572 | 565 | 571 | 568 | 564 | 571 |
| 2300-2400 | 565 | 561 | 573 | 560 | 569 | 566 | 568 | 566 | 566 | 564 | 568 | 562 |
| 2400-0100 | 570 | 567 | 565 | 563 | 567 | 563 | 566 | 564 | 566 | 563 | 559 | 562 |
| 0100-0200 | 567 | 555 | 554 | 557 | 559 | 552 | 556 | 560 | 555 | 558 | 557 | 553 |
| 0200-0300 | 560 | 553 | 558 | 555 | 555 | 561 | 549 | 559 | 553 | 555 | 551 | 551 |
| 0300-0400 | 556 | 554 | 557 | 561 | 554 | 560 | 547 | 551 | 552 | 554 | 557 | 550 |
| 0400-0500 | 546 | 551 | 551 | 548 | 548 | 552 | 553 | 555 | 550 | 545 | 551 | 557 |
| 0500-0600 | 547 | 545 | 543 | 549 | 550 | 550 | 547 | 551 | 549 | 548 | 549 | 550 |
| 0600-0700 | 557 | 554 | 546 | 550 | 548 | 555 | 547 | 549 | 552 | 548 | 552 | 555 |
| 0700-0800 | 556 | 550 | 549 | 564 | 547 | 550 | 554 | 552 | 555 | 554 | 547 | 554 |
| 0800-0900 | 553 | 549 | 554 | 550 | 550 | 549 | 549 | 549 | 554 | 550 | 554 | 552 |
| 0900-1000 | 554 | 551 | 555 | 547 | 553 | 554 | 557 | 551 | 555 | 553 | 543 | 550 |
| 1000-1100 | 551 | 552 | 551 | 548 | 553 | 548 | 552 | 552 | 550 | 553 | 553 | 556 |
| 1100-1200 | 555 | 551 | 554 | 552 | 552 | 553 | 550 | 557 | 555 | 549 | 554 | 551 |
| 1200-1300 | 554 | 554 | 550 | 553 | 556 | 550 | 554 | 555 | 553 | 558 | 551 | 557 |
| 1300-1400 | 554 | 553 | 561 | 553 | 554 | 556 | 554 | 558 | 555 | 561 | 554 | 552 |
| 1400-1500 | 552 | 557 | 557 | 559 | 552 | 551 | 553 | 552 | 559 | 559 | 553 | 551 |
| 1500-1600 | 551 | 555 | 555 | 552 | 553 | 554 | 545 | 550 | 559 | 556 | 549 | 551 |
| 1600-1700 | 549 | 553 | 551 | 547 | 558 | 548 | 554 | 553 | 550 | 549 | 544 | 556 |
| 1700-1800 | 546 | 551 | 554 | 545 | 557 | 549 | 545 | 553 | 554 | 552 | 545 | 550 |
| 1800-1900 | 551 | 551 | 543 | 546 | 549 | 549 | 553 | 545 | 550 | 546 | 539 | 543 |
| 1900-2000 | 545 | 548 | 552 | 551 | 542 | 545 | 549 | 550 | 548 | 545 | 548 | 545 |
| 2000-2100 | 551 | 541 | 540 | 546 | 545 | 545 | 546 | 541 | 546 | 542 | 544 | 547 |
| 2100-2200 | 549 | 553 | 543 | 550 | 541 | 542 | 539 | 544 | 543 | 543 | 545 | 543 |
| 2200-2300 | 538 | 545 | 544 | 543 | 546 | 543 | 549 | 545 | 542 | 549 | 544 | 538 |
| 2300-2400 | 542 | 545 | 540 | 548 | 540 | 543 | 549 | 544 | 545 | 544 | 548 | 544 |

Table 3 (continued)

LOMNICKY STIT 49.2N 20.22E CZECHOSLOVAKIA

IGY NEUTRON MONITOR

CORRECTED TO 550.0 MM HG

COEFFICIENT -1.024 PER CENT PER MM HG

REAL COUNTS 8 TIMES TABULATED COUNTS

TEN-MINUTE HOURLY RATES

SEPTEMBER 1-2, 1971

| TIME U.T. | MINUTES AT END OF INTERVAL 10 | 20 | 30 | 40 | 50 | 60 |
|---|---|---|---|---|---|---|
| 1900-2000 | 1818.3 | 1781.3 | 1774.5 | 1801.2 | 1798.0 | 1781.7 |
| 2000-2100 | 1790.3 | 1801.7 | 1793.1 | 1782.2 | 1815.9 | 1804.4 |
| 2100-2200 | 1802.2 | 1853.7 | 1768.9 | 1784.0 | 1774.3 | 1816.1 |
| 2200-2300 | 1820.4 | 1815.1 | 1788.6 | 1820.4 | 1800.1 | 1758.3 |
| 2300-2400 | 1827.9 | 1797.1 | 1821.8 | 1791.3 | 1812.4 | 1801.7 |
| 2400-0100 | 1802.8 | 1795.6 | 1802.0 | 1839.4 | 1781.7 | 1808.7 |
| 0100-0200 | 1792.7 | 1787.4 | 1757.5 | 1782.3 | 1809.0 | 1781.8 |
| 0200-0300 | 1790.9 | 1811.4 | 1781.6 | 1805.0 | 1790.4 | 1725.5 |
| 0300-0400 | 1785.4 | 1796.8 | 1798.9 | 1796.8 | 1737.5 | 1782.9 |
| 0400-0500 | 1801.0 | 1800.3 | 1791.7 | 1809.6 | 1799.2 | 1793.1 |
| 0500-0600 | 1787.0 | 1786.7 | 1796.0 | 0.0 | 0.0 | 1817.5 |
| 0600-0700 | 1813.0 | 1825.0 | 1792.0 | 1738.1 | 1770.8 | 1823.9 |
| 0700-0800 | 1770.8 | 1800.5 | 1805.1 | 1802.4 | 1809.0 | 1763.4 |
| 0800-0900 | 1767.1 | 1815.4 | 1805.8 | 1815.9 | 1817.3 | 1794.9 |
| 0900-1000 | 1776.3 | 1803.9 | 1818.6 | 1781.3 | 1822.6 | 1802.3 |
| 1000-1100 | 1801.3 | 1786.0 | 1793.5 | 1813.8 | 1815.6 | 1804.9 |

DALLAS 32.78N 96.80W TEXAS

NEUTRON MONITOR NM-64

REAL COUNTS 40 TIMES TABULATED COUNTS

FIVE-MINUTE BAROMETER CORRECTED HOURLY RATES

SEPTEMBER 1-2, 1971

| TIME U.T. | MINUTES AT END OF INTERVAL 05 | 10 | 15 | 20 | 25 | 30 | 35 | 40 | 45 | 50 | 55 | 60 | AVERAGE |
|---|---|---|---|---|---|---|---|---|---|---|---|---|---|
| 1700 | 1572 | 1565 | 1572 | 1555 | 1569 | 1584 | 1578 | 1542 | 1577 | 1549 | 1569 | 1598 | 1569.2 |
| 1800 | 1567 | 1577 | 1582 | 1568 | 1566 | 1559 | 1596 | 1591 | 1602 | 1588 | 1581 | 1574 | 1579.5 |
| 1900 | 1573 | 1579 | 1585 | 1600 | 1568 | 1576 | 1581 | 1572 | 1600 | 1580 | 1595 | 1565 | 1581.2 |
| 2000 | 1557 | 1580 | 1603 | 1573 | 1576 | 1569 | 1583 | 1579 | 1588 | 1595 | 1572 | 1582 | 1579.8 |
| 2100 | 1582 | 1579 | 1585 | 1577 | 1585 | 1569 | 1582 | 1586 | 1594 | 1576 | 1572 | 1579 | 1580.7 |
| 2200 | 1565 | 1592 | 1585 | 1592 | 1593 | 1589 | 1571 | 1565 | 1575 | 1589 | 1583 | 1586 | 1582.1 |
| 2300 | 1590 | 1580 | 1579 | 1586 | 1567 | 1597 | 1573 | 1567 | 1576 | 1580 | 1596 | 1583 | 1581.2 |
| 2400 | 1586 | 1575 | 1577 | 1595 | 1575 | 1567 | 1562 | 1592 | 1580 | 1560 | 1579 | 1587 | 1577.9 |
| 0100 | 1565 | 1560 | 1553 | 1565 | 1573 | 1596 | 1570 | 1566 | 1557 | 1586 | 1559 | 1565 | 1568.0 |
| 0200 | 1565 | 1576 | 1567 | 1570 | 1544 | 1582 | 1544 | 1572 | 1572 | 1556 | 1574 | 1578 | 1566.6 |
| 0300 | 1551 | 1551 | 1581 | 1549 | 1534 | 1561 | 1574 | 1570 | 1560 | 1564 | 1571 | 1569 | 1561.3 |
| 0400 | 1555 | 1586 | 1571 | 1547 | 1561 | 1571 | 1585 | 1559 | 1551 | 1543 | 1567 | 1569 | 1563.8 |
| 0500 | 1571 | 1562 | 1543 | 1561 | 1569 | 1558 | 1570 | 1556 | 1561 | 1538 | 1559 | 1558 | 1558.9 |
| 0600 | 1587 | 1553 | 1551 | 1589 | 1560 | 1568 | 1577 | 1564 | 1547 | 1550 | 1551 | 1565 | 1563.7 |
| 0700 | 1572 | 1557 | 1574 | 1565 | 1537 | 1575 | 1565 | 1556 | 1560 | 1577 | 1580 | 1557 | 1564.7 |
| 0800 | 1566 | 1584 | 1550 | 1584 | 1568 | 1549 | 1553 | 1542 | 1582 | 1564 | 1553 | 1570 | 1563.7 |
| 0900 | 1554 | 1558 | 1566 | 1570 | 1557 | 1585 | 1585 | 1560 | 1569 | 1559 | 1562 | 1574 | 1565.8 |
| 1000 | 1561 | 1560 | 1556 | 1580 | 1574 | 1575 | 1580 | 1559 | 1539 | 1556 | 1542 | 1576 | 1563.3 |
| 1100 | 1569 | 1575 | 1538 | 1573 | 1557 | 1554 | 1570 | 1575 | 1569 | 1561 | 1574 | 1566 | 1565.2 |
| 1200 | 1567 | 1552 | 1564 | 1562 | 1570 | 1565 | 1592 | 1571 | 1568 | 1586 | 1554 | 1572 | 1568.7 |
| 1300 | 1565 | 1551 | 1559 | 1566 | 1572 | 1577 | | | | | | | |

JUNGFRAUJOCH 46.6N 8.0E SWITZERLAND

IGY NEUTRON MONITOR

SCALING FACTOR 10

SIX-MINUTES BAROMETER CORRECTED HOURLY RATES

SEPTEMBER 1-2, 1971

| TIME U.T. | MINUTES AT END OF INTERVAL 6 | 12 | 18 | 24 | 30 | 36 | 42 | 48 | 54 | 60 | AVERAGE |
|---|---|---|---|---|---|---|---|---|---|---|---|
| 1700 | 5983 | 6071 | 6113 | 6112 | 6081 | 6105 | 6073 | 6119 | 6104 | 6090 | 6085.1 |
| 1800 | 6083 | 6052 | 6101 | 6035 | 6067 | 6076 | 6073 | 6103 | 6034 | 6021 | 6064.5 |
| 1900 | 6090 | 6067 | 6049 | 6071 | 6026 | 6074 | 6028 | 6111 | 6078 | 6054 | 6064.8 |
| 2000 | 6056 | 6118 | 6079 | 6115 | 6083 | 6053 | 6098 | 6120 | 6072 | 6063 | 6085.7 |
| 2100 | 6045 | 6105 | 6065 | 6131 | 6053 | 6026 | 6114 | 6026 | 5978 | 6002 | 6054.5 |
| 2200 | 6075 | 5966 | 6130 | 6030 | 6129 | 6006 | 6101 | 6026 | 6033 | 6129 | 6062.5 |
| 2300 | 6073 | 6048 | 6055 | 6048 | 6026 | 6050 | 6119 | 6052 | 5985 | 6032 | 6048.8 |

USHUAIA 54.8S 68.3W ARGENTINA

IGY NEUTRON MONITOR

REAL COUNTS 8 TIMES TABULATED COUNTS

FIFTEEN-MINUTE BAROMETER CORRECTED RATES

SEPTEMBER 1-2, 1971

| TIME U.T. | MINUTES AT END OF INTERVAL 15 | 30 | 45 | 60 |
|---|---|---|---|---|
| 1700-1800 | 848 | 851 | 866 | 863 |
| 1800-1900 | 875 | 844 | 873 | 873 |
| 1900-2000 | 832 | 860 | 852 | 853 |
| 2000-2100 | 842 | 861 | 839 | 831 |
| 2100-2200 | 873 | 863 | 868 | 845 |
| 2200-2300 | 858 | 0 | 842 | 845 |
| 2300-2400 | 835 | 844 | 870 | 885 |
| 2400-0100 | 854 | 873 | 836 | 860 |
| 0100-0200 | 851 | 847 | 830 | 836 |
| 0200-0300 | 851 | 849 | 845 | 839 |
| 0300-0400 | 847 | 882 | 856 | 840 |
| 0400-0500 | 842 | 873 | 851 | 828 |
| 0500-0600 | 829 | 856 | 851 | 856 |

Table 3 (continued)

MEXICO CITY 19.33N 99.18W MEXICO

NEUTRON MONITOR 6-NM-64

CORRECTED TO 778.9 MILLIBARS

COEFFICIENT -0.72 PER CENT PER MILLIBAR

REAL COUNTS 100 TIMES TABULATED COUNTS

FIVE-MINUTE HOURLY RATES

SEPTEMBER 1-2, 1971

| TIME U.T. | MINUTES AT END OF INTERVAL 05 | 10 | 15 | 20 | 25 | 30 | 35 | 40 | 45 | 50 | 55 | 60 | AVERAGE |
|---|---|---|---|---|---|---|---|---|---|---|---|---|---|
| 1800-1900 | 650 | 653 | 654 | 658 | 662 | 655 | 657 | 652 | 644 | 651 | 658 | 655 | 654.1 |
| 1900-2000 | 653 | 651 | 654 | 652 | 658 | 663 | 656 | 647 | 662 | 659 | 657 | 653 | 654.7 |
| 2000-2100 | 649 | 656 | 650 | 650 | 657 | 662 | 651 | 658 | 662 | 656 | 661 | 651 | 655.3 |
| 2100-2200 | 653 | 654 | 655 | 649 | 656 | 655 | 663 | 659 | 657 | 658 | 659 | 652 | 655.8 |
| 2200-2300 | 657 | 653 | 654 | 656 | 655 | 662 | 656 | 654 | 653 | 658 | 657 | 660 | 656.2 |
| 2300-2400 | 650 | 655 | 654 | 655 | 659 | 652 | 651 | 658 | 658 | 655 | 656 | 650 | 654.4 |
| 2400-0100 | 652 | 653 | 654 | 653 | 654 | 658 | 656 | 654 | 648 | 658 | 658 | 640 | 653.2 |
| 0100-0200 | 651 | 662 | 657 | 652 | 653 | 651 | 659 | 650 | 663 | 653 | 652 | 657 | 655.0 |
| 0200-0300 | 659 | 649 | 644 | 652 | 655 | 650 | 653 | 653 | 657 | 652 | 652 | 655 | 653.3 |
| 0300-0400 | 656 | 649 | 650 | 656 | 655 | 651 | 650 | 646 | 653 | 659 | 649 | 645 | 652.5 |
| 0400-0500 | 655 | 654 | 650 | 657 | 656 | 643 | 661 | 654 | 652 | 653 | 654 | 653 | 651.4 |
| 0500-0600 | 654 | 655 | 644 | 648 | 660 | 645 | 657 | 650 | 653 | 654 | 658 | 650 | 652.3 |
| 0600-0700 | 649 | 660 | 657 | 648 | 649 | 653 | 649 | 658 | 648 | 654 | 652 | 657 | 652.8 |
| 0700-0800 | 648 | 647 | 646 | 661 | 651 | 651 | 652 | 658 | 655 | 656 | 646 | 650 | 651.8 |
| 0800-0900 | 662 | 654 | 647 | 656 | 658 | 656 | 660 | 654 | 662 | 650 | 645 | 654 | 654.9 |
| 0900-1000 | 648 | 656 | 654 | 654 | 653 | 654 | 653 | 643 | 643 | 654 | 650 | 666 | 652.3 |

BUENOS AIRES 34.6S 58.49W ARGENTINA

NEUTRON MONITOR 18-NM-64

REAL COUNTS 32 TIMES TABULATED COUNTS

FIVE-MINUTE BAROMETER CORRECTED RATES

SEPTEMBER 1-2, 1971

| TIME U.T. | MINUTES AT END OF INTERVAL 05 | 10 | 15 | 20 | 25 | 30 | 35 | 40 | 45 | 50 | 55 | 60 | AVERAGE |
|---|---|---|---|---|---|---|---|---|---|---|---|---|---|
| 1700-1800 | 1126 | 1095 | 1093 | 1103 | 1118 | 1115 | 1103 | 1065 | 1129 | 1101 | 1108 | 1109 | 1105.4 |
| 1800-1900 | 1123 | 1111 | 1092 | 1088 | 1098 | 1099 | 1104 | 1104 | 1121 | 1092 | 1110 | 1116 | 1104.8 |
| 1900-2000 | 1076 | 1124 | 1087 | 1096 | 1109 | 1096 | 1086 | 1124 | 1100 | 1105 | 1090 | 1104 | 1099.7 |
| 2000-2100 | 1104 | 1095 | 1090 | 1103 | 1100 | 1119 | 1094 | 1106 | 1125 | 1086 | 1098 | 1092 | 1101.0 |
| 2100-2200 | 1102 | 1098 | 1096 | 1111 | 1105 | 1102 | 1107 | 1099 | 1095 | 1111 | 1123 | 1097 | 1103.8 |
| 2200-2300 | 1107 | 1109 | 1118 | 1117 | 1099 | 1090 | 1107 | 1106 | 1119 | 1118 | 1129 | 1085 | 1108.6 |
| 2300-2400 | 1101 | 1098 | 1115 | 1102 | 1099 | 1101 | 1110 | 1084 | 1113 | 1106 | 1109 | 1101 | 1103.2 |
| 2400-0100 | 1107 | 1081 | 1099 | 1091 | 1097 | 1112 | 1086 | 1115 | 1099 | 1080 | 1109 | 1096 | 1097.6 |
| 0100-0200 | 1091 | 1099 | 1105 | 1088 | 1100 | 1097 | 1099 | 1105 | 1099 | 1090 | 1091 | 1098 | 1096.8 |
| 0200-0300 | 1088 | 1092 | 1093 | 1122 | 1093 | 1103 | 1102 | 1100 | 1105 | 1095 | 1105 | 1081 | 1098.2 |
| 0300-0400 | 1103 | 1097 | 1075 | 1115 | 1088 | 1094 | 1077 | 1094 | 1097 | 1110 | 1095 | 1098 | 1095.2 |
| 0400-0500 | 1078 | 1092 | 1118 | 1096 | 1083 | 1095 | 1095 | 1091 | 1124 | 1103 | 1103 | 1093 | 1097.5 |
| 0500-0600 | 1091 | 1105 | 1102 | 1100 | 1108 | 1110 | 1105 | 1099 | 1106 | 1102 | 1092 | 1107 | 1102.2 |
| 0600-0700 | 1102 | 1086 | 1098 | 1097 | 1108 | 1109 | 1122 | 1093 | 1108 | 1111 | 1116 | 1102 | 1104.3 |
| 0700-0800 | 1097 | 1100 | 1101 | 1113 | 1113 | 1105 | 1098 | 1109 | 1108 | 1094 | 1085 | 1105 | 1101.9 |
| 0800-0900 | 1107 | 1106 | 1096 | 1082 | 1098 | 1107 | 1123 | 1097 | 1096 | 1098 | 1124 | 1082 | 1101.3 |
| 0900-1000 | 1101 | 1096 | 1097 | 1085 | 1107 | 1096 | 1105 | 1110 | 1106 | 1113 | 1108 | 1106 | 1102.5 |
| 1000-1100 | 1101 | 1112 | 1104 | 1107 | 1108 | 1128 | 1108 | 1117 | 1092 | 1092 | 1122 | 1125 | 1109.6 |
| 1100-1200 | 1103 | 1106 | 1111 | 1122 | 1105 | 1103 | 1091 | 1096 | 1104 | 1102 | 1117 | 1099 | 1104.9 |

Table 3 (continued)

MT NORIKURA 36.11N 137.55E JAPAN

NEUTRON MONITOR 4-NM-64

SCALING FACTOR 128

PRESSURE CORRECTED TO 720 MILLIBARS

COEFFICIENT -0.70 PER CENT PER MILLIBAR

FIFTEEN-MINUTE HOURLY RATES

SEPTEMBER 1-2, 1971

| TIME U.T. | MINUTES AT END OF INTERVAL 15 | 30 | 45 | 60 | AVERAGE |
|---|---|---|---|---|---|
| 1600 | 1315 | 1315 | 1309 | 1310 | 1312.2 |
| 1700 | 1316 | 1319 | 1310 | 1303 | 1312.0 |
| 1800 | 1322 | 1301 | 1316 | 1316 | 1313.7 |
| 1900 | 1314 | 1319 | 1310 | 1315 | 1314.5 |
| 2000 | 1329 | 1312 | 1312 | 1319 | 1318.0 |
| 2100 | 1331 | 1314 | 1307 | 1322 | 1318.5 |
| 2200 | 1319 | 1330 | 1311 | 1310 | 1317.5 |
| 2300 | 1322 | 1319 | 1322 | 1330 | 1323.2 |
| 2400 | 1324 | 1322 | 1322 | 1320 | 1322.0 |
| 0100 | 1322 | 1310 | 1316 | 1314 | 1315.5 |
| 0200 | 1319 | 1319 | 1324 | 1316 | 1319.5 |
| 0300 | 1316 | 1303 | 1315 | 1312 | 1311.5 |
| 0400 | 1322 | 1301 | 1311 | 1311 | 1311.2 |
| 0500 | 1307 | 1322 | 1309 | 1312 | 1312.5 |
| 0600 | 1312 | 1311 | 1310 | 1318 | 1312.7 |
| 0700 | 1314 | 1315 | 1314 | 1307 | 1312.5 |
| 0800 | 1316 | 1310 | 1306 | 1312 | 1311.0 |

ITABASHI 35.75N 139.71E JAPAN

NEUTRON MONITOR 18-NM-64

PRESSURE CORRECTED TO 1013.3 MILLIBARS

COEFFICIENT -0.666 PER CENT PER MILLIBAR

SCALING FACTOR 128

TEN-MINUTE HOURLY RATES

SEPTEMBER 1-2, 1971

| TIME U.T. | MINUTES AT END OF INTERVAL 10 | 20 | 30 | 40 | 50 | 60 | AVERAGE |
|---|---|---|---|---|---|---|---|
| 1600 | 591 | 586 | 598 | 593 | 591 | 593 | 592.0 |
| 1700 | 593 | 590 | 598 | 591 | 592 | 590 | 592.3 |
| 1800 | 593 | 592 | 590 | 589 | 593 | 589 | 591.0 |
| 1900 | 591 | 596 | 594 | 594 | 587 | 588 | 591.6 |
| 2000 | 587 | 592 | 594 | 598 | 586 | 590 | 591.1 |
| 2100 | 593 | 593 | 592 | 595 | 593 | 596 | 593.6 |
| 2200 | 605 | 593 | 595 | 594 | 594 | 595 | 596.0 |
| 2300 | 594 | 593 | 597 | 594 | 597 | 596 | 595.1 |
| 2400 | 593 | 604 | 589 | 592 | 603 | 602 | 597.1 |
| 0100 | 598 | 597 | 598 | 599 | 602 | 599 | 598.8 |
| 0200 | 591 | 598 | 596 | 600 | 586 | 602 | 595.5 |
| 0300 | 598 | 594 | 605 | 596 | 608 | 593 | 599.0 |
| 0400 | 593 | 591 | 594 | 599 | 602 | 592 | 595.1 |
| 0500 | 597 | 596 | 600 | 599 | 594 | 594 | 596.6 |
| 0600 | 594 | 592 | 594 | 594 | 600 | 595 | 594.8 |
| 0700 | 597 | 597 | 588 | 598 | 597 | 589 | 594.3 |
| 0800 | 589 | 602 | 591 | 589 | 597 | 594 | 593.6 |
| 0900 | 593 | 593 | 589 | 589 | 592 | 589 | 590.8 |

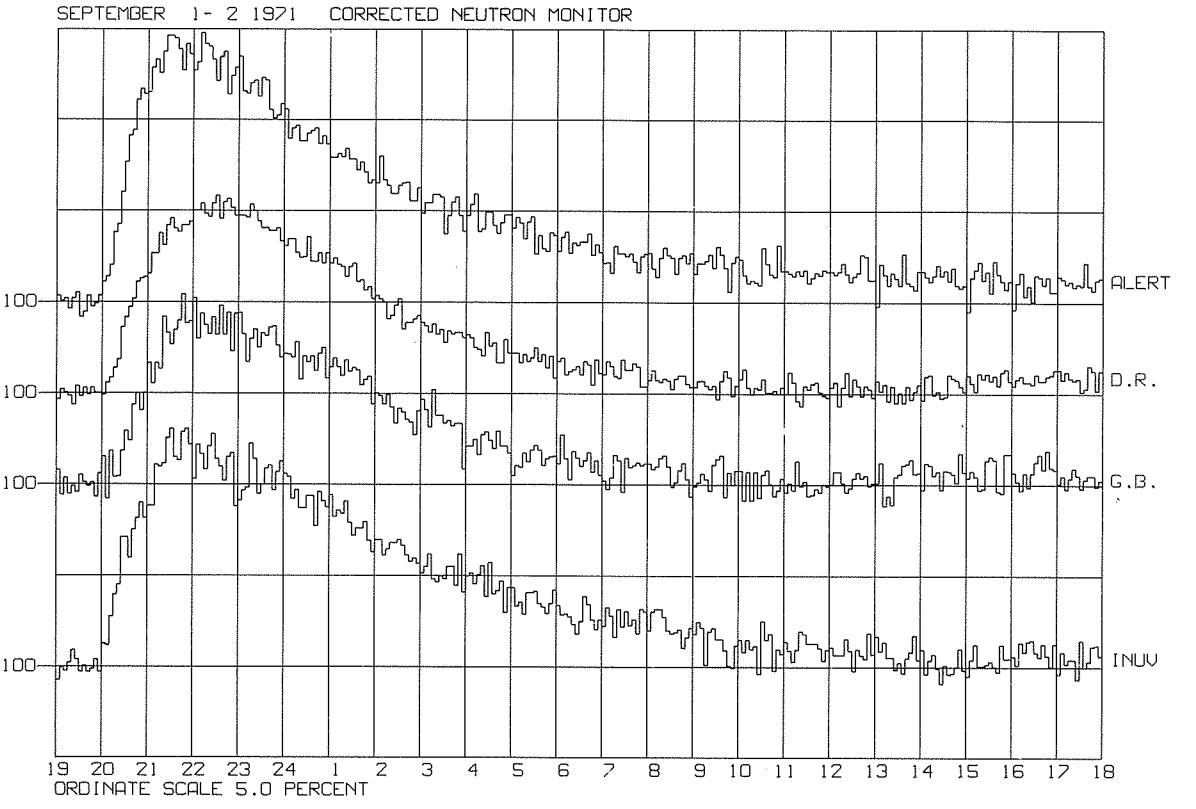


Fig. 1. 5-minute data from Alert, Deep River, General Belgrano and Inuvik, 1900 UT September 1 - 1800 UT September 2, 1971.
(Cutoff rigidities are 0.0, 1.02, 0.75 and 0.18, respectively.)

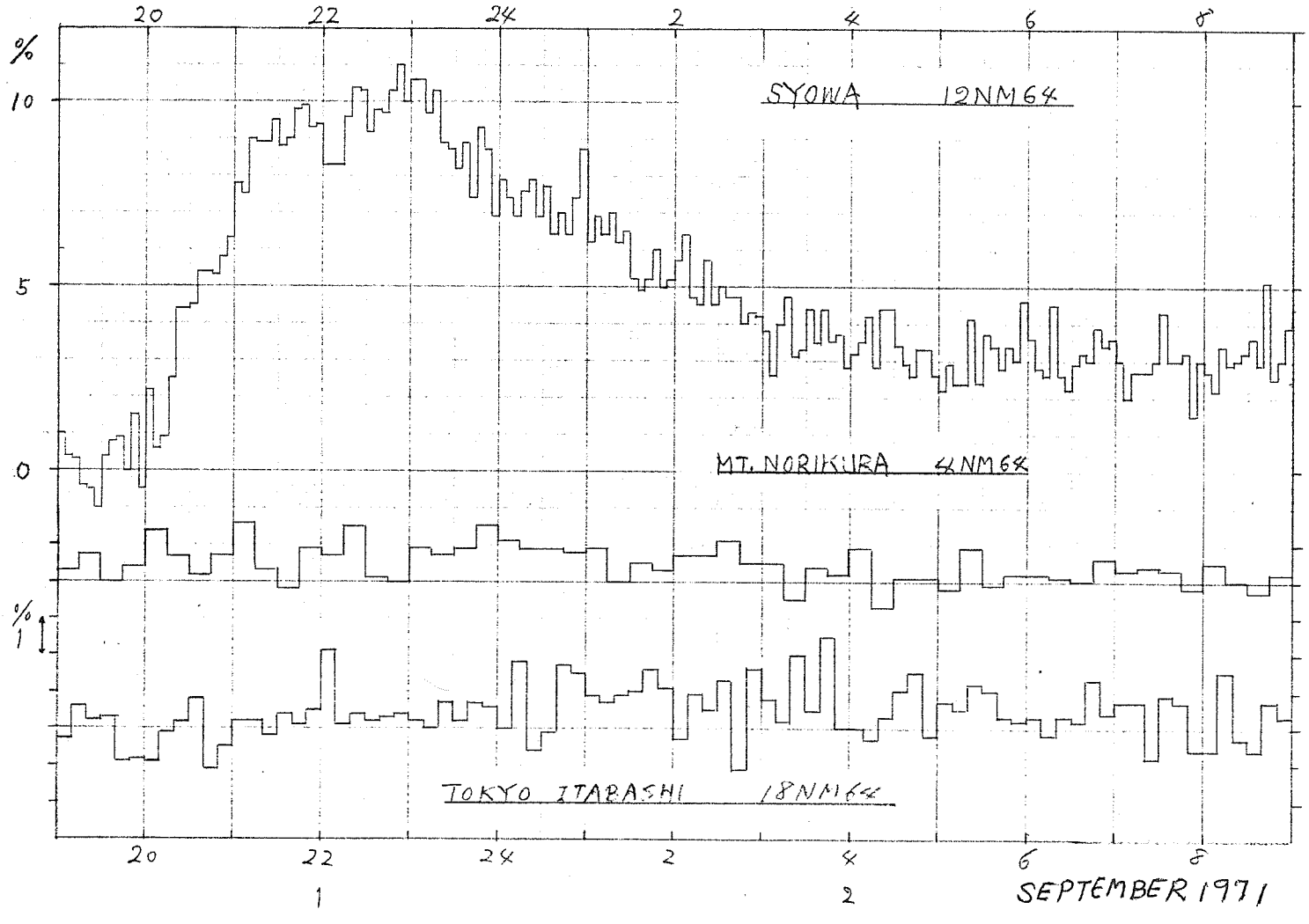


Fig. 2. 5-minute Syowa Base data, 15-minute Mt. Norikura data, and 10-minute Tokyo Itabashi data, 1800 UT August 31 - 1000 UT September 2, 1971. (Cutoff rigidities are 0.42, 11.39 and 11.61, respectively.)

# Relativistic Solar Cosmic Rays from the Invisible Disk on September 1-2, 1971

by

S. P. Duggal and M. A. Pomerantz
Bartol Research Foundation
of
The Franklin Institute

## 1. Introduction

The event of September, 1971, is the most recent of only three occasions on which relativistic solar cosmic rays originating on the invisible disk of the sun were observed to reach the earth. It is certainly the most unusual of this exceedingly rare class of occurrences, in that it displayed an unexpected and marked anisotropy for several hours following onset, despite the fact that the intensity profile bespoke a back-side source. This was confirmed by the absence of a candidate parent flare on the visible disk for at least 15 hours before the initial arrival of the energetic solar particles.

## 2. Observations

The extreme variability in the nucleonic intensity, as recorded by the Bartol network of polar neutron monitors prior to and following the event of September 1-2, 1971, is shown in Figure 1. Immediately after cessation of the relativistic solar particle precipitation, the galactic cosmic ray intensity appears to have recovered completely from the Forbush decrease that had been in progress since August 27.

The solar cosmic ray intensity, in hourly intervals, at four neutron monitor stations is plotted in Figure 2. The maximum nucleonic intensity increase, about 20%, was recorded at South Pole station and relativistic solar particles were observed there for about 16 hours. In contrast, the integral flux of particles with rigidities exceeding 1.9 GV, recorded at Swarthmore, reached a maximum level only 4% above the pre-event intensity, and the total duration of the event in this case was less than eight hours.

In Figure 3, the data from Bartol stations with asymptotic directions of arrival nearest the north and south poles are plotted on an expanded time scale (6 minute intervals). The data were corrected for pressure fluctuations by the application of two atmospheric coefficients, $\alpha$ and $\beta$, appropriate for solar and galactic particles respectively. For solar particles an absorption length of 104 gm/cm$^2$, derived earlier by Baird et al. [1967] was assumed. The Figure reveals a distinct north-south asymmetry of the relativistic solar cosmic rays.

## 3. Results of Analysis

### A. North-South Asymmetry

A quantitative evaluation of the north-south asymmetry was made by normalizing the data from Thule, Alert, McMurdo and South Pole to a standard pressure level of 760 mm Hg. The asymmetry $A = (N - S)100/N$, where N and S represent the average flux at the northern and the southern stations respectively, is plotted in Figure 4, which shows that A exceeded 44% during the first hour of the GLE, and decreased thereafter. By September 2, the solar flux became essentially isotropic.

### B. Spectrum

Figure 5 shows the nucleonic intensity enhancement at a number of stations during the period 0000-0100 UT on September 2, 1971, normalized to a standard pressure of 760 mm Hg and plotted as a function of threshold rigidity. Since the anisotropy was negligible during this period (cf. Figure 4) the primary differential rigidity spectrum can be determined from the data. The considerable scatter among the data points for various stations presumably arises from atmospheric effects, since the data available from only half of the stations included in Figure 5 could be corrected by the application of two pressure coefficients. Furthermore, appreciable fluctuations are attributable to pre-event variations in the galactic flux (see Figure 1) which affect the base level from which intensity increases were reckoned. In view of these uncertainties, the data plotted in Figure 5 are consistent with a knee location near 1.1 GV. The spectral index in the power-law representation of the spectrum determined from the observations at stations characterized by threshold rigidity > 1.4 GV and particle intensity > 1% is $\gamma = 5.7 \pm 0.6$.

## 4. Conclusion

Since this is the first back-side event which is characterized by an appreciable anisotropy persisting for more than 3 hours, further intensive study of the propagation mechanism is required. It has recently been shown that during anisotropic events ascribed to a source on the visible disk, the arrival of solar particles is not simultaneous on a global scale [Duggal and Pomerantz, 1971; Duggal et al., 1971]. However, during the September, 1971 event, in spite of the anisotropy, there was no difference in the times of the onset of particle arrival in the northern and southern hemispheres.

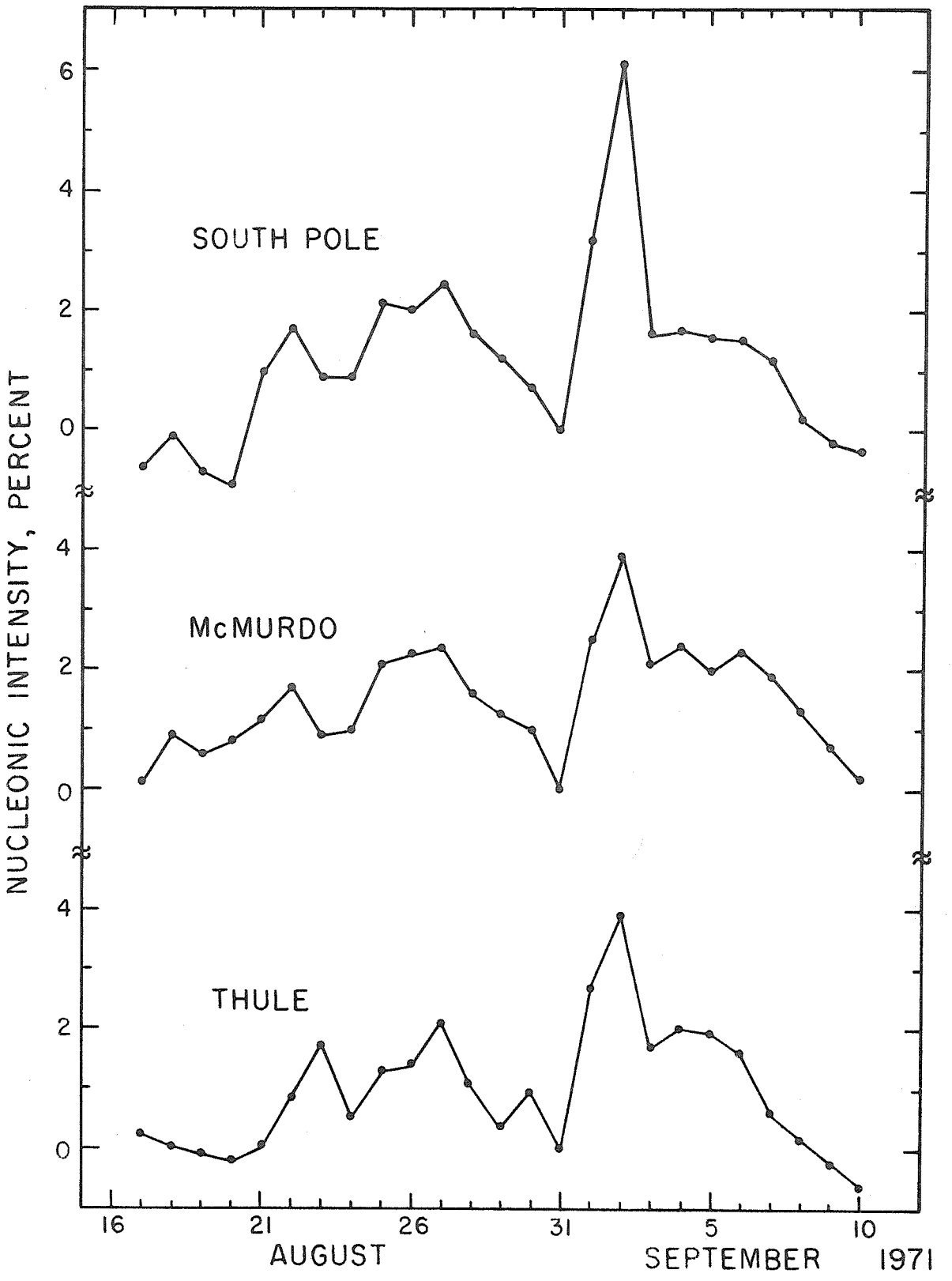


Fig. 1. Nucleonic intensity, expressed as percent of the pre-event level, at polar stations around the epoch of the September, 1971 ground level event (GLE).

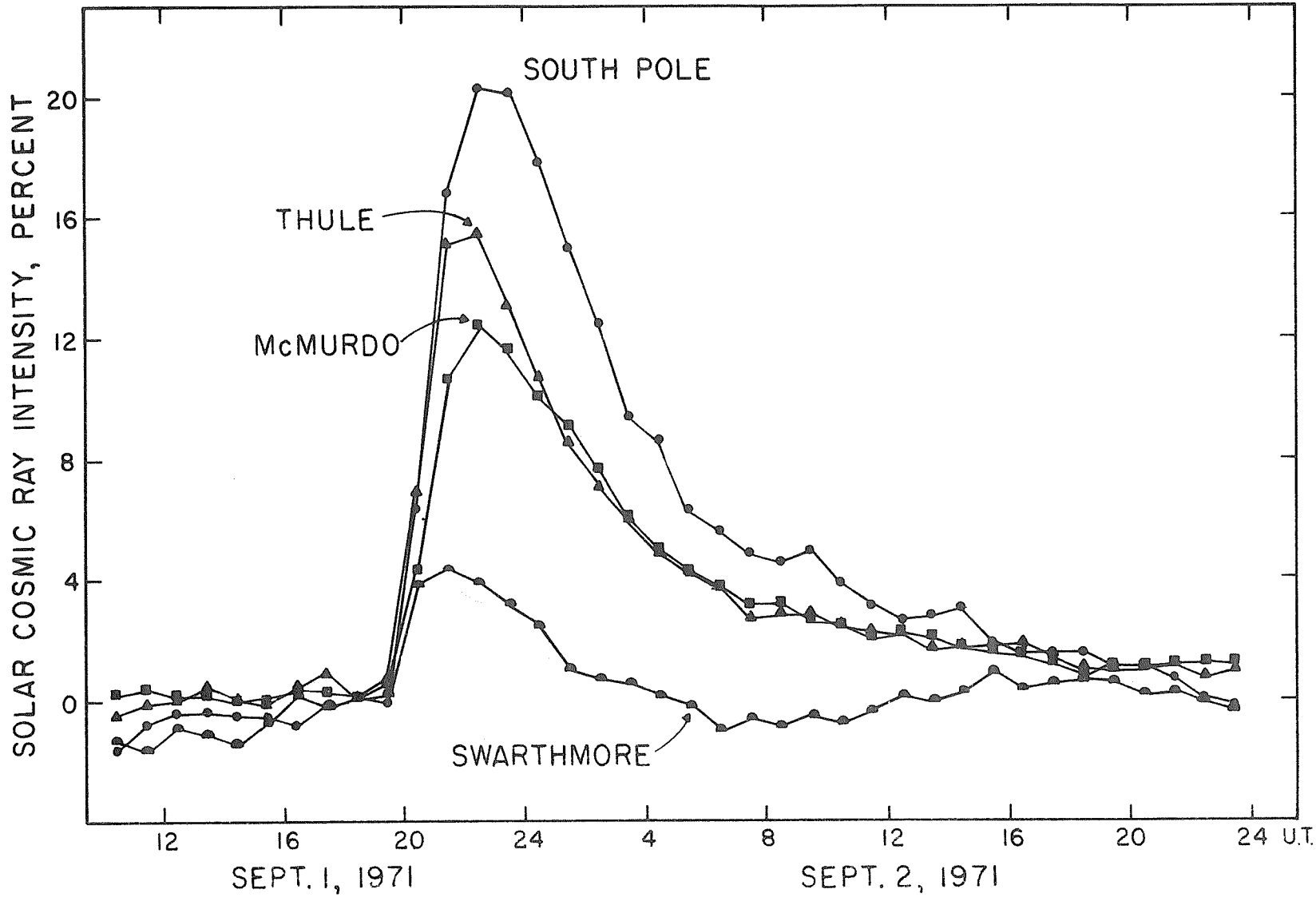


Fig. 2. The September 1-2, 1971 GLE neutron monitor observations at Bartol stations.

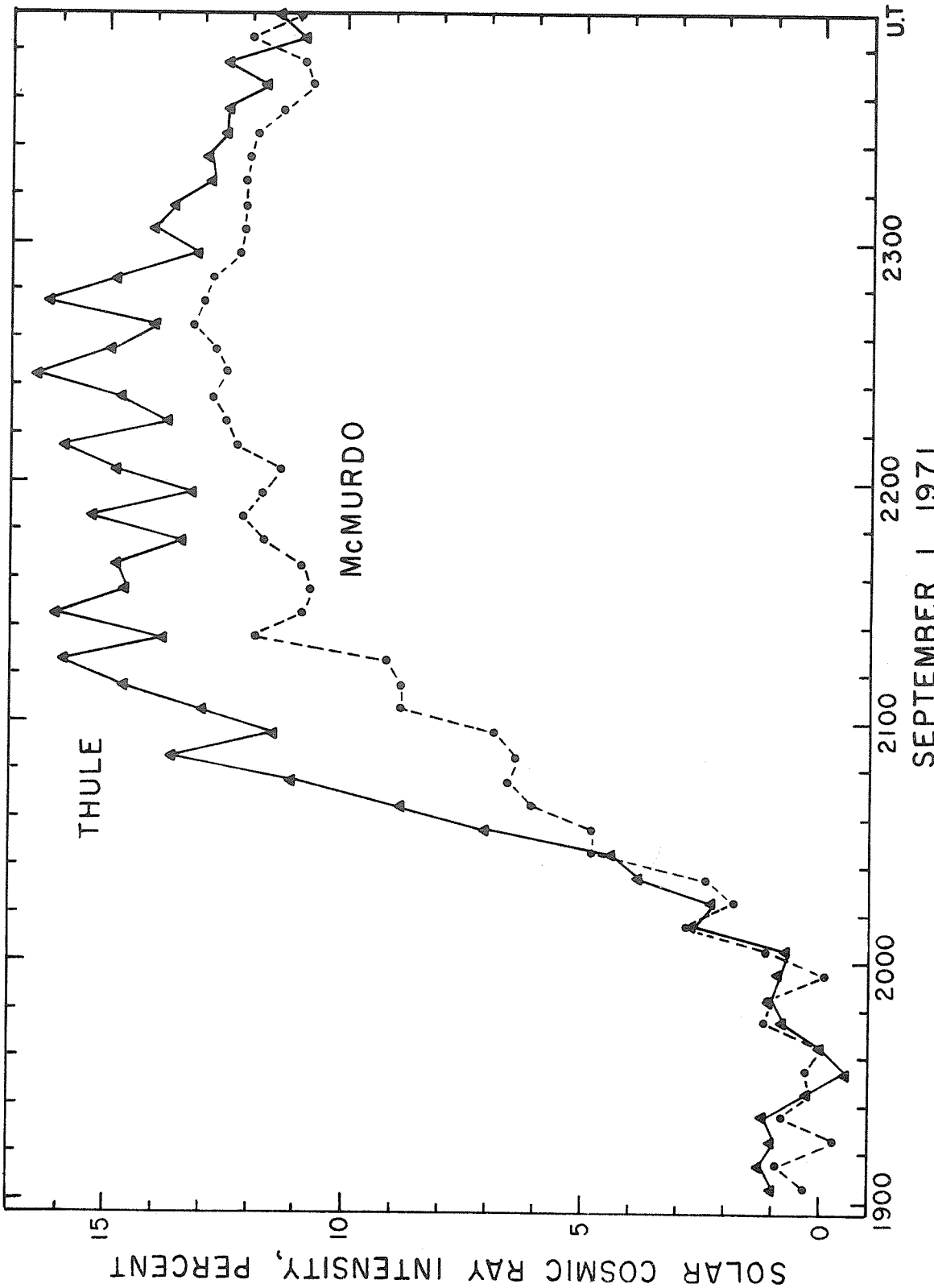


Fig. 3. Plot on an expanded time scale of the solar cosmic ray intensity at north (Thule) and south (McMurdo) polar stations.

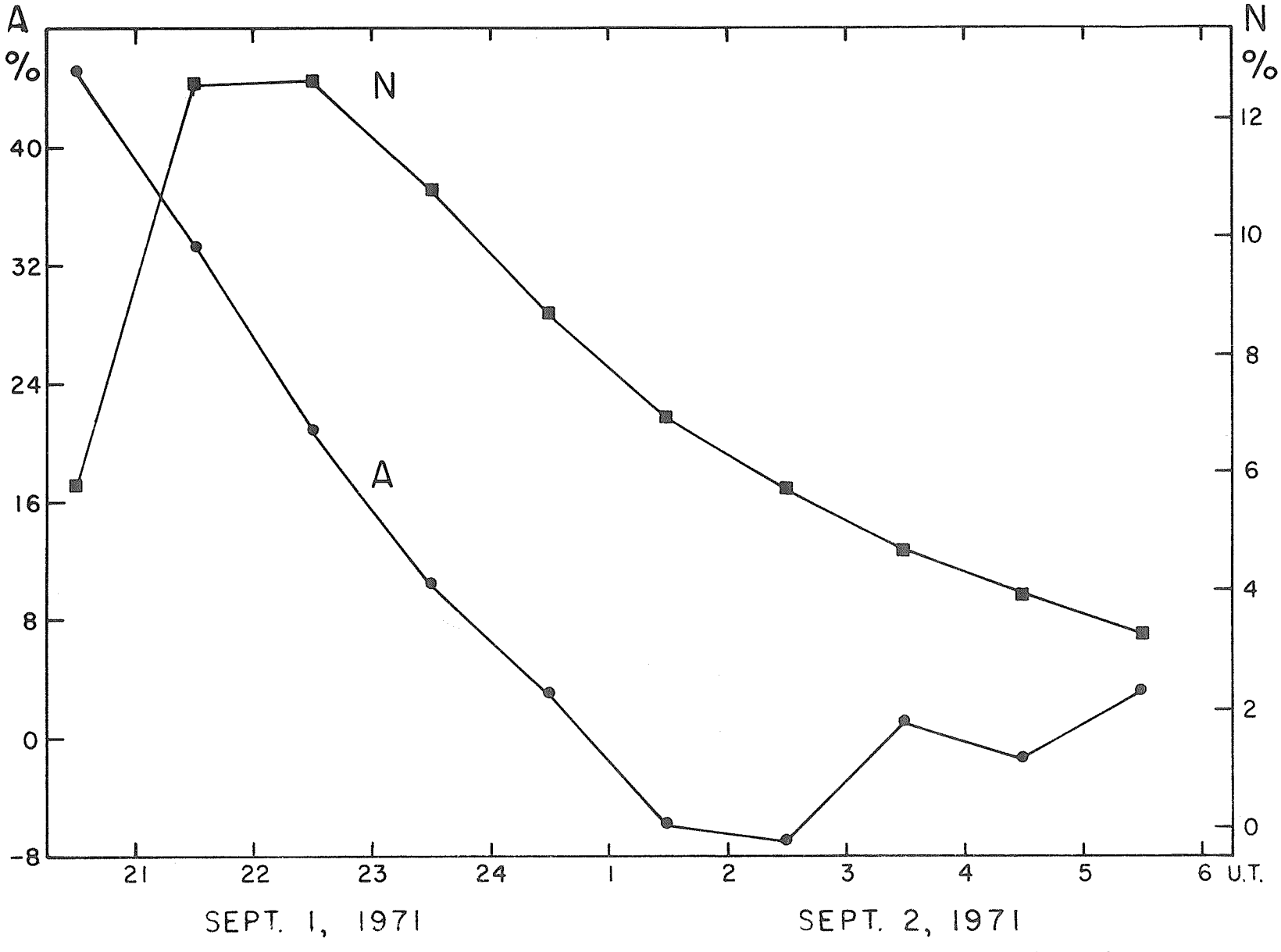


Fig. 4. The asymmetry, A, and the nucleonic intensity enhancement, N, in the northern polar region during the September, 1971 GLE.

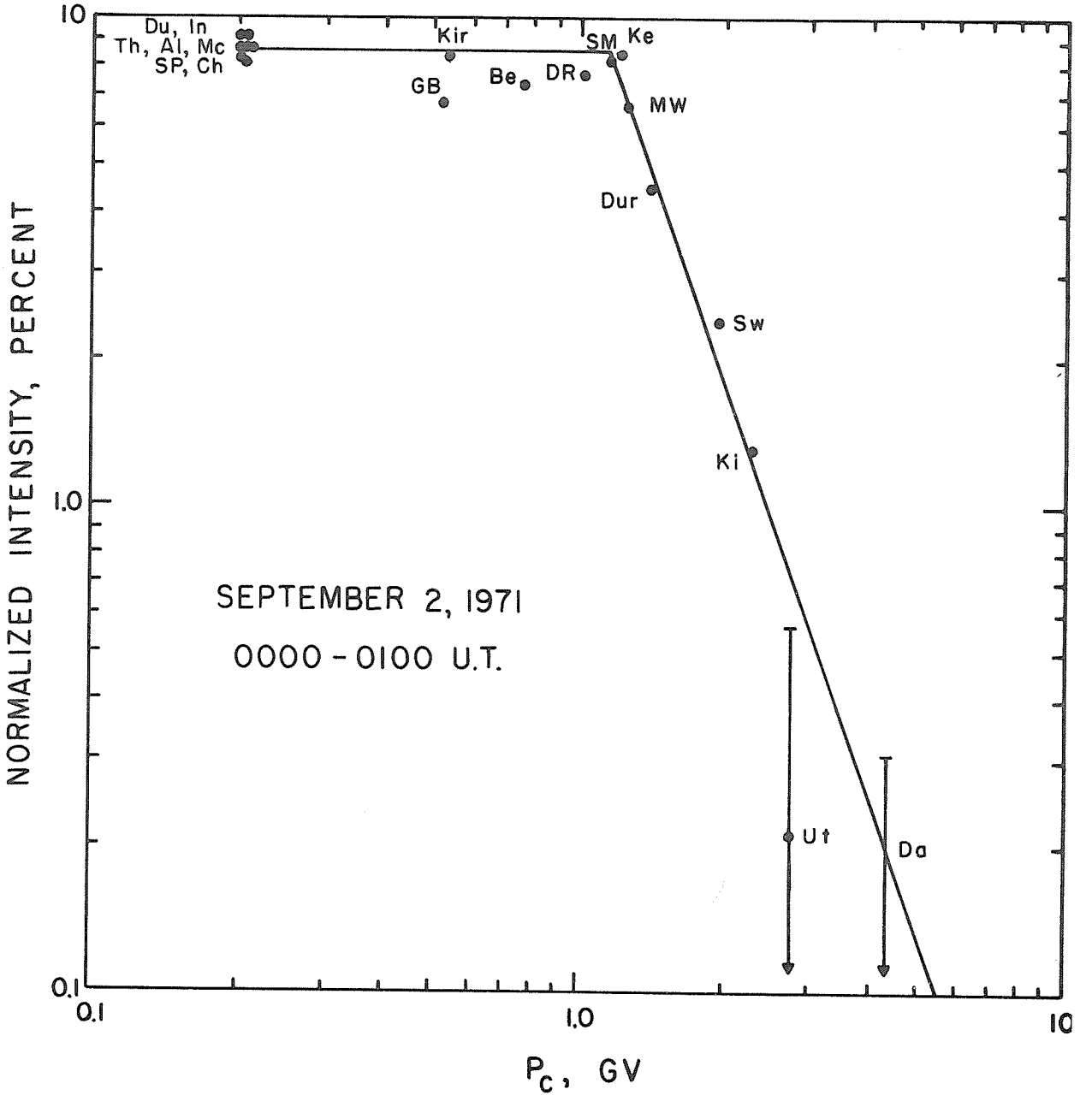


Fig. 5. Log-log plot of neutron monitor data recorded at a number of stations, and normalized to a standard atmospheric pressure, during the isotropic phase on September 2, 1971.

## REFERENCES


BAIRD, G. A., G. G. BELL, S. P. DUGGAL, and M. A. POMERANTZ, 1967, Solar Phys., 2, 491.

DUGGAL, S. P., I. GUIDI, and M. A. POMERANTZ, 1971, Solar Phys., 19, 234.

DUGGAL, S. P., and M. A. POMERANTZ, 1971, Proc. Int. Conf. Cosmic Rays, 12th, 2, 533.

# The Flare of Cosmic Rays on September 1, 1971

by

N. P. Chirkov, A. M. Novikov, G. V. Skripin, G. G. Todikov, A. T. Filippov
Institute of Cosmophysical Research and Aeronomy, Yakutsk Branch,
Siberian Department of the Academy of Sciences of the USSR, Yakutsk, USSR

Late on September 1, 1971 the Siberian net of stations observed the flare of solar cosmic rays. In the Table below geographical coordinates, threshold rigidities of stations [Shea et al., 1968], and amplitudes of the flare are listed. Stations were equipped with Superneutron Monitors.

Table 1

| Number | Station | P(GV) | Geographical | | Amplitude (per cent) | |
|---|---|---|---|---|---|---|
| | | | Latitude | Longitude | | |
| 1 | Tixie Bay | 0.52 | 71.5°N | 128.9°E | 12.1 | 12.3 |
| 2 | Norilsk | 0.60 | 69.3 | 88.1 | - | 11.4 |
| 3 | Yakutsk | 1.85 | 62.0 | 129.7 | 6.6 | 6.3 |
| 4 | Magadan | 2.16 | 60.1 | 151.0 | 4.0 | 3.7 |
| 5 | Irkutsk | 3.74 | 52.4 | 104.0 | 1.1 | 0.7 |
| 6 | Habarovsk | 5.55 | 48.5 | 135.2 | - | 0.4 |

5-, 15-minute, and hourly values of cosmic ray intensity during the flare are given in Figure 1. The statistical errors are indicated. From Figure 1 it is seen that the flare of cosmic rays started at 2010 UT, September 1, and reached its maximum at 2140-2200 UT, i.e., in 90-110 minutes.

In Figure 2 experimental and estimated according to Krymsky [1969] intensity values at various values of $\alpha$ in the equation

$$n(t) = B\tau^{\frac{3}{2-\alpha}} e^{-(1/\tau)}$$

are presented, where $\tau$ is a non-dimensional time. From Figure 2 it is evident that one can observe the best agreement between the theory and the experiment if $\alpha = 0$, and if we assume that particle emission on the Sun began at 1915 UT, i.e. 55 minutes earlier than the commencement of cosmic ray intensity increase observed on the Earth.

Knowledge of the emission commencement enables us to determine a path length L and a diffusion coefficient D for the present flare:

$$L = \frac{R_{\odot}^2}{(2-\alpha)ct_{max}} = 4\cdot10^{11} \text{ cm}; \quad D = \frac{Lc}{3} = 4\cdot10^{21} \text{ cm}^2/\text{sec}$$

where $R_{\odot}$ is a distance from the Sun to the Earth.

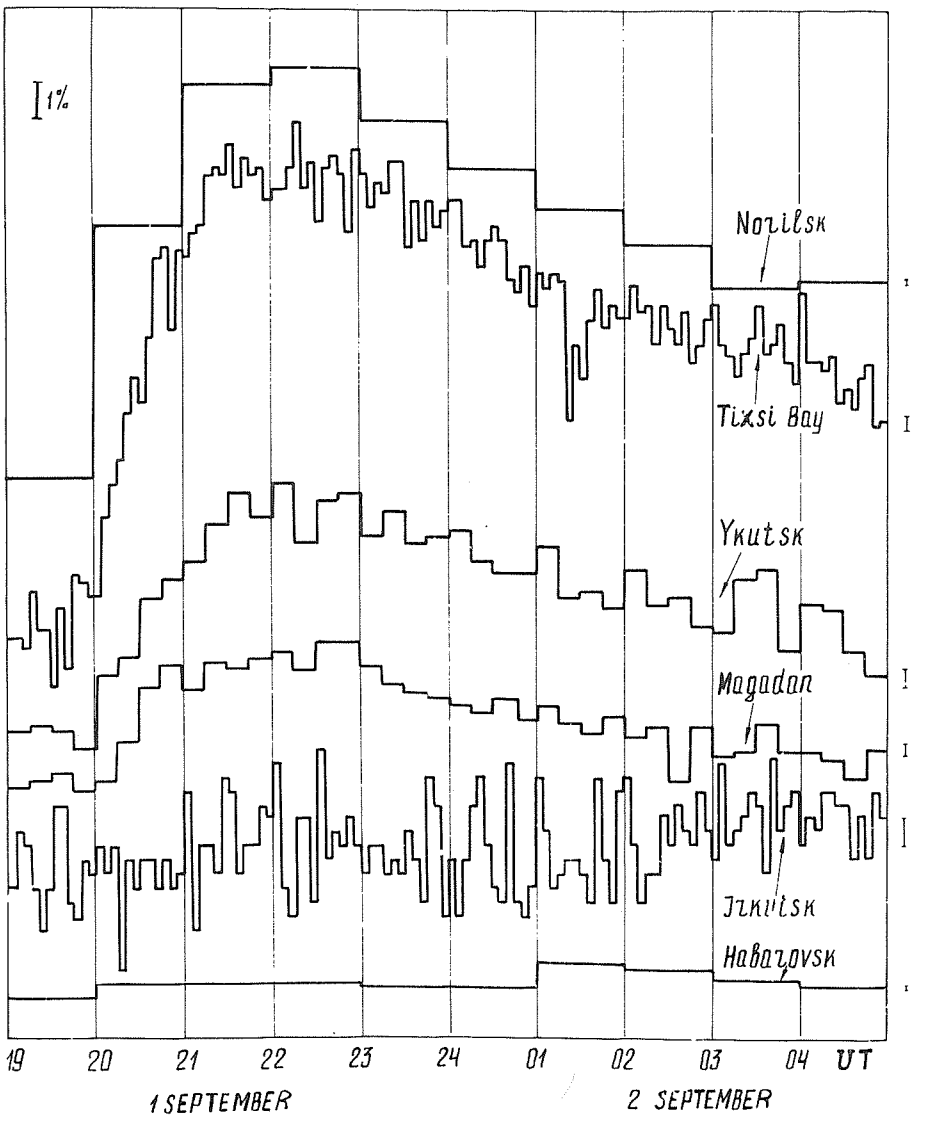


Fig. 1. Variations of cosmic ray intensity for the period 1900 UT September 1 - 0500 UT September 2, 1971 at stations Norilsk, Tixie Bay, Yakutsk, Irkutsk, Magadan and Habarovsk.

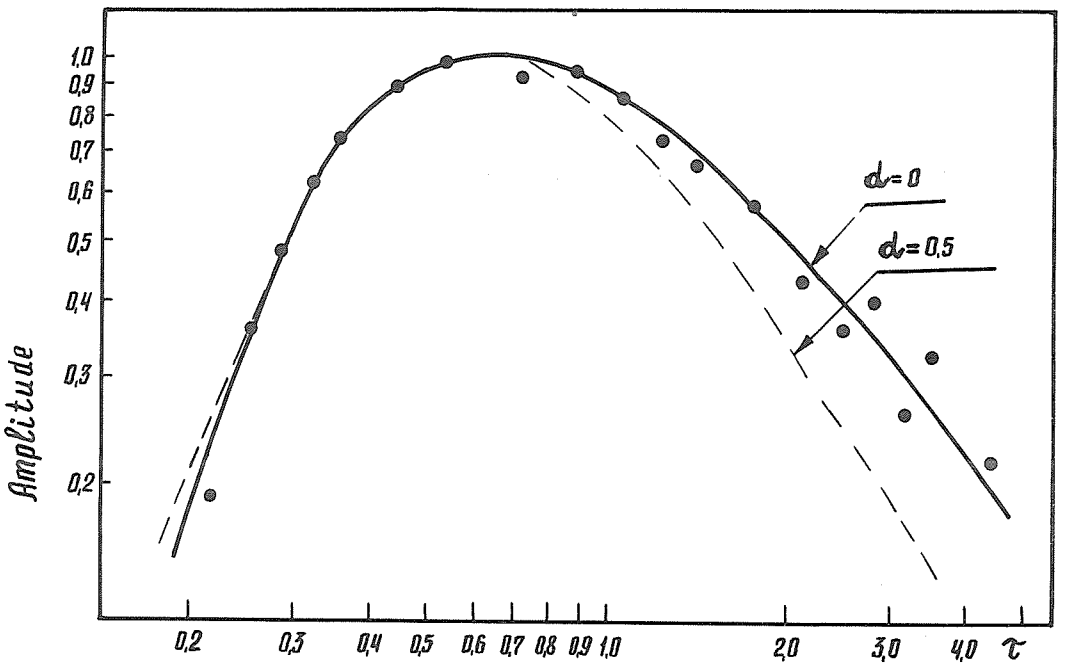


Fig. 2. Estimated values of cosmic ray intensities (curves) for $\alpha$ = 0 and 0.5, and experimental values (points) depending on time. Maximum amplitudes are normalized to 1.0.

In Figure 3 a latitudinal dependence of the flare amplitude is given. Points are amplitudes based on 15-minute values for 2245 - 2300 UT (amplitudes are presented in the Table in the next to the last column). Circles are amplitudes based on hourly values for 2300 UT September 1 (tne last column in the Table).

It is evident from Figure 3 that a latitudinal dependence of amplitudes is very well described by the expression

$$A(P) \sim P^{-\gamma}, \text{ where } \gamma = 2.6 \pm 0.1.$$

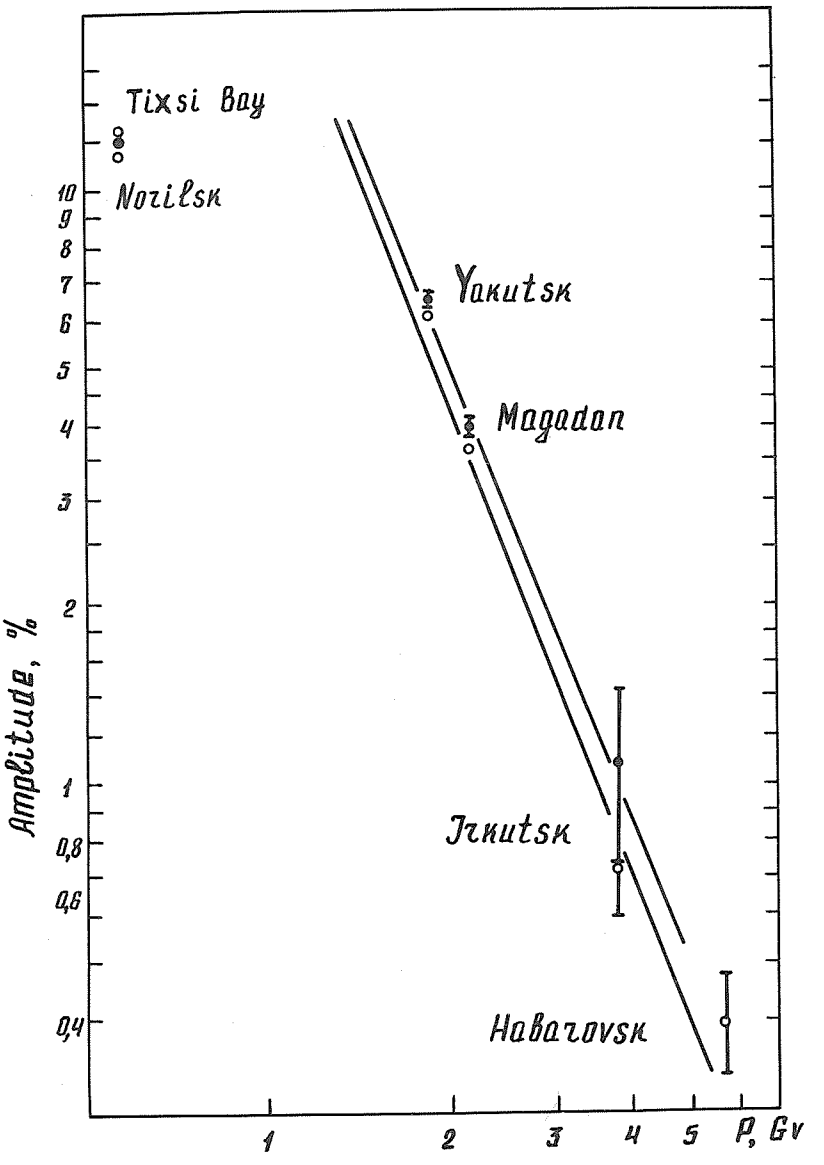


Fig. 3. Dependence of the flare amplitude on threshold rigidity. Points are amplitudes based on 15-minute data, circles are amplitudes based on hourly data.

REFERENCES


KRYMSKY, G. F. 1969 Modulyatsia kosmicheskikh luchei v mezhplanetnom prostranstve, Izd. "Nauka", Moscow.

SHEA, M. A., D. F. SMART, and J. R. MC CALL 1968 A Five Degree by Fifteen Degree World Grid of Trajectory-Determined Vertical Cutoff Rigidities, Canadian J. of Physics, 46, 10, 4, S1098-1103.

# The Ground Level Cosmic Ray Increase of September 1, 1971 Recorded by the Neutron Monitor in Bergen, Norway

by

R. Amundsen and H. Trefall
Department of Physics
University of Bergen, Norway

The Bergen neutron monitor data for the September 1, 1971 event is presented in Figure 1. The graph presents hourly values and is plotted as a percentage of the pre-event average count-rate. The data are pressure corrected to 990 mb (coefficient 0.74%/mb) and represent the mean of two sections. The 100% level is at 8370 counts per hour for the September event. The standard deviation is shown on the graph.

The neutron monitor station in Bergen is at sea level, and the geographical position is 60°24'N latitude and 5°24'E longitude. The cut-off rigidity is 1.2 GV.

For the September event, the maximum count-rate occurs in the interval 2200-2300 UT September 1, and the increase amounts to 13.2%. The September event has a markedly slower increase and decay rate than the January event.

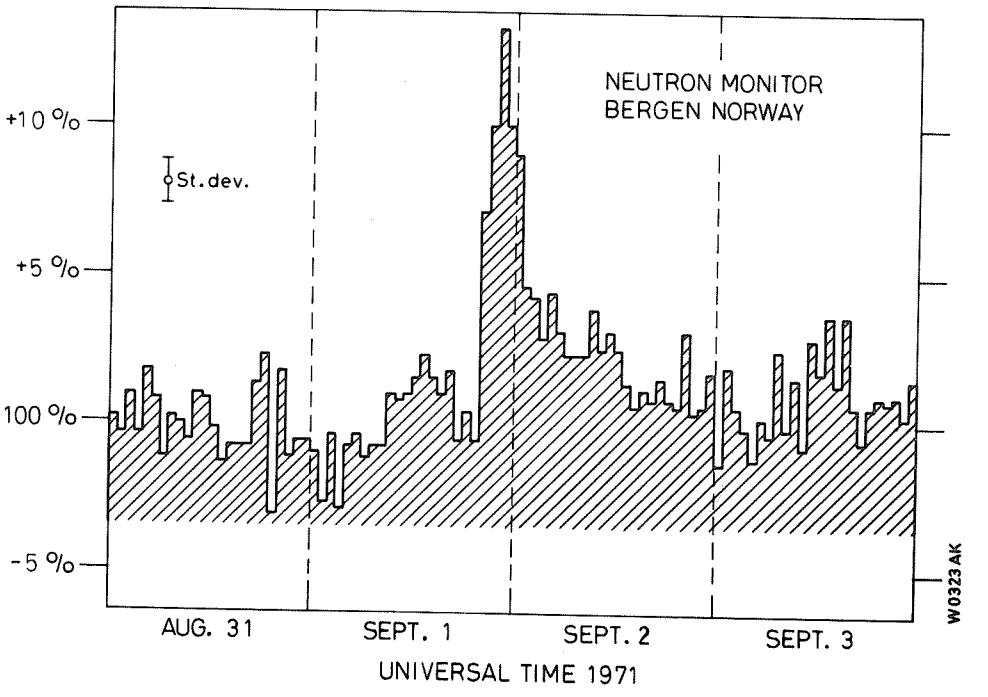


Fig. 1. Bergen neutron monitor data for the September 1, 1971 event.

"Scintillation Monitor, Bologna, Italy. 15-Minute Observations"

by

M. Galli, L. Fiandri
Istituto di Fisica "A. Righi"
Università degli Studi di Bologna

M.R. Attolini
Laboratori T.E.S.R.E.
Consiglio Nazionale delle Ricerche, Bologna

Figure 1 presents for August 28 to September 4, 1971 the total ionization (T), the atmospheric pressure at ground level (P), and the hard components: 45° inclined towards West (W), 45° inclined towards East (E) and vertical cubical coincidences (V).

Table 1 presents the data from the scintillation monitor at Bologna. The tabulated data should be read with a decimal point after the second figure of each number. The numbers are deviations in % units from a fixed value of pressure corrected data at the end of each 15-minute interval.

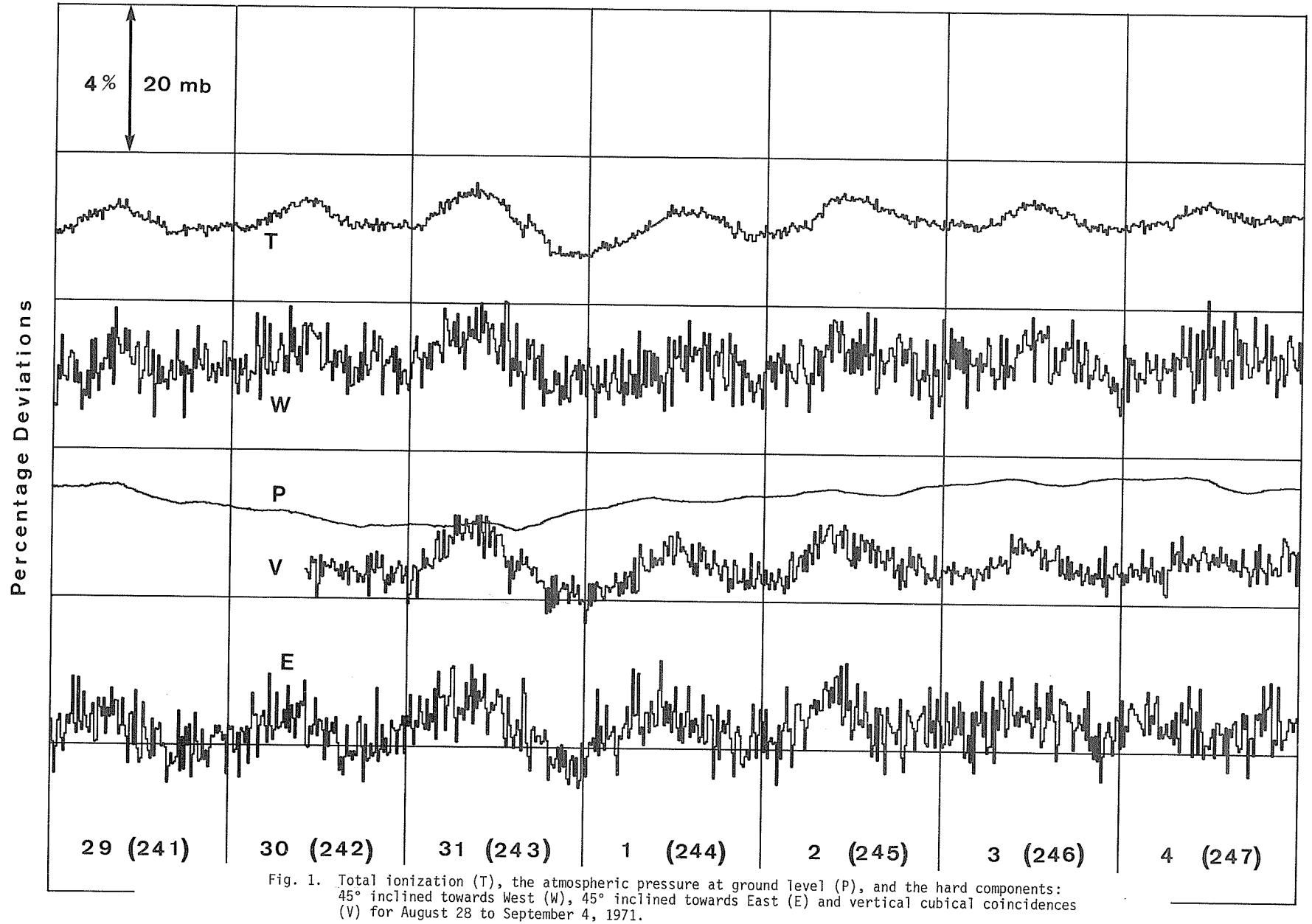


Fig. 1. Total ionization (T), the atmospheric pressure at ground level (P), and the hard components: 45° inclined towards West (W), 45° inclined towards East (E) and vertical cubical coincidences (V) for August 28 to September 4, 1971.

Table 1.

## 15-MINUTE COSMIC RAY DATA AT BOLOGNA DURING SEPTEMBER 1,2 1971

Scintillation Meniter for Cosmic Rays
Location Bologna 44.5 N 11.35 E 50 m a.s.l.
Tabulated Deviations in percent units from a fixed value of pressure corrected totals, at the end of each interval

* Total Ionizing Component counts under 5 gr/sqcm * S.D. 0.084%

* Coincidence counts 45 degrees inclined towards West filtered by 10 cm of lead * S.D. 0.54%

* Vertical Cubical coincidence counts filtered by 10 cm of lead * S.D. 0.30%

* Coincidence counts 45 degrees inclined towards East filtered by 10 cm of lead * S.D. 0.54%

Bar. coeff. 0.20 percent/mb
September 1,2 1971

| | Minutes at End of Interval | | | | | | | | | | | | | | | | | | | |
|---|---|---|---|---|---|---|---|---|---|---|---|---|---|---|---|---|---|---|---|---|
| U.T. hours | 15 | 30 | 45 | 60 | Mean | 15 | 30 | 45 | 60 | Mean | 15 | 30 | 45 | 60 | Mean | 15 | 30 | 45 | 60 | Mean |
| 1200-1300 | 4.43 | 4.55 | 4.67 | 4.49 | 4.54 | 4.63 | 5.18 | 4.31 | 4.24 | 4.59 | 4.25 | 4.89 | 4.72 | 4.35 | 4.55 | 4.03 | 4.70 | 3.59 | 3.25 | 3.89 |
| 1300-1400 | 4.45 | 4.53 | 4.48 | 4.60 | 4.51 | 4.93 | 3.96 | 5.61 | 4.64 | 4.79 | 4.49 | 4.37 | 4.29 | 4.08 | 4.31 | 3.98 | 3.18 | 3.63 | 4.03 | 3.71 |
| 1400-1500 | 4.51 | 4.47 | 4.40 | 4.51 | 4.47 | 4.50 | 4.89 | 4.68 | 4.81 | 4.72 | 3.95 | 4.56 | 3.75 | 4.04 | 4.07 | 4.72 | 3.34 | 3.80 | 3.48 | 3.83 |
| 1500-1600 | 4.67 | 4.56 | 4.54 | 4.39 | 4.54 | 4.86 | 3.73 | 5.29 | 4.95 | 4.71 | 3.70 | 4.60 | 4.10 | 4.49 | 4.22 | 3.85 | 3.67 | 3.21 | 3.35 | 3.52 |
| 1600-1700 | 4.47 | 4.46 | 4.37 | 4.43 | 4.43 | 4.25 | 5.26 | 4.04 | 3.47 | 4.25 | 4.39 | 3.90 | 4.03 | 3.73 | 4.01 | 4.49 | 3.17 | 3.22 | 3.95 | 3.71 |
| 1700-1800 | 4.34 | 4.42 | 4.26 | 4.34 | 4.34 | 4.68 | 4.78 | 4.39 | 4.75 | 4.65 | 3.91 | 4.39 | 4.04 | 3.99 | 4.08 | 3.94 | 3.82 | 2.22 | 3.10 | 3.27 |
| 1800-1900 | 4.42 | 4.15 | 4.26 | 4.13 | 4.24 | 5.11 | 4.07 | 3.74 | 3.86 | 4.19 | 3.76 | 3.58 | 3.97 | 4.14 | 3.86 | 4.21 | 2.75 | 3.50 | 3.80 | 3.56 |
| 1900-2000 | 4.15 | 3.96 | 3.85 | 3.97 | 3.98 | 5.27 | 4.72 | 3.30 | 4.96 | 4.56 | 3.95 | 3.28 | 3.63 | 3.37 | 3.56 | 3.46 | 3.71 | 4.08 | 3.32 | 3.64 |
| 2000-2100 | 4.29 | 4.08 | 4.02 | 4.02 | 4.10 | 4.50 | 4.42 | 4.52 | 3.35 | 4.20 | 4.14 | 4.00 | 3.52 | 3.57 | 3.81 | 2.93 | 2.29 | 3.49 | 3.64 | 3.09 |
| 2100-2200 | 3.81 | 3.78 | 3.94 | 3.94 | 3.87 | 4.55 | 4.09 | 4.20 | 3.72 | 4.14 | 3.55 | 3.91 | 3.35 | 3.60 | 3.60 | 3.39 | 2.63 | 2.55 | 2.83 | 2.85 |
| 2200-2300 | 3.76 | 3.76 | 3.93 | 3.93 | 3.85 | 3.99 | 3.43 | 3.69 | 3.94 | 3.76 | 3.38 | 4.33 | 3.44 | 3.38 | 3.63 | 3.02 | 2.75 | 3.39 | 4.25 | 3.35 |
| 2300-2400 | 4.03 | 3.98 | 3.88 | 4.19 | 4.02 | 4.16 | 3.78 | 3.24 | 4.23 | 3.85 | 3.64 | 4.10 | 3.76 | 3.52 | 3.75 | 3.48 | 2.80 | 3.42 | 4.11 | 3.45 |
| 0000-0100 | 4.00 | 3.97 | 3.99 | 3.85 | 3.95 | 4.53 | 4.32 | 4.67 | 3.98 | 4.38 | 3.46 | 3.38 | 3.50 | 3.36 | 3.55 | 3.78 | 2.96 | 4.11 | 2.79 | 3.41 |
| 0100-0200 | 3.95 | 4.07 | 4.08 | 3.85 | 3.99 | 4.51 | 3.78 | 4.75 | 4.63 | 4.42 | 3.80 | 3.59 | 3.36 | 3.56 | 3.58 | 3.25 | 3.35 | 3.18 | 3.23 | 3.25 |
| 0200-0300 | 4.04 | 4.14 | 3.93 | 4.03 | 4.04 | 4.22 | 4.97 | 4.46 | 4.32 | 4.24 | 3.91 | 3.67 | 3.46 | 3.25 | 3.57 | 2.07 | 3.69 | 2.78 | 3.55 | 3.02 |
| 0300-0400 | 4.18 | 4.27 | 4.19 | 4.13 | 4.19 | 4.46 | 4.26 | 4.08 | 4.01 | 4.20 | 3.72 | 3.39 | 4.16 | 4.37 | 3.91 | 3.75 | 4.73 | 3.53 | 3.60 | 3.90 |
| 0400-0500 | 4.04 | 4.20 | 4.17 | 4.13 | 4.14 | 3.94 | 4.48 | 5.12 | 4.96 | 4.63 | 3.58 | 3.65 | 3.99 | 4.23 | 3.86 | 2.56 | 3.17 | 4.25 | 4.27 | 3.56 |
| 0500-0600 | 4.33 | 4.14 | 4.12 | 4.08 | 4.17 | 4.35 | 4.15 | 3.94 | 3.17 | 3.90 | 4.28 | 3.86 | 4.43 | 3.85 | 4.10 | 4.27 | 3.83 | 3.84 | 3.02 | 3.74 |
| 0600-0700 | 4.36 | 4.39 | 4.45 | 4.53 | 4.43 | 4.22 | 3.92 | 4.93 | 4.86 | 4.48 | 4.58 | 4.35 | 4.05 | 4.94 | 4.48 | 3.63 | 3.90 | 4.24 | 4.16 | 3.98 |
| 0700-0800 | 4.54 | 4.43 | 4.80 | 4.73 | 4.63 | 4.16 | 4.82 | 3.75 | 4.67 | 4.35 | 4.59 | 4.21 | 5.11 | 4.63 | 4.63 | 4.39 | 3.99 | 4.37 | 4.10 | 4.21 |
| 0800-0900 | 4.79 | 4.88 | 4.94 | 4.92 | 4.88 | 4.98 | 4.87 | 5.53 | 4.53 | 4.98 | 4.69 | 4.83 | 5.01 | 5.11 | 4.91 | 4.10 | 4.68 | 4.87 | 4.64 | 4.57 |
| 0900-1000 | 4.88 | 4.98 | 4.91 | 4.93 | 4.90 | 5.66 | 5.61 | 5.35 | 4.79 | 5.35 | 5.12 | 4.62 | 4.37 | 4.85 | 4.74 | 4.18 | 4.73 | 4.32 | 5.00 | 4.56 |
| 1000-1100 | 5.00 | 5.08 | 4.91 | 4.90 | 4.97 | 5.63 | 5.27 | 4.29 | 4.79 | 5.00 | 4.85 | 4.96 | 4.50 | 5.12 | 4.86 | 5.03 | 4.28 | 5.31 | 3.72 | 4.58 |
| 1100-1200 | 4.89 | 5.00 | 4.88 | 4.94 | 4.93 | 4.87 | 4.22 | 5.16 | 4.24 | 4.62 | 4.99 | 4.21 | 4.17 | 4.02 | 4.35 | 3.94 | 5.38 | 4.12 | 4.38 | 4.46 |

# 6. IONOSPHERE

## The September 1971 Solar Cosmic Ray Event

by

A. J. Masley
Space Sciences Department
McDonnell Douglas Astronautics Company
Huntington Beach, California

## Introduction

The McDonnell Douglas Polar Observatories are located at McMurdo Sound, Antarctica (77°51'S, 166°43'E) and at magnetically conjugate Shepherd Bay, N. W. T., Canada (68°49'N, 93°26'W). These stations, at a geomagnetic latitude of 80°, are located inside the polar cap regions, removed poleward from the auroral zones to minimize auroral interference.

Radio techniques are used which allow effects taking place at altitudes from 30 to 90 kilometers to be observed with ground-based equipment. Riometers are operated which measure the signal strength of galactic radio noise at 30 and 50 MHz. The ionization produced by the interaction of the charged particles with the atmosphere increases the electron density so that radio waves passing through the ionosphere are significantly absorbed. The absorption of the radio waves at a given frequency is proportional to the square root of the intensity of charged particles. This technique is sensitive to protons from about 5 to 100 Mev. Other equipment operating at the stations includes magnetometers and photometers at 3914 Å and 5577 Å.

## 1 September 1971 Event

At 1935 UT September 1 a 10 minute radio noise burst was seen on the riometers in both polar regions. Absorption began on the McMurdo 30 MHz riometer at 2040 UT September 1, during sunlight hours (see Figure 1). The arrows in Figure 1 show the 30 km sunrise and sunset for each station. Maximum 30 MHz absorption at McMurdo was 3.4 dB at 0300 UT September 2 during daylight. The maximum at Shepherd Bay was 4.2 dB at 1400 UT September 2 during daylight. The actual peak intensity of the event may have occurred between these times while both stations were in darkness. The absorption level decreased to about 2 dB at 1500 UT September 4 at Shepherd Bay. There was a small decrease in absorption at both stations after the sudden commencement at 1646 UT September 4. The absorption remained near 1.5 dB for several days at Shepherd Bay until September 7. The absorption at Shepherd Bay was about 1 dB larger than at McMurdo Sound during most of the event, the difference increasing in the final days. If this difference is not due to ionospheric effects it suggests a 200% to 400% North-South asymmetry. During the 2 September 1966 event under similar sunlight conditions the absorption was nearly identical over both polar regions [Masley and Goedeke, 1968].

## Acknowledgement

This work was supported by the Polar Programs Office of the National Science Foundation under Contract NSF-C393 and the McDonnell Douglas Independent Research and Development Program.

## REFERENCE

MASLEY, A. J. and A. D. GOEDEKE — 1968 — The 1966-1967 Increase in Solar Cosmic Ray Activity, Canadian Journal of Physics, 46, S766-S771.

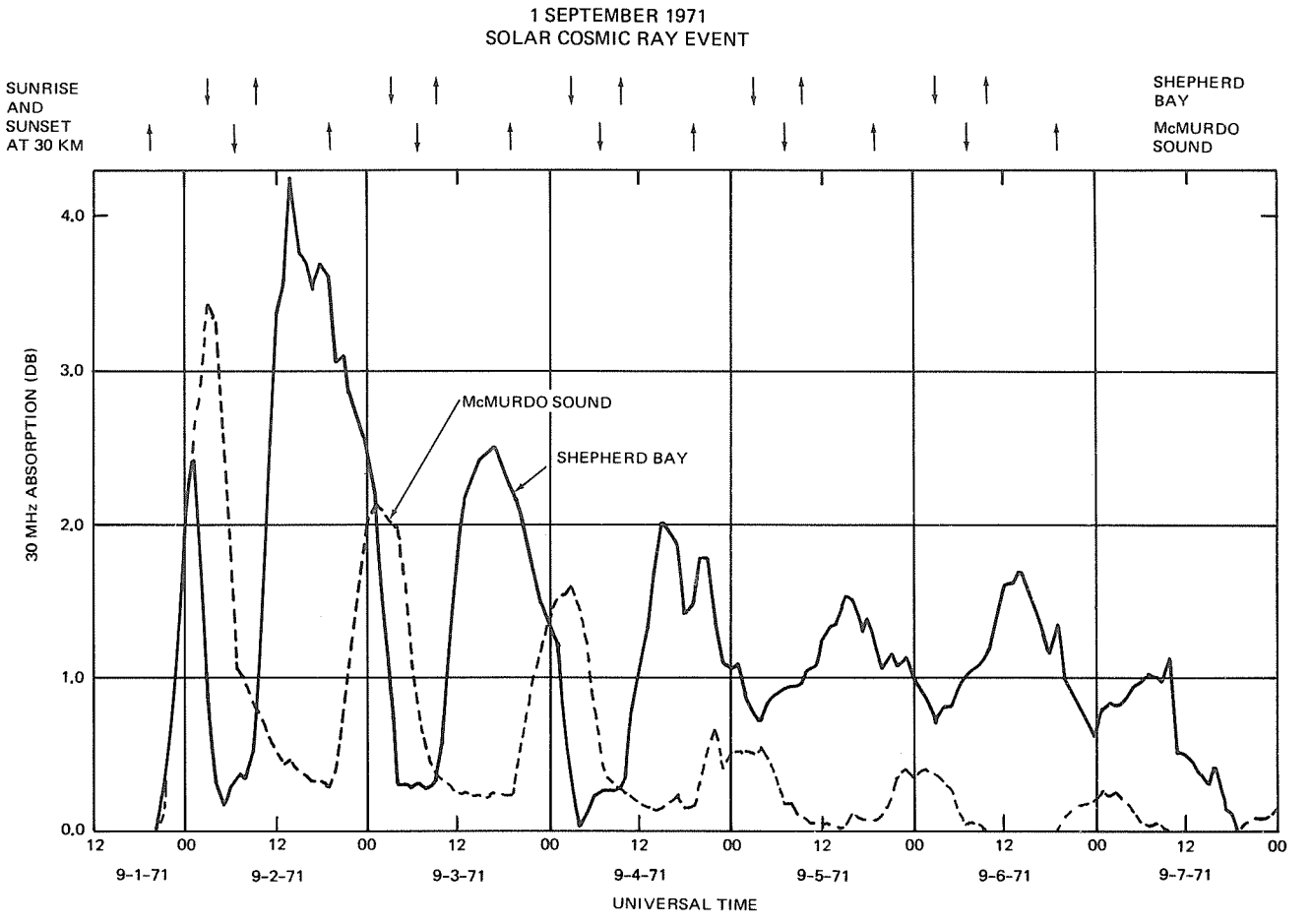


Fig. 1. 30 MHz riometer absorption data for Shepherd Bay and McMurdo Sound, September 1-7, 1971.

# 30 MHz RIOMETER DATA FOR SEPTEMBER 1971 SOLAR PARTICLE EVENT

RAYMOND J. CORMIER
IONOSPHERIC RADIO PHYSICS BRANCH
IONOSPHERIC PHYSICS LABORATORY
AIR FORCE CAMBRIDGE RESEARCH LABORATORIES
BEDFORD, MASS. 01730

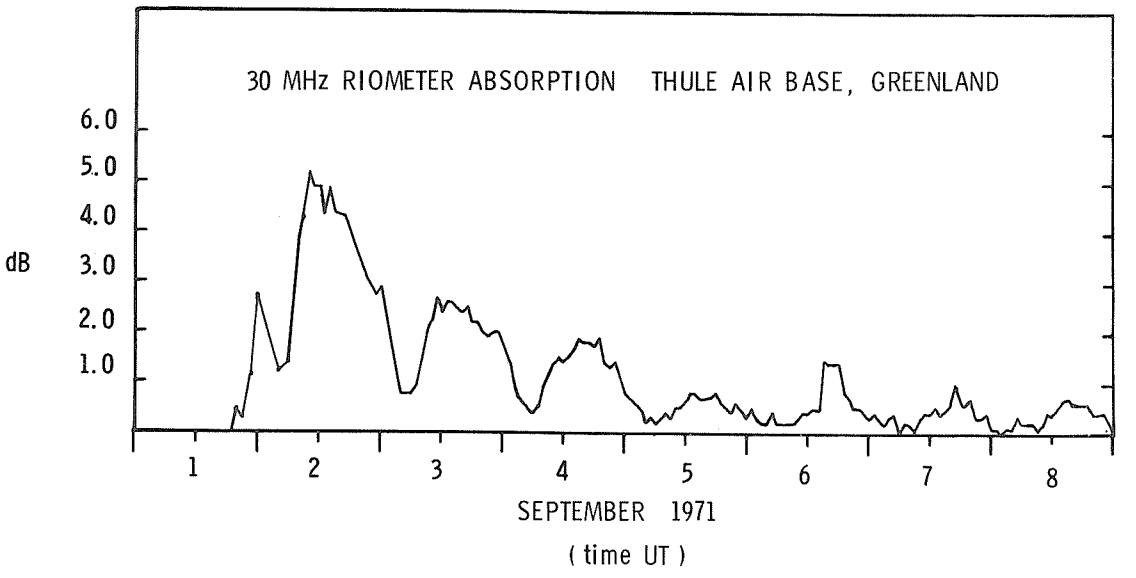


AFCRL Geopole Observatory 30 MHz Riometer Data
for September 1971 Solar Particle Event

Cormier, R. J. 1971 Geophysics & Space Data Bulletin
Vol. VIII; No. 4
AFCRL Bedford, Mass. 01730

# Polar Cap Absorption of September 1, 1971 by Riometer Data in the Arctic and Antarctic

by

V. M. Driatsky and V. A. Ulyev
The Arctic and Antarctic Research Institute, Leningrad
USSR

The present study is concerned with one of the two strongest Polar Cap Absorption events recorded in 1971. PCA data were obtained by riometers installed at the Soviet Arctic and Antarctic stations. Table 1 presents the station list, their geographical positions, invariant latitudes and the Sun's altitudes.

Table 1

STATION LIST

| | Station Name | Geographic Positions | | Φ' | Sun's Altitude 3 September 1971 | | Notes |
|---|---|---|---|---|---|---|---|
| | | Latitude | Longitude | | Noon | Midnight | |
| 1 | North Pole 19 | 83°17'N | 142°48'E | 76,0°N | +14°25' | + 0°59' | Positions for Sept. 3, 1971 |
| 2 | Dixon Island | 73 30 | 80 14 | 67,2 | +24 12 | - 8 48 | |
| 3 | Salekhard | 66 32 | 66 32 | 61,0 | +31 6 | -15 42 | |
| 4 | Vostok Station | 78°27'S | 106 52 | 84.3°S | + 3 50 | -19 14 | Data received by radio |
| 5 | Mirny | 66 33 | 92 01 | 76,8 | +15 45 | -31 9 | " " |
| 6 | Molodezhnaya | 67 10 | 45 51 | 67,6 | +15 8 | -30 32 | " " |

Notes: Riometer frequencies: Vostok Station - 30 and 50 MHz; Mirny - 31.8 and 40 MHz; other stations had riometers at 32 MHz.

Antennas at Vostok station are co-phasal, directed to zenith; at other stations antennas are of Yagi, directed to North Pole.

## PCA Event 1-6 September 1971

This event was not associated with any particular solar flare, since no optical solar flare data were readily available. We can, however, assume that a solar flare occurred at about 2000 UT 1 September on the basis of the data of radio emission bursts [Solar-Geophysical Data, 1971]. Vela Satellite measurements show that the proton flux with energies Ep > 25 Mev reached its maximum value F = 3640 particles/cm$^2$/sec at 0400 UT on the following day [Solar-Geophysical Data, 1971].

Figure 1 shows PCA intensity variations with data from 6 stations, three being in the Arctic, the other three in the Antarctic. North Pole-19 data show the absorption onset at 2000 UT, reaching its maximum at about 0600-0800 UT 2 September. Almost simultaneously, PCA maxima occurred at all other stations.

This PCA event occurred close to the autumn equinox, thus the night-day effect was well-pronounced at all the stations except NP-19. The evaluation of the ratio of the daytime absorption to the nighttime absorption has shown that it always decreased during PCA, having different values at the various stations, on an average ranging from 4 to 7. At Salekhard the effect of the geomagnetic cutoff was well-pronounced, and the absorption intensity was an order of magnitude less compared to other stations. At NP-19, though at midnight the Sun's altitude was + 0°59', the day-night effect was not observed. The equilibrium conditions at this station occurred because of the polar day during the

Sun's lower altitudes. An sc magnetic disturbance occurred on 4 September at 1646 UT. However, no marked changes related to it were observed in the PCA event. No midday recovery for this PCA event was observed.

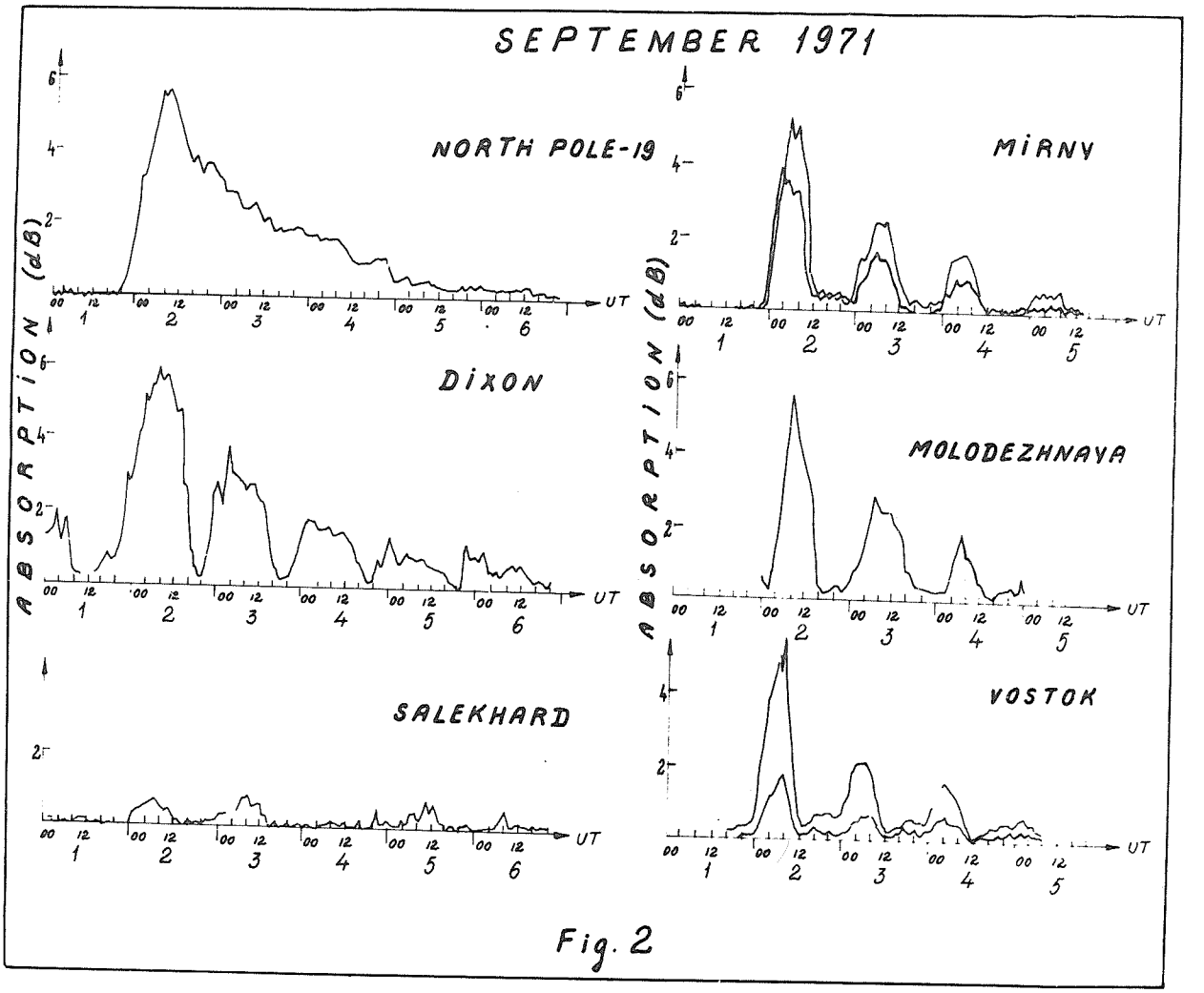


Fig. 1. Variations of PCA intensity over the period 1-6 September 1971.

REFERENCE

1971 Solar-Geophysical Data, 326 Part I, U.S. Department of Commerce, (Boulder, Colorado, U.S.A. 80302).

# Ground Based Ionospheric Observations from the Danish Geophysical Observatories in Greenland during the September 1 Event 1971

by

J. Taagholt and V. Neble Jensen
Ionosphere Laboratory
Technical University of Denmark
DK-2800 Lyngby, Denmark

The ionosphere data published below are reduced data based on routine measurements made at the field sites:

| | | |
|---|---|---|
| Narssarssuaq | (geomagnetic coordinates: | Lat. N 71.4° Long. E 37.1°) |
| Godhavn | (geomagnetic coordinates: | Lat. N 80.0° Long. E 33.1°) |
| Thule | (geomagnetic coordinates: | Lat. N 89.1° Long. E 357.5°). |

All three observatories, situated on the west coast of Greenland, are run by the Ionosphere Laboratory, a division of the Danish Meteorological Institute. The vertical sounder used at Narssarssuaq is a modified C-3/4, at Godhavn a J-5, and at Thule a C-4.

Additionally, Cosmic Noise Absorption (CNA) data obtained by means of IONLAB-Riometer at 30 MHz are shown from the same observatories as well as from Station Nord (geomagnetic coordinates: Lat. N 80.7° Long. E 134.5°), Sdr. Strømfjord (geomagnetic coordinates: Lat. N 77.6° Long. E 34.8°), and Godthaab (geomagnetic coordinates: N 75.0° Long. E 29.7°).

The three latter stations are operated for the Ionosphere Laboratory by the Greenland Technical Organization, Telesection.

## September 1 Event

The riometer observations for September 1 (see Figure 1) at the four southern stations and especially at Narssarssuaq show normal auroral observation events varying between 0 and 3 dB absorption. Only at Thule and Station Nord is another feature seen starting about 2000 UT with a steadily increasing absorption.

The CNA data for September 2 show high absorption at all 6 stations, indicating a real polar cap absorption event. Station Nord due to the extremely high geographic latitude and the time of year shows no diurnal solar effect corresponding to 24 hours of sunlight in the lower ionosphere. From about 5 dB maximum absorption at about 0730 UT on September 2 the absorption decreases slowly during the following 3 days at Station Nord. The diurnal variation is more pronounced farther south. The rapid increase of absorption at the four West Greenlandic stations shows a latitude time dependence, with the earliest occurrence at Thule and a delay of about 3 minutes per degree towards the south.

Some HF propagation data for the period September 1 to September 7 (Figure 2) illustrate the HF communication problems caused by such an absorption event. At Reersø near Copenhagen (N 55.1° E 11.0°) WWV signals from Fort Collins, Colorado (N 40.68° E 254.97°) are recorded every second hour. Figure 2 shows the signal strength received at Reersø with the scale from 1 = barely audible, 2 = poor, 3 = fair, 4 = good, to 5 = excellent, placed according to the different receiving frequencies in the range from 2.5 - 25 MHz. Additionally, information about HF communication from Godthaab, Greenland (N 64.2°E 308.2°) to Reersø is presented as a full line for normal communication, as a thin line for reduced communication, and marked with B for "black out" periods. On Figure 2 the 30 MHz riometer data from Godthaab are also presented, showing pronounced correlation between the CNA data and the HF communication data.

On Fiqure 3 the propagation paths are shown: Fort Collins - Reersø about 7000 km and Godthaab - Reersø about 3500 km. The normal propagation Godthaab - Reersø is usually a one hop propagation via F-layer with the reflecting point situated in the auroral zone over Iceland. The transmitter is situated on a small island on the West Greenland shore and the radiation angle is as small as about 4°.

The riometer data shown, giving information about absorption in D-region vertically above the transmitting station, could thus not be expected to give valuable information about the Godthaab - Reersø communication. However, based upon data from Figure 1 and Figure 4a and b, it can be expected that the PCA covers the total polar cap. The signal from Godthaab (as well as Fort Collins) therefore will be absorbed when crossing the D-region near Greenland's east coast. This is in agreement with Rybner and Ungstrup [1957] as seen on Figure 5 showing the area with high absorption based upon data collected during the 1932-33 international polar year. During the summer the Ionosphere Laboratory will start operation of a 30 MHz riometer at Angmagsalik. This riometer should give information about absorption in the area where the propagation path Godthaab - Reersø crosses the D-region.

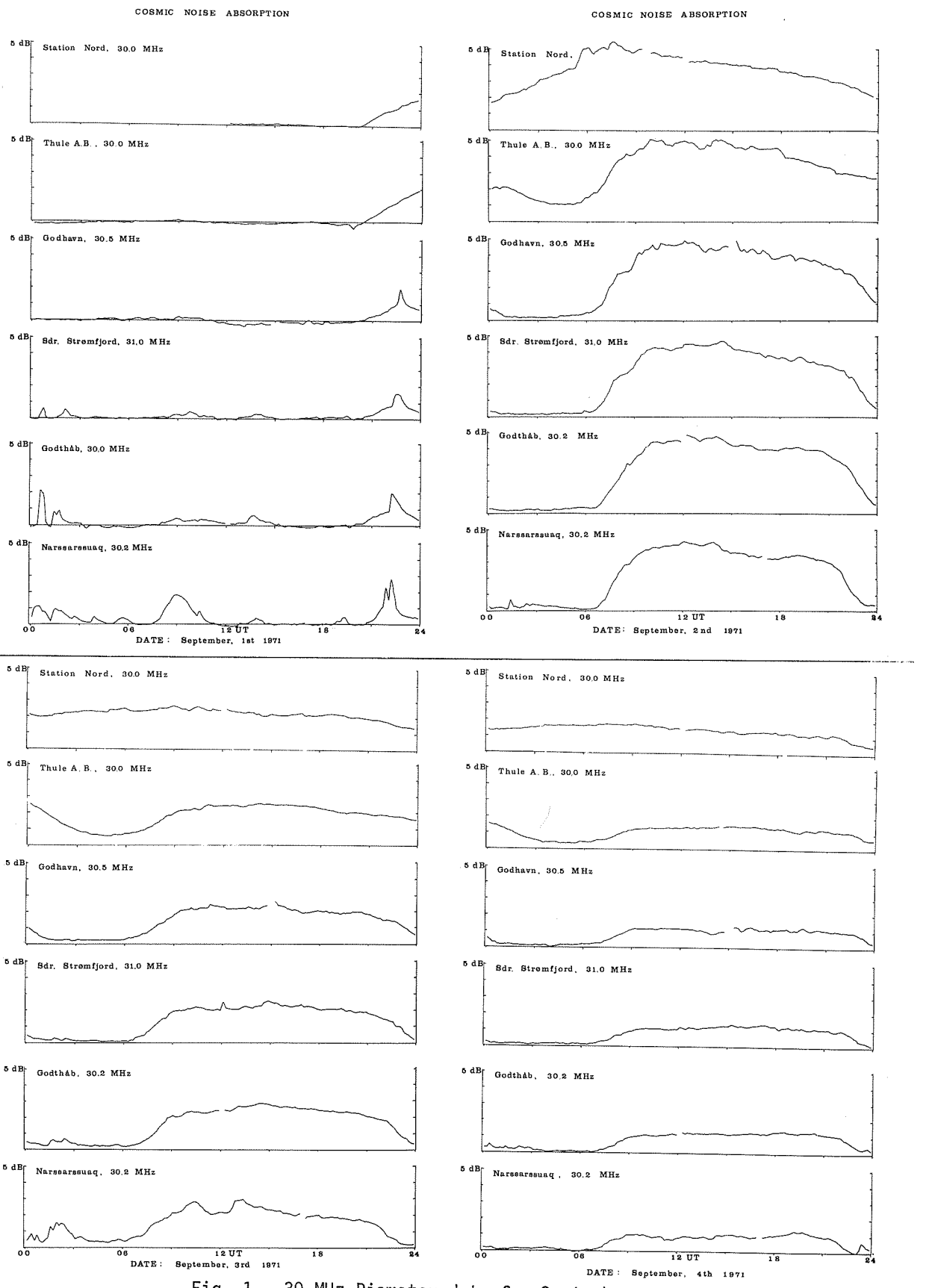


Fig. 1. 30 MHz Riometer data for September event.

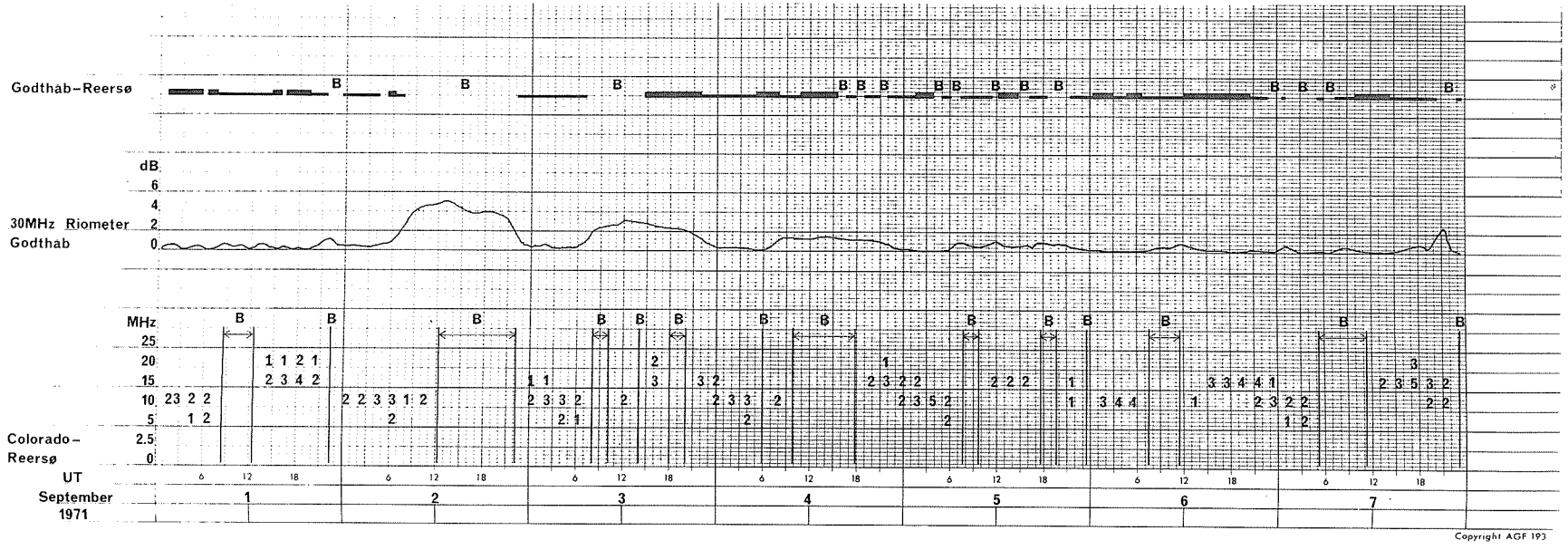


Fig. 2. HF communication data for September event.

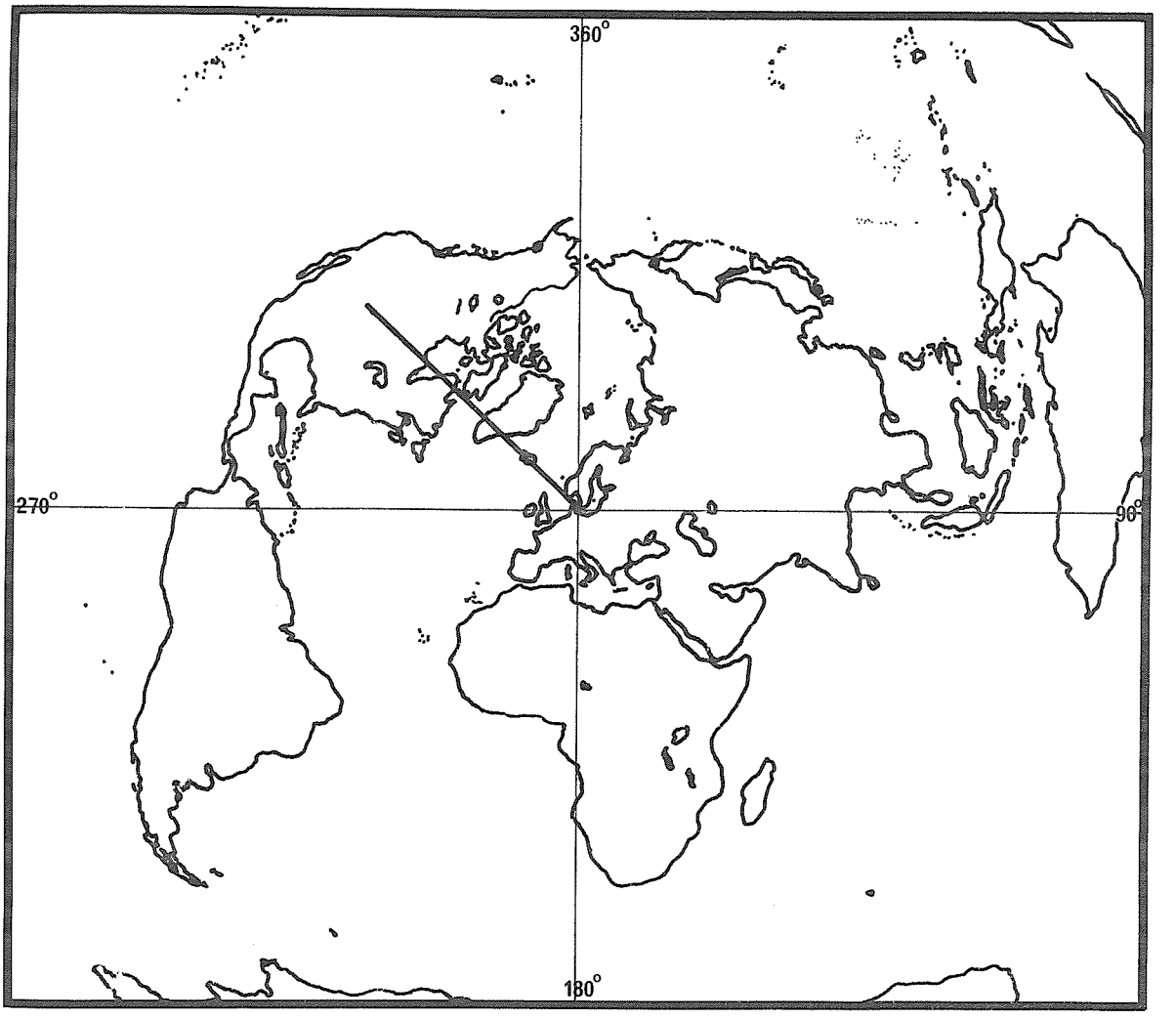


Fig. 3. HF communication path.

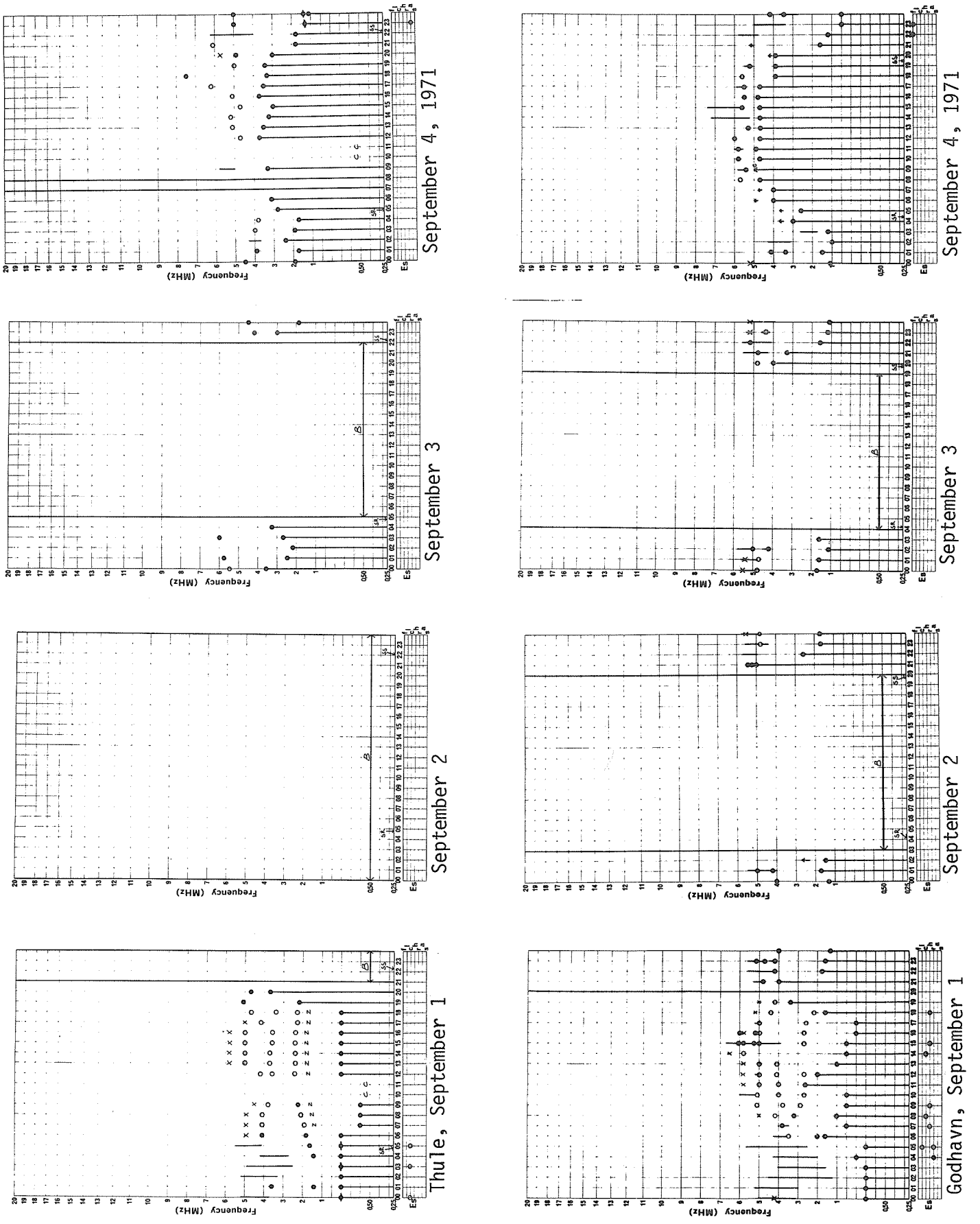


Fig. 4a. f-plots for September from Godhavn and Thule.

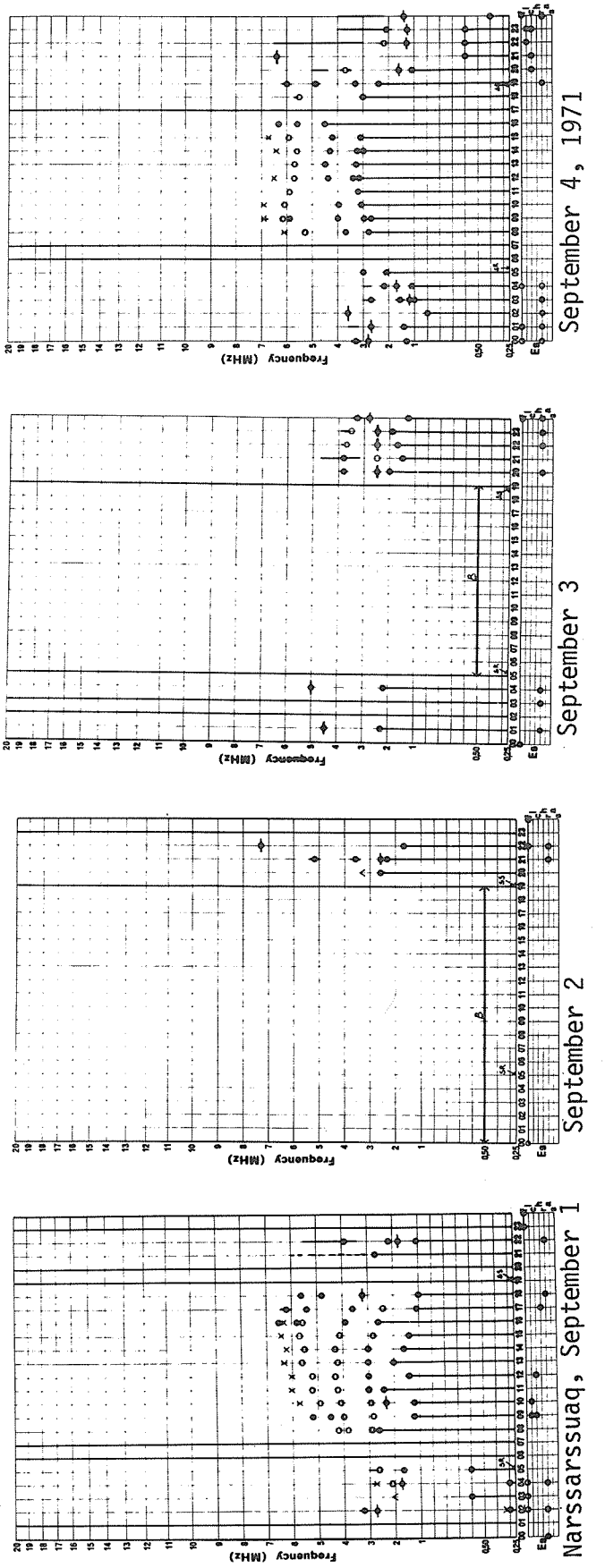


Fig. 4b. f-plots for September event from Narssarsuaq.

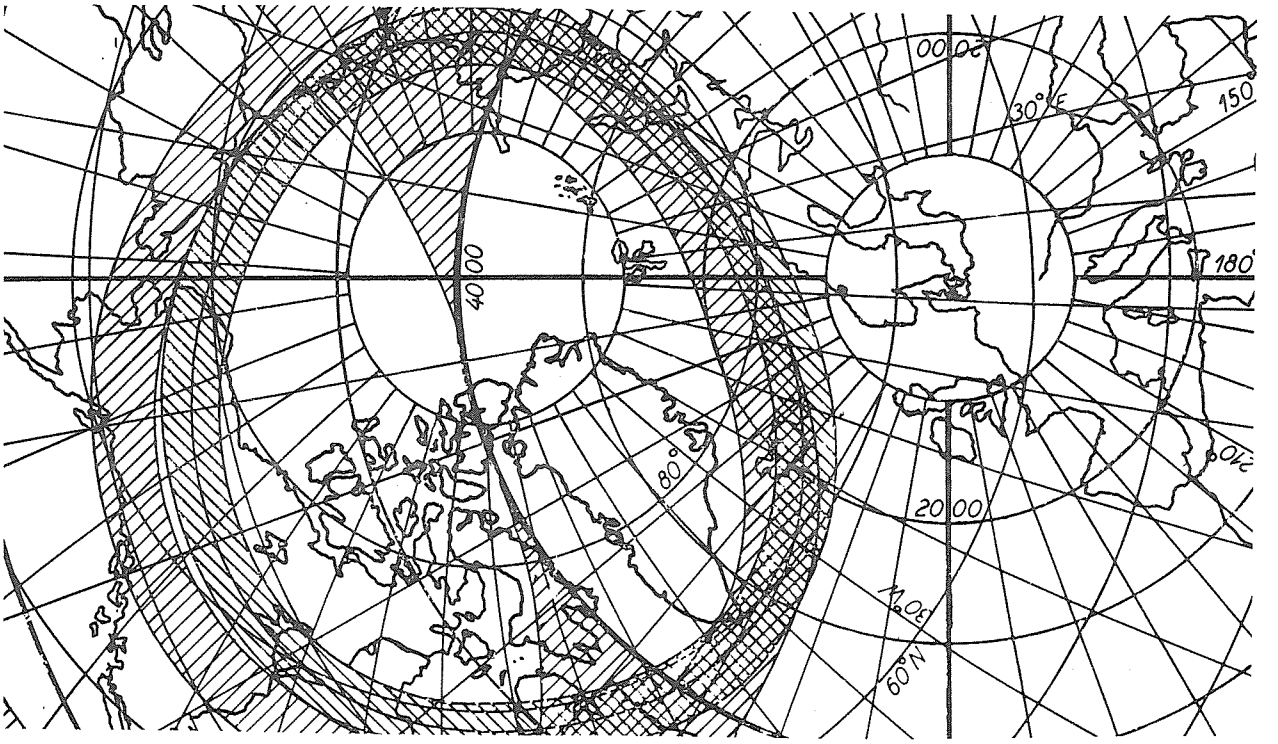


Fig. 5. Rybner and Ungstrup map showing area with max. geomagnetic disturbances during 1932-33 covering area with bad radio communication from Denmark.

REFERENCES

RYBNER, J. and E. UNGSTRUP 1957 L'influence de la zone d'aurores boréales sur les liaisons radioélectriques, Annales des Telecommunications, 12, 172-173.

# Ionospheric Observations in Kiruna of the PCA Event of 1 September 1971

by

C. Jurén and J. Svennesson
Kiruna Geophysical Observatory
S-981 01 Kiruna 1, Sweden

## Introduction

Ionospheric observations from Kiruna which may be related to the outstanding PCA event of September 1, 1971 and the associated geomagnetic events are collected and presented in synoptic figures. Reproductions of magnetometer and riometer records are given in separate figures. Ionosonde records from observing stations other than Kiruna have been included in the synoptic figures to show the latitudinal variations.

The coordinates of the stations are given in the table below:

| | Geographic | | Corrected Geomagnetic[+)] | |
|---|---|---|---|---|
| | Latitude | Longitude | Latitude | Longitude |
| Kiruna | 67.8°N | 20.4°E | 64.8°N | 104.2°E |
| Lycksele | 64.6°N | 18.7°E | 61.7°N | 100.6°E |
| Uppsala | 59.8°N | 17.6°E | 56.9°N | 97.1°E |

The riometer records from Kiruna are replaced by records from Down Range Station, ESRANGE, when, for longer periods, the riometer records in Kiruna are highly affected by radio interference. These records are marked with the letters DRS.

The ionosonde data used are from the bulletins published by the Research Institute of National Defence, Stockholm, Sweden.

The geographic coordinates of the transmitters of the VLF signals shown in this data report are as follows: NAA (17.8 kHz) 44.6°N, 67.3°W; NLK (18.6 kHz) 48.2°N, 121.9°W; and HAIKU (13.6 kHz) 21.4°N, 157.8°W.

## The PCA Event of 1 September 1971

A ground level cosmic ray increase started around 2015 UT on 1 September. The increase at Deep River was about 27% around 2200 UT.

The PCA onset was observed in Kiruna on the two VLF signals NLK (18.6 kHz) and HAIKU (13.6 kHz) around 2020 UT on 1 September.

No optical flare was observed which could be responsible for the emission of the particles causing the above two events. However, the Sagamore Hill Observatory recorded a complex radio burst with onset 1926 UT, and Type IV solar radio emission of medium intensity (with onset time 1937 UT) was observed in Boulder. It was probably a "behind limb event" with the particle emitting area supposedly (Ursigram) about 3 days behind the West limb of the Sun.

A general view of the event as observed in Kiruna is shown in Figure 1.

## VLF Propagation

The onset of the PCA event was observed as a phase advance starting about 2020 UT of both the VLF-signals. The maximum phase advance of the HAIKU signal was about 45 μsec and occurred early in the morning on 2 September (UT).

The amplitude of the NLK signal decreased and the maximum difference from the normal level was greater than 30 dB in the night of 1-2 September. About 6 September the amplitude began to increase slowly reaching normal level on 9 September.

## Radio Wave Absorption

The typical proton induced cosmic radio noise abosrption, showing smoothly varying and high absorption during day and low absorption during night, started early on 2 September and remained for 2 days. A moderately severe magnetic storm started with an sc at 1646 UT on 4 September and the absorption observed between 4 and 8 September was more variable.

+) G. Gustafsson, Arkiv för geofysik, 5, 595, 1970.

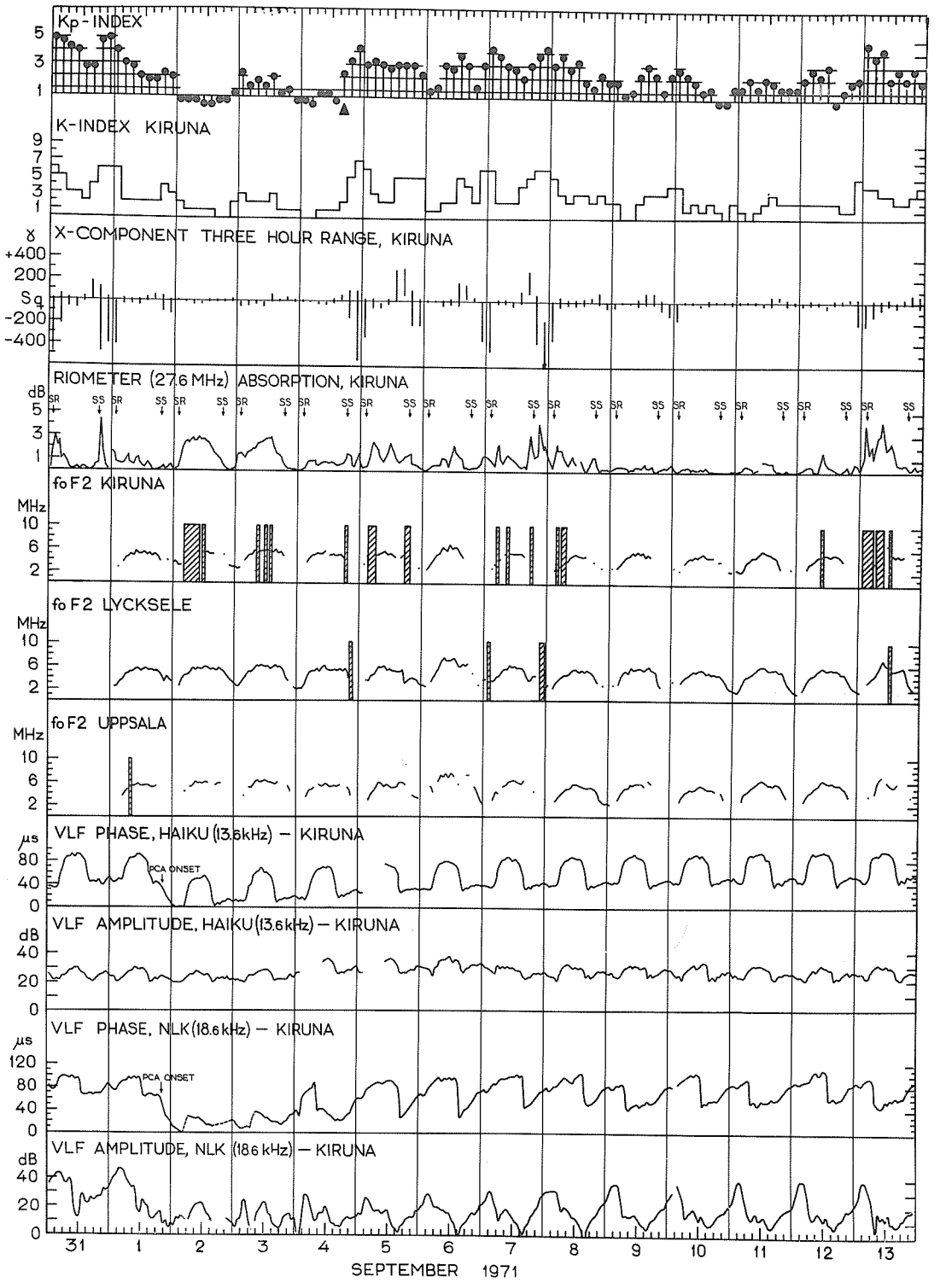


Fig. 1. Survey of ionospheric effects as recorded in Kiruna and nearby observatories. The foF2 plots are presented in the order of decreasing latitude.

The riometer absorption curve shows the maximum absorption during each hour. One-hour values of the critical frequency foF2 have been plotted. The hatched areas indicate periods when the critical frequency was not measured due to black-out, and empty areas correspond to periods when foF2 could not be measured for other reasons. The onset of the PCA is observed on the phase and amplitude records of the VLF signals.

A reproduction of the riometer records is shown in Figure 2.

The diagrams of the critical frequency of the F2-layer show black-out in Kiruna for some time every day between 2 and 8 September and only during very short time periods in Lycksele during the geomagnetic storm on 4 and 7 September. This indicates that the proton precipitation reached somewhat south of Kiruna. No black-out was recorded in Uppsala.

Geomagnetic Activity

The PCA onset occurred during a period with weak geomagnetic activity. The geomagnetic storm with the sc at 1646 UT on 4 September gave a smooth slowly growing X-component for two hours after the sc. At 2100 UT the X-component has a positive maximum. The X-component was negative with a minimum of about -500 $\gamma$ from the Sq curve at 2330 UT. At the same time there was a maximum in both the Y- and Z-components, 200 $\gamma$ and 250 $\gamma$, respectively. This indicates that the main activity occurred to the south of Kiruna. During the following nights the magnetic activity in Kiruna remained high.

Figure 3 shows the magnetometer records from Kiruna for the period 3 - 11 September 1971.

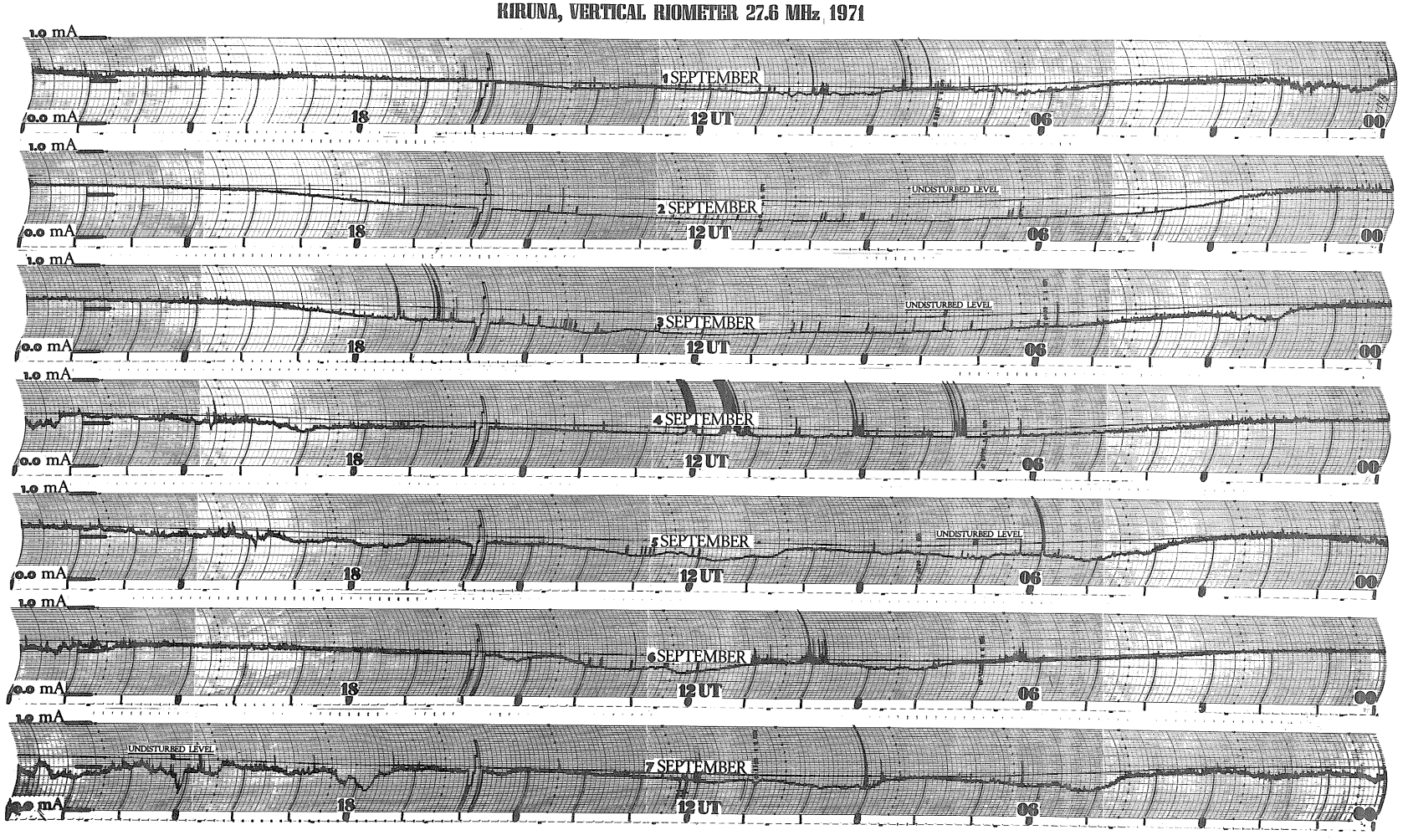
KIRUNA, VERTICAL RIOMETER 27.6 MHz, 1971
1.0 mA
0.0 mA
1 SEPTEMBER
2 SEPTEMBER
3 SEPTEMBER
4 SEPTEMBER
5 SEPTEMBER
6 SEPTEMBER
7 SEPTEMBER
UNDISTURBED LEVEL
18
12 UT
06
00

2a.

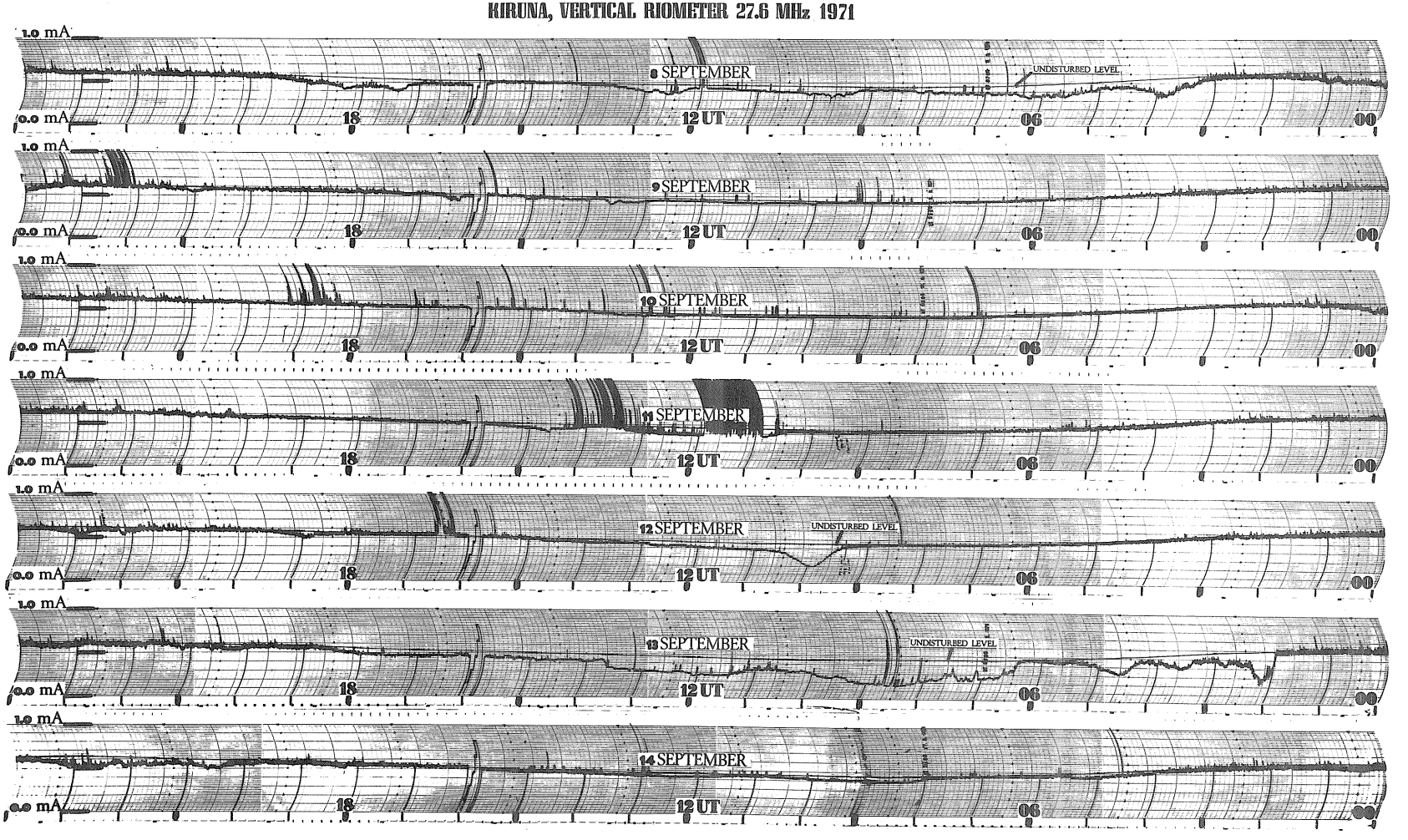


2b.

Fig. 2. Riometer records from Kiruna 27.6 MHz receiver. In case of severe interference in Kiruna, the less disturbed records of the Down Range Station (DRS) at ESRANGE, (27.6 MHz), have replaced the Kiruna records. The reproductions are extracted from "Kiruna Geophysical Data".

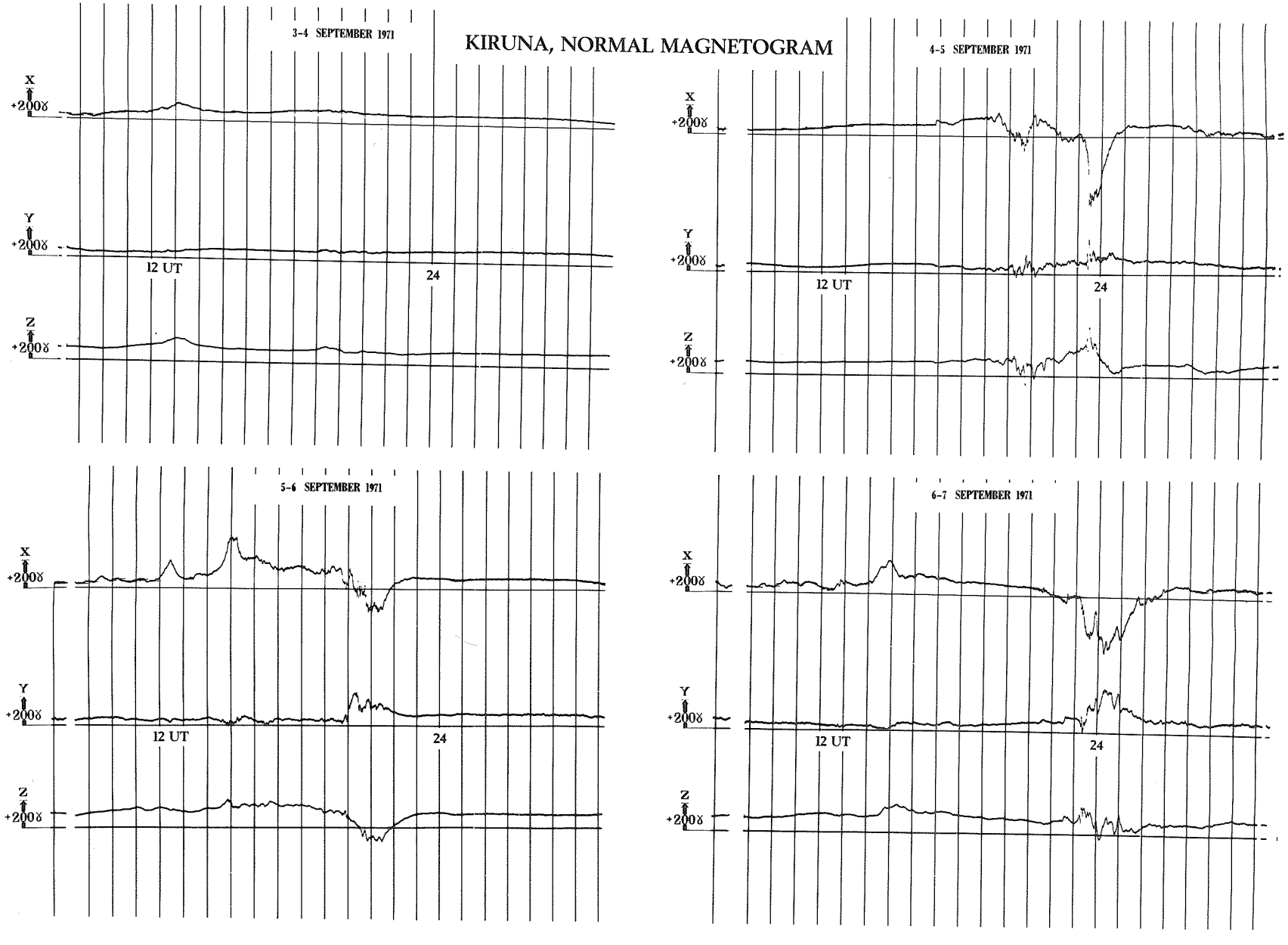
KIRUNA, NORMAL MAGNETOGRAM
3-4 SEPTEMBER 1971
4-5 SEPTEMBER 1971
5-6 SEPTEMBER 1971
6-7 SEPTEMBER 1971
X
Y
Z
+200γ
12 UT
24

3a.

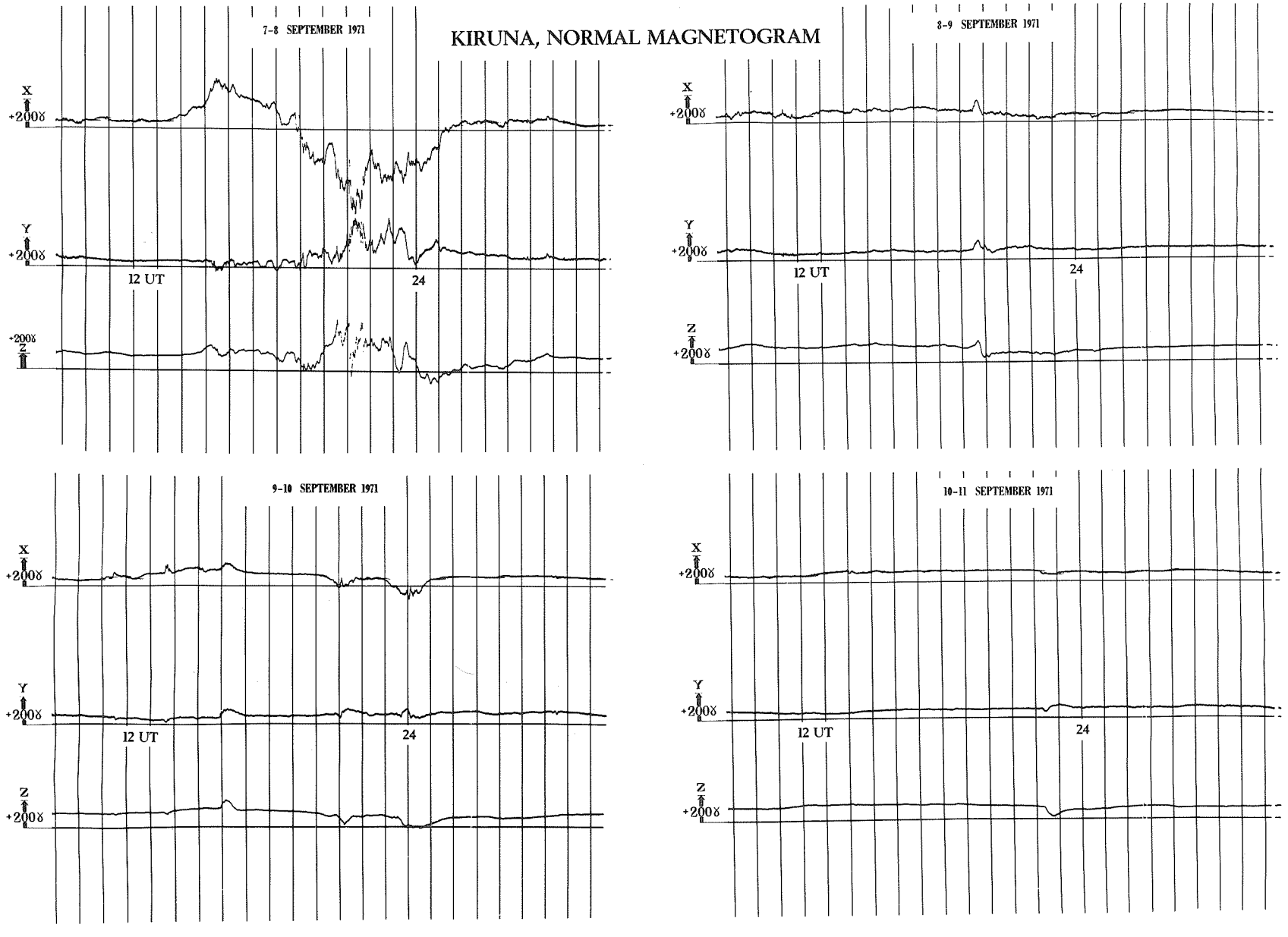


3b.

Fig. 3. Kiruna normal magnetogram. The reproductions are extracted from "Kiruna Geophysical Data".

# EFFECTS OF THE SEPTEMBER 1971 SOLAR PARTICLE EVENT ON POLAR VLF PROPAGATION

JOHN P. TURTLE
POLAR ATMOSPHERIC PROCESSES BRANCH
AERONOMY LABORATORY
AIR FORCE CAMBRIDGE RESEARCH LABORATORIES
BEDFORD, MASS. 01730

Measurements of VLF propagation in polar cap regions are made at the AFCRL Geopole Observatory at Thule AB in Greenland as a monitor of D-region particle precipitation disturbances. During the solar particle event on 1 September 1971 two transmitters were being monitored; one was GBR (16.0 kHz) in England and the other was NPG (18.6 kHz) in Washington. These paths are shown in Figure 1.

The effects of the 1 September 1971 solar particle event on the amplitude and phase of the signals from the two transmitters are shown in Figure 2. A rubidium frequency standard was used as the phase reference. Although both propagation paths were solar illuminated at the beginning of the event no definite SPA effects were recorded. The D-region particle disturbance began at about 2010 UT on 1 September. On the NPG-Thule path the maximum attenuation was about 12 dB at 0330 UT on 2 September and a maximum phase advance of 204° occurred at 0915 UT. On the GBR-Thule path the signal was lost during the daylight hours on 2 and 4 September due to the enhanced attenuation effects of the Greenland ice cap. The maximum attenuation on this path was probably more than 25 dB. Recovery to normal signal propagation conditions was not complete until 11 September 1971.

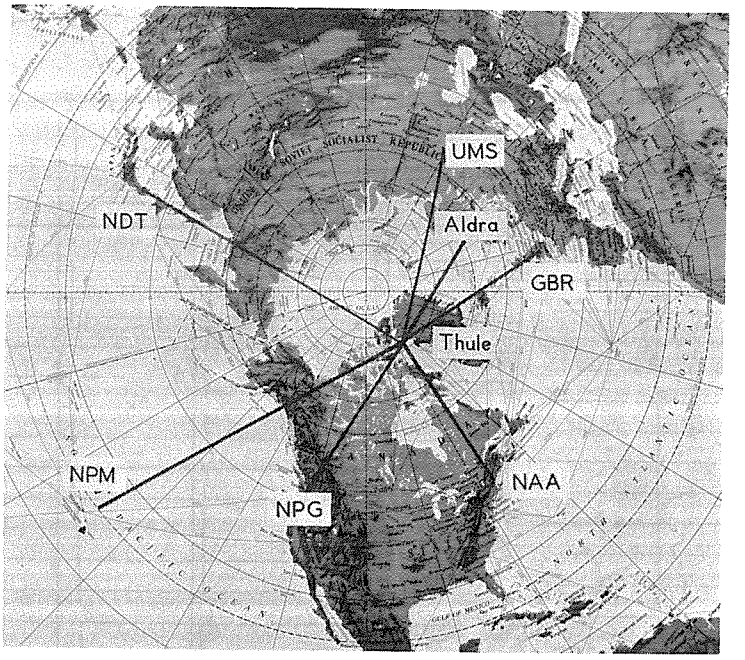


Fig. 1 Polar VLF Propagation Paths to the Geopole Observatory

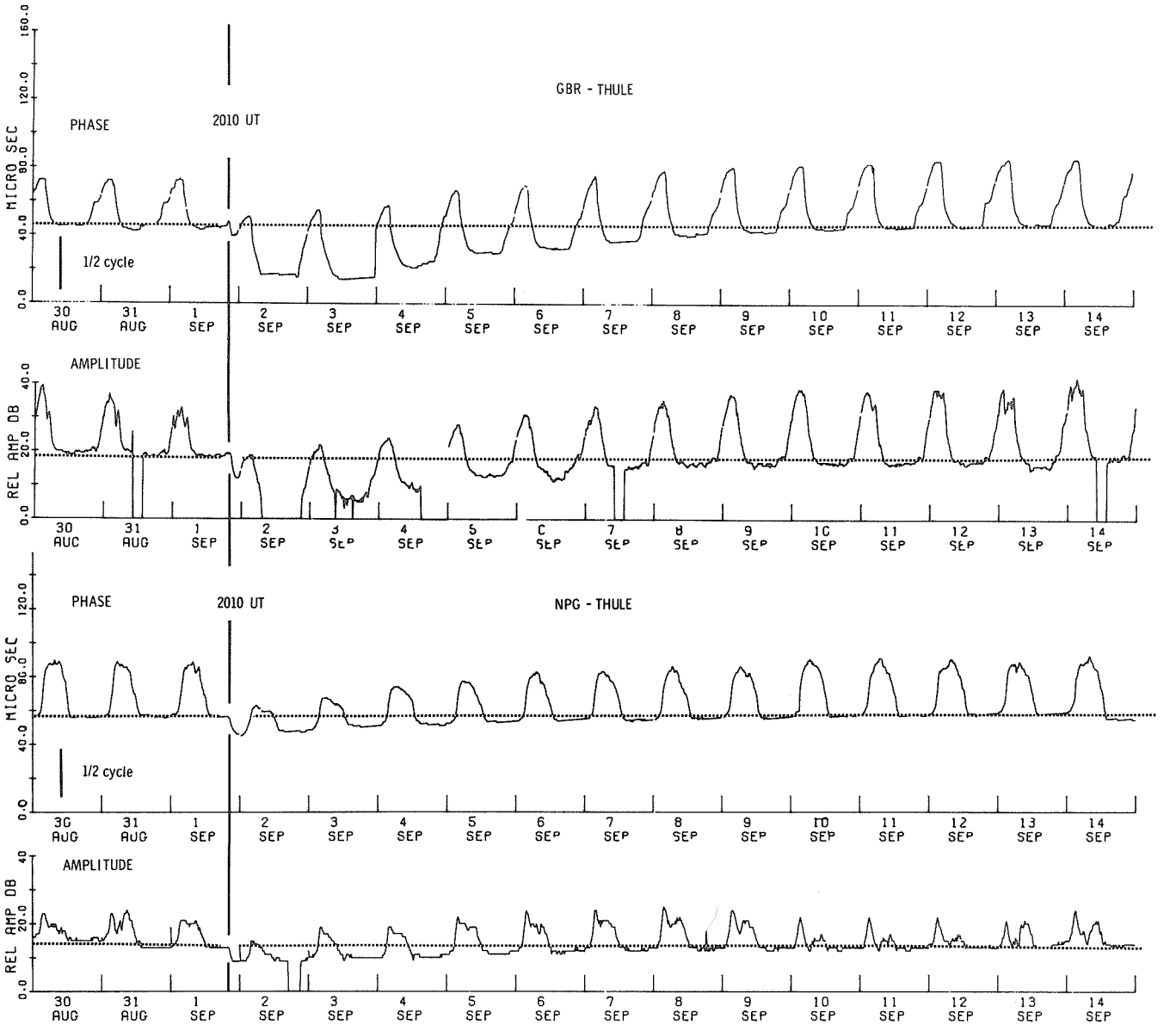


Fig. 2 VLF Amplitude and Phase Data for the September 1971 Solar Particle Event (The dotted line is an arbitrary reference level)

# Mid-Latitude Total Electron Content During Cosmic Ray Event September 1-2, 1971

by

J. A. Klobuchar
Air Force Cambridge Research Laboratories
Bedford, Massachusetts

and

M. J. Mendillo
Astronomy Department, Boston University
Boston, Massachusetts

Continuous measurements of the ionospheric total electron content (TEC) using the Faraday rotation technique are routinely made from Sagamore Hill, Hamilton, Massachusetts, by monitoring the VHF signal from the geostationary satellite, ATS-3. The TEC of the mid-latitude ionosphere consists mainly of the integrated electron densities of the F-region; that is, the lower layers contribute a negligible amount to the total. The equivalent vertical TEC values for September 1-2, 1971, are shown in the Figure below. The dashed curves give the monthly median behavior for the month. The small vertical arrow indicates the approximate time of the commencement of ground level cosmic ray increase. The September period was magnetically quiet, as indicated by the Ap values in the Figure. Geomagnetic storms typically cause large scale changes in TEC which last several days while large solar flares produce effects of much smaller magnitude and shorter duration. For this period, however, no changes occurred in TEC which could be directly associated with the cosmic ray increase.

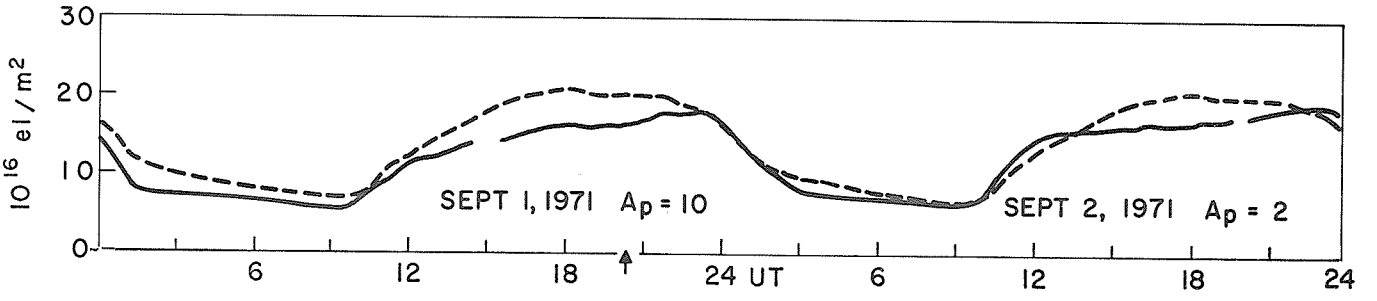


EQUIVALENT VERTICAL TOTAL ELECTRON CONTENT OBSERVED FROM SAGAMORE HILL, HAMILTON, MASS.

# Polar Cap Disturbances of September 1, 1971, Observed on the Phase of VLF Waves

by

Y. Hakura
Radio Research Laboratories
Koganei, Tokyo, Japan

and

T. Ishii, T. Asakura, and Y. Terajima
Inubo Radio Wave Observatory
Radio Research Laboratories
Choshi, Chiba, Japan

Phase measurements with a cesium frequency standard of VLF waves propagating over great distances have been made at Inubo Radio Wave Observatory, Choshi, Chiba, Japan (35°42'N, 140°52'E). Among them, transpolar VLF waves provide a very sensitive method of detecting solar proton events at the middle latitude [Nakajima et al., 1970]. The transpolar signal paths for NAA-17.8 kHz, GBR-16.0 kHz, and WWVL-20.0 kHz are shown in Figure 1, in which the corrected geomagnetic latitudes of 60° and 70° are shown by two elliptical lines.

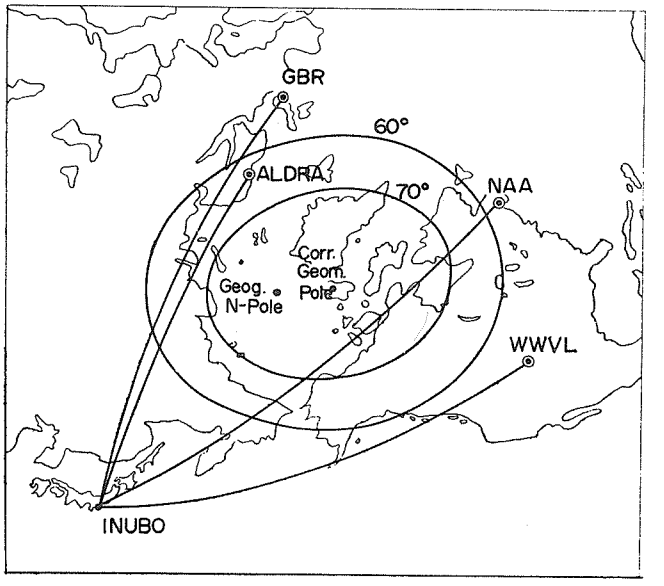


Fig. 1. Transpolar signal propagational paths.

Figure 2 shows solar proton flux with energy 5 - 21 Mev [Solar-Geophysical Data, October, 1971], phase deviations in the NAA and GBR signals and geomagnetic Kp indices on August 29 through September 11, 1971. Occurrence times of polar cap disturbances (PCD) and related solar-terrestrial events are listed in Table 1.

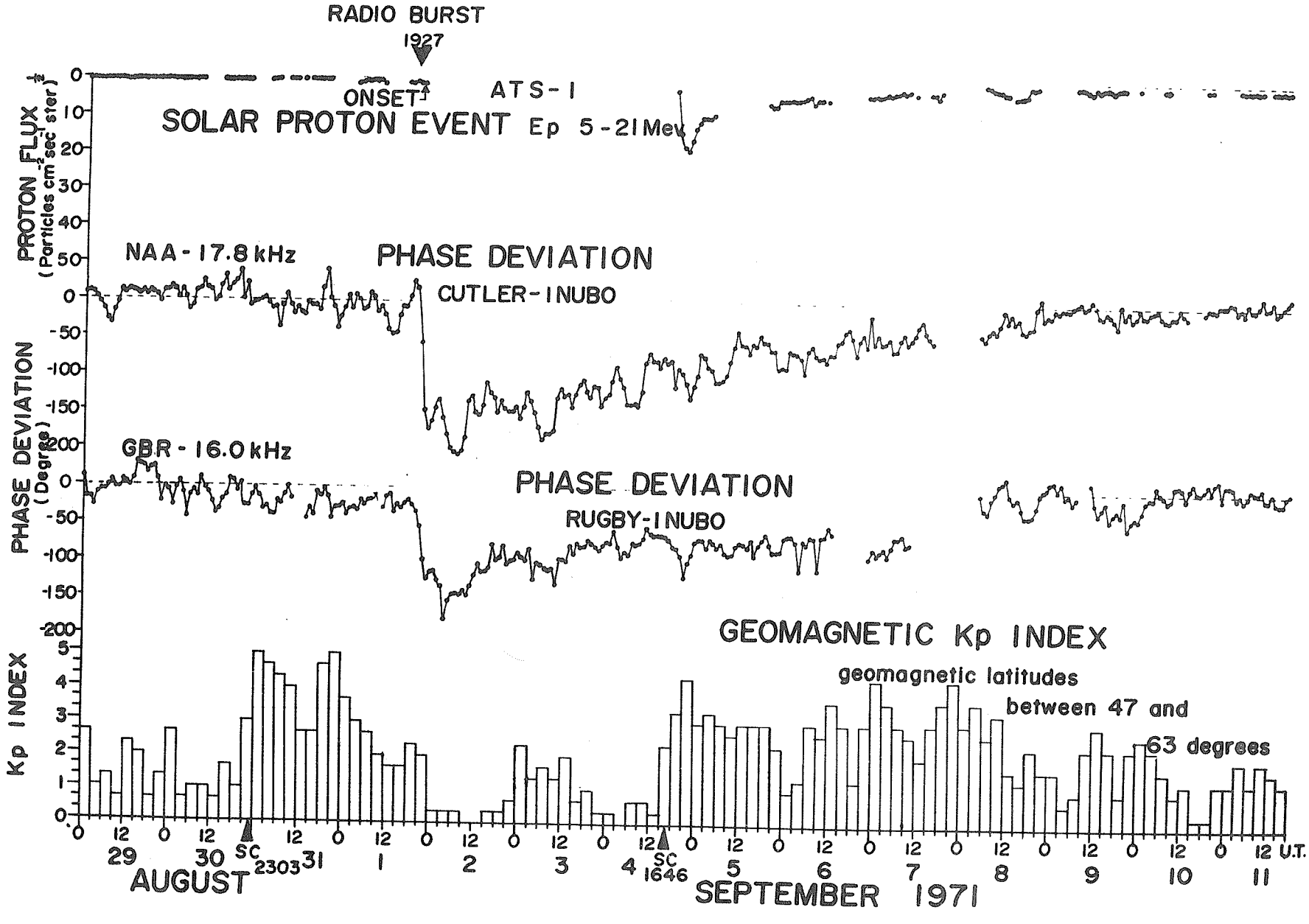


Fig. 2. Polar Cap Disturbance of September 1, 1971.

Table 1

PCD's observed at Inubo and related solar-terrestrial events of September 1, 1971

| Event | | Start time | Max. time | End | Flux, or Phase deviation |
|---|---|---|---|---|---|
| Radio burst at 2695 MHz ( Sagamore Hill ) | | 1/ 1926.9<br>2002.2 | 1940.5<br>2002.2 | 2002.2<br>2030D | $1.2 \times 10^{-20}$ wm$^{-2}$Hz$^{-1}$<br>$1.3 \times 10^{-20}$ |
| PCD | NAA-17.8 kHz | 1/ 2032 | 2/0741 | 9/08 | 218° |
| | GBR-16.0 kHz | 2045 | 0352 | 8/09 | 150° |
| Solar proton | ATS 1 (21-70 Mev) | 2100E | | 11/07 | |
| | Neutron monitor (Deep River) | 2020 | 2250 | 2/1230 | 11.5 % above background |

D = after
E = before

REFERENCES


NAKAJIMA, T., T. ISHII, K. TSUCHIYA, A. SAKURAZAWA, and Y. HAKURA. 1970. Results of special observations for the Proton Flare Project 1969: Polar cap disturbance of June 7, 1969, observed on the phase of VLF waves, J. Radio Res. Labs., Japan, 17, 49-54.

1971. Solar-Geophysical Data, 326 Part I, U.S. Department of Commerce, (Boulder, Colorado, U.S.A. 80302), 24-25.

# Report on Ionospheric and Whistler Activity at the Panská Ves and Průhonice Observatories on September 1, 1971

by

F. Jiricek, J. Lastovicka and P. Triska
Geophysical Institute
Czechoslovak Academy of Sciences
Prague, Czechoslovakia

The proton flare event on September 1, 1971 was accompanied by nearly no effect in the ionosphere above Central Europe. It is rather difficult to decide precisely what was the ionospheric response to the proton flare in question, because the flare influence was superimposed on the two magnetic storms that started on 30 August at 2303 UT and on 4 September at 1646 UT [NOAA, 1971].

The state of the upper ionosphere is studied using the foF2 data of the ionosonde located at Průhonice (49°59'N, 14°33'E). The foF2 values during the period August 31 - September 4 are close to monthly median values except the daytime values of August 31 and September 1, which are distinctly higher and lower, respectively, than median values. These two days, however, precede the proton flare event. Consequently, this proton flare event caused no observable changes in the upper ionosphere.

The X-ray burst accompanying this proton flare event was too weak to cause any SID-event, which is in agreement with observational SID data [NOAA, 1971]. The daytime lower ionosphere during the period August 30 - September 4 was fairly quiet according to the HF A3-absorption data obtained at Panská Ves (50°32'N, 14°34'E). The nighttime lower ionosphere is studied using the LF A3-measurements of the ionospheric absorption. The nighttime absorption data measured at 272 kHz (reflection point 49°34'N, 16°03'E) are presented in Table 1:

Table 1

| Date | Aug. 30-31 | Aug.-Sept. 31-1 | Sept. 1-2 | Sept. 2-3 | Sept. 3-4 | Sept. 4-5 | Sept. 5-6 | Median x) |
|---|---|---|---|---|---|---|---|---|
| L(dB) | 11.7 | 13.2 | 15 | 13.2 | 12.7 | 12.4 | 16.9 | 13 |

x) monthly median value

If we compare the results of absorption measurements made at 272 kHz (Table 1) and 185 kHz (reflection point 51°09'N, 14°06'E) with monthly median values and with the absorption values in the vicinity of the studied period, we obtain a general nighttime absorption characteristic of the period under study Table 2):

Table 2

| Night | Aug. 30-31 | Aug.-Sept. 31-1 | Sept. 1-2 | Sept. 2-3 |
|---|---|---|---|---|
| 272 kHz | low | normal | slightly enhanced | normal |
| 185 kHz | normal | enhanced | enhanced | more enhanced |

| Night | Sept. 3-4 | Sept. 4-5 | Sept. 5-6 |
|---|---|---|---|
| 272 kHz | normal | low | enhanced |
| 185 kHz | $B_0$ 2015 - 2125 UT; slightly enhanced | slightly enhanced | slightly enhanced |

The absorption enhancement starting on September 5-6 which continues during at least the next two nights may be attributed to the magnetic storm with ssc at 1646 UT on September 4 [NOAA, 1971]. The bay-like disturbance ($B_0$) observed at 185 kHz on September 3-4 seems to be of a random origin, because it is neither confirmed by any other absorption data nor supported by geomagnetic data. The time-development of absorption between the nights of August 30-31 - September 4-5 allows us to say that the absorption enhancement at 185 kHz and very probably also at 272 kHz is the absorption after-effect of the magnetic storm started at 2303 UT on August 30, but the possibility of some influence of the proton flare of Septmeber 1, 1971 cannot be excluded. The nighttime absorption

data of the Nagycenk Observatory (272 kHz; A3; reflection point 48.4°N, 17.1°E) indicate no observable influence of the given proton flare either [Bencze, 1972].

If we compare the lower ionosphere response to the solar proton flares of September 1, 1971, January 24, 1971 [Tríska et al., 1972] and November 2, 1969 [Krivský et al., 1972] and to the March 1970 event [Tríska and Lastovicka, 1971; Knuth et al., 1971], we can conclude that the effect of the proton flare itself probably does not occur in the lower ionosphere (except SID due to the EUV-radiation) above Central Europe (∿50°N, ∿15°E) nor somewhat more northerly. The main condition for the occurrence of the lower ionosphere disturbances accompanying the proton flare event seems to be a sufficiently disturbed geomagnetic situation caused by the given proton flare or by another solar event coinciding accidentally with the proton flare interval, e.g. by the mechanism proposed by Bednárová and Halenká [1969].

The whistler activity, as is usual in Czechoslovakia in this part of the year [Jiřícek, 1971], was so weak that it was impossible to obtain any results based on VLF-data. For instance, at the Panská Ves Observatory no whistler was observed during August 30 and only one was observed during September 1 in the routine observational program of 2 minute tape records every hours.

REFERENCES


BENCZE, P. 1972 Private communication.

BEDNAROVA-NOVAKOVA, B. and J. HALENKA 1969 A Universal Interpretation of the Generation of Geomagnetic Storms using Features of the Solar Corona, Planet. Space Sci., 17, 1039-1044.

JIRICEK, F. 1971 Whistler Activity in Central Europe during the Period of Increasing Solar Activity from 1964 to 1968, Trav. Inst. Géophys. Acad. Tchécosl. Sci., 1969, No. 313, 281-289, Academia, Praha.

KNUTH, R., W. LIPPERT and J. WEISS 1971 Midlatitude Ionospheric Effects in March 1970, Upper Atmosphere Geophysics Report UAG-12, Part II, 222-226.

KRIVSKY, L., A. TLAMICHA, J. HALENKA, J. LASTOVICKA, P. TRISKA, S. PINTER and L. ILENCIK 1972 Development and Spatial Structure of Proton Flares near the Limb and Coronal Phenomena. V. Emissions and Effects of the Proton Flare and Active Processes from November 2nd, 1969. Bull. Astron. Inst. Czechosl., 23, No. 2.

TRISKA, P., F. JIRICEK and J. LASTOVICKA 1972 Report on Ionospheric and Whistler Activity at the Panská Ves and Průhonice Observatories on January 24, 1971, this compilation.

TRISKA, P. and J. LASTOVICKA 1971 Ionospheric Disturbance during the Night of March 8-9, 1970, Upper Atmosphere Geophysics Report UAG-12, Part II, 211-212.

1971 Solar-Geophysical Data, 327 Part I, U.S. Department of Commerce, (Boulder, Colorado, U.S.A. 80302).

# Solar Particle Events in the Ionosphere during the Period of September 1 - 8, 1971

by

P. Velinov and G. Nestorov
Geophysical Institute
Bulgarian Academy of Sciences
Sofia, Bulgaria

## Introduction

The ground-level cosmic ray increase on September 1, 1971 is recorded only by the stations situated in higher latitudes, thereby distinct from the event on January 24, 1971. For instance in Europe on 1 September the event was observed at Kiel, Germany (geomagnetic threshold of rigidity $R_c \simeq 1.9$ BV), at Dourbes, Belgium with $R_c \simeq 3.2$ BV, etc. However, this event was not observed by the Pic-du-Midi ($R_c \simeq 5.6$ BV) neutron monitor.

Thus in our region of observation where $R_c \simeq 5$ BV, ionospheric effects caused directly by relativistic solar cosmic rays on September 1 are absent. However, in this case as well as during the event on January 24, a number of secondary ionospheric effects were observed of the soft as well as of the high energy solar particle fluxes throughout the high atmosphere during the period following September 1. These anomalies are ordinarily connected with geomagnetic field disturbances.

## Effects in the Low and Middle Ionosphere during the Period August 28 - September 8

Two days before the event on September 1 there was a strong geomagnetic storm with evident after-effects during the period of investigation September 1 - 8. Thus, it is only proper to begin the study of the case a few days earlier. In order to follow up more clearly the effects in the different ionospheric regions, Figure 1 represents a diagram of the absorption time - variations of the radio waves of different frequency ranges during the period August 28 - September 8. All measurements are performed at the Ionospheric Observatory, Sofia (N42.6, E 23.4) in typical middle latitudes.

In order to assess more objectively the absorption course in the given period it is necessary that we give the equivalent frequencies $f_i$ of the observed path for the A3 method. They are shown in the table below where the path length d is also given as well as the coordinates of the reflection points.

| f(kHz) | d(km) | $f_i$(kHz) | Coordinates North | Coordinates East |
|---|---|---|---|---|
| 155 | 380 | 75 | 44°13' | 24°27' |
| 164 | 1720 | 25 | 45°28' | 13°13' |
| 557 | 180 | 400 | 43°30' | 23°32' |
| 593 | 140 | 480 | 43°02' | 24°03' |

In the VLF range ($f_i$ = 25 kHz, $L_{164}$) on August 29 we observe a considerable absorption decrease which can partially be explained by the small Forbush effect in the cosmic rays on the same day. A similar decrease, but of a smaller amplitude, can be established in the $L_{155}$ curve. From the monthly median absorption values

$$L_{m,\,164} = 4 \text{ dB}; \quad L_{m,\,155} = 17 \text{ dB}$$

and the values on August 29

$$L_{164} = 2 \text{ dB} \quad ; \quad L_{155} = 15 \text{ dB}$$

We can determine the relative variation of electron production rate in the cosmic ray layer by means of the expression [Velinov, 1968 and 1971]:

$$\frac{\Delta q}{q} = \frac{\Delta L}{L}\left(2 + \frac{\Delta L}{L}\right) \qquad (1)$$

Hence the result obtained is

$$(\Delta q/q)_{164} = 125\% \text{ and } (\Delta q/q)_{155} = 25\%.$$

These values, however, cannot be explained only by cosmic ray Forbush decrease (3-hour Kp index reaches maximum 3) which can be easily established by the calculations made by Velinov [1971]. Similar estimations are given by Nestorov and Velinov [1972].

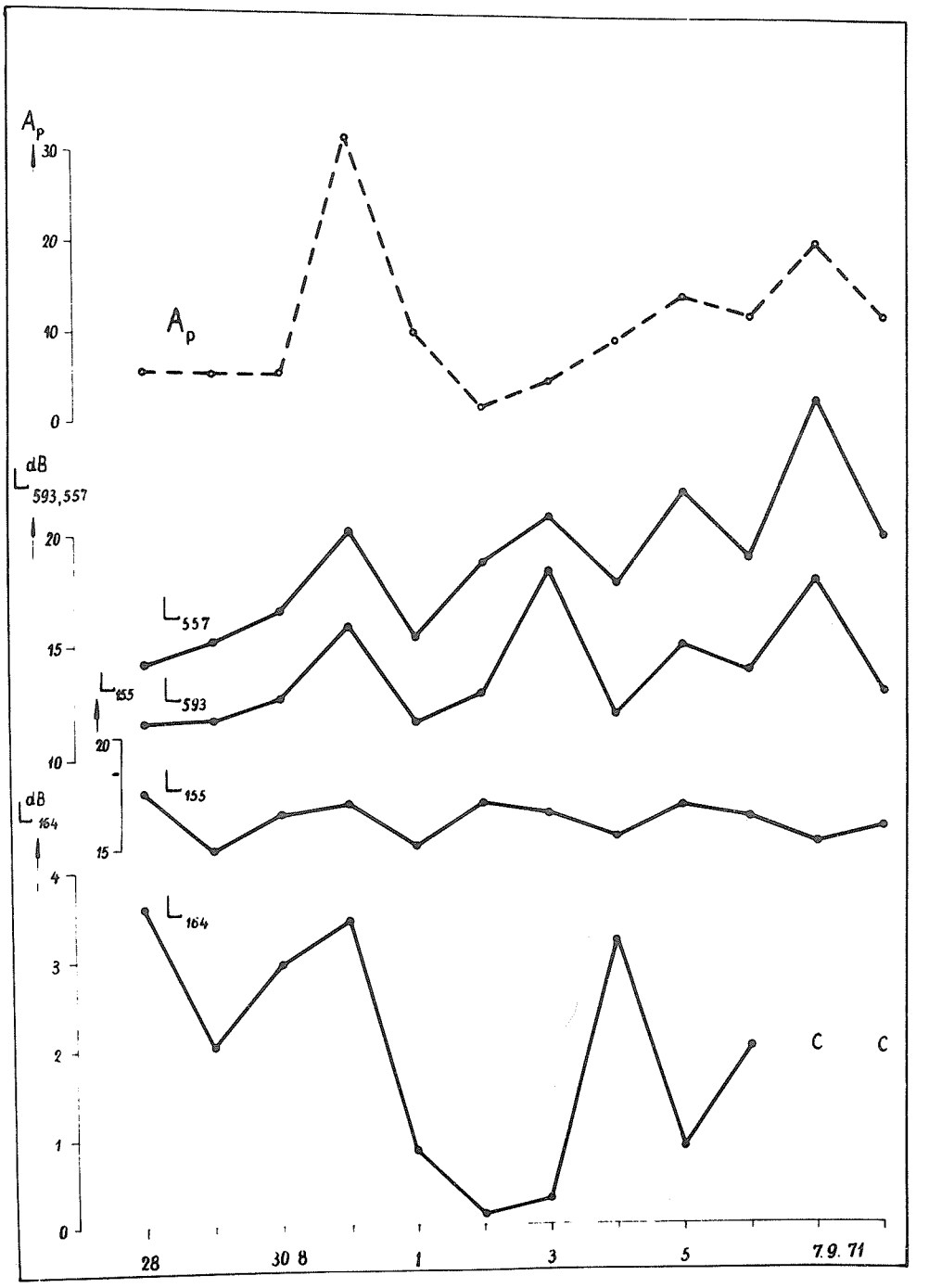


Fig. 1. Absorption in the low and middle ionosphere during the period of August 28 - September 8.

The absorption decrease effect on September 1 - 3 and 5 is much greater. The cause is as follows: since conditions of propagation for $L_{164}$ at night are determined mainly by a deviative component, i.e. according to Nestorov [1962] from the logarithmic gradient of the electron density in the reflection region, it can be expected that around and above this height there acts an excessive ionization course which increases the electron density in the night E-layer. This means that for radio waves crossing the layer the absorption will increase.

Actually from the absorption measurements $L_{557}$ and $L_{593}$ can be seen that they increase on August 31 and September 3, 5 and 7.

Similar to the January 24 - February 3 events [Nestorov and Velinov, 1972] as well as the established behavior of $L_{155}$ in other cases by Nestorov [1969], essential changes cannot be observed here. In the absorption on this path during the research period results confirm the compensation by opposite active factors in the reflection region during anomalies at the base of the thermosphere.

Thus in the studied case it is a confirmed fact that during as well as after the time of geomagnetic disturbances at the base of the thermosphere is formed increased ionization which favors VLF reflections and increases the absorption of the radio waves crossing this region.

The increased absorption $L_{557}$ and $L_{593}$ on August 31 coincides with the day of the geomagnetic storm, while the increase of L on September 3 is a well-known after-effect, taking place three days following the basic disturbance.

On September 5 and 7 there is a new increase in the geomagnetic activity accompanied by an L increase. Actually on September 7 the basic ionospheric effect is superimposed on the after-effect of September 5, thus the L value (especially $L_{557}$) greatly increases. It is to be regretted that records of $L_{164}$ are missing because of technical reasons.

The monthly median absorption value ($L_{m,\ 593}$ = 12.8 dB) as well as the current L values given in Figure 1 make it possible for us to estimate the intensity of the additional acting ionization source in the region $h_1$ to $h_2 \simeq 80$ to 120 km by means of the expression [Velinov, 1969]:

$$I = \frac{2Q(h_2 - h_1)}{E_{k,eff}} \Delta q \qquad (2)$$

where Q ≃ 30 ev is the energy required in the formation of 1 electron-ion pair, $E_{k,eff}$ is the effective energy of the particles.

For instance for the main effects on August 31 and September 5 we have

$$\Delta L_{31.8} = 3.2 \text{ dB} \quad \text{and} \quad \Delta L_{5.9} = 2.3 \text{ dB}$$

whence by means of equation (1) is obtained:

$$(\Delta q/q)_{31.8} = 0.55 \quad \text{and} \quad (\Delta q/q)_{5.9} = 0.4$$

From this at q = 0.3 $cm^{-3}sec^{-1}$ [for further details refer to Nestorov and Velinov, 1972] for the necessary flux of protons $E_{k,eff}$ = 300 kev we obtain

$$I \simeq (1 - 1.3)\times 10^2 \text{ particles } cm^{-2}sec^{-1},$$

and in the case of electron precipitation $E_{k,eff} \simeq 40$ kev from equation (2) is obtained:

$$I \simeq (0.7 - 1)\times 10^3 \text{ particles } cm^{-2}sec^{-1}$$

for the number of particles with pitch angle in the cone of losses. The total number of particles can be determined when I is divided by the factor $K \simeq 6\times 10^{-2}$ to $5\times 10^{-3}$ depending on the kind of distribution of the particles for the parameter of McIlwain L = 1.8.

## High Energy Solar Particle Effect on the Low Ionosphere

Figure 1 indicates that on September 4 there is an unusual increase of $L_{164}$ which indicates the presence of additional ionization in the low ionosphere which is absent in the night E-layer ($L_{557}$ and $L_{593}$ decrease). The calculations made by Velinov [1966, 1968 and 1970] show that for an explanation of the experimentally observed L increase it is necessary to postulate that a very small number of particles - less than 1% of the particles causing the polar cap absorption penetrate the mid-latitude ionosphere. Moreover the main problem is how a part of the PCA particles has been able to penetrate up to the middle latitudes where the geomagnetic threshold is high. Probably the weak geomagnetic disturbance on the night of September 4 - 5 with the 3-hour Kp index 3 to 4 caused an insignificant part (<1%) of PCA particles to precipitate at middle latitudes.

The detailed trend of the increased absorption $\Delta L_{164}$ on September 4 - 5 is shown in Figure 2. The base level taken here for the mean absorption includes the period September 1 - 7. In the same Figure the dashed line represents the trend of the 5 - 21 Mev energy level, showing hourly averages from the solar proton monitor ATS-1 (1966 - 110 A) [Solar-Geophysical Data, 1971]. As is well-known, the solar proton flux measured at ATS-1 is representative of the flux in interplanetary space and over the polar caps. Unfortunately, the data from ATS-1 for the energy level 21 - 70 Mev protons are incomplete. Nevertheless on Figure 2 the good correspondence between the trends of $\Delta L_{164}$ and 5 - 21 Mev protons to 2200 UT is seen. After that $\Delta L_{164}$ increases at 2300 UT, while the 5 - 21 Mev proton flux decreases. However, at the same time the number of 21 - 70 Mev energy protons increases. The Kp index also has its maximum value during the night.

It must be emphasized that the polar cap absorption begins about 1 hour after the ground-level cosmic ray increase on September 1 and effectively terminates in the morning on September 5. During this whole period however, there was no PCA influence because the geomagnetic field was comparatively quiet (Kp = 0 to 2). The geomagnetic storm (ssc) starts as late as September 4 with Kp = 3 to 4. The unsettled geomagnetic conditions that followed are believed to be the result of the passage of an interplanetary sector boundary rather than as a consequence of the behind-the-limb event on September 1. It is at this point that conditions for the middle latitude PCA event appear; it is also observed experimentally by $L_{164}$.

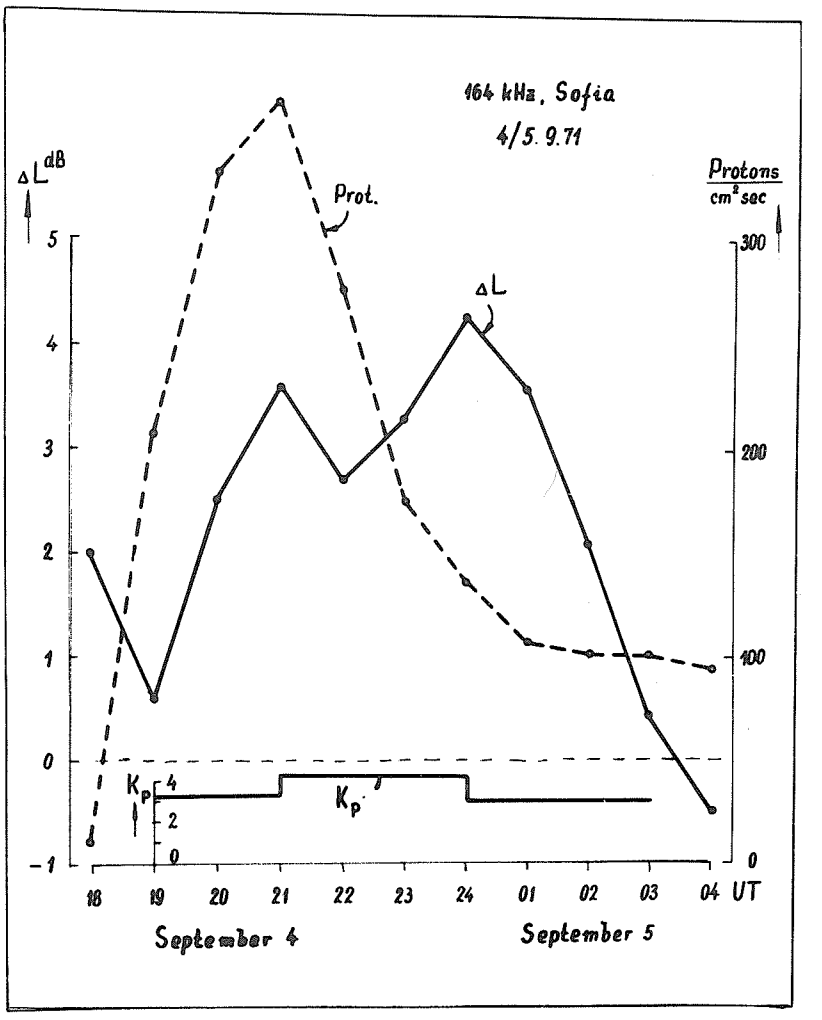


Fig. 2. The hourly trend of the additional absorption in the low ionosphere and 5 - 21 Mev protons during the night of September 4 - 5. The 3-hour Kp index is indicated also.

The behavior of the night E-layer (90 - 120 km) is of special interest. That layer is controlled by $L_{593}$ and $L_{557}$. As an illustration, in Figure 3 is shown a recording of the night of September 4 for the path 593 kHz. The monthly median absorption value is given by a dashed line. It is clear that a bay effect appeared in the absorption between 2000 and 2200 UT coinciding with the peak of 5 - 21 Mev protons. At the same time a strong polarization disturbance starts, continuing during the whole night (this conclusion is drawn from the observation of other MW paths). The bay effect is quite strong.

This shows that simultaneous with the high energy particles at the base of the thermosphere there is an influx of lower energy particles. This corresponds to our expectations because of the geomagnetic disturbance having taken place.

Effects in the High Ionosphere

Simultaneously with the current phenomena in the low and middle ionosphere were recorded disturbances in the higher level. In Figure 4 is shown the result of the ionogram interpretation obtained at the Sofia Ionospheric Station. In the upper part of the Figures is given the trend of foF2 averaged for 3-hour intervals during the period of August 28 - September 8. The averaging of foF2 for 3-hour intervals was performed in order that the trend of foF2 and of the geomagnetic index Kp((shown in the lower part of the Figures) could be compared more easily. The smooth trend of the monthly median values foF2 for August and September is shown by a dashed line. It can be easily seen that from the afternoon of August 30 to noontime on September 1 are obtained two positive and two negative anomalies of foF2 coinciding with the increased geomagnetic activity (the shaded parts of the diagram with the marks "+" and "-"). The relative amplitude of the anomalies is between 20 and 25% and can be assessed as medium magnetoionic disturbances. With the geomagnetic storm (ssc) on September 4 is connected the weak positive ionospheric disturbance during the pre-sunset period on the same day; on the contrary the ssc on September 7 evoked a negative ionospheric disturbance on the morning of September 8.

The disturbance series begins with the well-known sunset increase anomaly in the ionization of the F2-layer during the pre-sunset period on August 30. This increase of foF2 is not necessarily connected with the directly following geomagnetic storm ssc at 2303 UT. On the contrary the decrease of foF2 between the end of August 30 and the beginning of August 31 in the main phase of the storm is a regular phenomenon, connected most probably with an additional heating of the neutral gas at different heights of the F2-layer. The essential increase of foF2 during the whole day of August 31 is more interesting than the weak effect on September 4. Such positive disturbances are exceptions after a geomagnetic storm. According to a new investigation of Fatkullin [1971], such effects in the daytime ionosphere at medium latitudes during the time of geomagnetic anomalies could be even quantitatively explained by the increase of the concentration n(O) at the turbopause levels, i.e. on the basis of aeronomical processes. The anomaly series ends with a negative daytime disturbance in the F2-layer during the morning hours on September 2. In this way is established that the disturbances in the period of the geomagnetic storm and after it influence the entire ionosphere. Almost simultaneously the disturbances appear in the high and middle ionosphere. Later (by 1 - 3 days) they arise in the low ionosphere. This conclusion coincides with the previous results of Nestorov [1970].

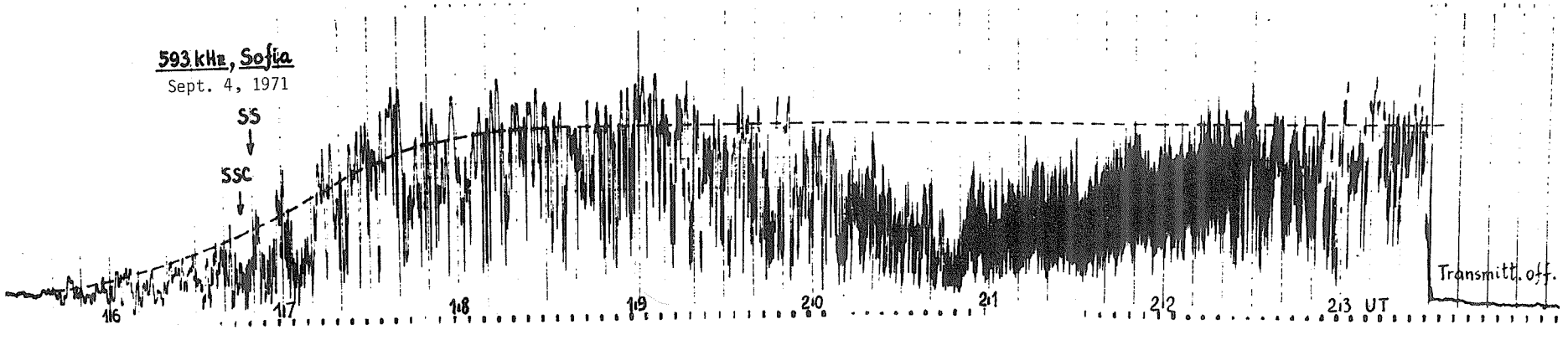


Fig. 3. Recording of the field strength of 164 kHz on September 4, 1971.

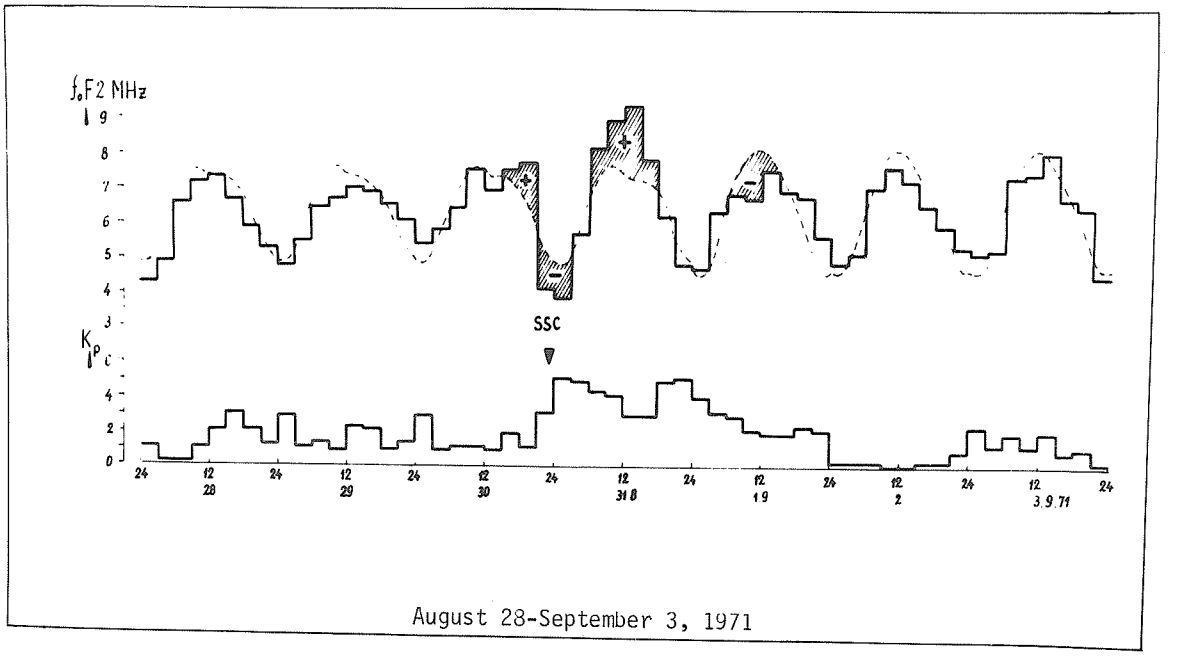


August 28-September 3, 1971

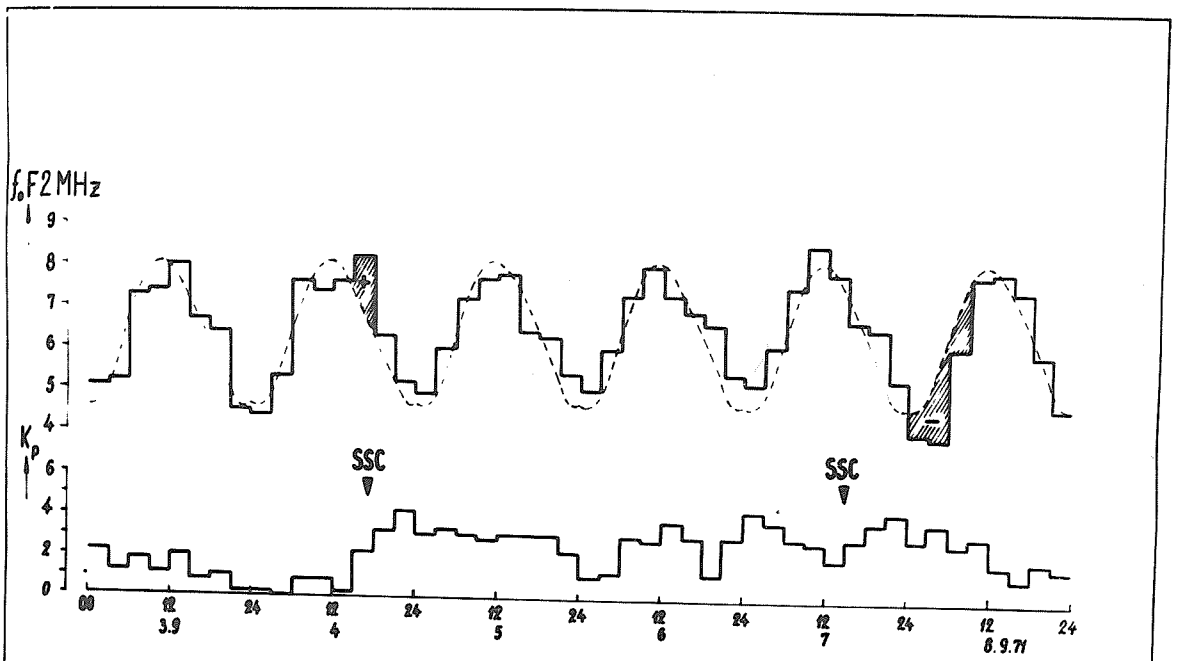


September 3-8, 1971

Fig. 4. 3-Hour values of the F2-layer critical frequency and geomagnetic Kp index during August 28 - September 8.

## REFERENCES


| | | |
|---|---|---|
| FATKULLIN, M. N. | 1971 | Some Ionospheric Indications for the Disturbances of Neutral Gas in the Turbopause during Geomagnetic Storms, Acad. Sci. USSR-- IZMIRAN, Moscow, Preprint No. 14. |
| NESTOROV, G. | 1969 | Effects in the Night Lower Ionosphere at Middle Latitudes Caused by Solar Corpuscular Fluxes, Proc. Geoph. Inst. Bulg., 14, 53. |
| NESTOROV, G. | 1970 | Development of Ionization Processes in Night Ionosphere with Geomagnetic Storms, Compt. rend. Acad. bulg. Sci., 23, 149. |
| NESTOROV, G. | 1972 | Positive Disturbances in the Night Ionosphere at Mesopause Region during Geomagnetic Anomalies, Compt. rend. Acad. bulg. Sci., 25 (in press). |
| NESTOROV, G. and P. VELINOV | 1969 | Effects in the Night Lower Ionosphere as a Result of Particle Precipitation on Middle Latitudes, Solar-Terrestrial Physics, Acad. Sci. USSR, 1, 181. |
| NESTOROV, G. and P. VELINOV | 1972 | Ionospheric Effects from Solar Particles during January 24 - February 3, 1971, this compilation p. 240. |
| VELINOV, P. | 1966 | An Expression for the Ionization in the Ionosphere, Cosmic Rays, Compt. rend. Acad. bulg. Sci., 19, 109. |
| VELINOV, P. | 1968 | On Ionization in the Ionospheric D-Region by Galactic and Solar Cosmic Rays, J. Atmos. Terr. Phys., 30, 1891. |
| VELINOV, P. | 1969 | On the Influence of Corpuscular Fluxes in the Magnetosphere on Night Ionosphere, Compt. rend. Acad. bulg. Sci., 22, 33. |
| VELINOV, P. | 1970 | Solar Cosmic Ray Ionization in the Low Ionosphere, J. Atmos. Terr. Phys., 32, 139. |
| VELINOV, P. | 1971 | On Variations of the Cosmic Ray Layer in the Lower Ionosphere, J. Atmos. Terr. Phys., 33, 429. |
| | 1971 | Solar-Geophysical Data, 327 Part I, U.S. Department of Commerce, (Boulder, Colorado, U.S.A. 80302). |

# The Effects of a Solar Proton Event and Associated Geomagnetic Disturbance on the Phase of VLF Signals Received at Leicester, UK

by

J. W. Chapman and R. E. Evans
Department of Physics
University of Leicester
Leicester, U. K.

## Introduction

This paper presents the effects of a period of enhanced solar proton flux and geomagnetic disturbance on the phase, recorded at Leicester, UK, of VLF radio signals propagated over medium and long distance paths. Details of the transmissions are given below.

| Transmitter | Frequency (kHz) | Path Length (km) |
|---|---|---|
| Trinidad | 12.0 | 7200 |
| Aldra | 10.2 | 1800 |

Aldra-Leicester is a high latitude path, the transmitter being situated in the northern auroral zone. The geomagnetic latitude ($\Phi$) is less than 40° for about half the Trinidad-Leicester path and hence charged particle effects might be expected to have the least influence on the signals for this circuit.

## The Disturbance of September 1971

All the available evidence suggests that this was a less severe disturbance than the January one (see page 237 this report). There is practically no data from ATS-1 during the first 3 days of the proton event (Figures 1d, e), but the maximum proton flux observed by the Vela satellite (3640 particles/cm$^2$ sec at 0400 UT on 2 September) was considerably less than for the earlier event (5640 particles/cm$^2$ sec at 0800 UT on 25 January). Comparison of ATS-1 measurements at the same time delay after the onset of the two events confirms that the flux is less for this event. The magnetic storm which began with a sudden commencement at 1646 UT on 4 September was only of relatively minor importance, Kp not exceeding $4^+$ at any time (Figure 1c).

Figures 1a and 1b show that the ionospheric effects are small for the 2 paths monitored (dashed lines indicate limits of undisturbed phase variation). There appears to be very little effect on the Trinidad phase immediately following the onset of the proton event, and only a small phase advance for the night-time following the onset of the storm (maximum advance $\sim 0.1\ \lambda$ on 5-6 September). Rather surprisingly the effect on the Aldra-Leicester path is even smaller, night-time phase advance at no time exceeding $\sim 0.05\ \lambda$ and there is also only a small effect on the day-time phase. A possible explanation of this is discussed below. The absence of short period irregular fluctuations at night and lack of distortion of the diurnal variation on the Aldra records is further evidence that the ionospheric disturbance was a relatively minor one.

## Discussion

Marked phase fluctuations at night were obtained on the 12.3 kHz Aldra-Leicester transmissions during the March 1970 event [Jones, 1971], and the lack of fluctuations during the September 1971 event suggests that the ionospheric disturbance at that time was not particularly severe. However, there is a small effect on the Trinidad phase, suggesting that a larger phase advance should be expected on a high latitude path. It seems possible that mode effects are involved for the Aldra-Leicester path, similar to the well-known effect on the 16 kHz Rugby-Rome transmission when phase retardation occurs as the reflecting region moves downwards during a solar flare [Burgess and Jones, 1967]. These 2 path lengths and frequencies are similar; there is a relatively small ($< \frac{1}{2}\ \lambda$) phase path change from day to night on both, and the shapes of the diurnal phase path variations are very similar. Further evidence for mode effects on the Aldra-Leicester path is provided by measurements at 13.6 kHz where there is very little change in phase path throughout the day. Calculations are being undertaken to determine which modes are important for the Aldra-Leicester circuits.

## REFERENCES

BURGESS, B. and T. B. JONES (1967) Solar Flare Effects and VLF Radio Wave Observations of the Lower Ionosphere, Radio Science, 2, 619.

JONES, T. B. (1971) VLF Radiowave Observations of Ionospheric Disturbances during the Period 4-18th March, 1970, World Data Center A, Upper Atmosphere Geophysics, Report UAG-12, 247.

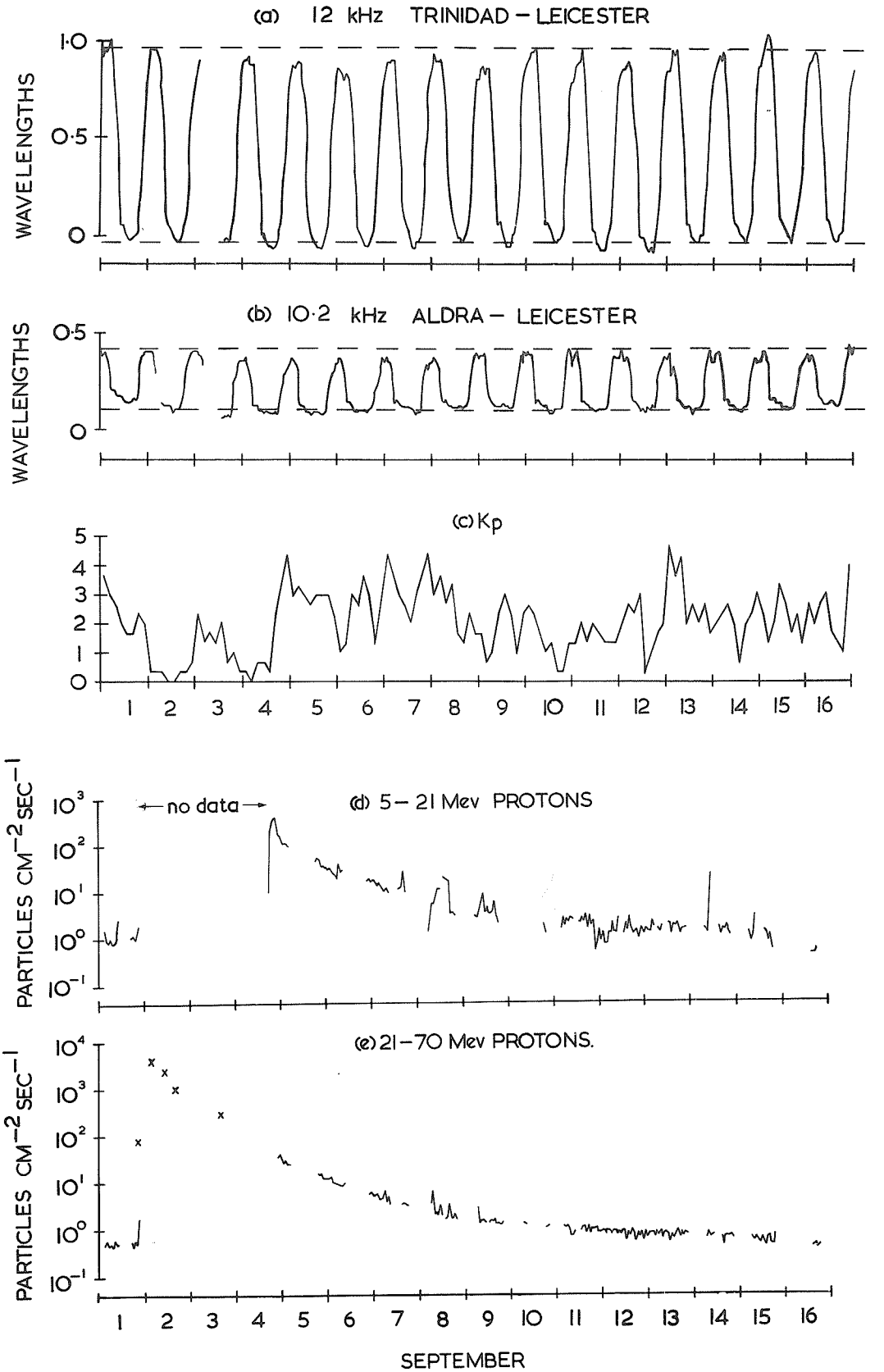


Fig. 1. DATA FOR THE SEPTEMBER 1971 EVENT. (a) and (b) VLF PHASE; (c) Kp; (d) and (e) ATS–1 SOLAR PROTON FLUX (CROSSES INDICATE VELA (>25 Mev) VALUES).

1971 Solar-Geophysical Data, 326 Part 1, October 1971, 327 Part 1, November 1971, U.S. Department of Commerce, (Boulder, Colorado, U.S.A. 80302).

7. AURORA

## The Auroral-Zone Effects of the September 1 Event over Cola Peninsula

by

B. E. Brunelli, L.S. Evlashin, S. I. Isaev, L. L. Lazutin,
G. A. Loginov, G. A. Petrova, V. K. Roldugin, N. V. Shulgina,
G. V. Starkov, G. F. Totunova, and E. V. Vasheniuk
Polar Geophysical Institute
Academy of Sciences of U.S.S.R.
Apatity, Murmansk Region, U.S.S.R.

Description of the 1-4 September 1971 event is given here using the same set of stations, observational technique and the manner of presentation as in our previous report [Brunelli et.al., 1971]. Development of the September 1971 event was similar to the January one (see p. 247 of this report) but with less intense solar proton flux and geomagnetic disturbance. Sudden commencement of the storm seen here as two moderate negative bays was delayed from the solar proton burst for 68.5 hours. The data are presented in Figures 1-4.

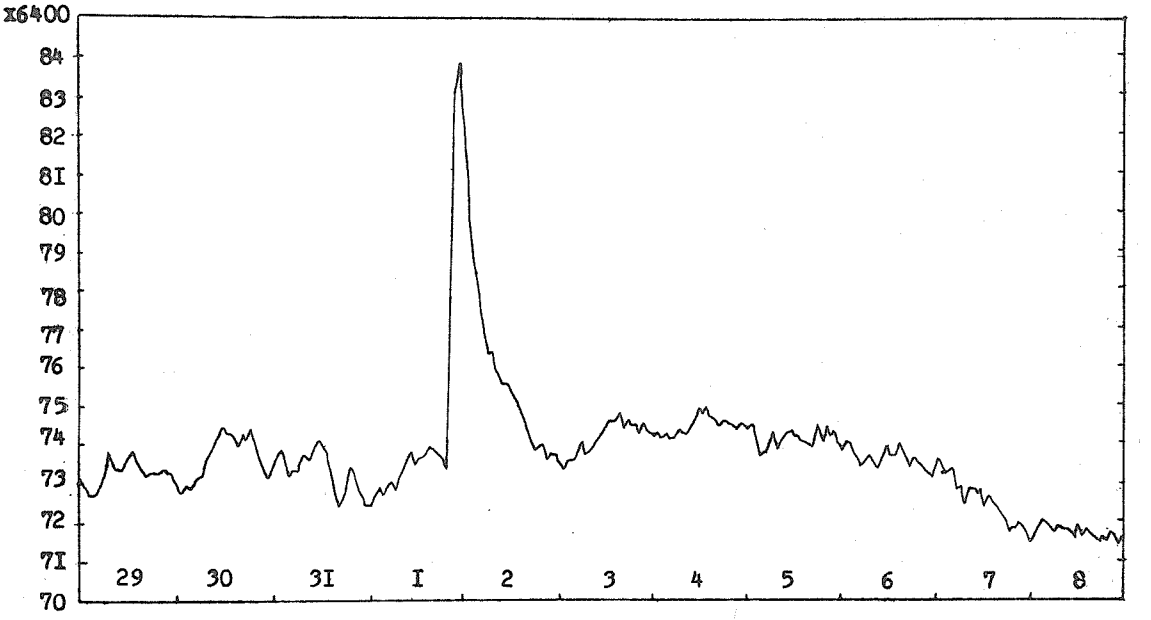


Fig. 1. Corrected hourly values of counting rate NM, Apatity, from August 29 to September 8.

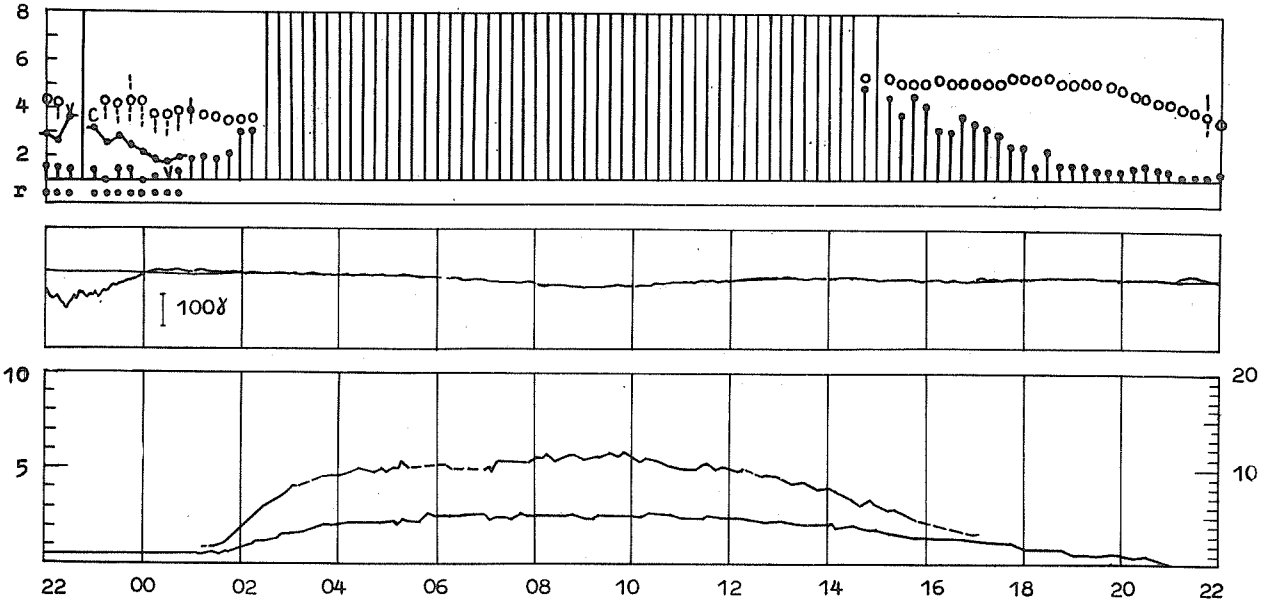


Fig. 2. Ground-based data, September 1-2: f-plot, ionosonde Murmansk; geomagnetic H-component on this day and undisturbed level; riometers 25 and 9 MHz left and right scales, respectively.

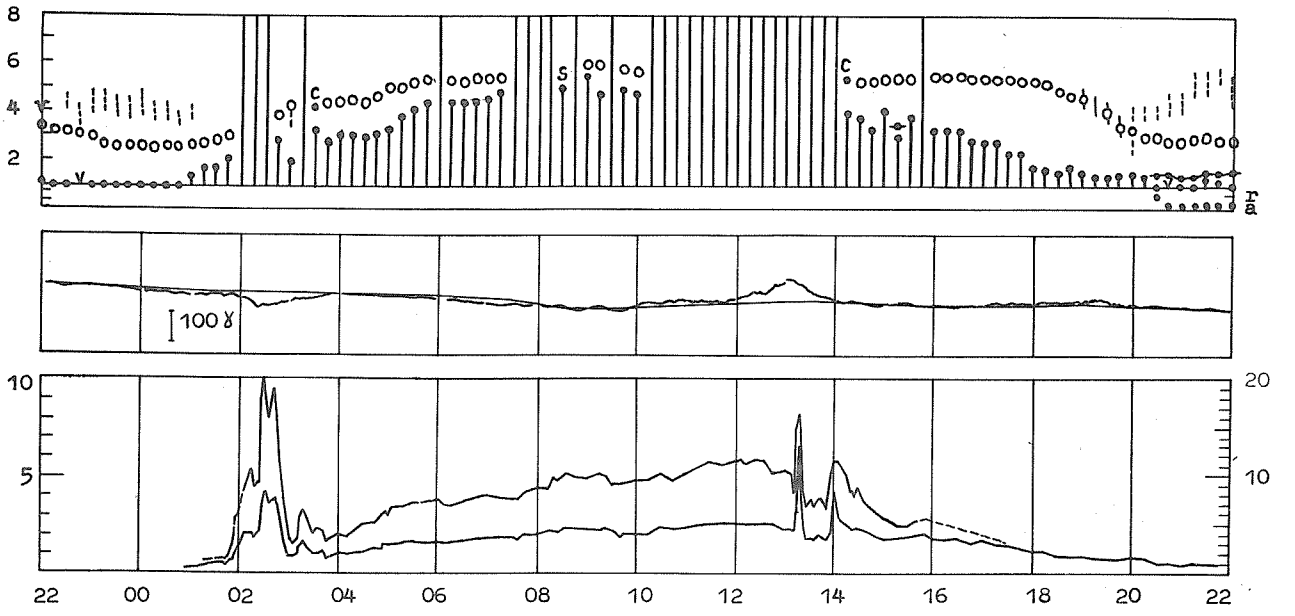


Fig. 3. The same as Figure 2, September 2-3.

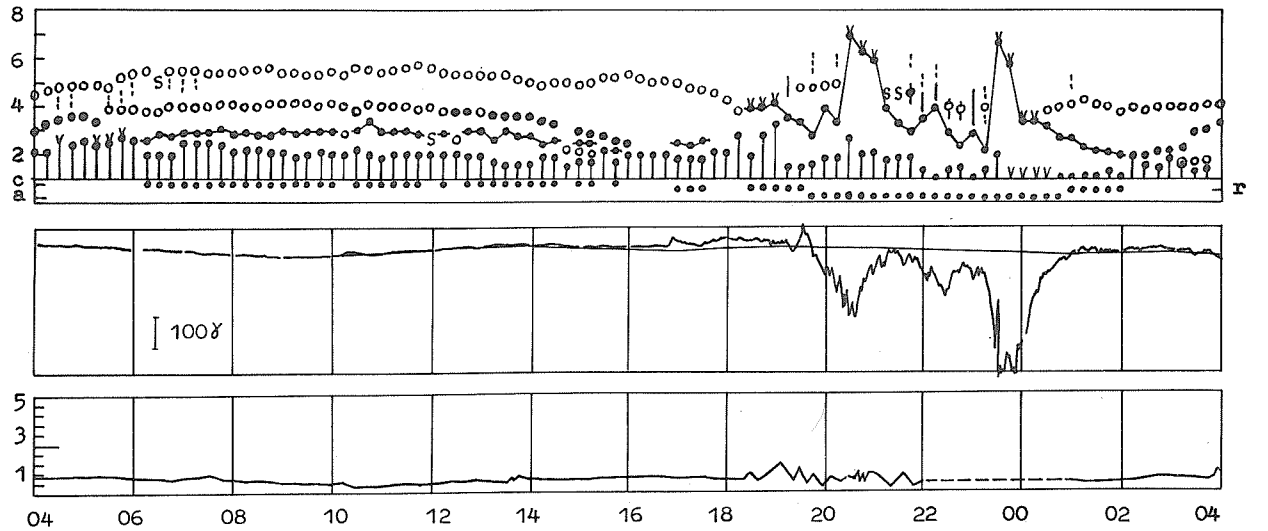


Fig. 4. The same as Figure 2, September 4-5.

Figure 1 presents Apatity neutron monitor data from August 29 to September 8, 1971. During this event the galactic cosmic ray background was fairly stable, no Forbush decrease was seen. The first 15-minute interval of enhanced counting rate at Apatity NM began at 2015 UT September 1. The geomagnetic field was quiet. In the ionosphere only a weak sporadic layer and the absorption near 0.5 dB at the frequency 25 MHz were observed. Gradual increase of cosmic noise absorption began at 0200 UT September 2, while the magnetic field remained undisturbed, Figure 2. This PCA event differs from the January one by showing a broader maximum due to the increase of the sunlit period. During the second day of event, Figure 3, September 3, the PCA value remains fairly large; in the morning hours PCA was mixed with the morning type of auroral absorption (AA), in the evening - with the second sharp increase of absorption, seen on all frequencies and accompanied by the small negative geomagnetic bay. On the third day after cosmic ray burst, Figure 4, September 4, a magnetic storm with sudden commencement at 1646 UT was registered. The main phase of the storm consisted of two negative bays accompanied by the appearance of a sporadic E-layer type "a" with large blanketing frequencies and sporadic structures in the F-region partially screened by the E-layer.

REFERENCES

BRUNELLI, B. E., L. S. EVLASHIN., S. I. ISAEV, L. L. LAZUTIN, G. A. LOGINOV, V. K. ROLDUGIN, G. V. STARKOV, N. S. SHULGINA, G. F. TOTUNOVA, and E. A. VASILKOVA 1971 Auroral-zone events of March 1970 on data of Cola Peninsula stations, World Data Center A, Upper Atmosphere Geophysics Report UAG-12, 325-336.

# K-Indices for August 23 - September 11, 1971

by

D. van Sabben
International Service of Geomagnetic Indices
Royal Netherlands Meteorological Institute
DeBilt, Netherlands

The geomagnetic K-indices from the individual observatories for August 23-September 11, 1971 are given below. Please refer to IAGA-Bulletins 12 or IAGA-Bulletin 32 for definition of the symbols.

| AUG | 23 | 24 | 25 | 26 | 27 | 28 | 29 | 30 | 31 |
|---|---|---|---|---|---|---|---|---|---|
| BT | 5554 4363 | 4434 4455 | 5434 3334 | 4444 4454 | 3322 2223 | 3223 3343 | 4343 3323 | 4333 2334 | 6664 3456 |
| CC | 6444 4253 | 3223 3444 | 3223 2534 | 4343 4354 | 3111 1232 | 2112 2533 | 3132 3423 | 4212 2344 | 5443 2556 |
| DI | 6444 4454 | 3223 4655 | 3323 3447 | 6354 6565 | 3222 2243 | 2122 3443 | 3233 4324 | 4223 3355 | 6554 3577 |
| TI | 4344 4452 | 3333 4544 | 3323 3334 | 3478 8877 | 2221 1111 | 1123 7633 | 2233 3323 | 3234 3554 | 5455 3677 |
| PB | 1023 3411 | 1000 1232 | 3555 5533 | 3223 2355 | 5457 4443 | 3256 5532 | 2243 3332 | 2356 6564 | ---- ---- |
| TR | 6323 4333 | 3212 3334 | 3212 2336 | 6233 3455 | 2111 1123 | 2000 3422 | 3011 2214 | 5011 1234 | 7533 2366 |
| GO | 3224 4322 | 2223 3432 | 2124 3443 | 3224 3433 | 2111 2323 | 2123 3532 | 2033 3323 | 3124 3333 | 4344 4555 |
| MM | 7233 4242 | 1121 3223 | 1112 2206 | 7133 3465 | 1111 1122 | 1011 3421 | 2011 2212 | 4111 1123 | 5433 2476 |
| KI | 7223 4232 | 2111 1223 | 1112 3217 | 7113 3454 | 2212 1122 | 1112 2421 | 2122 2303 | 4212 2223 | 6533 2466 |
| SO | 7223 3242 | 2112 2223 | 2112 2226 | 7122 3353 | 1000 0123 | 1001 3311 | 2011 2202 | 3011 1223 | 5433 2465 |
| WE | 3332 4122 | 2222 3133 | 2212 1323 | 2255 4432 | 2010 1112 | 0101 2421 | 1111 1112 | 2111 1213 | 3355 2333 |
| CO | 2333 5220 | 2113 3222 | 2213 3222 | 3266 5521 | 1010 0100 | 0000 2411 | 1111 1100 | 1112 0112 | 3466 1233 |
| RY | 7532 3344 | 4422 3434 | 4322 3336 | 6344 -354 | 4221 2235 | 3112 3432 | 5121 2324 | 6121 2235 | 7653 3587 |
| DO | 5333 3222 | 2333 3323 | 2323 3324 | 4233 3242 | 1122 2222 | 1023 4422 | 3122 3322 | 3122 3213 | 5543 3355 |
| YA | 5422 3132 | 3324 4324 | 3431 3424 | 4355 3454 | 3322 1123 | 3112 3533 | 3222 3234 | 4212 1245 | 5444 2465 |
| NU | 4333 3231 | 1112 2333 | 1112 2213 | 3122 2242 | 1122 0111 | 0012 3321 | 2122 2212 | 3111 1122 | 4444 3355 |
| LE | 5322 3121 | 1101 2222 | 1112 2214 | 4221 1132 | 1000 0112 | 1001 2321 | 3010 2201 | 2001 1212 | 5432 2254 |
| MG | 4342 3232 | 2222 3223 | 2222 2224 | 3245 2343 | 3331 0123 | 2222 2422 | 2122 2222 | 3322 2233 | 4343 2354 |
| LN | 4334 3231 | 1122 2233 | 2212 3324 | 3122 3243 | 1122 2222 | 1122 3422 | 2123 3312 | 3122 2223 | 4444 3355 |
| LO | 4233 3221 | 1111 2233 | 1112 3324 | 4122 3243 | 1112 1112 | 1011 3422 | 2022 3312 | 3012 2213 | 5444 3355 |
| SI | 3331 3221 | 2222 2211 | 0000 0022 | 2155 2210 | 1010 0100 | 0000 1221 | 2110 2110 | 2112 1212 | 3465 1233 |
| SV | 4323 2231 | 1111 2323 | 1212 1213 | 3122 2232 | 1100 0112 | 1001 2321 | 2121 3211 | 3011 1223 | 4334 2244 |
| RS | 4333 3221 | 2212 2233 | 2222 2313 | 3233 2242 | 1110 0112 | 1011 3322 | 2111 3322 | 3111 1223 | 5444 3355 |
| KN | 4433 2131 | 2232 1323 | 2322 2213 | 4222 2241 | 1321 1112 | 1331 2321 | 2211 2211 | 3232 1123 | 4434 2254 |
| MO | 4333 3232 | 1222 2333 | 2223 3324 | 3233 3342 | 2222 2222 | 2222 2322 | 2222 3312 | 3122 2223 | 4434 3355 |
| ES | 4222 2221 | 1111 2223 | 1212 2213 | 3111 1132 | 2010 0212 | 1002 3322 | 3111 3312 | 3011 1223 | 5433 3345 |
| ME | | | | | | | | | |
| HL | 4444 4443 | 2224 4444 | 3334 4434 | 4233 4343 | 2222 2223 | 2123 4543 | 3233 4433 | 4123 3434 | 5444 4455 |
| MN | 4343 3232 | 1132 3233 | 2123 2313 | 3132 3242 | 1112 2211 | 1121 2321 | 2122 3212 | 2122 2223 | 4433 3253 |
| WN | 5333 2221 | 2112 2223 | 2212 2323 | 3122 2242 | 2110 1122 | 1112 2322 | 3112 3312 | 3112 1223 | 5444 3355 |
| WI | 5323 2332 | 2212 2333 | 2222 2323 | 4233 2243 | 2110 0122 | 1002 2422 | 3111 3312 | 3012 1324 | 5444 4355 |
| IR | 3343 3233 | 2232 3223 | 3323 3323 | 4233 2343 | 3221 1212 | 3221 2421 | ---- ---- | 2222 1133 | ---- ---- |
| SW | 4333 3231 | 2222 2333 | 2233 2323 | 3233 2342 | 2223 1222 | 2123 2322 | 2233 3322 | 3222 2223 | 4433 3355 |
| NI | 4333 2232 | 2112 2223 | 2212 2323 | 3122 2242 | 2110 1112 | 1002 2422 | 3121 3312 | 3011 1223 | 5434 3354 |
| VL | 5222 3232 | 1212 2333 | 1112 3323 | 4133 1343 | 2111 1212 | 1022 2332 | 3132 2321 | 3012 1213 | 5433 4355 |
| BE | 4324 3232 | 2322 2233 | 2323 2323 | 3323 2242 | 2323 1122 | 2223 2422 | 3223 3312 | 3222 1223 | 4434 3354 |
| HA | 4323 2232 | 2212 2333 | 2222 3323 | 4232 1333 | 2110 0212 | 1002 2332 | 3021 3322 | 3011 1313 | 5433 4355 |
| KV | 3222 2221 | 1112 2222 | 1122 1212 | 2122 2232 | 2121 2211 | 1112 2321 | 2112 2211 | 2221 1122 | 3322 2244 |
| MA | 4333 3232 | 2222 2233 | 2222 2322 | 3222 2223 | 2222 2222 | 2223 2322 | 3222 3322 | 3112 2323 | 5333 3354 |
| DB | 4223 2231 | 2211 2223 | 2212 2313 | 3232 2232 | 2111 1112 | 1002 2322 | 3111 3312 | 3012 1213 | 5333 3255 |
| PR | 4333 2231 | 2211 2233 | 2222 3323 | 3132 2232 | 2211 1112 | 1112 2332 | 2122 3312 | 3112 1223 | 4334 3355 |
| LV | 4333 3121 | 1111 2123 | 2323 2212 | 3233 2332 | 1213 2222 | 1223 4322 | 1223 2211 | 2122 1223 | 4433 3354 |
| KD | 2222 2212 | 1110 2100 | 0112 1222 | 3022 1222 | 1001 1012 | 1011 2112 | 1112 2210 | 3112 2223 | 3233 2243 |
| VI | 3332 3212 | 2232 3223 | 2212 2223 | 3245 2211 | 1010 1101 | 0011 2322 | 2122 3211 | 3121 0213 | 5455 2333 |
| NE | 4331 2212 | 2232 1223 | 2212 1323 | 3244 2122 | 1010 1102 | 1011 2322 | 2121 3211 | 3121 0214 | 4454 1234 |
| FU | 4323 2221 | 2112 2223 | 2212 2213 | 3122 2131 | 2110 0112 | 1001 1321 | 2111 2211 | 3112 1113 | 4333 2244 |
| CF | 4322 2231 | 1211 2223 | 2212 2223 | 3222 2333 | 2100 2222 | 1001 2322 | 3111 2212 | 3011 1213 | 5433 3254 |
| HB | 4333 3221 | 1212 2233 | 2222 2213 | 3243 3343 | 2212 1212 | 1123 2422 | 2222 3211 | 3112 0223 | 5444 3355 |
| UB | 4443 3232 | 2332 3233 | 3322 3323 | 5333 2343 | 3323 0222 | 3223 3432 | 3332 3322 | 4323 2233 | 5444 3354 |
| JO | 4222 2222 | 2222 1223 | 2312 1323 | 4132 2121 | 2011 1112 | 1012 1221 | 3121 2222 | 3222 1213 | 4433 2244 |

| | | | | | | | | | | | | | | | | | | | | |
|---|---|---|---|---|---|---|---|---|---|---|---|---|---|---|---|---|---|---|---|---|
| SA | 4432 | 3333 | 3231 | 2325 | 4342 | 2322 | 2243 | 2332 | 3321 | 0224 | 3231 | 2434 | 3322 | 1234 | 4332 | 1224 | 5333 | 3235 |
| TY | 4333 | 4232 | 2112 | 3233 | 2212 | 3323 | 3233 | 3343 | 2112 | 2222 | 2112 | 3422 | 3212 | 3322 | 3023 | 2224 | 5534 | 3355 |
| OD | 4333 | 3222 | 1122 | 2223 | 2222 | 2223 | 3222 | 2232 | 1121 | 1112 | 2023 | 3422 | 2223 | 3322 | 3133 | 1224 | 4334 | 3254 |
| KK | 4333 | 3232 | 3333 | 2323 | 3333 | 3313 | 4333 | 3342 | 2343 | 2221 | 3342 | 3322 | 2233 | 2222 | 3432 | 1133 | 4334 | 3344 |
| OT | 4221 | 2222 | 3221 | 2133 | 2312 | 1224 | 4244 | 1022 | 2010 | 1111 | 1000 | 1321 | 2111 | 2211 | 3101 | 1113 | 4543 | 2245 |
| SU | 4343 | 3121 | 1111 | 2223 | 2222 | 2311 | 3043 | 1331 | 1122 | 1212 | 1213 | 2422 | 1132 | 3221 | 3122 | 1223 | 4234 | 3354 |
| GC | | | | | | | | | | | | | | | | | | |
| MT | 3332 | 3222 | 2221 | 2123 | 2222 | 2222 | 2233 | 2121 | 1110 | 0111 | 1122 | 2422 | 2222 | 2212 | 2221 | 1223 | 3343 | 2333 |
| VK | 3443 | 3223 | 3333 | 3233 | 3432 | 3223 | 3333 | 2332 | 3222 | 1112 | 4222 | 3423 | 3322 | 3223 | 3332 | 1224 | 5344 | 3343 |
| AT | 4433 | 3232 | 2233 | 2334 | 3223 | 3323 | 4233 | 2343 | 1243 | 2212 | 2232 | 3311 | 3332 | 3222 | 3332 | 2134 | 43-- | 3444 |
| LG | 5322 | 2221 | 2201 | 2233 | 2202 | 1223 | 3122 | 2232 | 2100 | 0113 | 2111 | 2322 | 3112 | 2312 | 4111 | 1214 | 5333 | 2266 |
| AQ | 4312 | 2132 | 2101 | 2223 | 1101 | 2223 | 3021 | 1132 | 1000 | 0112 | 2001 | 1322 | 2011 | 2212 | 3011 | 0213 | 4333 | 2155 |
| TF | 4444 | 4232 | 2343 | 2233 | 2443 | 3323 | 2434 | 3342 | 2443 | 3222 | 2444 | 4322 | 2434 | 2222 | 2333 | 3223 | 4444 | 3354 |
| TK | 3434 | 4322 | 2331 | 2224 | 1332 | 2214 | 3233 | 3342 | 2122 | 2222 | 2332 | 3312 | 3232 | 2223 | 3121 | 1124 | 4334 | 3354 |
| IK | 4323 | 2221 | 1111 | 1323 | 2112 | 2223 | 3122 | 1231 | 1110 | 0112 | 2112 | 2422 | 2112 | 3212 | 3111 | 1224 | 4433 | 3255 |
| CI | 4322 | 2121 | 2111 | 2233 | 1112 | 1323 | 3022 | 2132 | 1000 | 0101 | 2001 | 2422 | 2111 | 2211 | 3011 | 1213 | 4333 | 3244 |
| TL | 4222 | 1121 | 1211 | 2223 | 2111 | 2212 | 3122 | 1221 | 1110 | 0112 | 1111 | 2221 | 2111 | 1111 | 3011 | 1113 | 4333 | 2155 |
| FR | 4332 | 2122 | 3221 | 2233 | 2312 | 2223 | 4233 | 1121 | 2000 | 0102 | 2110 | 2221 | 2121 | 2111 | 3110 | 0113 | 5433 | 2244 |
| PE | 4342 | 2121 | 1111 | 2233 | 1101 | 1221 | 3011 | 1132 | 1110 | 0112 | 1111 | 1311 | 1111 | 2111 | 3111 | 1113 | 4333 | 2254 |
| AK | 3322 | 3332 | 2331 | 1112 | 1112 | 2111 | 3244 | 5433 | ---- | ---- | ---- | ---- | ---- | ---- | ---- | ---- | ---- | ---- |
| SM | 4333 | 2322 | 2332 | 2322 | 2323 | 2323 | 4232 | 2343 | 2222 | 2322 | 2222 | 3332 | 3234 | 4332 | 2232 | 3322 | 4323 | 2454 |
| AE | 4343 | 3231 | 2133 | 3333 | 2234 | 3323 | 3143 | 1231 | 2032 | 2103 | 2132 | 4412 | 2133 | 2212 | 3132 | 2213 | 4344 | 3455 |
| SF | 4433 | 3232 | 3211 | 3334 | 2123 | 3313 | 3233 | 2131 | 2200 | 1213 | 2122 | 3422 | 3213 | 3312 | 4213 | 1324 | 5544 | 4466 |
| KA | 3432 | 3222 | 1212 | 2123 | 1212 | 2212 | 2133 | 1131 | 1110 | 0111 | 1121 | 2421 | 2221 | 2211 | 1222 | 1213 | 4343 | 2333 |
| KS | 5442 | 1232 | 2122 | 2234 | 2211 | 1322 | 3122 | 2132 | 1110 | 0112 | 2112 | 2432 | 3232 | 3322 | 4132 | 2325 | 4334 | 3362 |
| AV | 4322 | 2221 | 1211 | 1133 | 1222 | 1313 | 3131 | 1131 | 2110 | 0111 | 1111 | 4311 | 2112 | 2212 | 3111 | 1213 | 3333 | 2244 |
| DS | 4432 | 3122 | 2321 | 3233 | 3322 | 3323 | 4243 | 2231 | 2110 | 1112 | 2121 | 2322 | 3231 | 2221 | 3222 | 2224 | 5544 | 3244 |
| TU | 4432 | 1212 | 1221 | 2223 | 2211 | 3313 | 4233 | 2121 | 2010 | 1101 | 2011 | 2322 | 2221 | 2211 | 3121 | 1214 | 5444 | 3243 |
| KY | 3432 | 3222 | 1212 | 2133 | 1211 | 1212 | 2133 | 1131 | 0100 | 0111 | 1121 | 3421 | 1221 | 2211 | 1122 | 1213 | 4334 | 3332 |
| QU | 3443 | 3231 | 1322 | 2123 | 1222 | 2223 | 2421 | 1341 | 1343 | 1113 | 2331 | 3322 | 3322 | 3222 | 2231 | 1222 | 4443 | 3353 |
| ML | 5543 | 4232 | 2332 | 3224 | 2322 | 2322 | 3342 | 2332 | 1232 | 2123 | 2333 | 3323 | 2332 | 3222 | 3344 | 3234 | 4444 | 4455 |
| SZ | 4333 | 3222 | 2111 | 3333 | 2112 | 3313 | 2132 | 1131 | 2110 | 2112 | 2011 | 3422 | 2112 | 2211 | 3112 | 3213 | 3333 | 3255 |
| LP | 454- | ---- | 3422 | 2223 | 3432 | 2123 | 3333 | 2332 | 1111 | 1001 | 3222 | 3422 | 3322 | 3222 | 2322 | 2223 | 5344 | 3344 |
| TA | 4332 | 2131 | 2111 | 2133 | 1111 | 1223 | 2222 | 1132 | 2110 | 1113 | 2111 | 2312 | ---2 | 2222 | 3122 | 1124 | 4334 | 3254 |
| HO | 2322 | 1111 | 1010 | 1123 | 1111 | 1111 | 1033 | 1000 | 0000 | 0000 | 2001 | 1211 | 1111 | 2111 | 1010 | 0113 | 4343 | 2132 |
| TE | 5432 | 2322 | 2222 | 2333 | 3222 | 3324 | 4233 | 3332 | 2111 | 2322 | 2221 | 2332 | 3231 | 2213 | 3222 | 3224 | 5443 | 3243 |
| AL | 3432 | 3231 | 1222 | 2223 | 2212 | 2223 | 2333 | 2341 | 1211 | 1122 | 2111 | 3322 | 2222 | 2223 | 3221 | 2223 | 5333 | 3453 |
| SJ | 4332 | 1111 | 2210 | 1222 | 1201 | 2204 | 4122 | 1222 | 2000 | 0100 | 2011 | 2221 | 2121 | 2212 | 2111 | 0223 | 5433 | 2153 |
| MB | 3322 | 2221 | 2101 | 2223 | 1111 | 1213 | 2021 | 1022 | 2010 | 0011 | 2011 | 2321 | 2111 | 2212 | 3121 | 1113 | 4333 | 3244 |
| MU | 4542 | 4223 | 3332 | 2233 | 4423 | 2222 | 4344 | 2342 | 3222 | 2223 | 4422 | 3323 | 3322 | 3222 | 3332 | 2314 | 5444 | 3343 |
| GU | 3432 | 3221 | 3312 | 2123 | 3211 | 1112 | 3133 | 1221 | 2110 | 1101 | 2111 | 3322 | 2231 | 2211 | 1212 | 1214 | 5333 | 2223 |
| BA | 4332 | 3232 | 2222 | 2223 | 2122 | 2322 | 2232 | 2232 | 2121 | 2113 | 2221 | 2322 | 3222 | 3222 | 3122 | 1323 | 4234 | 3254 |
| MC | 4333 | 2221 | 2101 | 0223 | 1003 | 2313 | 2022 | 2221 | 1000 | 0002 | 2012 | 3422 | 3222 | 2323 | 3021 | 0223 | 4234 | 3254 |
| TG | 5552 | 3222 | 4333 | 2123 | 4333 | 2221 | 4354 | 2353 | 4441 | 1103 | 5341 | 3333 | 4351 | 2212 | 4342 | 0324 | 4444 | 3243 |
| LU | | | | | | | | | | | | | | | | | | |
| PM | 3432 | 3122 | 2122 | 2123 | 1111 | 1222 | 2133 | 2222 | 2210 | 1110 | 1101 | 2311 | 2221 | 2211 | 2221 | 1213 | 3233 | 2233 |
| HU | 3322 | 4331 | 1221 | 3333 | 2211 | 4433 | 3122 | 2221 | 1011 | 2221 | 1021 | 2432 | 1111 | 3422 | 1111 | 3323 | 5533 | 4443 |
| PP | 3322 | 0101 | 1010 | 01-2 | 1001 | 0002 | 2131 | 1000 | ---- | ---- | 0000 | 1221 | 0011 | 1000 | 1000 | 0002 | 5242 | 1032 |
| TN | 3231 | 3120 | 0111 | 2122 | 2113 | 2211 | 2022 | 2121 | 1021 | 2012 | 1122 | 2311 | 2021 | 1111 | --22 | 1222 | 3123 | 2342 |
| PI | 4432 | 2222 | 3321 | 2323 | 3311 | 2314 | 4233 | 2243 | 2210 | 1112 | 2212 | 3322 | 3222 | 2323 | 3211 | 2223 | 5543 | 3354 |
| GN | 4321 | 2221 | 2122 | 2234 | 2111 | 1313 | 1133 | 3241 | 1110 | 0111 | 1011 | 1411 | 1121 | 2211 | 3111 | 1223 | 4343 | 2363 |
| HR | 4332 | 2121 | 3111 | 1223 | 1111 | 1112 | 3121 | 2031 | 1010 | 0002 | 1011 | 2311 | 2111 | 2101 | 3022 | 0113 | 4334 | 2354 |
| AC | ---- | ---- | ---- | ---- | ---- | ---- | ---- | --33 | 2100 | 1201 | 1111 | 2422 | 2211 | 2312 | 2111 | 1--- | ---- | ---- |
| TO | 3322 | 3121 | 1223 | 3123 | 1212 | 2212 | 2044 | 2130 | 0110 | 0000 | 1000 | 1410 | 1111 | 2200 | 2111 | 1112 | 3343 | 2344 |
| AM | 3333 | 2110 | 2121 | 2112 | 2102 | 1101 | 1144 | 2220 | 0100 | 0000 | 1010 | 2311 | 1111 | 2100 | 2110 | 1102 | 3444 | 1333 |
| TW | 4332 | 1222 | 2221 | 1222 | 2210 | 2224 | 4123 | 2232 | 2000 | 0121 | 1122 | 2421 | 2212 | 2222 | 2111 | 1223 | 5432 | 3343 |
| MI | 2333 | 4120 | 1114 | 4112 | 1112 | 2--- | 2266 | 5533 | 1110 | 0001 | 0000 | 2501 | 1111 | 0001 | 1111 | 1102 | 3355 | 1333 |
| MY | 4554 | 2243 | 4433 | 2233 | 3443 | 2234 | 3442 | 2243 | 3331 | 1133 | 3332 | 1332 | 3342 | 3223 | 4443 | 2334 | 5565 | 3676 |
| MW | 7433 | 3244 | 3322 | 2255 | 4332 | 2336 | 5453 | 3364 | 3221 | 1124 | 2211 | 2332 | 3222 | 2225 | 5222 | 2245 | 7563 | 2377 |
| NL | 6332 | 2122 | 3211 | 1124 | 2212 | 1115 | 5332 | 2132 | 3101 | 0102 | 1001 | 1211 | 4111 | 1113 | 5222 | 1112 | 7742 | 2265 |
| SB | 4232 | 3222 | 2221 | 2223 | 3212 | 2232 | 3233 | 2233 | 0011 | 1111 | 1011 | 1312 | 2111 | 1102 | 3111 | 2223 | 4432 | 2344 |
| VO | 3323 | 3122 | 2222 | 2222 | 3222 | 2222 | 3232 | 2233 | 1221 | 1112 | 2111 | 1322 | 2222 | 2112 | 3222 | 1213 | 3433 | 2245 |

TABLE 1 THREE-HOUR-RANGE INDICES, K S E P T E M B E R 1971

| SEP | 1 | 2 | 3 | 4 | 5 | 6 | 7 | 8 | 9 | 10 | 11 |
|---|---|---|---|---|---|---|---|---|---|---|---|
| BT | 5543 3554 | 3322 1223 | 4444 5253 | 3323 2445 | 4544 4543 | 3344 5545 | 4553 4645 | 5445 3433 | 3433 4633 | 3433 3332 | 3344 4332 |
| CC | 5323 3435 | 2111 1223 | 2233 5142 | 1112 2444 | 4334 6645 | 3335 5524 | 5343 5546 | 6334 5534 | 3333 4633 | 3233 3432 | 2133 4323 |
| DI | 6333 3556 | 3222 1223 | 3234 5252 | 2222 2466 | 5435 6676 | 3235 5545 | 7344 6666 | 6444 3565 | 3223 4734 | 3223 3333 | 2233 4444 |
| TI | 3444 3444 | 1111 1212 | 2235 4232 | 2222 2565 | 3436 7665 | 3345 5554 | 4454 7674 | 3353 2222 | 3444 5734 | 3334 4422 | 2334 4433 |
| PB | | | | | | | | | | | |
| TR | 7533 2366 | 5321 0102 | 3212 3122 | 0001 1356 | 5422 5465 | 2023 5325 | 5322 4466 | 5423 3213 | 3112 3434 | 4211 1114 | 2101 2333 |
| GO | 3234 3344 | 1121 2322 | 3234 4222 | 1122 1433 | 3234 5433 | 2134 5533 | 4334 4433 | 3223 4322 | 2223 4433 | 3233 3211 | 1233 4332 |
| MM | 5222 1243 | 1011 0001 | 2212 3121 | 0111 1255 | 5233 5554 | 1123 5415 | 6232 4566 | 6223 2142 | 1013 3314 | 3111 1011 | 1011 3222 |
| KI | 6222 2243 | 2111 1002 | 3222 3111 | 0011 1257 | 6322 5555 | 1122 5426 | 6222 4566 | 5323 3232 | 2002 3334 | 4121 2102 | 1012 3222 |
| SO | 5211 2243 | 1000 0001 | 2211 3121 | 0001 0256 | 5222 5554 | 1012 4325 | 6222 3565 | 5323 2232 | 1112 3323 | 3111 1112 | 1101 3322 |
| WE | 3332 3112 | 0000 0111 | 1123 4112 | 0110 0233 | 2346 6632 | 1134 6523 | 3243 5643 | 3335 3321 | 1112 2421 | 1133 2101 | 1223 3222 |
| CO | 3333 3112 | 1000 0000 | 1134 4000 | 0000 0122 | 2346 6622 | 1145 5512 | 3345 5623 | 2345 3211 | 2112 3311 | 1134 3000 | 1225 4210 |
| RY | 6532 3345 | 2121 1112 | 5432 2232 | 2121 2357 | 6553 4453 | 3132 4436 | 6533 4566 | 5533 2334 | 4222 3326 | 5422 2213 | 3222 2333 |
| DO | 3333 3333 | 1222 2112 | 2332 2121 | 1122 2345 | 3322 3343 | 1132 4313 | 5333 3345 | 3223 3232 | 2123 4313 | 3221 2112 | 1222 3322 |
| YA | 5444 4243 | 1322 0112 | 3322 3133 | 2312 1356 | 3435 6544 | 3334 5435 | 4555 5655 | 4536 4333 | 3222 4424 | 3344 4213 | 2234 4242 |
| NU | 3222 2223 | 1011 0001 | 2101 2020 | 0112 1224 | 2223 3342 | 1032 4313 | 4322 2344 | 3212 2132 | 1012 3412 | 3221 1102 | 1111 1222 |
| LE | 4321 2222 | 1000 0001 | 2210 1110 | 0000 0235 | 4321 2333 | 0021 3213 | 4211 2344 | 3212 1132 | 1001 3212 | 3100 1002 | 1100 1111 |
| MG | 4343 3233 | 3221 1123 | 2323 3123 | 3321 1335 | 4434 4344 | 4334 3334 | 4344 3444 | 3426 3323 | 3333 3434 | 3333 2213 | 2223 3232 |
| LN | 4233 2223 | 1112 2112 | 2123 2121 | 0122 2334 | 2323 3352 | 1133 3323 | 4333 3354 | 3324 2233 | 1123 4413 | 3222 2112 | 1213 2333 |
| LO | 3222 2333 | 0000 1101 | 2122 2110 | 0112 2224 | 3322 3343 | 1133 3313 | 5332 2344 | 3223 2232 | 1113 3313 | 3212 1112 | 2212 3333 |
| SI | 2331 1012 | 0000 0000 | 1122 2000 | 1000 0233 | 2335 4421 | 1133 3222 | 2344 3423 | 2444 1211 | 1112 2211 | 1232 2000 | 1114 3210 |
| SV | 3221 2232 | 0000 0001 | 1022 2010 | 0000 0234 | 3323 4432 | 1123 3323 | 3232 3333 | 2223 2232 | 1012 3412 | 2111 1101 | 0011 2222 |
| RS | 3222 2232 | 0000 0101 | 2112 2111 | 0011 0324 | 3333 3343 | 1133 3423 | 4322 2345 | 3222 2232 | 1112 3323 | 3212 2112 | 2221 2333 |
| KN | 4322 2232 | 1232 1111 | 1234 2121 | 0233 2235 | 2434 3341 | 1223 3322 | 3332 2343 | 1324 1231 | 1232 3412 | 3222 1101 | 1122 2322 |
| MO | 4233 2233 | 2221 2112 | 2222 2121 | 1222 2334 | 2333 3342 | 1233 3423 | 4332 2344 | 3333 2232 | 2123 3423 | 3223 2112 | 1222 3333 |
| ES | 3222 2232 | 1000 0101 | 2111 2111 | 0001 1334 | 3222 3333 | 0121 4323 | 4322 2344 | 3323 2132 | 2112 3212 | 3211 2112 | 2211 2232 |
| ME | 3343 2222 | 1111 1212 | 2132 3221 | 1011 1224 | 3456 3322 | 2245 4323 | 4365 3333 | 3566 2221 | 2112 2222 | 2342 2211 | 1125 2212 |
| HL | 4334 3343 | 2222 2222 | 3232 3232 | 0132 2444 | 4333 4443 | 2343 4423 | 4343 2444 | 3334 3342 | 2224 4423 | 4333 3323 | 2323 3332 |
| MN | 3223 3232 | 1023 2202 | 2133 3211 | 1033 3323 | 2323 3342 | 1133 3323 | 5332 3344 | 3223 2232 | 1113 3412 | 3223 2112 | 2221 3332 |
| WN | 4222 2333 | 1111 0111 | 2121 2111 | 1111 1334 | 3322 3342 | 1122 3313 | 5323 2345 | 3322 2132 | 2113 3313 | 3211 2112 | 1212 2222 |
| WI | 4232 2342 | 0000 0112 | 2111 2121 | 0011 1335 | 4332 3343 | 1133 4423 | 5332 3345 | 3323 2232 | 2013 4313 | 3211 2113 | 1212 2232 |
| IR | ---- ---- | 2232 1112 | 3342 2122 | 2222 1344 | 3334 5443 | 3343 4323 | 3344 4443 | 3334 3322 | 2323 3422 | 3223 3322 | 3223 3232 |
| SW | 3233 3233 | 1122 2112 | 2222 2221 | 1123 2334 | 3233 2342 | 1132 3323 | 4333 2344 | 3333 2232 | 1123 3323 | 3222 2222 | 1232 2232 |
| NI | 4222 2233 | 1010 0112 | 2111 2121 | 0011 1334 | 3233 3343 | 1132 3323 | 4322 2345 | 3323 2132 | 1113 3313 | 3111 2112 | 1212 2222 |
| VL | 4222 2232 | 1011 1101 | 2112 2111 | 1012 2234 | 3223 3343 | 1123 3313 | 4332 2345 | 3322 1131 | 1112 3223 | 3223 1112 | 1213 2222 |
| BE | 3323 1333 | 1222 1212 | 2222 2221 | 0123 2334 | 3333 3342 | 1232 3323 | 4323 3344 | 3323 2232 | 2224 3423 | 3222 2112 | 2222 2233 |
| HA | 4322 3232 | 0000 0101 | 2111 2111 | 0002 0334 | 3232 2343 | 0122 3413 | 4322 2345 | 3322 2132 | 2013 3223 | 3211 2002 | 2212 2222 |
| KV | 3222 2122 | 1112 1211 | 2123 2110 | 0122 2223 | 2223 3332 | 2122 3322 | 3222 2233 | 2222 1222 | 2222 2312 | 2212 1101 | 1222 2222 |
| MA | 4322 2232 | 1000 0011 | 2222 2121 | 0000 0334 | 2223 3342 | 2222 3423 | 4332 2335 | 3333 2232 | 2103 3322 | 3221 2112 | 2222 2222 |
| DB | 4332 2232 | 0000 0101 | 2121 2111 | 0011 1334 | 3233 3343 | 1123 3413 | 4332 2345 | 3333 2231 | 2123 3323 | 3212 2112 | 1222 2222 |
| PR | 4222 2233 | 1022 1111 | 2122 2111 | 1122 2334 | 3333 3332 | 1132 3323 | 3322 2344 | 3322 2232 | 1112 3312 | 3112 2212 | 1222 2222 |
| LV | 3324 1232 | 1212 1111 | 1222 2111 | 1223 2234 | 3233 3332 | 1222 3323 | 3233 2233 | 2323 2131 | 1123 3212 | 2111 2111 | 1331 3322 |
| KD | 2222 3232 | 1021 0000 | 0221 3010 | 0112 2234 | 3323 3434 | 1103 4313 | 2221 3343 | 2322 1222 | 1221 2403 | 2122 1000 | 1222 1212 |
| VI | 4432 1112 | 0000 0000 | 2112 3000 | 0010 0234 | 2444 3322 | 2244 3213 | 3353 2323 | 2455 1111 | 2122 3302 | 2332 1000 | 1224 2110 |
| NE | 3332 2123 | 1000 0001 | 2122 3111 | 0010 0334 | 3444 3222 | 2234 3223 | 4442 2323 | 2445 2211 | 2112 2312 | 2232 1101 | 1224 1111 |
| FU | 4212 1232 | 1010 0101 | 2111 1010 | 0011 1223 | 2222 2232 | 1122 2213 | 4222 2234 | 2212 1131 | 1112 2312 | 2111 1102 | 1112 1122 |
| CF | 4222 1232 | 0011 1101 | 2121 1111 | 1022 1234 | 3222 3343 | 1122 3313 | 4321 2245 | 3323 2131 | 2012 3313 | 3112 1112 | 1112 2332 |
| HB | 4323 2233 | 1112 1201 | 2222 2111 | 1133 2335 | 3333 3343 | 1232 3423 | 5333 3345 | 3322 2132 | 2103 3413 | 3121 1101 | 1212 3332 |
| UB | 3343 3232 | 3333 1112 | 3333 3123 | 3332 1345 | 3335 5444 | 3343 5434 | 3344 4544 | 3335 3332 | 3223 3523 | 4232 2222 | 3223 3332 |
| JO | 5322 1122 | 0011 0111 | 3221 1121 | 1111 0234 | 3332 3332 | 1132 3223 | 3323 2334 | 3332 3221 | 2012 2222 | 3221 1111 | 2222 2121 |
| SA | 3332 2122 | 2330 0012 | 3232 2011 | 2321 0234 | 3434 4433 | 4333 2433 | 4333 2433 | 3334 2223 | 3222 2322 | 3232 0122 | 2232 2233 |
| TY | 4333 3232 | 2233 2211 | 2333 3221 | 1233 3335 | 3334 3343 | 2233 3423 | 5343 3453 | 3333 3332 | 2223 3313 | 3333 2112 | 1323 2332 |
| OD | 4223 2232 | 1111 0101 | 2122 2011 | 0122 1335 | 3334 3342 | 1233 4423 | 3233 3333 | 2223 2232 | 2123 4423 | 2222 2212 | 2222 2232 |
| KK | 2222 2221 | 0221 1101 | 2223 2011 | 1233 1223 | 2322 3331 | 1122 3312 | 2222 2222 | 1222 1121 | 0222 2311 | 1222 1101 | 1222 2221 |
| OT | 3333 1123 | 0000 0001 | 3222 2001 | 0010 0244 | 2443 3232 | 1143 3313 | 4434 1234 | 2534 2121 | 2011 3223 | 2231 1001 | 2233 2010 |

| | | | | | | | | | | | | | | | | | | | | | | | | |
|---|---|---|---|---|---|---|---|---|---|---|---|---|---|---|---|---|---|---|---|---|---|---|---|---|
| SU | 4322 | 1232 | 0101 | 2111 | 1213 | 2110 | 0121 | 3235 | 3334 | 4331 | 1223 | 4323 | 3232 | 3233 | 1312 | 3232 | 2112 | 4212 | 3113 | 2112 | 1323 | 3322 |
| GC | | | | | | | | | | | | | | | | | | | | | | |
| MT | 2222 | 2122 | 0000 | 0001 | 1111 | 2010 | 0110 | 0234 | 1335 | 4422 | 1233 | 3213 | 2233 | 2422 | 1234 | 2221 | 1122 | 2412 | 2112 | 1101 | 1112 | 2221 |
| VK | 4433 | 2223 | 3322 | 2123 | 3222 | 2123 | 3332 | 2345 | 2345 | 4433 | 3343 | 3434 | 4354 | 3434 | 3335 | 3323 | 2343 | 3424 | 3333 | 2212 | 2333 | 3233 |
| AT | ---- | ---- | ---- | ---- | -343 | 3121 | 1343 | 3344 | 3434 | 5442 | 2333 | 4323 | 3-33 | 4433 | 2334 | 2232 | 2222 | 2412 | 2232 | 32-- | ---- | 3331 |
| LG | --11 | ---- | ---- | ---- | ---- | ---- | ---- | ---- | ---- | ---- | ---- | ---- | ---- | ---5 | 3312 | 2232 | 2112 | 3213 | 3210 | 1112 | 1210 | 1122 |
| AQ | 4311 | 1132 | 1000 | 0001 | 2111 | 1010 | 0000 | 0234 | 3222 | 3342 | 1122 | 3313 | 4221 | 2244 | 2212 | 1032 | 1002 | 3312 | 2100 | 1002 | 2201 | 1122 |
| TF | 3444 | 2232 | 1334 | 2112 | 1443 | 2111 | 1333 | 2335 | 2442 | 4332 | 1332 | 4423 | 3434 | 4233 | 2434 | 3232 | 1334 | 4222 | 2333 | 3222 | 2333 | 4322 |
| TK | 3333 | 1222 | 2221 | 1022 | 2231 | 2011 | 2220 | 1344 | 3334 | 3343 | 1222 | 3312 | 3333 | 3244 | 2224 | 1130 | 0211 | 3422 | 2221 | 2112 | 1332 | 3322 |
| IK | 4212 | 2233 | 1001 | 0111 | 2111 | 2111 | 0011 | 1335 | 3223 | 3342 | 1212 | 431- | ---2 | 333- | 2313 | 2132 | 1112 | 3312 | 2111 | 2112 | 1212 | 1222 |
| CI | 4222 | 2222 | 0000 | 0000 | 2111 | 1000 | 0000 | 0234 | 3222 | 2232 | 0111 | 3313 | 3322 | 2334 | 3322 | 1021 | 1002 | 2212 | 2100 | 1001 | 1112 | 1121 |
| TL | 4211 | 1132 | 1000 | 0101 | 2111 | 1111 | 0011 | 1135 | 3222 | 2332 | 1121 | 2313 | 3221 | 1234 | 2212 | 1121 | 1101 | 1212 | 2111 | 1112 | 1212 | 1121 |
| FR | 4332 | 1122 | 1000 | 0000 | 3123 | 2111 | 0011 | 0244 | 3433 | 3232 | 1233 | 3223 | 4432 | 2234 | 3433 | 2122 | 2112 | 3212 | 2231 | 1001 | 2233 | 1012 |
| PE | 4111 | 1132 | 0000 | 0101 | 2110 | 1011 | 0111 | 0235 | 3211 | 2232 | 1211 | 2213 | 4211 | 1133 | 2212 | 1121 | 1111 | 3312 | 2111 | 1112 | 1112 | 2121 |
| AK | ---- | ---- | ---- | ---- | -111 | 1011 | 1123 | 2223 | 1123 | 3331 | ---- | ---- | --22 | 1432 | 1213 | 1111 | 0212 | 2101 | 1221 | 1112 | 2311 | 3211 |
| SM | 3222 | 2332 | 2222 | 3222 | 2223 | 3222 | 2233 | 3225 | 4333 | 3233 | 2233 | 2323 | 3332 | 2344 | 3333 | 3222 | 2223 | 2222 | 4332 | 3222 | 2333 | 3222 |
| AE | 4343 | 2231 | 1033 | 2301 | 3323 | 2311 | 0033 | 2335 | 3232 | 4332 | 2132 | 3322 | 3344 | 3324 | 2233 | 2122 | 2124 | 4323 | 3132 | 2211 | 2233 | 3232 |
| SF | | | | | | | | | | | | | | | | | | | | | | |
| KA | 2222 | 2121 | 1000 | 0000 | 1001 | 1010 | 0110 | 0234 | 2235 | 3412 | 1233 | 3212 | 2233 | 2422 | 1224 | 2221 | 1112 | 2422 | 2112 | 1100 | 1012 | 2221 |
| KS | 4313 | 2242 | 0011 | 1102 | 2010 | 2011 | 0011 | 1345 | 1143 | 4432 | 1212 | 3212 | 3232 | 2224 | 2223 | 2231 | 1012 | 4322 | 1111 | 2222 | 2212 | 2132 |
| AV | 3321 | 1122 | 1011 | 0111 | 2111 | 1111 | 0101 | 1234 | 2222 | 3233 | 1221 | 2213 | 3322 | 2244 | 2222 | 1122 | 2012 | 2212 | 2111 | 2101 | 1111 | 1222 |
| DS | 4332 | 1112 | 1110 | 0001 | 2122 | 2111 | 0020 | 0244 | 4433 | 2221 | 2242 | 3324 | 4432 | 2234 | 2434 | 2121 | 2222 | 3213 | 3231 | 2001 | 2223 | 2111 |
| TU | 4432 | 1212 | 1000 | 0000 | 2122 | 3001 | 0020 | 0234 | 3334 | 3232 | 2233 | 3213 | 4442 | 2233 | 3444 | 3111 | 1122 | 3212 | 2231 | 1000 | 2223 | 1122 |
| KY | 2222 | 2122 | 0000 | 0000 | 1011 | 1011 | 0011 | 1233 | 2325 | 3322 | 1233 | 3312 | 2232 | 2422 | 1224 | 2211 | 1112 | 2412 | 2112 | 1101 | 1012 | 3221 |
| QU | 2334 | 2221 | 1223 | 0001 | 2231 | 3010 | 2223 | 1334 | 2433 | 3332 | 1232 | 3312 | 3334 | 3343 | 1233 | 1131 | 1323 | 3312 | 2222 | 1111 | 1322 | 3221 |
| ML | 4434 | 3232 | 1333 | 3222 | 2332 | 3222 | 2332 | 2345 | 4433 | 4333 | 2342 | 4324 | 3444 | 4333 | 2354 | 3233 | 2333 | 4223 | 3334 | 2222 | 2354 | 3233 |
| SZ | 4222 | 2132 | 1012 | 1101 | 3211 | 2211 | 0012 | 2342 | 3233 | 2321 | 2222 | 3213 | 4323 | 3324 | 2224 | 2122 | 2112 | 4312 | 2112 | 3211 | 2113 | 3222 |
| LP | 3322 | 2122 | 2222 | 1112 | 2222 | 2122 | 2121 | 2334 | 3535 | 3423 | 2335 | 3323 | 3433 | 3333 | 3323 | 2223 | 3222 | 3423 | 4322 | 2113 | 4423 | 3222 |
| TA | 4321 | 1232 | 1001 | 0111 | 3211 | 1010 | 0111 | 0235 | 3323 | 3232 | 2222 | 2222 | 3321 | 1223 | 2233 | 1122 | 2112 | 3213 | 3111 | 1111 | 1211 | 1132 |
| HO | 2222 | 0011 | 0000 | 0000 | 1111 | 3000 | 0010 | 0243 | 1112 | 2121 | 1212 | 1212 | 1322 | 1212 | 1333 | 1110 | 1111 | 2212 | 1121 | 1100 | 1012 | 1111 |
| TE | 3433 | 3122 | 3111 | 3322 | 2222 | 3222 | 1121 | 1444 | 3433 | 3343 | 2242 | 4334 | 4333 | 3444 | 3433 | 4332 | 2222 | 4123 | 3332 | 2222 | 2323 | 2233 |
| AL | | | | | | | | | | | | | | | | | | | | | | |
| SJ | 3211 | 1112 | 0000 | 0101 | 2012 | 1000 | 0010 | 0233 | 3323 | 3234 | 1232 | 2213 | 4322 | 2133 | 3323 | 1110 | 2001 | 1110 | 2210 | 1100 | 1112 | 0022 |
| MB | 3211 | 1121 | 1000 | 0011 | 2211 | 1011 | 0010 | 0234 | 1222 | 3333 | 1212 | 3323 | 4312 | 3334 | 3212 | 1122 | 2012 | 3322 | 2101 | 1101 | 1111 | 1022 |
| MU | 3322 | 2222 | 2332 | 0102 | 3322 | 3123 | 3322 | 1334 | 3434 | 3333 | 2334 | 3313 | 2323 | 2332 | 3333 | 2222 | 3212 | 3422 | 3312 | 2212 | 3332 | 3322 |
| GU | 3221 | 2112 | 1110 | 0101 | 1111 | 2011 | 0110 | 0234 | 2224 | 3311 | 2223 | 3213 | 3222 | 2313 | 2223 | 2111 | 2112 | 2322 | 2112 | 1111 | 2111 | 2221 |
| BA | 42-- | -232 | 1111 | 0112 | 3221 | 1121 | 1121 | 0235 | 3233 | 5232 | 2222 | 3222 | 3232 | 2223 | 2223 | 2222 | 2122 | 3212 | 2101 | 2112 | 2222 | 2122 |
| MC | 4222 | 1132 | 0000 | 0112 | 3212 | 2111 | 0010 | 0245 | 4223 | 4331 | 1212 | 3223 | 4223 | 3334 | 2123 | 2122 | 2122 | 3222 | 2100 | 1001 | 2102 | 4222 |
| TG | 3341 | 2223 | 4440 | 0112 | 2340 | 3122 | 4340 | 0333 | 4554 | 3333 | 3354 | 3312 | 3352 | 2343 | 3453 | 2022 | 3343 | 3403 | 3341 | 1212 | 2353 | 3333 |
| LU | | | | | | | | | | | | | | | | | | | | | | |
| PM | 4221 | 2122 | 1110 | 0012 | 2211 | 2012 | 1120 | 1233 | 3234 | 3322 | 1233 | 3222 | 3332 | 2322 | 2333 | 2112 | 2222 | 2412 | 2222 | 1111 | 2111 | 2121 |
| HU | 3212 | 2323 | 1101 | 2221 | 21-- | -220 | 0111 | 2444 | 3333 | 4432 | 1121 | 4423 | 4311 | 3334 | 3322 | 2220 | 1112 | 4312 | 1221 | 2221 | 1222 | 2321 |
| PP | 3321 | 0001 | 0000 | 0000 | 1112 | 2000 | 0000 | 0233 | 2333 | 1011 | 0122 | 1011 | 2222 | 1110 | 2332 | 0000 | 1001 | 2101 | 1211 | 0001 | 2222 | 1010 |
| TN | 2031 | 2122 | 2101 | 1101 | 1131 | 3001 | 0010 | 1124 | 2123 | 2131 | 2122 | 2212 | 2221 | 3333 | 2223 | 2120 | 1023 | 2011 | 1011 | 2001 | 1131 | 1010 |
| PI | 3321 | 1223 | 1110 | 1112 | 3222 | 2212 | 0121 | 1344 | 4432 | 3344 | 2232 | 3324 | 4322 | 3344 | 3432 | 2223 | 211- | 4223 | 2221 | 2212 | 2222 | 2242 |
| GN | 3222 | 2332 | 1010 | 0001 | 1111 | 3021 | 1000 | 0234 | 2234 | 4342 | 1223 | 3323 | 2232 | 4433 | 1223 | 3221 | 1111 | 2411 | 1011 | 1110 | 1011 | 2121 |
| HR | 4221 | 0132 | 0000 | 0001 | 2011 | 1010 | 0011 | 0235 | 3324 | 3332 | 1123 | 3113 | 3332 | 2334 | 2122 | 1021 | 1022 | 2213 | 2111 | 1001 | 1133 | 1021 |
| AC | ---- | ---- | 1000 | 0000 | 2111 | 1010 | 0010 | 0333 | 3322 | 3233 | 2232 | 3333 | 4321 | 3334 | 3322 | 2122 | 2112 | 3222 | 1211 | 1111 | 2111 | 2232 |
| TO | 3232 | 2112 | 0100 | 0001 | 2221 | 3010 | 0000 | 1223 | 3324 | 4332 | 1233 | 3312 | 2332 | 3432 | ---- | ---- | 1112 | 2311 | 1122 | 1100 | 1222 | 2111 |
| AM | 3332 | 1111 | 0100 | 0000 | 2122 | 3010 | 0000 | 0123 | 1234 | 3211 | 2233 | 3202 | 2333 | 2321 | 2334 | 1112 | 1111 | 3202 | 2122 | 1000 | 1122 | 2000 |
| TW | 3221 | 2212 | 1000 | 0001 | 2210 | 2110 | 0021 | 1234 | 3432 | 3243 | 1232 | 2324 | 4321 | 2334 | 3322 | 2121 | 2112 | 3222 | 2220 | 1110 | 1212 | 2221 |
| MI | 3232 | 3011 | 1000 | 0001 | 1135 | 4001 | 1101 | 0122 | 1346 | 7722 | 1135 | ---2 | 3344 | 5633 | 2345 | 4311 | 1112 | 3411 | 2124 | 3012 | 1224 | 4110 |
| MY | 4454 | 3464 | 2333 | 1233 | 3343 | 3243 | 3333 | 1244 | 3454 | 3343 | 3455 | 3334 | 4454 | 3334 | 3454 | 3244 | 3343 | 3322 | 4345 | 2222 | 3343 | 2222 |
| MW | 6543 | 2365 | 2221 | 1124 | 5434 | 4244 | 3211 | 1366 | 6554 | 3566 | 2243 | 3336 | 6434 | 3465 | 4543 | 4345 | 4223 | 4334 | 4532 | 2225 | 4433 | 4334 |
| NL | 5422 | 1133 | 1111 | 1111 | 4221 | 1111 | 1111 | 1245 | 4542 | 2233 | 1133 | 2214 | 4422 | 1346 | 3422 | 1122 | 211- | 2213 | 3212 | 1002 | 2222 | 1111 |
| SB | 3332 | 2322 | 1221 | 1222 | 3322 | 3221 | 1010 | 0223 | 2323 | 3322 | 3133 | 3323 | 3333 | 2322 | 3333 | 2222 | 2112 | 2222 | 2211 | 1111 | 1223 | 2222 |
| VO | 3332 | 2233 | 2222 | 2112 | 3232 | 3222 | 1122 | 1223 | 3333 | 3333 | 3333 | 3313 | 3333 | 3323 | 3333 | 2222 | 3222 | 3312 | 2222 | 2111 | 2222 | 2222 |

Provisional Equatorial Dst

by

M. Sugiura
Laboratory for Space Physics
Goddard Space Flight Center, Greenbelt, Maryland 20771

Provisional equatorial Dst is plotted below for the period August 27 to September 7, 1971. The Dst data presented here are provisional. The base line, which is based on extrapolations of the base lines for the four observatories, Kakioka, Hermanus, San Juan, and Honolulu, from the 1957-1970 series [Sugiura and Poros, 1971], will be redetermined later when the final Dst values are calculated.

REFERENCE

SUGIURA, M., and D. J. POROS 1971 Hourly values of equatorial Dst for the years 1957 to 1970, Goddard Space Flight Center, X-645-71-278.

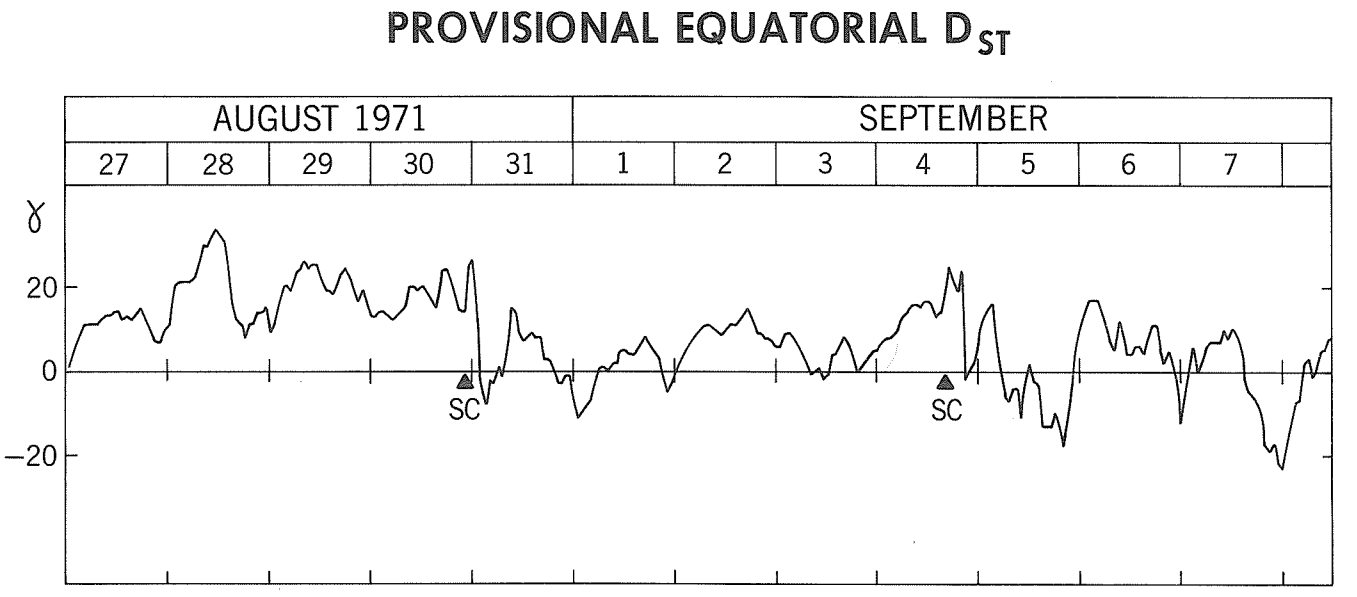

# Geomagnetically Active Plages and Flares Observed during the Interval Including September 1, 1971

by

M. C. Ballario
Osservatorio Astrofisico di Arcetri
Florence, Italy

## Abstract

The moderate geomagnetic disturbance observed on September 1 (Kp max = 5), 1971, is related to an importance 2 flare recorded on August 30 (Time-lag of about 2 days).

The other geomagnetic storms and disturbances observed during the interval August 14-September 20, including the selected day, are well-correlated either with CMPs of positive plages or with occurrences of "specific flares", namely proton flares (Figure 1).

## Introduction

Solar phenomena occurring during the interval August 14-September 20, 1971 are examined.

In Figure 1 are marked:

A. The CMPs of all recurrent and non-recurrent plages as given in the McMath calcuim plage list ("Solar-Geophysical Data", Part I, Boulder, Colorado).

B. The CMPs of recurrent positive plages only.

The positive plages are never associated, before the meridian transit, with spot-groups type C or greater but, at the most, with spot-groups type A or B (spots without penumbra).

The CMPs of positive plages are generally associated with geomagnetic storms or disturbances; the correlation being about 78% [Ballario, 1970a].

On the contrary the negative plages are associated, before the meridian transit and at least for part of their life, with spot-groups type C or greater (spot with penumbra).

The CMPs of negative plages, as well as their CMPs in the subsequent rotations, are generally associated with quiet or slightly disturbed geomagnetic conditions [Ballario, 1970a], unless a resurgence takes place.

It is also seen that the CMPs of non-recurrent plages, whatever the associated spot-group type may be, are geomagnetically inactive.

The subdivision into negative and positive plages, depending on the associated spot-group type, is based on the Fraunhofer Institut Solar Maps.

The plage subdivision into recurrent and non-recurrent is given in the McMath calcium plage list. However, we have to note that, particularly when the active centers show only very small and negligible plages which appear and disappear during their life, some classified non-recurrent plages may be considered as recurrent ones. Thus, in this regard, some changes have been made.

C. The geomagnetic index Kp (Bartels).

D. The geomagnetically active flares.

We are not able, at present, to give the characteristics distinguishing the geomagnetically active flares from the inactive ones. Only "a posteriori" we may correlate geomagnetic storms and disturbances with flare occurrences.

In a previous paper [Ballario, 1970a] we have found that 48% of importance 2 and 3 flares, 53% of importance 1 proton flares and 21% of importance S proton flares were followed by geomagnetic storms or disturbances with Kp maximum value $\geq$ 4+ (time-lag of about 2 days), while the others were followed by quiet or slightly disturbed geomagnetic conditions. On the other hand it is well-known that importance 1 and S flares are geomagnetically inactive.

In some cases the geomagnetic storms or disturbances are related both with CMPs of positive plages and with flare occurrences. Only when there are not CMPs of positive plages associated with the disturbance, can we consider the flare entirely responsible for the disturbance itself.

E. All the flares observed as given in the Quarterly Bulletin on Solar Activity.

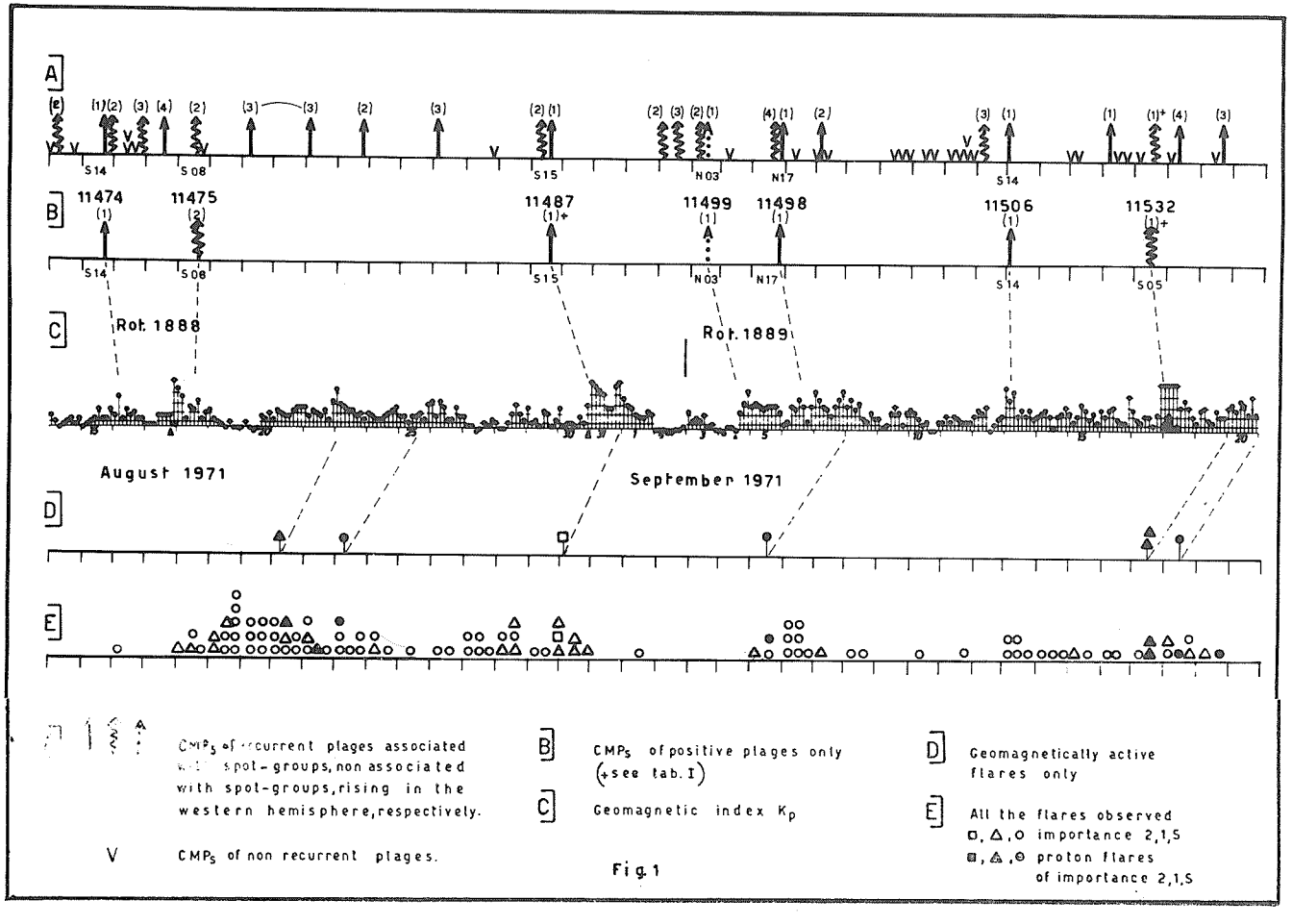
A
B
11474
11475
11487
11499
11498
11506
11532
S14
S08
S15
N03
N17
S14
S05
C
Rot. 1888
Rot. 1889
August 1971
September 1971
D
E
CMPs of recurrent plages associated with spot-groups, non associated with spot-groups, rising in the western hemisphere, respectively.
V CMPs of non recurrent plages.
B CMPs of positive plages only (+see tab. I)
C Geomagnetic index Kp
D Geomagnetically active flares only
E All the flares observed □, △, ○ importance 2,1,S
■, ▲, ● proton flares of importance 2,1,S

Fig. 1

## The Events of August 14-September 20

### Plages

The CMPs of recurrent and non-recurrent plages observed during this interval and their subdivision into positive and negative plages are presented in Table 1 and marked in Figure 1A.

The positive plages are 7 in number and are marked in Figure 1B.

Broken lines relate the CMPs of positive plages with geomagnetic storms or disturbances (Figures 1B-1C).

### Flares

The data referring to importance 2 flares and importance 1 and S proton flares are presented in Table 2. They are 9 in number and seven of them (two of which occurred in the same day) are followed by geomagnetic disturbances.

These geomagnetically active flares are marked in Figure 1D.

Broken lines relate the maxima of the flares with the maxima of the disturbances (Figures 1D-1C).

### Conclusion

From Figure 1 it is seen that the geomagnetic storms and disturbances recorded during this interval are related either to CMPs of recurrent positive plages or with flare occurrences.

Particularly we note:

1.) The moderate disturbance of September 1 (Kp max = 5) is entirely due to the importance 2 flare recorded on August 30 (time-lag of about 2 days), since no CMPs of positive plages are correlated with the disturbance itself.

2.) The sc disturbance of August 31 and the storms of August 17 and September 18 are correlated with the CMPs of the recurrent positive plages McMath Nos. 11487, 11475, 11532 respectively.

3.) The geomagnetic disturbance of September 5 (Kp max = 4+) is not preceded by any reported flare for more than 3 days. It is correlated with the CMP of the recurrent positive plage McMath No. 11499 rising in the western hemisphere. During its central meridian transit this center of activity does not show chromospheric-photospheric phenomena, but appears to be geomagnetically active. Thus we think it possible to identify this center as a Bartels "M solar region".

The results here obtained are in good agreement with those found in examining the solar and geomagnetic phenomena recorded during the year 1968 [Ballario, 1970a] and in other selected intervals [Ballario, 1969a, 1969b, 1970b, 1971, 1972].

### REFERENCES


BALLARIO, M. C. 1969a On the special events of March 1966, Ann. Geophys., 25, fasc. 1, 135-146.

BALLARIO, M. C. 1969b The IQSY 27-day recurrence sequence for 1964, Mem. SAIt., 40, fasc. 3, 271-294.

BALLARIO, M. C. 1970a Solar and geomagnetic events of the year 1968, Ann. Geophys., 26, 459-473.

BALLARIO, M. C. 1970b On the solar and geomagnetic events of Oct.-Nov., 1968, World Data Center A Upper Atmosphere Geophysics Report UAG-8, 231-238.

BALLARIO, M. C. 1971 March 1970: Solar and geomagnetic events, World Data Center A Upper Atmosphere Geophysics Report UAG-12, Part III, 349-358.

BALLARIO, M. C. 1972 On the geomagnetically active flares of September 1963, Mem. SAIt., in press.

Table 1

CMPs of plages recorded during the interval Aug. 14 - Sept. 20, 1971 and their subdivision into positive and negative plages.

| Mc Math Data | | | | | | Characteristics | Remarks (group types from Fraunhofer Institut solar maps) |
|---|---|---|---|---|---|---|---|
| CMP 1971 | Lat. | Hel. long. | McMath plage number | Return of region | Age | | |
| Aug. | | | | | | | |
| 14.2 | N14 | 36° | 11471 | New | 1 | non-rec. negative | - - |
| 14.3 | N07 | 35 | 11466 | 11425 | 2 | recurrent " | E groups in the prec.rot. |
| 14.7 | N31 | 29 | 11476 | New | 1 | non-rec. " | - - |
| 15.8 | S14 | 15 | 11474 | New | 1 | rec. positive | Eastern A group |
| 15.9 | N08 | 14 | 11473 | 11429 | 2 | rec. negative | J groups in the prec.rot. |
| 16.4 | N17 | 7 | 11483 | New | 1 | non-rec. " | - - |
| 16.4 | N04 | 7 | 11485 | New | 1 | non-rec. " | - - |
| 16.5 | S03 | 6 | 11481 | New | 1 | non-rec. " | - - |
| 16.9 | S16 | 0 | 11472 | 11432 | 3 | rec. " | C groups in the prec.rot. |
| 17.7 | N14 | 350 | 11467 | 11433 | 4 | rec. " | E,J groups in prec.rot. |
| 18.7 | S08 | 336 | 11475 | 11434 | 2 | rec. positive | No spots |
| 18.7 | N48 | 336 | 11477 | New | 1 | non-rec. negative | - - |
| 20.3 | N15 | 315 | 11478 | 11438 | 3 | rec. " | D,C groups in the prec.rot |
| 22.1 | N17 | 292 | 11480 | 11438 | 3 | rec. " | - - |
| 23.8 | S12 | 269 | 11482 | 11445 | 2 | rec. " | Eastern E groups |
| 26.2 | S12 | 237 | 11484 | 11442 | 3 | rec. " | Eastern C groups |
| 27.8 | N09 | 216 | 11493 | New | 1 | non-rec. " | - - |
| 29.4 | N06 | 195 | 11486 | 11447 | 2 | rec. " | C groups in the prec.rot. |
| 29.6 | S16 | 193 | 11487 | New | 1 | rec. positive$^{+}$(a) | A spots |
| Sept. | | | | | | | |
| 2.1 | N11 | 146 | 11489 | 11465 | 2 | rec. negative | C groups in the prec.rot. |
| 2.5 | S11 | 141 | 11490 | 11455 | 3 | rec. " | D groups in the prec.rot. |
| 3.5 | N13 | 128 | 11491 | 11456 | 2 | rec. " | D groups in the prec.rot. |
| 3.5 | N03 | 128 | 11499 | New | 1 | rec. positive | Rising in the W hemisph. |
| 4.2 | S06 | 119 | 11496 | New | 1 | prob.rec. negative | Eastern C groups |
| 5.8 | S11 | 97 | 11492 | 11457 | 4 | rec. " | E groups in the prec.rot. |
| 5.8 | N17 | 97 | 11498 | New | 1 | rec. positive | Eastern A,B groups |
| 6.2 | N03 | 92 | 11495 | New | 1 | non-rec. negative | - - |
| 7.0 | S14 | 82 | 11507 | New | 1 | non-rec. " | - - |
| 7.1 | N21 | 80 | 11494 | 11479 | 2 | rec. " | J groups in the prec.rot. |
| 7.2 | S19 | 79 | 11505 | New | 1 | non-rec. " | - - |
| 9.5 | N13 | 49 | 11512 | New | 1 | non-rec. " | - - |
| 9.6 | N03 | 47 | 11500 | New | 1 | non-rec. " | - - |
| 9.9 | S09 | 43 | 11510 | New | 1 | non-rec. " | - - |
| 10.4 | N24 | 37 | 11502 | New | 1 | non-rec. " | - - |
| 10.6 | N11 | 34 | 11520 | New | 1 | non-rec. " | - - |
| 11.2 | N25 | 26 | 11513 | New | 1 | non-rec. " | - - |
| 11.3 | N06 | 25 | 11517 | New | 1 | non-rec. " | - - |
| 11.4 | N14 | 23 | 11508 | New | 1 | non-rec. " | - - |
| 11.6 | S29 | 21 | 11503 | New | 1 | non-rec. " | - - |
| 11.7 | S17 | 20 | 11504 | 11474 | 2 | rec. " | C groups in the prec.rot. |
| 12.1 | N16 | 14 | 11501 | 11473 | 3 | rec. " | J groups in the prec.rot. |
| 13.1 | S14 | 1 | 11506 | New | 1 | rec. positive | Eastern B groups |
| 13.9 | N15 | 350 | 11509 | 11467 | 5 | rec. negative | E groups in prec.rot. |
| 15.0 | N03 | 336 | 11521 | New | 1 | non-rec. " | - - |
| 15.2 | S12 | 333 | 11529 | New | 1 | non-rec. " | - - |
| 16.2 | N13 | 320 | 11511 | New | 1 | rec. " | Eastern J groups |
| 16.4 | S27 | 318 | 11519 | New | 1 | non-rec. " | - - |

Table 1 continued

| Mc Math Data | | | | | | Characteristics | Remarks (group types from Fraunhofer Institut solar maps) |
|---|---|---|---|---|---|---|---|
| CMP 1971 | Lat. | Hel. long. | McMath plage number | Return of region | Age | | |
| Sept. | | | | | | | |
| 16.8 | S13 | 312 | 11522 | New | 1 | non-rec. negative | - - |
| 17.1 | S18 | 308 | 11526 | New | 1 | non-rec. " | - - |
| 17.7 | S05 | 300 | 11532 | New | 1 | rec. positive+(b) | Rising in the W hemisph |
| 18.2 | N01 | 294 | 11518 | New | 1 | non-rec. negative | - - |
| 18.4 | N14 | 291 | 11514 | 11480 | 4 | rec. " | Eastern C groups |
| 19.4 | N05 | 278 | 11515 | New | 1 | prob. rec. " | Eastern J groups |
| 19.6 | S13 | 275 | 11516 | 11482 | 3 | rec. " | Eastern E,D groups |

+(a) Plage 11487 at L = 193° is recurrent with the negative plage 11531 at S15 and L = 190° (see McMath footnotes in Solar Geophysical Data n° 327) CMP: Sept. 26.1

+(b) Plage 11532 at L = 300° is recurrent with the positive plage 11553 at S05 and L = 305° (see McMath footnotes in Solar Geophysical Data n° 327) CMP: Oct. 14.5

Table 2

Importance 2 flares and importance 1,S proton flares observed during the interval Aug. 14 - Sept. 20, 1971 (from Quarterly Bulletin on Solar Activity)

| Date 1971 | Time U.T. | Max U.T. | Position | Imp. | App. and corr. aerea | Charac. | McMath Region | Proposed correlation between Kp max. and flare max. (time-lag of about 2 days) |
|---|---|---|---|---|---|---|---|---|
| Aug. | | | | | | | | |
| 21 | 0930<br>0950 | 0936 | 09S-25E | 1B | 2.9<br>3.2 | FHQUVW | 11482 | Kp max = 4+ on Aug. 23.1 |
| 22 | 0730<br>0817 | 0735<br>0752 | 09S-11E | 1B | 2.9<br>3.0 | FHKUWZ | 11482 | Geomagnetically inactive |
| 23 | 0719<br>0743 | 0727 | 10S-12E | SN | 1.1<br>1.1 | HU | 11482 | modest Kp fluctuation |
| 30 | 0303<br>0410 | 0332 | 12S-87W | 2F | 1.9<br>- | - | 11482 | Kp max = 5 on Aug. 31.9 |
| Sept. | | | | | | | | |
| 5 | 1323<br>1405 | 1329<br>1339 | 17S-05E | SN | 1.7<br>1.7 | HU | 11492 | Kp max = 4+ on Sept. 7.9 |
| 17 | 1400<br>1525 | 1415<br>1429 | 11S-21E | 1B | 2.6<br>2.7 | FLU | 11516 | Modest Kp fluctuation |
| 17 | 1544<br>1610 | 1549 | 17S-22E | 1B | 2.1<br>2.3 | HRU | 11516 | |
| 18 | 1330<br>1410 | 1338 | 03N-08E | SB | 1.6<br>1.6 | EUZ | 11545 | Kp max = 4 on Sept. 20.7 |
| 19 | 1122<br>1212 | 1132 | 10S-04W | SN | 1.4<br>1.4 | KU | 11516 | Geomagnetically inactive |

## ACKNOWLEDGEMENTS

This Report would not have been possible without the many contributions from the worldwide scientific community.

## ALPHABETICAL INDEX

# AUTHOR INDEX

Publication Notice

WORLD DATA CENTER A for SOLAR-TERRESTRIAL PHYSICS REPORT UAG
(Prepared by World Data Center A for Solar-Terrestrial Physics, NOAA, Boulder, Colorado)

These reports are for sale through the National Climatic Center, Federal Building, Asheville, NC 28801, Attn: Publications. Subscription price: $9.00 a year; $2.50 additional for foreign mailing; single copy price varies. These reports are issued on an irregular basis with 6 to 12 reports being issued each year. Therefore, in some years the single copy rate will be less than the subscription price, and in some years the single copy rate will be more than the subscription price. Make checks and money orders payable to: Department of Commerce, NOAA.

Upper Atmosphere Geophysics Report UAG-1, "IQSY Night Airglow Data" by L. L. Smith, F. E. Roach and J. M. McKennan of Aeronomy Laboratory, ESSA Research Laboratories, July 1968, single copy price $1.75.

Upper Atmosphere Geophysics Report UAG-2, "A Reevaluation of Solar Flares, 1964-1966" by Helen W. Dodson and E. Ruth Hedeman of McMath-Hulbert Observatory, The University of Michigan, August 1968, single copy price 30 cents.

Upper Atmosphere Geophysics Report UAG-3, "Observations of Jupiter's Sporadic Radio Emission in the Range 7.6-41 MHz, 6 July 1966 through 8 September 1968" by James W. Warwick and George A. Dulk, Department of Astro-Geophysics, University of Colorado, October 1968, single copy price 30 cents

Upper Atmosphere Geophysics Report UAG-4, "Abbreviated Calendar Record 1966-1967" by J. Virginia Lincoln, Hope I. Leighton and Dorothy K. Kropp, Aeronomy and Space Data Center, Space Disturbances Laboratory, ESSA Research Laboratories, January 1969, single copy price $1.25.

Upper Atmosphere Geophysics Report UAG-5, "Data on Solar Event of May 23, 1967 and its Geophysical Effects" compiled by J. Virginia Lincoln, World Data Center A, Upper Atmosphere Geophysics, ESSA, February 1969, single copy price 65 cents.

Upper Atmosphere Geophysics Report UAG-6, "International Geophysical Calendars 1957-1969" by A. H. Shapley and J. Virginia Lincoln, ESSA Research Laboratories, March 1969, single copy price 30 cents.

Upper Atmosphere Geophysics Report UAG-7, "Observations of the Solar Electron Corona: February 1964-January 1968" by Richard T. Hansen, High Altitude Observatory, Boulder, Colorado and Kamuela, Hawaii, October 1969, single copy price 15 cents.

Upper Atmosphere Geophysics Report UAG-8, "Data on Solar Geophysical Activity October 24-November 6, 1968", Parts 1 and 2, compiled by J. Virginia Lincoln, World Data Center A, Upper Atmosphere Geophysics, ESSA, March 1970, single copy price (includes Parts 1 and 2) $1.75.

Upper Atmosphere Geophysics Report UAG-9, "Data on Cosmic Ray Event of November 18, 1968 and Associated Phenomena" compiled by J. Virginia Lincoln, World Data Center A, Upper Atmosphere Geophysics, ESSA, April 1970, single copy price 55 cents.

Upper Atmosphere Geophysics Report UAG-10, "Atlas of Ionograms" edited by A. H. Shapley, ESSA Research Laboratories, May 1970, single copy price $1.50

Upper Atmosphere Geophysics Report UAG-11, "Catalogue of Data on Solar-Terrestrial Physics", compiled by J. Virginia Lincoln and H. Patricia Smith, World Data Center A, Upper Atmosphere Geophysics, ESSA, June 1970, single copy price $1.50.

Upper Atmosphere Geophysics Report UAG-12, "Solar-Geophysical Activity Associated with the Major Geomagnetic storm of March 8, 1970", Parts 1, 2 and 3, compiled by J. Virginia Lincoln and Dale B. Bucknam, World Data Center A, Upper Atmosphere Geophysics, NOAA, April 1971, single copy price (includes Parts 1-3) $3.00.

Upper Atmosphere Geophysics Report UAG-13, "Data on the Solar Proton Event of November 2, 1969 through the Geomagnetic Storm of November 8-10, 1969", compiled by Dale B. Bucknam and J. Virginia Lincoln, World Data Center A, Upper Atmosphere Geophysics, NOAA, May 1971, single copy price 50 cents.

Upper Atmosphere Geophysics Report UAG-14, "An Experimental Comprehensive Flare Index and its Derivation for 'Major' Flares 1955-1969", by Helen W. Dodson and E. Ruth Hedeman, McMath-Hulbert Observatory, University of Michigan, July 1971, single copy price 30 cents.

Upper Atmosphere Geophysics Report UAG-15, "Catalogue of Data on Solar-Terrestrial Physics", prepared by Research Laboratories, NOAA, Boulder, Colorado, July 1971, single copy price $1.50. (Supersedes Report UAG-11, June 1970.)

Upper Atmosphere Geophysics Report UAG-16, "Temporal Development of the Geographical Distribution of Auroral Absorption for 30 Substorm Events in each of IQSY (1964-65) and IASY (1969)" by F. T. Berkey, V. M. Driatskiy, K. Henriksen, D. H. Jelly, T. I. Shchuka, A. Theander and J. Yliniemi, September 1971, single copy price 70 cents.

Upper Atmosphere Geophysics Report UAG-17, "Ionospheric Drift Velocity Measurements at Jicamarca, Peru (July 1967 - March 1970)", by Ben B. Balsley, Aeronomy Laboratory, National Oceanic and Atmospheric Administration, Boulder, Colorado, and Ronald F. Woodman, Jicamarca Radar Observatory, Instituto Geofisico del Perú, Lima, Peru, October 1971, single copy price 35 cents.

Upper Atmosphere Geophysics Report UAG-18, "A Study of Polar Cap and Auroral Zone Magnetic Variations", by K. Kawasaki and S. I. Akasofu, Geophysical Institute, University of Alaska, June 1972, single copy price 20 cents.

Upper Atmosphere Geophysics Report UAG-19, "Reevaluation of Solar Flares 1967", by Helen W. Dodson and E. Ruth Hedeman of McMath-Hulbert Observatory, The University of Michigan, and Marta Rovira de Miceli, San Miguel Observatory, Argentina, June 1972, single copy price 15 cents.

Report UAG-20, "Catalogue of Data on Solar-Terrestrial Physics", prepared by Environmental Data Service, NOAA, Boulder, Colorado, October 1972, single copy price $1.50 (supersedes Report UAG-15, 1971.)

Report UAG-21, "Preliminary Compilation of Data for Retrospective World Interval July 26 - August 14, 1972", compiled by J. Virginia Lincoln and Hope I. Leighton, WDC-A for Solar-Terrestrial Physics, November 1972, single copy price 70 cents.

Report UAG-22, "Auroral Electrojet Magnetic Activity Indices (AE) for 1970", by Joe Haskell Allen, National Geophysical and Solar-Terrestrial Data Center, Environmental Data Service, November 1972, single copy price 75 cents.

Report UAG-23, "U.R.S.I. Handbook of Ionogram Interpretation and Reduction", Second Edition, November 1972, edited by W. R. Piggott, Radio and Space Research Station, Slough, U.K., and K. Rawer, Arbeitsgruppe für Physikalische Weltraumforschung, Freiburg, G.F.R., November 1972, single copy price $1.75.

USCOMM-NOAA-ASHEVILLE,NC-1-73-1325